

The Effects of Acidosis,
Glutamine Starvation and Inhibition of the pH
Sensitive SNAT2 Amino Acid Transporter on Protein
Metabolism in L6 Muscle Cells.

Thesis submitted for the degree of
Doctor of Philosophy
At the University of Leicester

By

Mrs Kate Florella Evans
Department of Infection, Immunity and Inflammation
And
Department of Cell Physiology and Pharmacology
University of Leicester

September 2008

Abstract

Uraemia in end-stage renal disease patients leads to wasting of lean tissue, partly through the effects of acidosis that induce negative protein balance. Insulin resistance in these patients is also a major cause of muscle wasting, suggesting that low pH has a significant effect on insulin signalling in uraemic muscle. The pH sensitive SNAT2 amino acid transporter has been implicated in this because it is strongly inhibited by low pH, and amino acids are a well-established stimulus for the key protein kinase mTOR which regulates protein synthesis. The aims of this study were to determine: (a) the effects of amino acids, (especially L-Gln), and acidosis on insulin signalling and global protein synthesis/proteolysis rates; (b) whether these effects are mimicked by selective inhibition of SNAT2, and (c) whether intracellular amino acid depletion is sufficient to account for the functional effects of SNAT2 inhibition.

In the L6 skeletal muscle cell-line, inhibition of SNAT2 with the non-metabolisable SLC38 substrate methylaminoisobutyrate, metabolic acidosis (pH 7.1), or silencing of SNAT2 expression with small-interfering RNAs, all decreased intracellular amino acid concentrations, mTOR activation, and global protein synthesis; and increased global proteolysis. Acidosis and small-interfering RNA inhibition both decreased phosphatidylinositol-3-kinase and protein kinase B activation, even though this is not regarded as an amino acid sensitive pathway. Extracellular amino acid depletion yielded decreases in intracellular amino acid levels similar to those observed during SNAT2 inhibition, but this failed to mimic the impairment of mTOR signalling observed when SNAT2 was inhibited.

It is concluded that, in this muscle model, SNAT2 is able to regulate mTOR activation and protein synthesis rates; and that SNAT2 links acidosis, activity of the phosphatidylinositol-3-kinase/PKB signalling pathway and proteolysis, suggesting that SNAT2 is a key player in the acid-induced insulin resistance which is a prime cause of cachexia in acidotic uraemic patients.

Publications, Presentations and Posters

Papers

Evans K, Nasim Z, Brown J, Clapp E, Amin A, Bin Y, Herbert TP and Bevington A (2008) pH-sensing amino acid transporter SNAT2 regulates signals to proteolysis through PI-3-kinase/mTOR in L6 myoblasts and myotubes Journal of the American Society of Nephrology (In Press).

Evans K. Nasim Z. Brown J. Butler H. Kauser S. Varoqui H. Erickson JD. Herbert TP. Bevington A (2007). The acidosis-sensing glutamine pump SNAT2 determines amino acid levels and mTOR signalling to protein synthesis in L6 muscle cells. Journal of the American Society of Nephrology 18, 1426 – 36.

Oral presentations

KF Evans, J Brown, Z Naseem, E Gomez, and TP Herbert. A Bevington. The SNAT2 amino acid transporter is a key requirement for insulin signalling to protein metabolism in L6 skeletal muscle cells. Kidney Research UK Fellows Day Conference, Royal College of Surgeons, London, 3 October 2006.

Kate Evans, Jeremy Brown, Edith Gomez, Terry Herbert & Alan Bevington. Glutamine restriction, a potent cachexia signal in L6 skeletal muscle cells, renders global protein synthesis resistant to insulin. NKRF Fellows' Day Conference, Belfast, 4-5 Apr 2005.

Posters

Kate Evans, Terence P. Herbert and Alan Bevington. Biochemical Society Focussed Meeting. mTOR signalling, nutrients and disease, Oxford. Amino-Acid Transporter SNAT2 Can Regulate PI3K/Akt and mTOR Independent of Amino-Acids 16 September 2008.

George Kosmadakis, Emma Clapp, Joao Viana, Jeremy Brown, Kate Evans, Alice Smith, Nicolette Bishop and Alan Bevington. Renal Association/British Renal Society Meeting, Glasgow. Inhibition of the acidosis-sensing L-Gln transporter SNAT2 impairs proliferation of LBRM-TG6 T-lymphocytes, May 13 – 16, 2008.

KF Evans, J Brown, TP Herbert and A Bevington. The acidosis-sensing amino acid transporter SNAT2 activates protein catabolism in L6 muscle cells by signalling through PI-3-kinase and protein kinase B. Kidney Research UK Fellow's Day Conference, Cambridge, 17-18 September 2007.

Bevington, K. F. Evans, J. R. Brown, S. Kauser, T. P. Herbert. L-Glutamine transporter SNAT2 controls signalling to protein synthesis through Mammalian Target of Rapamycin in skeletal muscle cells. Life Sciences 2007 Joint Biochemical Society/Physiological Society Meeting, Glasgow, 11-12 July 2007. And Renal Association Meeting, Brighton, 23 May 2007.

A Bevington, KF Evans, J Brown, Z Naseem, E Gomez, and TP Herbert. The SNAT2 amino acid transporter is a key requirement for insulin signalling to protein metabolism in L6 skeletal muscle cells. Abstracts of Diabetes UK Annual Professional Conference, Glasgow, 14-16 March 2007 published in Diabetic Medicine 24 (2007) Supplement 1, 39.

Kate Evans, Zeerak Naseem, Jeremy Brown, Edith Gomez, Terry Herbert & Alan Bevington. SNAT2 determines levels of anabolic amino acids L-Gln and L-Leu and signals to protein metabolism through mTOR in L6 muscle cells. Abstracts of the Transporters 2006 Workshop, Parma, Italy, 6-9 September 2006 published in Acta Bio Medica 77 (2006) Supplement 3, 60.

Kate Evans, Jeremy Brown, Edith Gomez, Terry Herbert & Alan Bevington. Glutamine restriction, a potent cachexia signal in L6 skeletal muscle cells, renders global protein synthesis resistant to insulin. Renal Association Meeting, Belfast, 5-8 Apr 2005.

Acknowledgements

Firstly, a big thank you to both my supervisors, Dr Alan Bevington and Dr Terry Herbert, for their excellent supervision, advice and guidance throughout the whole of my PhD. I really appreciate all the time you both spent with me practicing presentations, planning experiments, discussing results and correcting my thesis. Thank you very much, it has been a real pleasure working with you both.

Thanks are also due to Mr J. Brown for his assistance with the Northern blot and L-Gln synthetase experiments in Figures 3.1, 4.11 and 4.1, and for allowing me to show some of his unpublished data in Appendix D to explain the rationale behind some of my experiments. Also, thank you Jez for teaching me everything you know about laboratory techniques and for always having a great sense of humour.

To Dr Z. Nasim and Mr A. Amin thank you for your assistance in producing additional replicates of the HPLC experiments and Western blot experiments for figures 3.2, 4.1 and 5.15. And thank you to Dr Z. Nasim for allowing me to show some of his data in Appendix D.

Love and thanks to everyone I have worked with over the past 4 years; Emma, Jez, Iza, Tricia, Karen, Samita, Alice, Bin, George, Edith, Claire and Mike. Thank you all for your friendship, support and advice in all things. "A true **friend** is someone who thinks that you are a good egg even though they know that you are slightly cracked!"

Also, I must thank my family (old and new!) for all their support and encouragement, phone calls and love over the past four years. A special thank you to my Mum and Dad for supporting me during my first degree and for never once saying, "haven't you finished yet" during this one!

Thank you to George and Matilda, who have both helped and hindered in equal measure!

Finally I need to say a massive "I love you" and "thank you" to my lovely husband, Phil, for loving me, marrying me! for supporting me financially and emotionally in every way during my writing up year, for always encouraging me when I needed encouragement, for putting up with every possible mood I could throw at him and for never ever letting me run out of Ribena!

Abbreviations.

4EBP1	Eukaryotic initiation factor 4E binding protein 1
5' TOP	5' tract of pyrimidines
AARE	Amino acid response element
AE	Anion exchanger
AMP	Adenosine-mono-phosphate
APS	Ammonium Persulfate
ASIC	Acid sensing ion channel
ATF4	Activating transcription factor 4
ATP	Adenosine-tri-phosphate
BCAA	Branched-chain amino acid
BCKAD	Branched-chain ketoacid dehydrogenase
BSA	Bovine serum albumin
BSO	L-Buthionine-Sulfoximine
CA	Carbonic anhydrase
CD	Cytochalasin D
CHO	Chinese hamster ovary
CKD	Chronic kidney disease
CQ	Chloroquine
DEPC	Diethylpyrocarbonate
DMEM	Dulbecco's Modified Eagle's Medium
DNA	Deoxy-ribonucleic acid
DTT	Dithiothreitol
EDTA	Ethylenediaminetetraacetic acid
eEF	Eukaryotic elongation factor
EGTA	Ethylene glycol tetraacetic acid
eIF	Eukaryotic initiation factor
eRF	Eukaryotic release factor
ERK	Extracellular signal-regulated kinase
ESRD	End-stage renal disease
FBS	Foetal bovine serum
FKBP38	FK506-binding protein, 38kDa
GADD34	Growth arrest and DNA damage 34
GAG	Glycosaminoglycan
GAP	GTPase activator protein
GCN2	General control non-derepressible -2
GDP	Guanine di phosphate
GEF	Guanine nucleotide exchange factor
GFR	Glomerular filtration rate
GPCR	G-protein coupled receptor
GSH	Glutathione
GSK-3	Glycogen synthase kinase-3
GTP	Guanine tri phosphate
GβL	G-protein β-subunit-like protein
HBS	Hepes Buffered Saline
HBSS	Hank's Balanced Salts Solution
HECT	Homologous to E6-AP Carboxy Terminus
HEK	Human embryo kidney

HPLC	High Performance Liquid Chromatography
HPRG	Histidine-Proline-rich glycoprotein
HRI	Haem-regulated inhibitor
IP	Inositol phosphate
IRES	Internal ribosome entry site
IRS	Insulin receptor substrate
JNK	c-Jun N-terminal kinase
L-DON	L-Diazo-oxo-norleucine
m ⁷ G	7-methylguanosine
MAPK	Mitogen activated protein kinase
MeAIB	α-Methyl-aminoisobutyrate-
MEF	Mouse embryonic fibroblast
MEK	Mitogen activated ERK kinase
MEM	Minimum Essential Medium
Met-tRNA _i	Methionyl initiator-tRNA
MHC I	Major histocompatibility complex class I proteins
Mnk	Map kinase-interacting kinases
mRNA	Messenger ribonucleic acid
mRNP	Ribonucleoprotein complex
mTOR	Mammalian target of rapamycin
mTORC1	mTOR complex 1
mTORC2	mTOR complex 2
MuRF1	Muscle ring finger-1
NAE	Net acid excretion
NHE	Sodium hydrogen exchanger
OGR1	Ovarian cancer G-protein coupled receptor 1
p38	p38 mitogen activated protein kinase
PAT	Proton assisted transporter
PBS	Phosphate buffered saline
PBST	Phosphate buffered saline Tween
PCA	Perchloric acid
PCR	Polymerase chain reaction
PDK1	PI-dependent protein kinase 1
PERK	PKR-like endoplasmic reticulum (ER) kinase
PH domain	Pleckstrin homology domain
PI	Phosphatidylinositol
PI(3)P	Phosphatidylinositol (3) phosphate
PI3K	Phosphatidylinositol-3-kinase
PIP ₃	Phosphatidylinositol 3,4,5-tris-phosphate
PKB	Protein kinase B
PKR	RNA dependent protein kinase
PMSF	Phenylmethylsulphonyl fluoride
PP1	Protein phosphatase 1
PTB	Phosphotyrosine binding
PTEN	Phosphate and tensin homolog on chromosome 10
PUGNAc	O-(2-Acetamido-2-deoxy-D-glucopyranosylidene) amino N-phenyl carbamate
Raptor	Regulatory associated protein of mTOR
Rheb	Ras homolog enriched in brain
Rictor	Rapamycin insensitive companion of mTOR
rpS6	Ribosomal protein S6

RSK	Ribosomal S6 kinase
RTK	Receptor tyrosine kinase
RT-PCR	Reverse-transcriptase polymerase chain reaction
RVI	Regulatory Volume Increase
S6K1	S6 kinase 1
S6K2	S6 kinase 2
SDS	Sodium Dodecyl Sulphate
SDS-PAGE	Sodium Dodecyl Sulphate Polyacrylamide Gel electrophoresis
SH2	Src homology-2
SH3	Src homology-3
Shp2	Src homology-2 domain containing protein tyrosine phosphatase-2
shRNA	Small hairpin RNA
siRNA	Small interfering RNA
SNAT	Sodium dependent neutral amino acid transporter
Sos	Son of sevenless
TASK	TWIK-related acid sensitive K ⁺ channel
TBS	Tris buffered saline
TBST	Tris-buffered saline- Tween
TCA	Trichloro-acetic Acid
TCTP	Translationally controlled tumour protein
TEMED	Tetramethylethylenediamine
TLC	Thin layer chromatography
TOP	Tract of pyrimidines
TOS	TOR signalling
tRNA	Transfer-ribonucleic acid
TSC1	Tuberous sclerosis complex 1 (Hamartin)
TSC2	Tuberous sclerosis complex 2 (Tuberin)
Ub	Ubiquitin
UIC	Universal inhibitor cocktail
UPS	Ubiquitin-proteasome system
UT	Urea transporter
UTR	Untranslated region
Wt	Wild-type

Table of Contents

Abstract	ii
Publications, Presentations and Posters	iii
Acknowledgements	iv
Abbreviations	v
Contents	viii
Chapter 1: Introduction	1
1.1 The clinical problem	1
1.2 Normal kidney function	1
1.2.1 The glomerular filter	2
1.2.2 Transport processes within the nephron	7
1.3 The kidneys and pH homeostasis	10
1.4 Renal failure and progression of disease	13
1.4.1 Diabetic nephropathy	15
1.4.2 Metabolic acidosis	15
1.4.3 Basic Muscle Physiology	16
1.4.4 Cachexia	19
1.5 Sensing of metabolic acidosis	21
1.5.1 pH sensing in the plasma membrane	22
1.5.2 Plasma membrane nutrient transporters as pH sensors	26
1.5.3 Amino acid transporters	27
1.5.3.1 Theoretical considerations	27
1.5.4 The SNAT transporters	32
1.5.4.1 Expression, structure and function of SNAT transporters	32
1.5.5 Regulation of SNAT2	37
1.5.5.1 Adaptive regulation of SNAT2	37
1.5.5.1.1 The acute phase of adaptive regulation	37
1.5.5.1.2 The chronic phase of adaptive regulation	38
1.5.5.1.3 Cell recovery from amino acid starvation	39
1.5.5.2 Activity of SNAT2 is modulated by hormones.	42
1.5.5.3 The role of SNAT2 in cell volume regulation	44
1.5.5.4 The pH-sensitivity of SNAT2	46
1.5.6 System A, SNAT2 and metabolic acidosis	47
1.6 Control of protein synthesis	50
1.6.1 An overview of translation	50
1.6.1.1 Translation initiation	51
1.6.1.2 Translation elongation	54
1.6.1.3 Translation termination	56
1.6.1.4 Regulation of translation initiation	57
1.6.2 Insulin signalling pathway	57
1.6.2.1 Insulin binding triggers a signalling cascade	57
1.6.2.2 Phosphatidylinositol 3- kinase	59
1.6.2.3 PKB	62
1.6.2.4 Downstream targets of PKB.	64
1.6.2.5 Mammalian Target of Rapamycin.	64
1.6.2.5.1 mTORC1	66

1.6.2.5.2 mTORC2	66
1.6.2.5.3 mTOR as an amino acid sensor.	68
1.6.2.6 Downstream of mTOR	74
1.6.2.7 4EBP1	74
1.6.2.8 S6 Kinases	75
1.6.2.9 Phosphorylation targets of S6K1	76
1.6.2.10 Ribosomal protein S6	76
1.6.2.10.1 eIF4B, eEF2 kinase and SKAR	78
1.6.2.11 The MEK-ERK signalling pathway	79
1.6.2.11.1 ERK	80
1.6.2.12 Insulin signalling to translation initiation via eIF2	81
1.6.2.12.1 eIF2B	82
1.6.2.12.2 eIF2- α	82
1.6.2.12.3 eIF2 kinases	82
1.7 Control of proteolysis.	85
1.7.1 Coupling of Proteolysis to the Insulin/PI3K/PKB Signalling Pathway.	89
1.8 Thesis Aims	91
1.9 Summary	92
Chapter 2: Materials and methods	94
2.1 General reagents and materials	94
2.2 Cell culture	94
2.3.1 Maintenance of cell lines	95
2.3.2 Routine cell passaging	95
2.3.3 Differentiation to myotubes	96
2.3 Experimentation	96
2.4 Protein Assays	97
2.4.1 Lowry protein determination	97
2.4.2 Bio-Rad DC Assay	98
2.5 Radio-isotope techniques	98
2.5.1 Protein synthesis measurements	98
2.5.2 Proteolysis measurements	99
2.5.3 ^{14}C - MeAIB uptake measurements	101
2.6 Protein techniques	102
2.6.1 Cell Membrane Preparation	102
2.6.2 Sodium Dodecyl Sulphate Polyacrylamide Gel electrophoresis (SDS- PAGE) gels.	103
2.6.2.1 Casting the gels	103
2.6.2.2 Preparation of samples for SDS-PAGE	104
2.6.2.3 Running the gels	104
2.6.3 Western Blotting	105
2.6.3.1 Blocking the membranes	105
2.6.4 Immunostaining	106
2.7 Assay of Phosphatidylinositol-3-kinase (PI3-K) Activity	108
2.7.1 Autoradiography of radio labelled lipids	111
2.7.2 Quantifying PI(3)P by liquid scintillation counting	111
2.8 L-Glutamine Synthetase assay	113
2.9 RNA techniques	113
2.9.1 Preparation and Screening of siRNA for Silencing of SNAT2	113

2.9.2 Calcium Phosphate mediated siRNA transfection	115
2.9.2.1 Transfection of unfused myoblasts	115
2.9.2.2 Transfection of myotubes	116
2.9.3 SNAT2 mRNA determination	118
2.9.3.1 RNA isolation and RT-PCR	118
2.9.3.2 Northern Blotting	119
2.10 Measurement of intracellular amino acids and their derivatives by High Performance Liquid Chromatography (HPLC)	119
2.11 Quantification of bands in blots and autoradiographs	120
2.12 Statistical analyses	121
Chapter 3: The effect of the SNAT2 transporter on mammalian target of Rapamycin (mTOR) signalling and global protein synthesis	122
3.1 Introduction	122
3.1.1 SNAT2 inhibition depletes intracellular amino acids	123
3.2 Results	125
3.2.1 Silencing of SNAT2 gene expression	125
3.2.2 SNAT2 is a potential regulator of mTOR signalling to protein synthesis	128
3.2.3 Functional effects of SNAT2 on protein metabolism	132
3.2.3.1 Effects of pH and MeAIB	132
3.2.3.2 Effects of SNAT2 silencing	135
3.3 Discussion	137
3.3.1 SNAT2 determines L-Gln concentration in L6-G8C5 cells	137
3.3.2 Inhibition of SNAT2 depletes amino acids not transported on SNAT2	138
3.3.3 SNAT2 regulates mTOR and influences protein metabolism	138
3.3.4 SNAT2 inhibition mimics the effects of acidosis in vivo	139
Chapter 4: The effect of the SNAT2 transporter on phosphatidylinositol-3-kinase (PI3K) signalling and global proteolysis.	141
4.1 Introduction	141
4.1.1 Increased proteolysis arising from insulin resistance during acidosis can be modelled in vitro using L6-G8C5 myotubes	142
4.2 Results	144
4.2.1 Time course of intracellular L-Gln depletion by SNAT2 inhibition	144
4.2.2 Role of SNAT2 up-regulation and L-Gln synthetase in restoring L-Gln levels during acidosis	144
4.2.3 Proteolysis maintains intracellular L-Gln levels during acidosis	147
4.2.4 Increased proteolysis in response to acid involves SNAT2	152
4.2.5 Involvement of mTOR and PI3K signalling in acid-induced proteolysis	152
4.2.6 Mechanism of SNAT2 effects on PI3K and PKB	157
4.2.7 SNAT2 effects on other insulin signals	161
4.3 Discussion	161

4.3.1 SNAT2 regulates mTOR, PI3K, PKB and proteolysis	161
4.3.2 Linkage between protein synthesis and degradation during acidosis	162
4.3.3 SNAT2 signalling to proteolysis through amino acid depletion	163
4.3.4 SNAT2 signalling independent of amino acid transport	164
4.3.5 Mechanism(s) of SNAT2 coupling to PI3K	166
4.3.6 Implications for SNAT2 signals to mTOR and protein synthesis	166
Chapter 5: The role of free amino acids in the effect of SNAT2 on global protein synthesis.	167
5.1 Introduction	167
5.1.1 Pathways of L-Gln metabolism	168
5.1.2 Previous work on the metabolic effects of L-Gln starvation in L6-G8C5 myotubes	169
5.2 Results	171
5.2.1 Role of mTOR signalling in the L-Gln deprivation effect	176
5.2.2 Phosphorylation of eIF2 α	177
5.2.3 Relevance of L-Gln deprivation effects to SNAT2	187
5.3 Discussion	192
5.3.1 L-Gln restriction is an imperfect model for the effect of SNAT2 inhibition on protein synthesis	192
5.3.2 L-Gln restriction is a metabolic stress	193
5.3.3 Partial depletion of L-Gln and branched chain amino acids fails to mimic the effect of SNAT2 inhibition	194
Chapter 6: General Discussion and Future Directions	196
6.1 SNAT2 Coupling to Amino Acid Dependent Proteins	196
6.2 SNAT2 Coupling to Proteins Independent of Amino Acids	200
6.3 Temporal Relationships	201
6.4 Summary	202
Appendix A: DMEM and MEM Components	203
Appendix B: Buffers and Reagents	206
Appendix C: Buffers and Reagents used in PI3K assay	208
Appendix D: Specimen Calculation of Global Proteolysis Rate of Cultures of L6-G8C5 Myotubes	209
Appendix E: Supporting Data	211
References	219

Chapter 1: Introduction

1.1 The clinical problem

The kidneys work to excrete waste products from the blood into the urine and to resorb water and solutes back into the blood in order to allow all other bodily organs to function in a normal extracellular environment. These processes include the excretion of acid and resorption of bicarbonate. Consequently the disruption of this process in patients suffering from end-stage renal failure frequently leads to metabolic acidosis which can cause fatigue, growth retardation in children, (1), inflammation, cardiac disease, bone disease and cachexia, (2).

1.2 Normal kidney function

The kidneys are situated in the region of the lower back. Each kidney is approximately 12cm long and weighs around 150g. Despite making up less than 0.5% of total body weight the kidneys receive approximately 25% of the cardiac output meaning that the kidneys filter over 1L of blood/min, (3).

Each kidney has two distinct regions; the outer cortex and the darker inner medulla, (Figure 1.1). Within the medulla lie the renal pyramids, at the point of which there is located a region known as the papilla where urine is collected from the nephron and drained into the minor calyces, then into the major calyces, and eventually into the pelvis which leads to the ureter, where urine is drained into the bladder, (3).

The functional units of the kidney which produce the urine that drains into the papilla are called the nephrons, (Figure 1.2). There are two different types of nephron; the cortical nephrons, which are situated in the cortex and do not enter the medulla at all or only protrude a short way into it, and the juxtamedullary nephrons which protrude deeply into the medulla, (3). Nephrons are made up of several distinct regions; Bowman's capsule and the glomerulus, the proximal tubule, the loop of Henle, the distal tubule and the collecting duct. Blood flowing into the kidneys via the renal artery passes along the afferent arteriole and then into a series of capillaries, that are collectively known as the glomerulus, (3), which is situated in Bowman's capsule, (Figure 1.2).

1.2.1 The glomerular filter

The capillaries of the glomerulus are supported on one side by the Mesangium allowing blood flowing through the glomerular capillaries to be unidirectionally filtered into the nephrons in order to facilitate primary urine production. The glomerular filtration unit consists of three layers; the fenestrated endothelial cells of the capillary wall, the glomerular basement membrane and the epithelial cell layer (or podocytes), which make up the filtration surface partly surrounded by Bowman's capsule, (4), (Figure 1.3). Small positively charged molecules pass more easily through the glomerular filter than large negatively charged molecules. This is owing to the size restriction determined by the fenestrations in the endothelial cells and the slit-diaphragm, (see below), and the negatively charged endothelium and glomerular basement membrane, (as a result of the presence of negatively

charged proteoglycans), (5). Although both the capillary endothelial cells and the glomerular basement membrane are able to filter solutes dependent on their size and charge, the main filtration barrier is now thought to be the podocyte cell layer, (4,5). Podocytes are specialised epithelial cells that have large cell bodies with elongated projections called trabeculae, from which smaller foot processes called pedicels are projected. These pedicels interdigitate to encircle the capillaries, leaving small gaps called filtration slits in which the main filtration barrier is thought to arise from a complex of junction proteins (e.g. nephrin, (6)) which are known collectively as the slit diaphragm. The slit diaphragm prevents any molecules of approximately 70kDa or greater passing through into Bowman's space and the tubular lumen. As each of the filtration layers is negatively charged, proteins smaller than 70kDa, such as albumin, may be largely prevented from passing through the filter as they are repelled, but some positively charged molecules with a molecular weight greater than 70kDa may pass through, (5). Therefore at this stage the glomerular filtrate still contains some low molecular weight proteins, such as insulin, and contains small molecules and ions, such as; glucose, amino acids, urea, sodium and potassium, in concentrations almost equal to those in blood plasma. Therefore further processing of the glomerular filtrate must occur before primary urine in Bowman's space is drained into the papilla. After passing through Bowman's space the glomerular filtrate, or the tubular fluid, as it will be referred to from this point onwards, passes into the proximal tubule. The small proteins which are able to pass through the filter in a healthy kidney are efficiently taken up in the proximal tubular epithelial cells by receptor-mediated endocytosis via the megalin-cubulin complex. They are

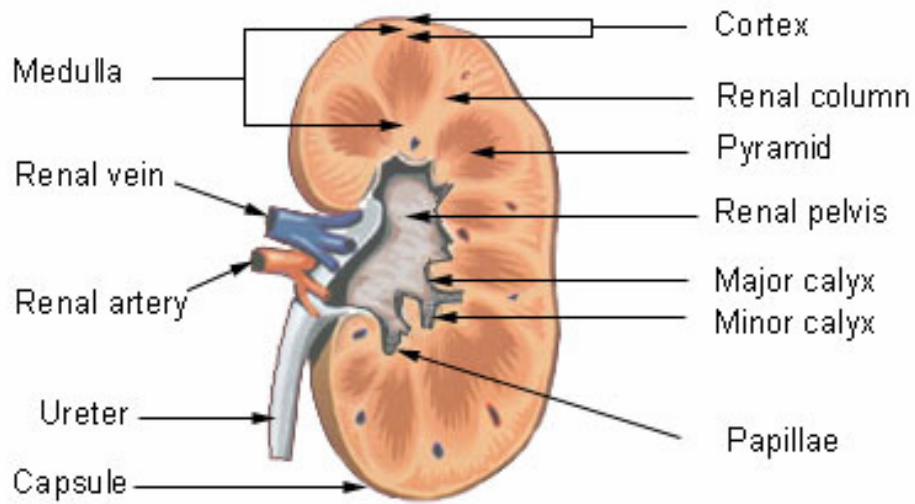


Figure 1.1: Frontal section through the kidney.

This figure shows a frontal section through the kidney with all major components, as discussed in section 1.2 in the text, labelled for clarity.

Copied from Wikimedia Commons free access figures.
http://commons.wikimedia.org/wiki/Image:Illu_kidney2.jpg last accessed 27.9.08.

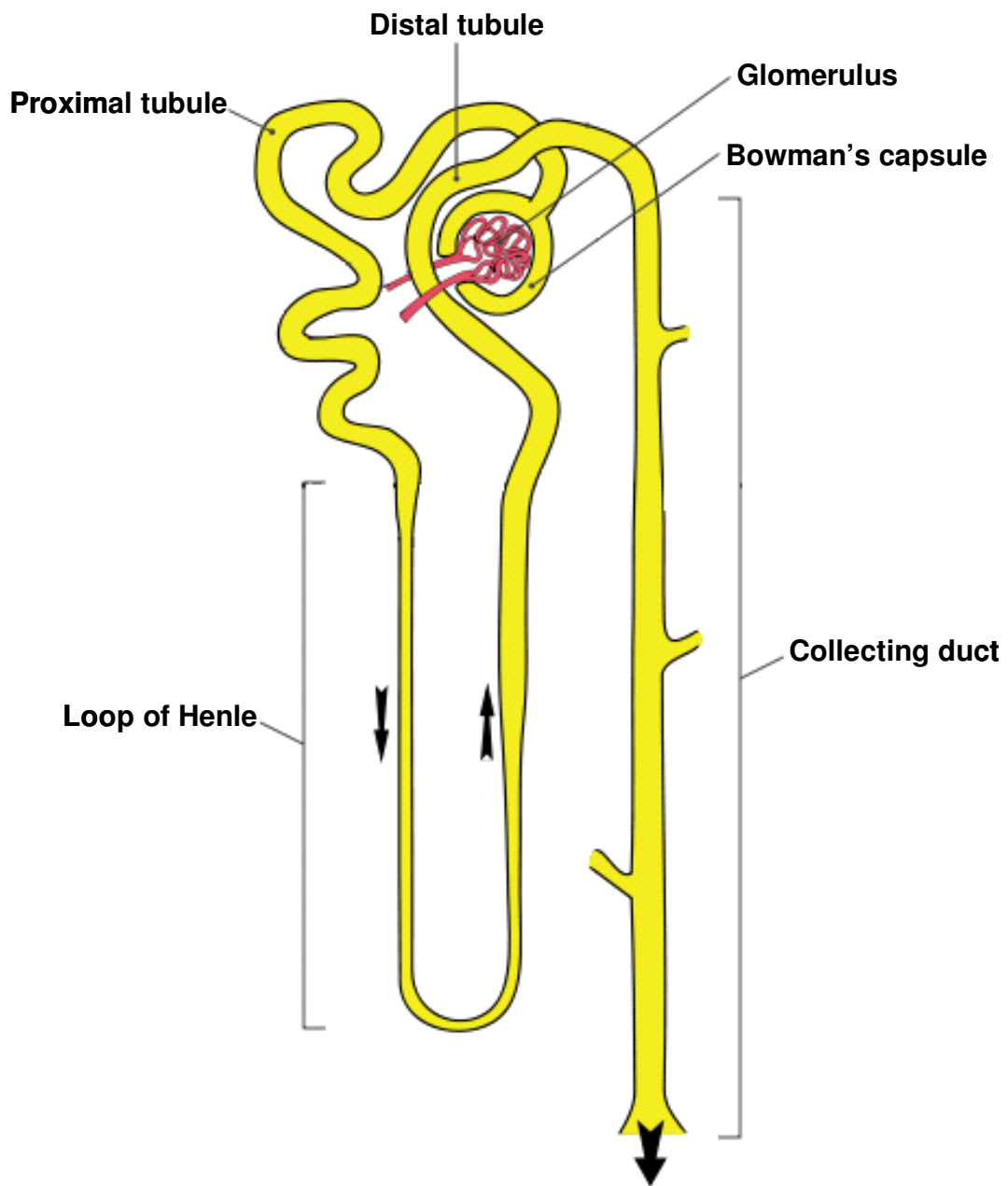


Figure 1.2: A nephron

This figure depicts a nephron and shows the distinct functional regions as discussed in the text in section 1.2. The situation of the glomerulus within Bowman's capsule is also shown.

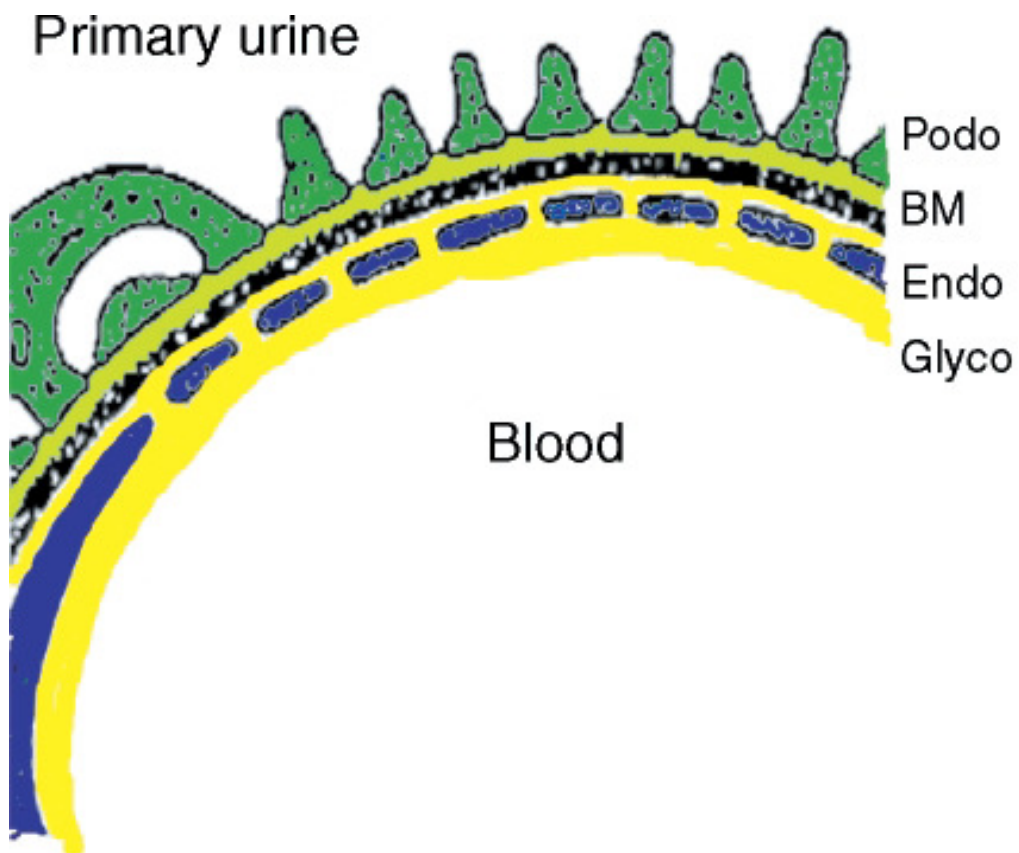


Figure 1.3: The filtration unit

Schematic drawing of the glomerulus and its four major layers, (4).

This figure shows the filtration slits in the podocyte layer (Podo), the glomerular basement membrane (BM), and the endothelium cell wall of the capillaries (Endo) and the endothelial cell surface layer (Glycocalyx), (which are referred to collectively as the endothelial cell layer in the text). Described in the text in section 1.2.1

Diagram taken from Haraldsson, B. and Sörensson, J. (2004), (4).

then degraded in the lysosomes before being released back into the circulation as amino acids, (4). Therefore appearance of these small proteins in the urine is referred to as tubular proteinuria, as they result from damage to the tubular epithelia cells and not to the glomerular filter, (5). The presence of large proteins in the urine is referred to as glomerular proteinuria as an indicator of glomerular damage and inefficient protein filtration, (5).

1.2.2 Transport processes within the nephron

In the tubules the two processes of resorption, (whereby solutes and water are transported into the cells of the tubular walls and then into the blood), and secretion, (whereby solutes are transported from the cells of the tubular wall into the tubular fluid for excretion), are very important as they allow the tubules to control the volume and composition of the urine and therefore the volume, osmolality, composition and pH of the extracellular fluid, (3). The proximal tubule consists of an initial convoluted segment followed by a straight segment which goes down into the medulla and eventually becomes the loop of Henle. Virtually all of the glucose and amino acids and about 67%, (3), of the filtered water, Na^+ , Cl^- , K^+ and other solutes are reabsorbed from the proximal tubular lumen in the initial convoluted segment. In this region of the tubule, Na^+ enters the cells from the tubule either via a $\text{Na}^+\text{-H}^+$ antiporter, (using intracellular H^+ which is in ready supply owing to the production of H^+ and HCO_3^- from CO_2 and H_2O , catalysed by carbonic anhydrase), or via symporter mechanisms whereby Na^+ is transported into the cell with glucose, amino acids, Pi, or lactate, (3). The $\text{Na}^+\text{-K}^+\text{-ATPase}$ which is situated in the basolateral membrane removes Na^+ from the tubular epithelial cells into the

intercellular space in exchange for K^+ . The operation of this transporter allows HCO_3^- , glucose and other organic solutes to leave the cell via passive diffusion and leads to water passing from the tubular fluid into the blood via osmosis. This movement of water leads to an increased concentration of Cl^- within the proximal tubule, (3). This is removed in the second part of the tubule where a Cl^- -anion antiporter in the cell membrane facilitates entry of Cl^- into the cell at the apical membrane whilst a Cl^-K^+ symport allows Cl^- removal at the basolateral membrane. In addition to this, the high Cl^- levels in the tubule mean that NaCl can passively diffuse through the tight junctions between the cells that make up the tubule wall. This is known as paracellular transport. Transport of NaCl is evenly split between the cellular and paracellular routes and leads to further movement of water from the tubules into the blood, (3).

As the tubular fluid proceeds down into the loop of Henle, the majority of resorption of water and solutes back into the blood has already taken place. Any resorption of solutes in the loop of Henle occurs in the thick ascending limb, and water resorption occurs in the thin descending limb as the thin ascending limb is impermeable to water and has a low resorptive capacity, (3). As in the second half of the proximal tubule, cationic solute transport in the loop of Henle is evenly split between cellular and paracellular transport. This is due to the positive electrical potential of the tubular fluid, relative to the blood. Cellular transport is again mediated in part by the Na^+H^+ antiporter on the apical membrane and the $Na^+K^+ATPase$ on the basolateral membrane, but, in addition to this, there exists, on the apical membrane, a $Na^+2Cl^-K^+$

symport, and separate Cl^- , K^+ and HCO_3^- transporters on the basolateral membrane, (3).

The final sections of the nephron are the distal tubule and the collecting duct which resorb approximately 7% of total NaCl and secrete variable levels of K^+ and H^+ . The early section of the distal tubule is impermeable to water, but between 8-17% of the filtered water is resorbed in the late distal tubule and collecting duct, dependent on the plasma levels of the anti-diuretic hormone (ADH)/vasopressin which increases the permeability of the collecting duct to water, (3). The late distal tubule and collecting duct both consist of two different types of cells called principal cells and intercalated cells. In the principal cells the resorption and secretion of solutes is again driven by the $\text{Na}^+\text{K}^+\text{ATPase}$ in the basolateral membrane. The activity of this transporter leads to high levels of K^+ in the cells so K^+ is excreted into the tubular fluid, and as Na^+ is resorbed this leads to a negative electrical potential in the tubular lumen which drives Cl^- resorption via paracellular pathways, (3). The intercalated cells resorb some of the K^+ that is secreted by the principal cells; either by coupling to secretion of H^+ into the tubular fluid, or by resorption of HCO_3^- into the blood, making these cells very important in the regulation of acid-base balance (see Section 1.3).

It is by these mechanisms of solute and water resorption in the nephrons that the kidneys are able to generate 180L of filtrate per day but excrete less than 1% of the filtered water and solutes in the urine, (3).

1.3 The kidneys and pH homeostasis

In addition to ensuring adequate resorption of water and solutes, the kidneys also maintain the pH of extracellular fluid. In arterial blood this is usually stated to fall within a tight range of 7.35-7.45. However, even in healthy individuals, this pH can be affected by several factors, most notably end products of cellular metabolism, and acid and alkali ingested from the diet or generated from dietary components. On a conventional Western diet, the high intake of animal protein, rich in sulphur amino acids, leading ultimately to generation of sulphuric acid, (7), is thought to be a significant factor in depressing the extracellular pH even in individuals with healthy renal function, (8). A significant daily acid load (~40-70mEq of H⁺ per day, (8)) must therefore be excreted in order for there to be stringent control of pH. The lungs and, more controversially, the liver also play a role in pH homeostasis, but here the discussion will focus on the dominant role played by the kidneys and on non-volatile acid (i.e. not carbonic acid, which is a volatile acid owing to its ability to generate CO₂ after dehydration).

Acids do not circulate the body as free acid but are immediately buffered to produce salts (principally sodium salts), a process which consumes NaHCO₃⁻. This is rectified by the kidneys excreting an amount of acid equal to the acid produced (in the form of sodium and ammonium salts) and reabsorbing much of the filtered HCO₃⁻. Net acid excretion (NAE) is the rate of excretion of titratable acid, excreted as salts of acids e.g. sodium salts, and NH₄⁺ minus the HCO₃⁻ lost in urine. HCO₃⁻ resorption and acid secretion occurs in the

nephrons and, as with water and solute reabsorption, the majority of the resorption occurs in the proximal tubule, (3).

Within the proximal tubular cells the enzyme Carbonic Anhydrase (CA) is involved in solute resorption and HCO_3^- resorption. CA catalyses the hydration of CO_2 to carbonic acid (H_2CO_3), which is in equilibrium with H^+ and HCO_3^- . H^+ is secreted into the tubular fluid, via a H^+ -ATPase and a Na^+ - H^+ antiporter, where it combines with intra-luminal HCO_3^- to form carbonic acid, and the residual intracellular HCO_3^- is resorbed into the blood mainly via a 1Na^+ - 3HCO_3^- symporter, (3), CA is also present on the tubular luminal cell surface where it catalyses the dehydration of H_2CO_3 in the tubular fluid to produce water and CO_2 . The latter can then diffuse back into the proximal tubular cells to act as a substrate for intracellular CA and complete the cycle, (3). The resorption mechanisms in the ascending loop of Henle are the same, but there is no CA present in the tubular luminal membrane, presumably because over 80% of HCO_3^- resorption has already taken place by this stage, (3). In the collecting duct the intercalated cells also contribute to acid-base balance as described later.

As can be seen from the definition of NAE above, HCO_3^- resorption and excretion of titratable acids alone does not replenish HCO_3^- lost during the buffering of acids, so more HCO_3^- must be produced. Some HCO_3^- is produced in the CA catalysed hydration of CO_2 , but in order to achieve overall acid-base balance the kidneys produce ammonia, (which combines with up to two thirds of the acid excreted by the kidneys under normal conditions), in the

process of ammoniogenesis. Renal ammoniogenesis occurs mainly in the proximal tubular cells and results in bicarbonate and ammonium production due to L-Gln catabolism, (9), as shown below:



The oxidation of the divalent anion α -keto-glutarate then leads to production of 2HCO_3^- , (9,10). Ammoniogenesis can be regulated depending on acid-base balance because the enzymes glutaminase and glutamate dehydrogenase, which catalyse the first and second stages in NH_4^+ production respectively, can be up-regulated by increased gene expression in acidosis, (9). The increased production of both ammonium and bicarbonate in situations of extreme acid load helps the kidneys to regain pH homeostasis as the bicarbonate is returned to the blood to replace bicarbonate used up by the acid load and ammonium is excreted in the urine to an even greater extent, (9). Initially the NH_4^+ is secreted from the proximal tubular cells via a $\text{Na}^+\text{-H}^+$ antiporter where NH_4^+ takes the place of H^+ , (9). A significant proportion of the NH_4^+ secreted in the proximal tubule is then resorbed into the blood from the thick ascending limb of the loop of Henle where NH_4^+ substitutes for K^+ on the $\text{Na}^+1\text{K}^+2\text{Cl}^-$ symporter, the activity of both these transporters may be increased in acidosis due to increased gene expression, (9). In addition to this, NH_4^+ is resorbed via a paracellular pathway due to the positive electrical potential of the tubular lumen relative to the epithelial cell layer, (3). Due to this resorption of NH_4^+ into the blood there is an accumulation of NH_4^+ and NH_3 in the medullary interstitium. As the cells of the collecting duct are permeable to NH_3 , NH_3 diffuses into the tubular fluid from the blood. In the

lumen of the collecting duct the tubular fluid is at its most acidic, with a pH as low as 4, meaning that once NH_3 has entered the tubular fluid it is protonated to produce NH_4^+ . The collecting duct is not permeable to NH_4^+ so that it is trapped in the tubular fluid and is therefore excreted in the urine, (9). By these means acid and base balance are regulated to maintain the arterial blood pH in the tight range of 7.35-7.45 in a healthy individual.

1.4 Renal failure and progression of disease

The term acute kidney failure is used to describe cases where renal failure occurs rapidly over days or even hours leading to a sudden decrease in glomerular filtration rate. This is usually caused by trauma or injury to the kidneys, often involving ischemia and acute tubular necrosis, (11). It can often be reversed if the cause of the kidney failure is treated rapidly but, in spite of strenuous efforts by nephrologists to improve therapy, mortality from acute kidney injury is still high, (12).

In contrast chronic kidney disease, (CKD), usually progresses gradually and can be separated into five stages of progression (CKD1-5), (13), see Table 1.1, according to the glomerular filtration rate (GFR), which is a measurement of renal function, i.e. the volume of filtrate generated per minute, (2). Patients who have progressed to stage 5 CKD, end-stage renal disease (ESRD), have a decreased renal mass, are highly uraemic and require regular dialysis to facilitate the removal of systemic waste products and partly restore normal acid-base balance, (2). In ESRD the GFR will have decreased to lower than

20% of normal, (2), and will usually decrease further as the disease progresses.

Table 1.1: Stages of CKD.

CKD stage	Description	GFR (ml/min/1.73m ²)
1	Evidence of kidney damage, such as proteinuria. GFR may be normal or slightly raised.*	>90
2	Loss of renal reserve [#] . Mildly decreased GFR*.	60-89
3	Renal insufficiency [#] . Moderately decreased GFR*.	30-59
4	Chronic renal failure [#] . Severely decreased GFR*.	15-29
5	End-stage renal disease [#] . Chronically decreased GFR.	<15

Adapted from (13) *(13) [#](14).

One of the first signs of CKD is proteinuria, where trace amounts of plasma protein, especially albumin, can be detected in the urine, (5), suggesting that the glomerular filter, discussed in Section 1.2, is no longer functioning properly. Often kidney disease is not diagnosed until this stage, (6). Glomerular damage can occur as a result of; diseases such as diabetes mellitus (diabetic nephropathy), as discussed below, hypertension, or renal diseases such as glomerulonephritis, (5). The glomerular damage may have occurred some time before proteinuria becomes apparent as there are many more nephrons in the kidneys than are required to maintain normal kidney function. Initially the remaining functioning units are able to maintain a normal GFR, but as the loss of renal reserve puts extra strain on the nephrons further glomerular damage occurs, leading to renal insufficiency and the resultant proteinuria.

In addition to being a valuable diagnostic marker of kidney disease, proteinuria may also contribute to progression of the disease. Because of the excess of proteins passing through the glomerular barrier, the epithelial cells of the proximal tubule are unable to cope with the increased need for protein re-absorption and this is thought to be an important contributor to tubulo-interstitial disease, (5,15,16).

1.4.1 Diabetic nephropathy

Diabetes Mellitus is the most common of a number of risk factors which predispose patients to developing chronic kidney disease, (17). As many as 60% of ESRD patients suffer from diabetes, (18). Contrary to what was formerly believed, Type II as well as Type I diabetes also strongly predisposes patients to diabetic nephropathy, (18). In diabetic nephropathy initial damage to the glomerulus is caused by hyper-filtration occurring during hyperglycaemia which leads to a state of glomerular capillary hypertension which further damages the kidneys leading initially to microalbuminuria, (5), and ultimately to progression to ESRD as detailed above. Patients suffering from diabetic nephropathy have a decreased chance of survival compared to non-diabetic ESRD patients of the same age, (14) and, of relevance to this thesis, cachexia is particularly severe in these patients when compared with the rest of the CKD population, (18).

1.4.2 Metabolic acidosis

As chronic disease progresses and glomerular filtration declines, a fall in plasma bicarbonate concentration becomes apparent, falling from the normal

range of ~24-30mEq/L down to 12-22mEq/L. This decrease in bicarbonate concentration is the most readily measured manifestation of metabolic acidosis, an acid-base disorder which affects pre-dialysis CKD patients, (CKD4), but is evident to a much greater extent in ESRD patients undergoing dialysis, (1), because dialysis techniques are usually unable to completely correct the systemic base deficit, (19). Metabolic acidosis occurs in CKD and ESRD patients because of a decrease in bicarbonate resorption and a decrease in ammonium and bicarbonate production arising from the marked decrease of functional units within the kidneys. A net decrease in excretion of hydrogen ions occurs once the GFR has decreased below 15ml/min, (2). This inability to excrete non-volatile acids is called increased anion gap acidosis (1). Metabolic acidosis may cause further progression of kidney disease, (2), but not all studies have confirmed this, (20). More reproducibly metabolic acidosis also adversely affects the cardiovascular system, (21), and bone composition, due to mobilisation of minerals from bones, (2), and leads to wasting of the lean body mass (see Section 1.4.4). Cardiac disease is a major cause of mortality in CKD and ESRD patients, with many stage 3 and 4 CKD patients dying from cardiovascular disease before progressing to ESRD, (21). The exact mechanisms by which chronic metabolic acidosis in ESRD leads to impairment of cardiac function are not yet clear, (2).

1.4.3 Basic Muscle Physiology

Skeletal muscle makes up just under half of the total human body mass, (22), with the function of converting chemical energy into kinetic energy through the production of muscle contractions. Each skeletal muscle is made up of a

massive number of individual multinucleated cells called muscle fibers, and in turn, each of these fibers is then made up of a large number of myofibrils consisting of contractile units known as sarcomeres, containing overlapping thick and thin myofilaments, (22). The edge of each sarcomere is defined by two Z-lines which have thin myofilaments anchored to them on both sides, meaning that sarcomeres, arranged in parallel, have overlapping Z-lines (Z-lines on adjacent sarcomeres are linked together by intermediate filaments, (3)). The thin myofilaments are made up of the contractile protein, actin, and two other proteins called troponin and tropomyosin. The thick myofilaments are arranged in the centre of each sarcomere, attached to the Z-lines only by titin filaments, and are made up of bundles of 300-400 molecules of the contractile protein myosin, (22). Each myosin molecule consists of two light chains and two heavy chains, (22). The carboxy-terminal ends of the heavy chains form coils and bundle together to form the backbone of the thick myofilaments, with the remaining section of the heavy chains sticking out from the thick myofilament towards the Z-lines. The light chains of myosin then connect to the protruding sections of the myosin heavy chain and form the myosin head or cross-bridge which binds to the thin myofilament, (22). It has been determined that the myosin light chain contains two subfragments called S1 and S2, and that the S1 fragment contains three functional domains; the N-terminal domain, containing both the actin binding site and the active site for ATP hydrolysis; the neck domain, which allows the myosin head to bend once bound to actin, thus forcing the thin myofilaments in towards the centre of the sarcomere, and the converter domain which lies between the N-terminal domain and the neck domain and allows the production of force, due

to a conformational change in S1 occurring once it is bound to actin, (22). The combined action of these functional domains allows cross bridge cycling, and therefore muscle contraction to occur. The initial step in this cycle is the binding of ATP to the myosin light chain N-terminal domain, and then its subsequent hydrolysis to ADP + Pi, producing the myosin-ADP-Pi complex which has a high affinity for actin. Rapid binding of the myosin-ADP-Pi complex to the thin myofilament then occurs, producing a high energy actin-myosin complex and pivoting of the neck domain, (22), which draws the thin myofilament in towards the centre of the sarcomere, resulting in shortening of the sarcomere as the two Z-lines move closer together. The shortening of each individual sarcomere only has a tiny effect but the shortening of all of the parallel and adjacent sarcomeres combined produces a large overall effect on muscle contraction, (3). Once the thin myofilament has attached to the myosin head ADP and Pi are released causing a conformational change in the myosin head and a low energy actin-myosin complex. Myosin then once again binds an ATP molecule resulting in formation of an actin-myosin-ATP complex. As the cross-bridge has low affinity for the thin myofilament in this conformation the two become dissociated. Upon hydrolysis of ATP to produce ADP+ Pi the cycle repeats itself with one ATP molecule being utilised per cycle, (3). In a relaxed state the cross-bridges are detached from the thin myofilament and are only able to bind to the thin myofilaments in a Ca²⁺ regulated manner. The release of Ca²⁺ occurs as a result of an action potential, which causes release of acetylcholine from neurons and ultimately mobilisation of Ca²⁺ from the sarcoplasmic reticulum. Troponin, in the thin myofilaments, contains Ca²⁺ binding sites, which, when occupied, result in the

“turning on” of the thin myofilaments allowing cross-head cycling to occur as described above, (3).

1.4.4 Cachexia

The literal meaning of cachexia in Greek is “poor condition”, (23). Cachexia is defined as a wasting illness in which wasting of lean tissue (particularly skeletal muscle) predominates, (24). Cachexia occurs in many chronic illnesses such as cancer, heart failure, AIDS and renal failure, (23). Cachexia in CKD patients is associated with increased mortality, (18,23), higher incidence of hospitalisation, (18), and a decrease in their quality of life, (25). It is therefore important that the underlying mechanisms of cachexia, (which may differ depending on the primary disease), are understood, (25). The present study will only focus on the mechanisms leading to cachexia which are most relevant to uraemic metabolic acidosis.

Cachexia should not be confused with anorexia (anorexia being defined as a decreased sensation of appetite), although both can occur in CKD patients, with anorexia being a contributing factor to cachexia in patients and animals with metabolic acidosis, (26). It has been suggested that anorexia in CKD patients is the result of a defect, caused by CKD, in the neuroendocrine pathways which regulate food intake, (27). A normal response to food deprivation is a decrease in protein catabolism, (24), but in acidosis that metabolic response is impaired and protein catabolism and increased branched-chain amino acid (BCAA) oxidation occur, (24). These changes are also observed in CKD patients with uraemic metabolic acidosis, (28), and can

be modelled in cultured L6 rat skeletal muscle cells and cultured BC3H1 myocytes *in vitro* by exposing the cells to acidified culture medium, (29-31). Studies in rats and isolated muscle have shown that the increase in oxidation of BCAAs is the result of an increase in the activity of the regulatory enzyme, branched-chain ketoacid dehydrogenase (BCKAD), (19).

In healthy humans the daily protein turnover rate is approximately 3.5-4.5g of protein/kg per day, (32). Proteolysis and protein synthesis within a given tissue must therefore be tightly balanced, because even a slight imbalance through decreased protein synthesis or increased proteolysis, or both, will ultimately lead to cachexia, (24).

It is known that metabolic acidosis causes negative protein balance, (19,33), which indicates that increased proteolysis and/or decreased protein synthesis is occurring. A study by May et al, (34), using partially nephrectomised rats as a model of CKD, provided the first evidence that metabolic acidosis increases proteolysis in uraemia. It was observed that proteolysis in the uraemic rats was increased and could be corrected by oral bicarbonate administration, implying that uraemic metabolic acidosis was the dominant contributor to the problem. The catabolic pathway was subsequently identified as the ATP-dependent ubiquitin-proteasome pathway which will be discussed in more detail in Section 1.7. Interestingly it was also found that protein synthesis rates in these rats were not altered, however more recent studies have shown that, at least initially, protein synthesis is decreased by metabolic acidosis. *In vitro* L6 rat skeletal muscle cells incubated in medium at a low pH of 7.1

showed a significant decrease in protein synthesis when compared to a pH 7.4 control, (35). The same was seen in BC3H1 myocytes, (36). *In vivo* acute metabolic acidosis has also been shown to decrease albumin synthesis, (33), and the fractional synthesis rate of muscle protein, (37), in human subjects.

1.5 Sensing of metabolic acidosis

An obvious mechanism for sensing of acidosis by skeletal muscle cells would be for an extracellular decrease in pH to lead to a corresponding decrease in intracellular pH which might then affect cell metabolism, leading to the observed catabolic state. It has been determined however that, at least in skeletal muscle cells in the resting state, this is not the case. Intracellular pH in cultured L6 cells was not found to decrease significantly in the presence of an extracellular pH of 7.1, when measured with the fluorescent cytosolic pH indicator BCECF, (31). Measurements of sarcosolic pH in resting rat skeletal muscle *in vivo* by ³¹P nuclear magnetic resonance spectroscopy also failed to detect a significant change in response to systemic metabolic acidosis, (38), and, by the same technique, the resting sarcosolic pH in uraemic patients was found to be similar to that in healthy individuals, (39), the only abnormality being that the profound decrease in sarcosolic pH observed in healthy individuals during exercise was more marked in uraemic patients, (39). As the marked fall in sarcosolic pH in healthy subjects during exercise has not been reported to trigger significant protein wasting, it seems unlikely that intracellular pH is the main signal through which muscle cells sense metabolic acidosis.

It has also been suggested that metabolic acidosis may be sensed indirectly *in vivo*, for example through the rise in the circulating glucocorticoid concentration that occurs during acidosis, (40). However, in moderate metabolic acidosis like that observed in CKD patients, the rise in glucocorticoid is probably too small to account for the protein wasting state, (41).

1.5.1 pH sensing in the plasma membrane

This leads to the possibility that the decrease in extracellular pH is sensed at the plasma membrane. A number of proteins expressed in the plasma membrane of mammalian cells are known to be responsive to physiologically relevant changes in extracellular and/or intracellular pH. These include Sodium-Hydrogen Exchangers (NHEs), potassium channels (e.g. TASK), proton-sensing G-protein coupled receptors (OGR1 and GPR4), the AE2/Slc4A2 anion exchanger, the Histidine-Proline-rich Glycoprotein (HPRG), the urea transporter UT-A /Slc14A2, Acid Sensing Ion Channels (ASICs), and the pH-sensitive System A and System N neutral amino acid transporters of the Slc38 gene family (to be discussed later in Section 1.5.4).

The TWIK -related acid sensitive K⁺ channel (TASK), (43), sub-family belong to the tandem pore domain acid-sensitive K⁺ channel, (44), family of K⁺ channels which allow K⁺ leakage to occur and therefore play a role in setting resting membrane potential, (42). To date there are thought to be five members of the TASK family (TASK1-5), (42-45), which are widely expressed and sensitive to deviations from physiologically normal extracellular pH.

Table 1.2: Acid-sensitive proteins

pH sensitive proteins expressed at the plasma membrane	Relevant literature
TWIK-related acid sensitive K ⁺ channels, (TASKs).	Discussed in (42-45).
G-protein-coupled receptors OGR1 and GPR4.	Discussed in (46).
Anion exchanger 2 (AE2)	Discussed in (47,48).
Histidine - Proline – rich glycoprotein	Discussed in (49,50).
Urea transporter UT-A	Discussed in (51).
Na ⁺ -H ⁺ exchanger 3 (NHE3)	Discussed in (52).
Acid sensing ion channels (ASICs)	Discussed in (53-55).

TASK-1 and TASK-3 are most notably sensitive to acid inhibition as protonation of a conserved L-His residue (H⁹⁸) leads to channel closure in both isoforms, (45). The physiological implications of this pH sensitivity are unclear although TASK isoforms located in the brain, such as TASK-3, would undoubtedly be inhibited in ischemia and seizure when the pH falls to around pH 6, (43,44).

There has also been evidence to suggest that some G-protein-coupled receptors (GPCRs) may be sensitive to extracellular pH changes. In the case of the closely related GPCRs; ovarian cancer G-protein-coupled receptor 1 (OGR1) and GPR4, both neutral and slightly acidic extracellular environments appear to increase formation of the second messengers inositol phosphate (IP) and cyclic AMP, with IP formation decreasing at pHs lower than 6.5, (46). The pH sensitivity of these two receptors is thought to arise from conserved histidine clusters at the extracellular surface of the GPCRs that are involved in hydrogen bonding, (46). Both of these GPCRs are widely expressed but

the presence of OGR1 in osteoblasts and osteocytes may suggest a role for OGR1 in mediating acidosis effects in bones. (46).

Members of the Slc4 gene family: anion exchanger (AE) 1, AE2 and AE3, are widely expressed Na^+ -independent Cl^- - HCO_3^- exchangers that regulate intracellular volume, Cl^- concentrations and pH, (48). As might be expected, AE2 is sensitive to both intracellular and extracellular proton inhibition with its activity at pH 6.8 being decreased by up to 90% relative to that at pH 7.4. However AE1 is not inhibited in milder acidosis as it must be able to retain its function in the acidic environment of the respiratory tissues, (47).

HPRG is a plasma membrane glycoprotein which contains a unique His-Pro rich domain that acts as a pH sensor due to the protonation of its Histidine side chains that occurs at low pH, (50). Histidine protonation at a pH of approximately 6.8 produces a positively charged HPRG that binds strongly to negatively charged glycosaminoglycans (GAGs), (50). As HPRG is able to interact with a large number of proteins a clear picture of its function has not yet been determined, but its ability to bind simultaneously to GAG surfaces and to plasminogen, suggests a role for HPRG in the regulation of fibrinolysis, (49). When plasminogen is complexed with HPRG on a GAG surface its activator, tissue plasminogen activator, is better able to convert plasminogen to plasmin, a key fibrinolysis enzyme, (49).

It is well documented that acidosis occurs in damaged, inflamed or ischaemic tissue, (53,55). The acid-sensing ion channel (ASIC) family of proton-gated

cation ($\text{Na}^+/\text{Ca}^{2+}$) channels have been implicated in transmitting the sensation of pain that accompanies tissue acidosis, (53,54). This is because ASIC1, ASIC2 and ASIC3 are widely expressed throughout the sensory neurons and CNS, (53). They are all pH sensitive, with low pH (and resultant multi-site protonation, (53)) increasing transporter activity, (55).

The four UT-A urea transporters; UT-A1, UT-A2, UT-A3 and UT-A4 are all expressed in the kidneys and two UT-A isoforms have also been found to be expressed in rat liver, (51). Decreased blood pH of 7.12 in rats was found to up-regulate the overall expression of the UT-A2b transporter in hepatocyte membranes and the kidney inner medulla, (51). This up-regulation of UT-A2b in hepatocytes is thought to occur in order to allow increased transport of urea out of the hepatocytes, to prevent urea build-up during increased ureagenesis in uraemic rats, and is reversed by bicarbonate treatment, (51).

Another group of transporters which are regulated by acidotic conditions are the Na^+/H^+ exchangers (NHEs) located in the kidneys. NHE3 specifically is known to be up-regulated in acidosis, and incubation of opossum kidney OKP cells in acidic media for 24 hours led to increased activity of the antiporter and increased expression of NHE3 mRNA. *In vivo* this increased activity is important in mediating increased bicarbonate absorption, (52).

Although all of the transporters mentioned above are responsive to pH, considering their functional properties it is not immediately obvious how they

might have a role in signalling to global protein metabolism. For this reason the focus here shall be on pH sensitive nutrient transporters.

1.5.2 Plasma membrane nutrient transporters as pH sensors

The possibility of acid inhibition of nutrient transporters leading to the observed catabolic state was considered by Bevington et al, (56), who examined the effects of extracellular pH on transporters of inorganic phosphate (Pi), glucose and neutral amino acids in L6 skeletal muscle cells with the hypothesis that low pH, instead of exerting its multiple metabolic effects by acting at a number of different sites, might act at one site, exerting multiple effects via a common initial intracellular signal. Pi transporters were found to be only weakly pH sensitive. Glucose transporter activity was found to be significantly impaired by low pH, but inhibition of glucose metabolism only partly mimicked the effects of acid on protein metabolism, (31,56). In contrast low extracellular pH strongly inhibited the activity of the System A neutral amino acid transporters, assayed from the rate of influx of the substrate methylaminoisobutyrate (MeAIB); and selective competitive inhibition of these transporters with a saturating dose of MeAIB was found to mimic a number of the metabolic effects of low pH on the cells. Such transporters were therefore considered a likely site of action for acid inhibition, (56). See Section 1.5.6 below.

1.5.3 Amino acid transporters

1.5.3.1 Theoretical considerations

As the intracellular concentration of most amino acids in mammalian cells is generally higher than, or at least equal to, the extracellular amino acid concentration, (57), many amino acids seem to be transported actively into the cell against their electrochemical gradient. This active transport (“pumping”) is thought to occur mainly through coupling to the inwardly directed transmembrane gradient of Na^+ which is maintained by the $\text{Na}^+\text{K}^+\text{ATPase}$. The $\text{Na}^+\text{K}^+\text{ATPase}$ is one of the most widely expressed and active transporters in the body, accounting for up to 23% of the resting ATP turnover rate. It functions by using energy derived from the hydrolysis of ATP to drive 3Na^+ out of the cell and 2K^+ into the cell for every ATP hydrolysed, (58). Sodium dependent active amino acid transporters such as the System A transporters of the Slc38 gene family use this sodium gradient to pump amino acids into the cell via secondary active transport and are listed in Section (a i) of Table 1.3.

In contrast, sodium independent amino acid transporters (e.g. the LAT1 and LAT2 System L transporters of the Slc7 gene family), and some sodium-dependent transporters (e.g. ASCT1 and ASCT2 in the Slc1 gene family) (Section aii, Table 1.3) are unable to utilise this sodium gradient to drive active amino acid flux into the cell. They function instead as amino acid exchange proteins, (57), but this does not mean that they have no role in the active accumulation of amino acids inside the cell. They are thought to

function by utilising the amino acid gradient (set up by the sodium-linked amino acid pumps), to transport other amino acids into the cell by so-called “tertiary” active transport. For this to occur the amino acid exchangers must be expressed in the same cell as a sodium-linked amino acid pump which has overlapping amino acid specificity, (59). The unidirectional sodium-linked amino acid pumps therefore indirectly control the activity of the amino acid exchangers.

A well-documented example of such coupling between sodium-dependent active transporters and sodium-independent exchangers is seen in the case of System A and System L transporters, (59-61). System L (LAT1 and LAT2), which will be discussed in further detail later, imports large neutral branched and aromatic amino acids, most favourably L-Leu and the other branched-chain amino acids (BCAAs), (59), and exports mainly neutral amino acids, (57). The amino acid specificity of System L overlaps with that of the System A transporters (e.g. L-Gln is efficiently transported by both types of transporter), making it possible for the transmembrane gradient of L-Gln maintained by System A to drive BCAA influx through System L (Figure 1.4). In this way System A can indirectly control intracellular accumulation of BCAAs, which it does not carry itself. It is worth noting that this relationship between System A and System L could lead to a decrease in System L activity in situations of System A inhibition, where a disruption of the L-Gln gradient could occur, thus affecting the System L amino acid gradient.

Table 1.3: Amino acid transporters

(a i) Neutral-amino-acid transporters: sodium-dependent

System	Protein	Gene	Amino acid substrates (one-letter code)
A	SNAT1	SLC38A1	G, A, S, C, Q, N, H, M, T, Me-AIB, P, Y, V
	SNAT2	SLC38A2	G, P, A, S, C, Q, N, H, M, Me-AIB
	SNAT4	SLC38A4	G, P, A, S, C, N, M, H, K, R
ASC	ASCT1	SLC1A4	A, S, C
	ASCT2	SLC1A5	A, S, C, T, Q
B ^o	ASCT2	SLC1A5	A, S, C, T, Q, F, W, Y
	GAT1	SLC6A1	GABA
BETA	GAT2	SLC6A13	GABA, betaine, P, β -A
	GAT3	SLC6A11	GABA, betaine, taurine
	BGT1	SLC6A12	GABA, betaine
	TAUT	SLC6A6	Taurine
Gly	GLYT1	SLC6A9	G, sarcosine
	GLYT2	SLC6A5	G, sarcosine
IMINO	–	–	P
N	SNAT3	SLC38A3	Q, N, H
	SNAT5	SLC38A5	Q, N, H, S, G
Nm	–	–	Q, N, H
Nb	–	–	Q, N, H
PHE	–	–	F, M
PROT	PROT	SLC6A7	P

(a ii) Neutral-amino-acid transporters: sodium-independent

asc	Asc1	SLC7A10	G, A, S, C, T
	Asc2	-	G, A, S, T
imino			P, G, A, β -A,

	PAT1/LYAAT1	SLC36A1	GABA Me-AIB
	PAT2/LYAAT2	SLC36A2	P, G, A, β -A, GABA Me-AIB
L	LAT1	SLC7A5	H, M, L, I, V, F, Y, W, Q
	LAT2	SLC7A8	A, S, C, T, N, Q, H, M, L, I, V, F, Y, W
T	TAT1	SLC16A10	F, Y, W
<i>(b i) Anionic-amino-acid transporters: sodium-dependent</i>			
	EAAT1	SLC1A3	E, D
	EAAT2	SLC1A2	E, D
X_{AG}^-	EAAT3	SLC1A1	E, D, C
	EAAT4	SLC1A6	E, D
	EAAT5	SLC1A7	E, D
<i>(b ii) Anionic-amino-acid transporters: sodium-independent</i>			
x^{-c}	xCT	SLC7A11	E
–	XAT2	–	D, E
<i>(c i) Cationic-amino-acid transporters: sodium-dependent</i>			
$B^{o,+}$	ATB(o,+)	SLC6A14	K, R, A, S, C, T, N, Q, H, M, I, L, V, F, Y, W
y^+L	y+ LAT1	SLC7A7	K, R, Q, H, M, L
	y+LAT2	SLC7A6	K, R, Q, H, M, L, A, C
<i>(c ii) Cationic-amino-acid transporters: sodium-independent</i>			
$b^{o,+}$	b(o,+) AT	SLC7A9	K, R, A, S, C, T, N, Q, H, M, I, L, V, F, Y, W, Ci
y^+	Cat-1	SLC7A1	R, K, H
	Cat-2	SLC7A2	R, K, H
	Cat-3	SLC7A3	R, K
	Cat-4	SLC7A4	Unknown

Reproduced from Hyde et al 2003, (57).

Figure 1.4: The Na⁺-K⁺ ATPase, System A and System L transporters as examples of Primary, Secondary and Tertiary active transport

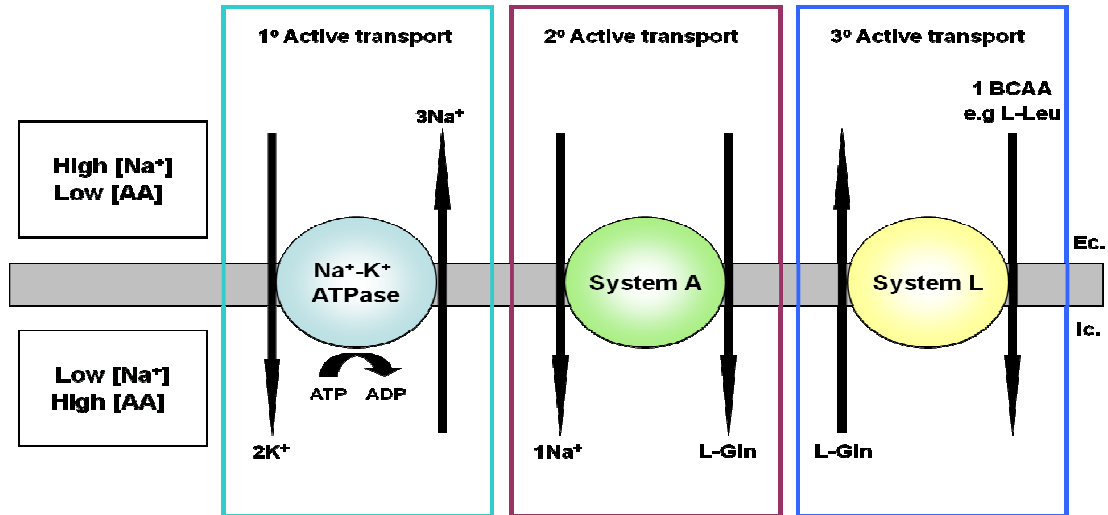


Figure 1.4: The Na⁺-K⁺ ATPase, System A and System L transporters as examples of Primary, Secondary and Tertiary active transport

This figure depicts the coupling of the Na⁺-K⁺ ATPase (1° active transport), the System A transporter (2° active transport), and the System L transporter

1.5.4 The SNAT transporters

System A and System N sodium-coupled neutral amino acid transporters (SNATs) are all members of the Slc38 gene family, (62). This gene family comprises 5 genes, SNAT1 (Slc38A1) – SNAT5 (Slc38A5), which encode well characterised amino acid transporters, and six “orphan” genes SNAT6 (Slc38A6) -SNAT11 (Slc38A11), (see Table 1.4), of unknown biological function which are also thought to encode transporters, and show wide variation in their expression between different tissues, (63).

1.5.4.1 Expression, structure and function of SNAT transporters

The System A transporters are SNAT1, SNAT2 and SNAT4, and the System N transporters are SNAT3 and SNAT5, (64). The System A subtypes co-transport 1Na⁺ and 1 substrate amino acid into the cell, (with Na⁺ binding preceding amino acid binding, (64)), via secondary active transport using the sodium gradient (as described in Section 1.5.3 above), (62). The System A transporters preferentially transport small zwitterionic, or net neutral, amino acids, (64), such as L-Gln, (57), but neutral amino acids with bulky side chains (e.g. BCAAs) are poor substrates (62). An important feature of System A transporters is that they are prone to the phenomenon of trans-inhibition, (65), i.e. influx through these transporters is strongly inhibited by intracellular accumulation of their substrates.

SNAT1 is mainly expressed in the central nervous system, retina, heart and placenta, with its maximal expression being in the central nervous system. Its favoured substrates are L-Gln, L-Ala, L-Asn, L-Cys, L-His and L-Ser, (64).

Table 1.4: Slc38 orphan genes.

Protein	Gene	Species	Source
		Rat	GENBANK NM_001013099
SNAT6	Slc38a6	Mouse	MGI:3648156
		Human	HGNC:19863
		Rat	GENBANK BC086369
SNAT7	Slc38a7	Mouse	GENBANK BC031853
		Human	GENBANK NM_018231
		Rat	GENBANK XM_577668
SNAT8	Slc38a8	Mouse	GENBANK NM_001009950
		Human	GENBANK NM_001080442
		Rat	RGD1311881
SNAT9	Slc38a9	Mouse	MGI:1918839
		Human	HGNC:26907
		Rat	RGD1306356
SNAT10	Slc38a10	Mouse	MGI:1919305
		Human	HGNC:28237
		Rat	RGD1306005
SNAT11	Slc38a11	Mouse	MGI:2443383
		Human	HGNC:26836

The SNAT2 transporter is widely expressed and is found in the brain and spinal cord, placenta, adrenal glands, testis, thymus, muscle, liver, intestine, kidney, lung, adipose tissue, spleen and skin, (64). The favoured SNAT2 substrates are; L-Ala, L-Ser and L-Gln, (66), although it also transports L-Gly, L-Pro, L-Asn, L-Cys, L-His and L-Met, (57,64). The proposed structure of the SNAT2 transporter, Figure 1.5, with eleven transmembrane domains, was first documented in 2000 by Yao et al, (66).

SNAT4 is maximally expressed in the liver but is also found in muscle, kidney and pancreas tissues. Its favoured substrates are L-Ala, L-Asn, L-Cys, L-Gly, L-Ser and L-Thr, (64).

The System N transporters have a narrower range of substrates than the System A transporters, only transporting L-Gln, L-His, L-Ser, L-Asn and L-Gly, between them, (57,64). In addition to this, System N transporters differ from System A in that they perform influx of 1Na^+ and 1 amino acid in exchange for counter-transport (efflux) of 1H^+ , and have a much weaker ability than System A to transport the non-metabolisable substrate methyl-aminoisobutyrate (MeAIB). Traditionally these transporters have been regarded as incapable of transporting MeAIB, but more recently this has been challenged, (67).

SNAT3 only transports L-Gln, L-His and L-Asn and is found in the brain, retina, liver, kidney and adipose tissue, (64). Interestingly System N transporters have also been found to mediate L-Gln efflux in astrocytes, (68), this has been particularly noted in the SNAT3 transporter due to its abundant expression in astrocytes throughout the brain, (64). An increase in the expression of SNAT3 transporters in the kidneys has been observed during metabolic acidosis, and is believed to mediate an increase in basolateral glutamine uptake into the proximal tubule from the blood, thus, facilitating increased ammoniogenesis and therefore increased acid excretion, (70).

SNAT5 transports L-Gln, L-Asn, L-His, L-Ser and L-Gly and is found in the stomach, brain, liver, lung, small intestine, spleen, colon and kidney, (64). In addition to mediating amino acid influx, efflux of L-Gln via the SNAT5 transporter has also been observed, (70).

The ability of SNAT1, 2 and 4 (and possibly SNAT3 and 5) to transport the non-metabolisable substrate methyl-aminoisobutyrate (MeAIB), is a property which distinguishes the Slc38 gene family from most other amino acid transporters. Exceptions are the Proton-Assisted Transporters (PATs) of the Slc36 gene family which also transport MeAIB. These were originally described as endosomal proton-coupled amino acid transporters, (71), but are expressed in the apical plasma membrane of intestinal epithelial cells, (72). Their expression in the plasma membrane of other cell types has not been studied in detail, but the relative contribution of Slc36 and Slc38 transporters to MeAIB transport in a given cell type can be assessed by measuring the extracellular pH dependence of MeAIB influx. This should be activated by low pH if Slc36 transporters are carrying the flux, and inhibited by low pH if Slc38 transporters predominate. At least in L6 cells, corresponding effects on intracellular pH should be small, and hence should have little effect on endosomal Slc36 transporters

SNAT2 is the main subtype of System A expressed in the tissue of interest here, i.e. skeletal muscle, (73,74), and is discussed in further detail in Section 1.5.5.

1.5.5 Regulation of SNAT2

Owing to its ability to transport MeAIB (which provides a convenient assay for the transporter's activity) and its widespread expression, SNAT2 has been extensively studied in a number of different cell types. A striking feature of the biology of SNAT2 is that its expression and activity is strongly increased in response to extracellular amino acid deprivation, (62,74,75), a phenomenon known as adaptive regulation.

1.5.5.1 Adaptive regulation of SNAT2

Adaptive regulation of SNAT2 has been observed in a number of different cell types; L6 myotubes and 3T3-L1 adipocytes, (74), mouse embryonic fibroblasts, (76), rat mammary gland, (62), C6 glioma cells, (75), and BeWO cells, (77). It occurs in two phases; an acute phase in which SNAT2 is translocated from intracellular stores to the plasma membrane, and a chronic phase with increased levels of SNAT2 synthesis, (75).

1.5.5.1.1 The acute phase of adaptive regulation

SNAT2 is constitutively recycled at the plasma membrane, (78), and has been found in intracellular membranes fractionated from L6 cells, (74). It therefore appears that SNAT2, in muscle cells at least, is stored in intracellular compartments ready to be translocated to the plasma membrane when increased uptake of amino acids is required. Increased levels of the SNAT2 protein have been observed in plasma membrane preparations from L6 cells after 4 hours of amino acid starvation, (74). The high protein turnover

rate of SNAT2 allows activity of the transporter to be tightly regulated, (62). The mechanism(s) controlling this acute phase of adaptive regulation are still uncertain, but it is thought that proteins activated as part of the insulin signalling pathway may be involved, as discussed in Section 1.6.

1.5.5.1.2 *The chronic phase of adaptive regulation*

The chronic phase of adaptive regulation requires increased synthesis of SNAT2 transporters. It has been observed in several studies that SNAT2 mRNA, (62), (75), and functional expression of SNAT2, (78), are increased in prolonged amino acid starvation, and that this increase is inhibited by actinomycin D and cycloheximide, (62), (78), inhibitors of transcription and translation respectively. This increase in gene expression, following increased mobilisation of SNAT2 from intracellular stores, ensures that these intracellular stores are replenished, (75). The mechanisms by which this increase in SNAT2 expression occurs, under conditions in which protein synthesis would be expected to be decreased, were poorly understood. However, characterisation of an amino acid response element (AARE) in the SNAT2 gene, (76) has given rise to the suggestion of the involvement of the kinase, general control non-derepressible -2, (GCN2), which phosphorylates the alpha-subunit of eukaryotic initiation factor 2 (eIF2). eIF2- α phosphorylation decreases translation in general but leads to increased translation of mRNA encoding activating transcription factor 4 (ATF4), (76). ATF4 is known to target and increase transcription of certain genes, including those which have an amino acid response element. The adaptive response of SNAT2 to amino acid starvation was blocked in mouse embryonic fibroblasts

(MEFs) deficient for GCN2, or expressing a S51A mutated eIF2 α subunit which could not be activated, but not in wild-type MEFs. In addition to this, amino acid starvation in wild type MEFs led to an increase in the expression of ATF4, the induction of SNAT2 mRNA, and MeAIB uptake, and all of these observed increases were severely blunted in amino acid starved MEFs containing a S51A mutated eIF2 α , (79). This group, (79), also investigated the translational control of SNAT2 during amino acid starvation. By constructing expression vectors expressing mRNAs containing the SNAT2 5' UTR and a luciferase reporter and transfecting them into HeLa, MEF and C6 cells, they determined that the SNAT2 5' Untranslated Region (5'UTR) contains an internal ribosome entry site (IRES) which they found to be constitutively active in both amino acid replete and depleted conditions, (79). This suggests that the increased expression of SNAT2 in amino acid starvation is due to a combination of increased transcription of SNAT2 mRNA, (because its AARE is recognised by ATF4, which is expressed at increased levels in amino acid starvation as a result of GCN2 and eIF2 α activation), (76,79), and continuation of SNAT2 mRNA translation (in conditions where cap-dependent translation is inhibited) due to the constitutive cap-independent translation of mRNAs containing an IRES region, (79).

1.5.5.1.3 Cell recovery from amino acid starvation

When cells are exposed to amino acids, after a period of amino acid starvation, SNAT2 activity decreases, (62,80), possibly as a result of polyubiquitination of SNAT2 by the ubiquitin ligase Nedd4-2, (81), (for an

explanation of proteolysis by the ubiquitin proteasome system see Section 1.7).

Interestingly, exposure of the cells to a single amino acid is enough to suppress adaptive regulation and lead to a decrease in SNAT2 activity. This mainly occurs in the presence of SNAT2 substrates and as such L-Gln, L-Ala and MeAIB, all decreased expression of SNAT2 at the plasma membrane in C6 glioma cells, (75), and L6 myotubes, (80), and decreased the transport activity of SNAT2 in L6 myotubes when compared to conditions of amino acid starvation, however this was also seen to occur with the re-addition of L-Tyr, (80).

The MeAIB mediated suppression of SNAT2 adaptive regulation is interesting as it suggests that the presence of a substrate at the transporter and/or transportation of that substrate into the cell is enough to return SNAT2 activity to normal, with metabolism of that substrate being un-necessary, (75,80). It was determined that this effect was not simply a result of trans-inhibition because MeAIB (and L-Gln, L-Ala and L-Tyr) addition to amino acid starved L6 cells, expressing SNAT2-luciferase vectors, led to a decrease in luciferase activity to a level comparable with that seen in amino acid replete cells, (80).

Treatment of amino acid starved L6-myotubes with L-Gln, L-Ala and MeAIB *during* a transport assay, measuring uptake of radio-labelled MeAIB into the cells, was again found to decrease SNAT2 transport activity but this was not observed when L-Tyr was added at the same concentration under the same

conditions, (80) This confirms that L-Tyr (or an impurity in the sampled used) does not directly interact with the SNAT2 transporter and suggests that it inhibits SNAT2 activity by an alternative method, (80). In order to determine which signalling pathways could be involved in the suppression of adaptive regulation, the effect on adaptive regulation of the inhibitors of; extracellular-signal regulated kinase (ERK), phosphatidylinositol-3-kinase (PI3K), c-Jun N-terminal kinase (JNK), p38 mitogen activated protein kinase (p38) and mammalian target of rapamycin (mTOR), was determined, (80). Inhibition of ERK, p38 and mTOR had no effect, but PI3K and JNK inhibition decreased adaptive regulation of SNAT2 in L6-myotubes. Phosphorylation of both JNK and ERK was increased in amino acid depletion and then decreased by addition of L-Gln and L-Tyr (and to a lesser extent L-Ala), but not by addition of MeAIB, (80).

To re-cap, these experiments determined that L-Gln, L-Tyr, L-Ala and MeAIB all decrease SNAT2 activity but that L-Tyr does so without having a direct interaction with SNAT2. L-Gln, L-Tyr and L-Ala all decrease phosphorylation of JNK and ERK in amino acid starved conditions, an effect not observed in the presence of MeAIB. This is indicative of a system where two amino acid sensitive pathways, with overlapping responsiveness, are able to mediate the observed decrease in SNAT2 adaptive regulation.

The results above, (80), led to the suggestion that SNAT2 may act as a “transceptor” involved in both amino acid transport and signal transduction. This model suggests that SNAT2 functions as an amino acid sensor which

undergoes a conformational change upon substrate binding or during the transport cycle, thus inhibiting SNAT2 adaptive regulation. In addition to this, the presence of a separate plasma membrane amino acid sensor, sensing large neutral amino acids, which inhibits the amino acid starvation mediated phosphorylation of JNK and/or ERK was suggested. As both of these pathways were thought to be equally important, (80), it was suggested that they would both inhibit the induction of SNAT2 mRNA, (80) Inhibition of JNK/ERK activation could achieve this by signalling through transcription factors, (82), but the pathway through which the activated SNAT2 “transceptor” could signal is less certain. As inhibition of PI3K partly inhibited the adaptive regulation of SNAT2, it is possible that this occurs through an as yet undefined, PI3K dependent, adaptive regulation pathway, (80).

1.5.5.2 Activity of SNAT2 is modulated by hormones.

SNAT2 activity can also be increased in response to hormones such as insulin, but in this case the increase in activity is not dependent on increased synthesis of the transporter, (78). SNAT2 transporters are constitutively recycled at the plasma membrane, making regulation of SNAT2 levels at the plasma membrane dependent on levels of exocytosis and endocytosis, (78). It was shown by Hyde et al that insulin activation of SNAT2 occurs due to an increase in translocation of SNAT2 from intracellular compartments, (78), a mechanism analogous to that thought to occur in the acute phase of adaptive regulation. Chloroquine, (CQ), which disrupts exocytosis, and cytochalasin D, (CD), which disrupts endocytosis, were used to determine where insulin exerts its effects. As expected, treating the cells with CQ led to a decrease,

and CD to an increase, in MeAIB uptake. The CD induced increase in MeAIB uptake, presumably due to the prevention of internalisation of SNAT2 transporters at the plasma membrane, was further increased in the presence of insulin but not beyond the levels observed from insulin treatment alone. Insulin signalling itself was not found to be inhibited by CQ suggesting that CQ inhibition of insulin-stimulated SNAT2 exocytosis was a result of inhibition occurring at the intracellular compartment, (78). The mechanisms by which insulin signalling increases SNAT2 exocytosis are not fully understood, but as constitutively active protein kinase B (PKB) mimics the insulin effect, and inhibition of phosphatidylinositol-3-kinase (PI3K) blocks the increase in exocytosis, signalling via PI3K and PKB is thought to play a role, (78).

The role of other hormones in regulating System A activity was described by McGivan & Pastor-Anglada, (83), who stated that, "System A is under hormonal and nutritional control in all cell types so far studied", although the majority of examples outlined in their review focus on liver cells. Interestingly, (in light of the normally antagonistic roles of glucagon and insulin), glucagon up-regulates System A activity in liver parenchymal cells, (83), via undetermined mechanisms. Catecholamines and glucocorticoids in liver parenchymal cells, and adrenaline in rat hepatocytes, also up-regulated System A, (83). As the up-regulation of System A mediated by adrenaline can be inhibited by actinomycin D and cycloheximide, (83), this response may be the result of increased transcription and translation of System A genes or genes encoding System A regulatory proteins. As these reports pre-date the

cloning of the Slc38 genes, the precise System A isoform involved remains to be determined.

1.5.5.3 The role of SNAT2 in cell volume regulation

Hypertonic stress, like insulin stimulation and amino acid starvation, leads to an increase in SNAT2 availability at the plasma membrane in human fibroblasts, (84,85). The SNAT2 up-regulation response in hypertonic stress is not a result of increased translocation of SNAT2 to the plasma membrane from intracellular stores but instead seems closely related to the chronic phase of adaptive regulation, in that there is an increase in the amount of newly synthesised SNAT2, (84). These transporters are distributed both to intracellular stores and the plasma membrane but, as there is a much greater increase in the number of transporters located at the plasma membrane than in intracellular stores in hypertonic conditions, it has been suggested that, under these conditions, new transporters are preferentially targeted to the plasma membrane, (84). It takes around 6 hours incubation in hypertonic media for SNAT2 induction to reach its maximal response, (84), and around 24 hours for an increase in transporters of other osmolytes to occur, (84). This cellular response to hypertonicity is called the regulatory volume increase (RVI) which can be split into the short term RVI (involving activation of SNAT2) and the long term RVI (involving activation of other osmolyte transporters) (85). SNAT2 up-regulation in the RVI response is functionally important because SNAT2 plays a major role in regulating both the total intracellular amino acid concentration and the specific composition of the intracellular free amino acid pool, (85). SNAT2 drives intracellular

accumulation of its substrates, particularly L-Gln, which increases the rate of cell volume recovery. Increases in non-System A substrates, such as leucine, were also observed probably as a result of SNAT2-coupled tertiary active transport through the System L transporter as explained in Figure 1.4, (84).

In hypertonic stress, cell shrinkage occurs as a result of the osmotic movement of water out of the cell. The increase in SNAT2 activity increases the intracellular concentration of amino acid osmolytes leading to movement of water back into the cell until cell volume has been restored. Key evidence for SNAT2 involvement in cell volume recovery comes from SNAT2 siRNA silencing experiments, in which increased expression of SNAT2 is prevented, intracellular amino acids are not immediately increased via other mechanisms and volume recovery is delayed, (85). The cell responds in the opposite way to a hypotonic environment, leading to the regulatory volume decrease response which involves down-regulation of SNAT2, (84).

It is worth noting that cell shrinkage also occurs in total amino acid starvation, because of marked efflux of amino acids from the cell, (84). This is interesting given that both amino acid starvation and cell shrinkage lead to a protein synthesis dependent up-regulation of the SNAT2 transporter, (79). An important difference between the amino acid starvation response and the hyper-osmotic stress response however is that different signalling pathways are involved. It has recently been determined that SNAT2 mRNA induction in amino acid starvation requires the activation of eIF2 α , see Section 1.5.5.1.2,

but that S51A mutation of eIF2 α does not affect the increase in SNAT2 mRNA observed in hypertonic stress, (79).

1.5.5.4 The pH-sensitivity of SNAT2

All members of the Slc38 gene family, of known biological function, (ie SNAT 1-5), are sensitive to regulation by extracellular pH, (73). Increases in extracellular pH above 7.4 increase the activity of the System A, (86), and System N, (73), transporters and the activity of both is decreased when the extracellular pH is lowered below 7.4, (68,73,86). Initially inhibition of the activity of the System N transporters was thought to occur as a result of the increased extracellular proton concentration at low pH preventing the efflux of H⁺ by the transporter, (64), and System A inhibition was thought to be caused by H⁺ competing with Na⁺ for its binding site on System A, (68). However, the pH sensitivity of SNAT2 in skeletal muscle and SNAT2, (86), and SNAT5 overexpressed in *Xenopus* oocytes, (73), is blunted in the presence of the histidine modifying agent diethylpyrocarbonate (DEPC), suggesting a conserved mechanism of pH regulation throughout the Slc38 gene family involving protonation of histidine residues, (73).

Histidine to alanine mutation of conserved histidine residues, His⁵⁰⁴ in SNAT2 and His⁴⁷¹ in SNAT5, was found to decrease the pH sensitivity of SNAT2 and SNAT5, (73). The mutated transporters were also less sensitive to DEPC than their wild-type counterparts, (73). The affinity of Na⁺ for its transporter was decreased as pH was lowered, which supports the idea of H⁺ competing with Na⁺ for its binding site, however, no decrease in Na⁺/SNAT affinity was

observed for DEPC treated or mutated transporters in the pH range 7-8, (73). This suggests that protons must act at C-terminal histidine residues and therefore allosterically inhibit Na⁺/SNAT binding, as direct interaction of H⁺ at the Na⁺ binding site would bypass the effects of histidine mutation and DEPC treatment and have the same affect on Na⁺/SNAT affinity as seen in wild-type transporters.

It was concluded from this study that protonation of a conserved C-terminal histidine residue on both SNAT2 and SNAT5 partially decreases activity of the transporters, by allosterically regulating Na⁺ binding to the transporter, but that synchronized proton interaction at a distinct pH sensing site, (yet to be determined), is likely to result in total inhibition of the SNAT transporters, (73). Decreases in System A activity have also been observed as a result of lowering intracellular pH in skeletal muscle, (86), suggesting that there may also be acid sensitive histidine residues within the cytoplasmic domain of the SNAT transporters.

1.5.6 System A, SNAT2 and metabolic acidosis

As SNAT2 studies in the stress states of amino acid depletion and hypertonic stress suggest that SNAT2 plays an important role in maintaining intracellular amino acid homeostasis, and its transport activity is inhibited by low pH, SNAT2 is a plausible candidate for the hypothetical “sensor” linking the low extracellular pH signal to intracellular signalling pathways and protein metabolism.

In cultured L6 rat skeletal muscle cells, low extracellular pH exerts a number of metabolic effects, (31): it decreases DNA synthesis rate, protein synthesis rate, glycolytic rate, and glucose transporter activity, and increases proteolysis rate. Treatment of L6 myotubes with a saturating dose of MeAIB, to bring about competitive inhibition of System A transporters, mimics all of these metabolic effects of low pH, (56). In particular it increases proteolysis and decreases protein synthesis, effects similar in magnitude to those observed at low pH (56). As MeAIB is mainly transported at the plasma membrane by System A transporters, and as SNAT2 is the dominant form of System A expressed in skeletal muscle cells, (74), these results support the argument that it is System A/SNAT2, inhibited at low pH, which leads to the catabolic intracellular consequences of extracellular acidosis.

It has been suggested that catabolism in metabolic acidosis is the result of inhibition of a pathway common to all of the affected metabolic variables, triggered by extracellular sensing of acidosis, (56). As decreases in protein synthesis, DNA synthesis, glucose transport and glycolysis are observed in both acidosis and insulin withdrawal, it is possible that System A inhibition by low pH could be inhibiting anabolic insulin signalling, (56). Insulin signalling involves proteins that are nutrient sensors, such as mTOR, (87), implying that the metabolic effects of acidosis and System A inhibition could, at least in part, be the result of decreased amino acid availability within the cell.

More specifically, the amino acid L-Gln (which is a substrate for SNAT1 and SNAT2, (66,88)) appears to have an anabolic effect within L6 cells and, at

high concentration, decreases the catabolic effects of MeAIB, (56). A ten-fold increase in extracellular L-Gln concentration inhibited protein degradation at pH 7.4, but not at pH 7.1, possibly because System A transporters were inhibited at this pH, decreasing the influx of L-Gln into the cell, (56). It was also shown that L-Gln starvation increased proteolysis, but addition of MeAIB did not increase this further, (56). The lack of an additive effect was taken as further evidence that L-Gln and MeAIB were acting via the same transporter. This suggests that L-Gln depletion occurring through acidotic inhibition of SNAT2 transport may have contributed to the enhanced proteolysis, an idea which was supported by the finding that the pH sensitivity of proteolysis was blunted in a L-Gln-free environment, (56).

Cell volume is regarded as an important regulator of global protein metabolism in some cell types such as 3T3 fibroblasts and hepatocytes, (89)). But, although System A is thought to be important in regulation of cell volume, (Section 1.5.3.3), the water content of L6 myotubes was found to be unaltered at pH 7.1 compared with pH 7.5, (31), suggesting that cell volume does not play a major role in the cellular response to acidosis. Furthermore deliberately altering water content of the cells with an osmolyte (mannitol) did not affect proteolysis, (56). This also makes it unlikely that manipulating MeAIB and L-Gln concentrations could produce changes in proteolysis through changes in cell volume.

1.6 Control of protein synthesis

Proteins make up around 44% of the human body's dry weight, (90), making control of protein synthesis rates vitally important. The process of gene expression occurs in two broad stages; transcription and translation, both of which can be acutely regulated dependent on the environment and requirements of the cell. Translational regulation is preferable when a rapid response to changes in the rate of protein synthesis is required as it does not require mRNA production or nuclear export of mRNA intermediates.

In order for translation to occur the transcribed pre-mRNA must undergo post transcriptional modifications: the addition of a 7-methylguanosine (m^7G) cap structure at the 5' end of the pre-mRNA, splicing to remove introns, and polyadenylation of the 3' end, (91). As these modifications occur export factors are recruited to the pre-mRNA forming a complex particle of mRNA and proteins, known as a ribonucleoprotein complex (mRNP), (91). Properly assembled mRNP complexes are recognised by the nuclear export machinery and exit the nucleus via the nuclear pore complex, (92). This highly regulated mechanism allows a substantial degree of quality control ensuring that mRNAs only enter the cytoplasm if they are "complete" and ready to undergo translation.

1.6.1 An overview of translation

Translation occurs in the cytoplasm and is a procedure with three steps; initiation, reviewed in (93), elongation, reviewed in (94), and termination, reviewed in (95,96). Initiation is the process which brings together the 40S

ribosome, the mRNA and the initiator tRNA in order to promote scanning of the mRNA and initiation codon recognition. Initiation ends upon formation of the 80S ribosome where the initiator tRNA is in the ribosomal P site. Elongation is a cyclic process which ensures elongation of the polypeptide chain until a stop codon reaches the ribosomal A site and termination ensues. Termination involves the release of the nascent polypeptide chain from the ribosome and ribosomal and mRNA dissociation.

1.6.1.1 Translation initiation

Initiation, Figure 1.6, is the most complex step in translation and requires the activity of many eukaryotic initiation factors (eIFs), which assist in recruiting the initiator tRNA and the mRNA to the 40S ribosome and the subsequent scanning of mRNA for the start codon AUG.

The initiator tRNA, methionyl initiator-tRNA, (Met-tRNA_i), is brought to the 40S ribosome as part of an eIF2.GTP.Met-tRNA_i ternary complex. In order for the ternary complex to bind to the 40S ribosome the 40S and 60s ribosomal subunits must be separated, (97). In order to prevent their association eIF6 binds to the 60s subunit, (98) and eIF3 to the 40S ribosomal subunit, where the added presence of eIF1A, eIF1 and the ternary complex stabilise this binding reaction, (97).

The binding of the ternary complex to the 40S ribosome to produce the 43S pre-initiation complex; eIF2.GTP.Met-tRNA_i.40S, (97), is facilitated by the initiation factors eIF1, eIF1A, and eIF3, (93). This stage of translation initiation

is particularly highly regulated and can be inhibited by phosphorylation of the alpha subunit of eIF2, which indirectly prevents formation of the ternary complex, (98), and will be discussed in further detail in Section 1.6.2.12.

The m⁷G-capped 5' end of the mRNA is recognised by the cap binding protein eIF4E that makes up part of the eIF4F complex, which also consists of a scaffolding protein, eIF4G, and an ATP dependent RNA helicase, eIF4A, (98). eIF4E binds to the 5'cap of the mRNA and the RNA helicase activity of eIF4A, (which is enhanced in the presence of eIF4H and eIF4B, (99)), facilitates the unwinding of any secondary structures present in the 5' untranslated region (UTR), thus promoting ribosomal binding to the mRNA, (100).

The 43S pre-initiation complex now binds to the mRNA at or near the 5'cap, due to the association of eIF3 and eIF4G, (101), and begins scanning along the 5' UTR searching for the AUG initiation codon, (93). Once the ribosome encounters the AUG codon it stops scanning due to interaction of the mRNA AUG codon and the Met-tRNA_i anti-codon, (98). During ribosomal scanning eIF2 bound GTP is hydrolysed to GDP in an irreversible reaction mediated by eIF5, a GTPase activator protein (GAP), but phosphate release from GDP is temporarily inhibited by eIF1. Upon AUG recognition eIF1 is released from its binding site, allowing phosphate release and causing eIF2.GDP to be ejected from the ribosome, (97). The remaining eIFs dissociate as the 60s subunit binds to the 40S subunit to form the 80S ribosome in a process involving the activity of eIF5.GTP, (97).

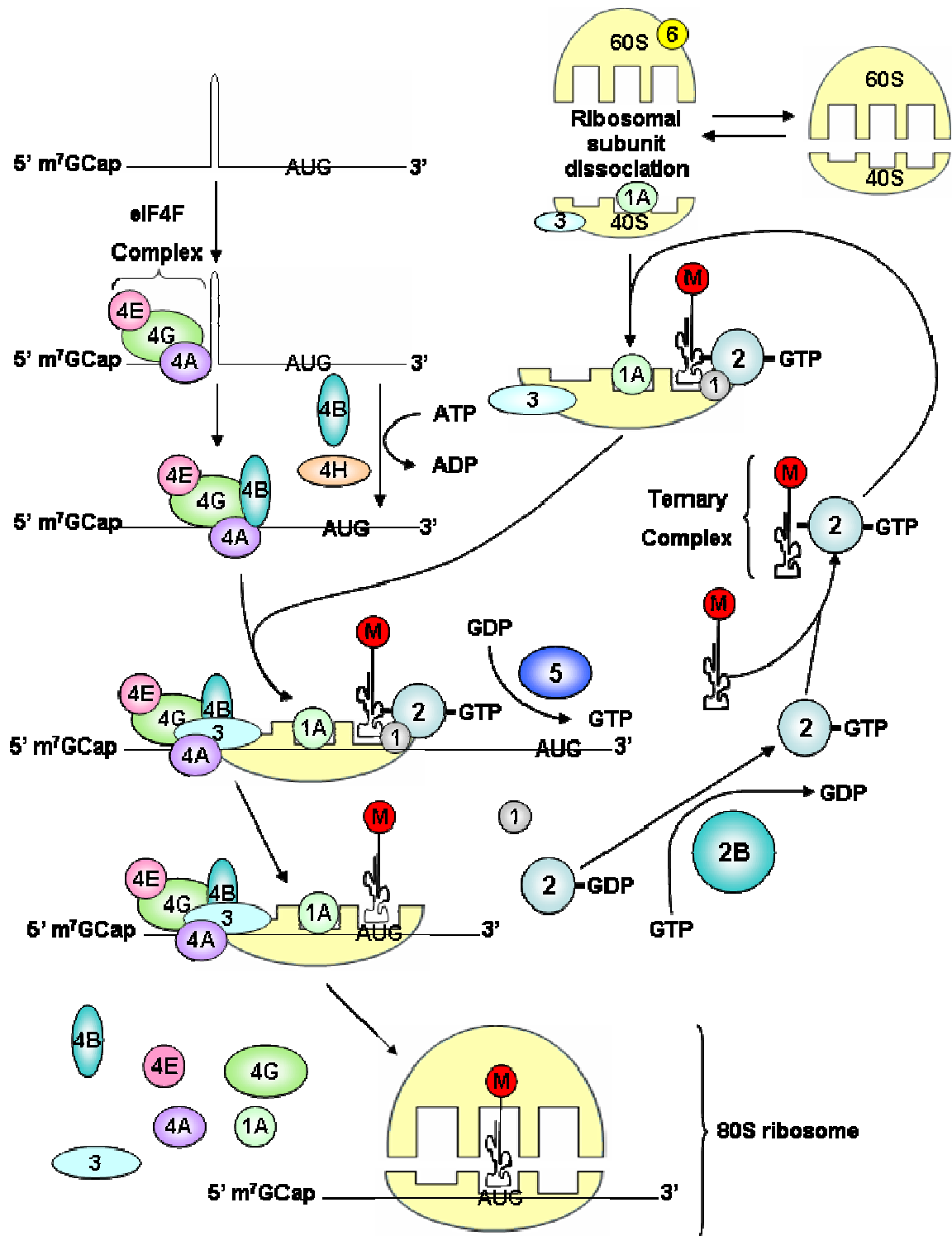


Figure 1.6: Translation Initiation

This figure depicts translation initiation, discussed in the text in section 1.6.1.1. Initiation factors are shown schematically as individually labelled coloured circles or ellipses. This diagram is drawn from information obtained from sources referenced in the main text and items are not drawn to relative scale.

Upon release of eIF2.GDP from the 40S ribosome the inactive eIF2.GDP complex is recognised by eIF2B which then catalyses the exchange of GDP for GTP producing an active eIF2 bound to GTP and ready to bind to Met-tRNA_i, (98).

1.6.1.2 Translation elongation

The currently accepted explanation of the elongation cycle is based on the half site model suggested by Moazed and Noller in 1986, (94). As can be seen in Figure 1.7 there are three tRNA binding sites within the ribosome termed the exit site, E, the peptidyl-RNA site, P, and the aminoacyl-tRNA site, A. There are three main steps in the elongation cycle; binding of aminoacyl-tRNA to the A site, peptidyl transfer, and translocation. The peptidyl transfer step, where a new peptide bond is formed between the polypeptide chain and the aminoacyl-tRNA, occurs rapidly and is catalysed by the peptidyl transferase enzymatic activity of the large ribosomal subunit, (94). The other two steps occur more slowly and require the activity of elongation factors. Eukaryotic elongation factor 1 (eEF1) consists of four subunits; eEF1A, eEF1B α , eEF1B γ and eEF1B β , (102). eEF1A is a GTPase. In its GTP bound form eEF1A is able to bind to aminoacyl-tRNA and transport it to the ribosomal A site where the tRNA binds once the mRNA codon is recognised by the tRNA anti-codon via complementary base pairing. Upon aminoacyl-tRNA binding to the A site the GTP bound to eEF1A is hydrolysed and eEF1A is released from the tRNA and binds to the eEF1B complex, (103). The eEF1B complex functions as a guanine nucleotide exchange factor, (GEF), and reactivates eEF1A by stimulating GDP release and GTP binding,

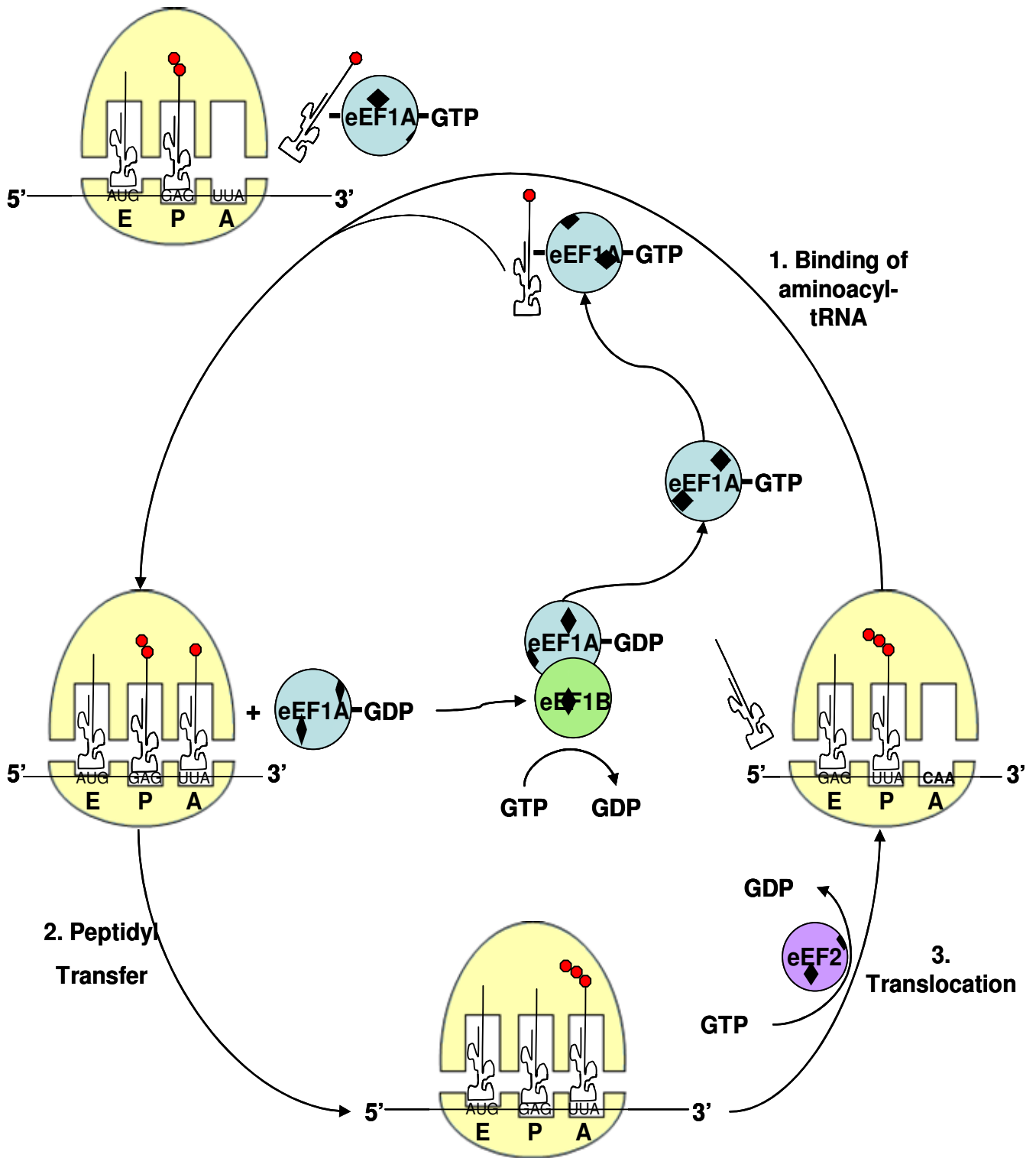


Figure 1.7: Translation Elongation

This figure depicts the elongation stage of translation, described in the text in section 1.6.1.2.

Elongation factors are shown schematically as individually labelled coloured circles. The 80S ribosome is shown in yellow and amino acids are shown as small red circles attached to the tRNA or as part of a growing polypeptide chain. This diagram is drawn from information obtained from sources referenced in main text and items are not drawn to relative scale.

therefore preparing eEF1A for another elongation cycle, (102). Once the peptidyl transfer step has occurred the ribosome undergoes a translocation phase catalysed by eukaryotic elongation factor 2, (eEF2), in a GTP dependent manner, (94). This step involves the release of the deacylated-tRNA from the E site and the movement of; the peptidyl-tRNA from the A site to the P site, the deacylated-tRNA from the P site to the E site, and a movement of the mRNA by 3 nucleotides in a 5' direction in order to expose the next codon in preparation for another elongation cycle.

1.6.1.3 Translation termination

Translational termination in eukaryotes occurs when one of three possible stop codons reaches the ribosomal A site, (95). This stop codon is recognised by a class I release factor called eukaryotic release factor 1, (eRF1), which hydrolyses the final peptidyl-tRNA bond, held in the P site, leading to release of the nascent polypeptide chain, (96), and dissociation of the ribosomal subunits and mRNA, for re-use in another translational cycle, (94). Translation termination is dependent upon the activity of eRF1 and stop codon read-through is increased upon eRF1 depletion in HeLa and 293 cells, (95). Peptide release efficiency is increased by the activity of a class II release factor, eukaryotic release factor 3, (eRF3), a GTPase. eRF3 activity is dependent upon the presence of the 80S ribosome and eRF1, which acts as a GTP dissociation inhibitor, (TDI), stabilising the eRF3-GTP bond, (96). eRF3 increases the efficiency of eukaryotic translation termination but may not be an absolute necessity as its depletion increases stop codon read-through in some cell types but not in others, (95).

1.6.1.4 Regulation of translation initiation

The majority of the regulation of translation occurs at the initiation step, (90). Many of the initiation factors involved in translation initiation can be regulated by phosphorylation events dependent on hormonal control.

1.6.2 Insulin signalling pathway

Some of the proteins involved in translational control can be phosphorylated in response to increases in insulin levels making the study of the insulin signalling pathway important in understanding the control of protein synthesis.

1.6.2.1 Insulin binding triggers a signalling cascade

The insulin receptor consists of two α and two β subunits. When insulin binds to its receptor it causes a conformational change and triggers the tyrosine kinase activity of the receptor β subunits leading to autophosphorylation and phosphorylation of tyrosine residues on a number of substrates including: insulin receptor substrate 1 and 2 (IRS1 and IRS2) and Shc, (104,105). Tyrosine phosphorylation of IRS1/2 increases their affinity for other signalling proteins that contain Src homology-2 (SH2) domains, (105), and phosphotyrosine binding (PTB) domains, such as the p85 regulatory subunit of phosphatidylinositol-3-kinase (PI3K), Src homology-2 domain containing protein tyrosine phosphatase-2 (Shp2), a tyrosine specific phosphatase, and Grb2 an adaptor molecule, (106), as shown in Figure 1.8. Binding of the p85 regulatory subunit of PI3K to IRS1/2 increases the activity of the p110

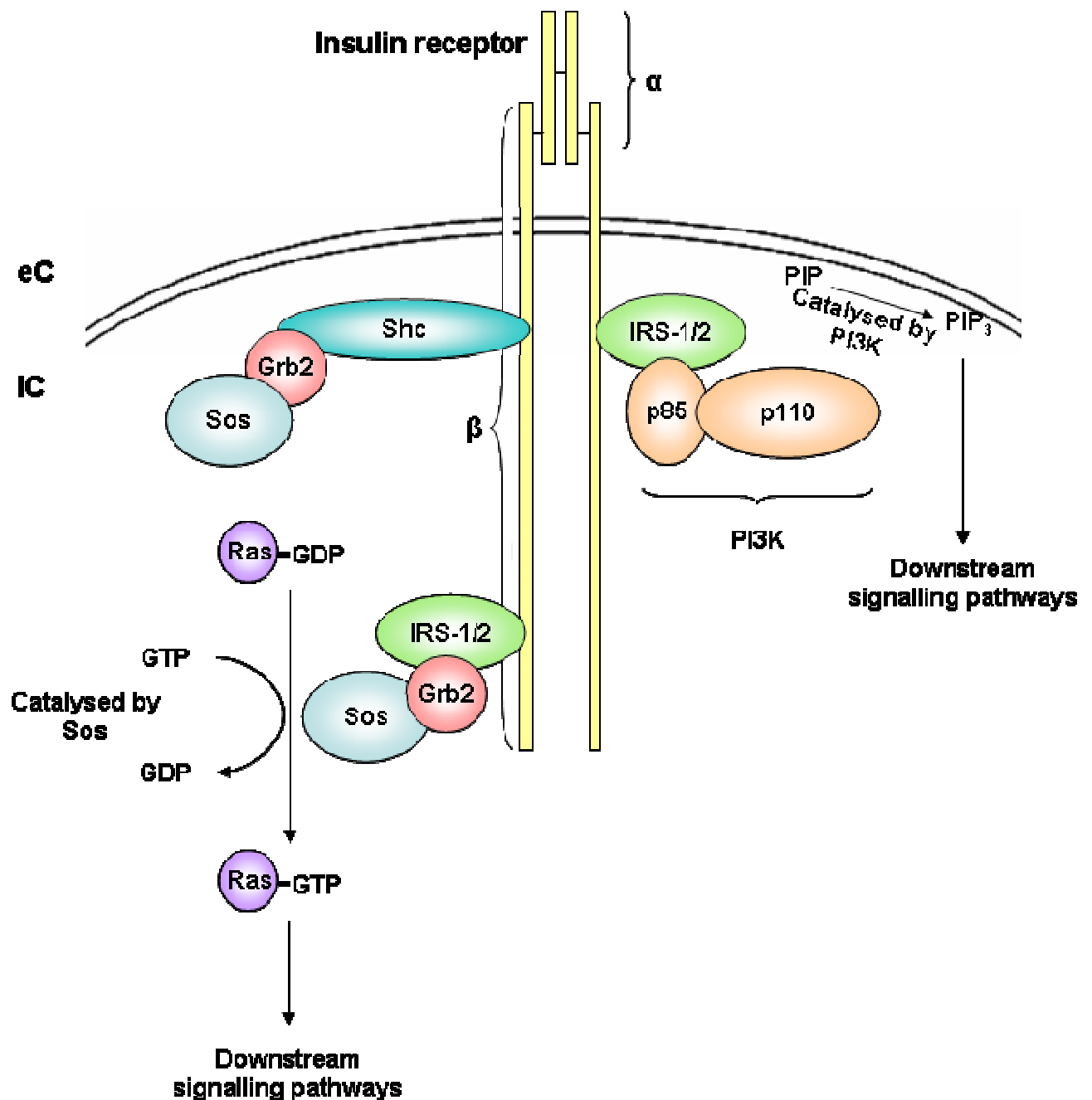


Figure 1.8: The insulin signalling pathway

This figure depicts the initial phase of the insulin signalling pathway, described in the text in section 1.6.2.1.

Proteins are shown schematically as individually labelled coloured circles. This diagram is drawn from information obtained from sources referenced in the main text and items are not drawn to relative scale.

catalytic domain of PI3K leading to an increase in the levels of phosphatidylinositol 3,4,5-tris-phosphate (PIP₃) and to activation of PI-dependent protein kinase 1, which in conjunction with mammalian target of rapamycin complex 2 (mTORC2) then activates downstream protein kinases such as PKB, (107). This signalling pathway is discussed in further detail in Section 1.6.2.2.

Grb is constitutively bound to Son of sevenless (Sos), a guanine nucleotide exchange factor (GEF), (108), in an “SH3 (Src homology-3) domain dependent protein complex”, (109). Phosphorylated IRS1/2 and Shc both bind to Grb2.Sos, leading to the activation of a small membrane bound G-protein, called Ras, (105). The active, GTP bound, Ras then activates the serine-threonine kinase Raf, (108), leading ultimately to downstream activation of the MEK-ERK pathway, discussed in Section 1.6.2.12. Binding of Shp2 to IRS1/2 also promotes activation of the MEK-ERK pathway but its mechanism of action is unclear, (108).

1.6.2.2 Phosphatidylinositol 3- kinase

Phosphatidylinositol 3-kinase (PI3K) consists of two subunits, a p85 regulatory subunit and a p110 catalytic subunit, (110). There are three different classes of PI3K; class I, class II and class III, with class II being split into three different isoforms; PI3K-C2 α , PI3K-C2 β and PI3K-C2 γ and class I being split initially into sub-classes PI3K-C1a and PI3K-C1b, with PI3K-C1a then being split into three different isoforms, PI3K-C1a α , PI3K-C1a β and

PI3K-C1a δ , dependent on the p110 subunit, see Table 1.5, (110,111). The class II and III PI3-kinases are all unable to generate phosphatidylinositol 3,4,5-tris-phosphate (PI(3,4,5)P₃ or PIP₃) suggesting that they are not involved in insulin signalling to PIP₃ dependent downstream effectors. Class II PI3K mediated increases in PI(3)P are thought to play a role in insulins ability to increase glucose transport, (110), and the PI3K-Class 3 isoform is thought to play a role in sensing amino acid deprivation and regulating activation of mTOR, (112,113). This idea is discussed in detail in Section 1.6.2.5.3. All of the class I PI3-kinases are able to generate PIP₃ and thus activate downstream effectors but PI3K-C1a δ and PI3K-C1b are unlikely to be involved in insulin signalling as they are not highly expressed in insulin sensitive tissues, leading to the conclusion that PI3K-C1 α and/or PI3K-C1 β must play the major role in PIP₃ generation in insulin signalling to protein synthesis, (110), and will be referred to as PI3K in the rest of this thesis unless another class is specifically mentioned.

PI3K is activated when it is recruited to IRS1/2 upon tyrosine phosphorylation of IRS1/2 as discussed in Section 1.6.2.1. The two SH2 domains on the PI3K p85 adaptor sub-unit dock with IRS1/2 phosphorylated tyrosines. This leads to activation of the p110 catalytic subunit which phosphorylates the D-3 position on the inositol ring of phosphoinositides, (111), located in the plasma membrane, leading to increased PIP₃ generation from the substrate PI(4,5)P₂, (110). This local increase in PIP₃ triggers the PI3K mediated signal transduction cascade by facilitating co-localisation of PIP₃-dependent protein

Table 1.5: Different classes of PI3K

<i>PI3K Class</i> <i>(named dependent on P110 subunit)</i>	<i>Expression in insulin-responsive tissues/ Insulin sensitivity</i>	<i>Sensitivity to PI3K Inhibitors</i>	<i>Phosphoinositide generated</i>
PI3K-Class 1α	Expressed in insulin sensitive tissues. Stimulated by insulin.*	Sensitive to Wortmannin and LY294002.+	PI(3,4,5)P3
PI3K-Class 1β	Expressed in insulin sensitive tissues. Stimulated by insulin*	Sensitive to Wortmannin and LY294002.+	PI(3,4,5)P3
PI3K-Class 1δ	Not highly expressed in insulin sensitive tissues. Stimulated by insulin*	Sensitive to Wortmannin and LY294002.+	PI(3,4,5)P3
PI3K-Class 1b	Not highly expressed in insulin sensitive tissues.* No evidence of insulin activation.+	Decreased sensitivity to Wortmannin and LY294002.+	PI(3,4,5)P3
PI3K-Class 2α	Widely expressed. Stimulated by insulin.+	Decreased sensitivity to Wortmannin and LY294002.#	PI(3)P
PI3K-Class 2β	Widely expressed. Stimulated by insulin.+	Sensitive to Wortmannin but decreased sensitivity to LY294002.#	PI(3)P
PI3K-Class 2γ	Widely expressed. Stimulated by insulin.+	Decreased sensitivity to Wortmannin and LY294002.+	PI(3)P
PI3K-Class 3	Widely expressed.+	Sensitive to Wortmannin and LY294002.+	PI(3)P

(110)* (111)+ (115)#

kinase1 (PDK1), and PKB which contain PH domains that tightly bind to PIP₃, (111). PDK1 and mTORC2 then phosphorylate PKB leading to its activation. The PI3K signal is attenuated by the activation of a protein known as phosphate and tensin homolog on chromosome 10 (PTEN), which dephosphorylates the PIP₂ and PIP₃ generated by PI3K, (114).

1.6.2.3 PKB

There are three different isoforms of the serine threonine kinase protein kinase B (PKB) (also known as Akt); PKB- α , PKB- β and PKB- γ , (116,117). All three isoforms have a pleckstrin homology domain (PH domain), a kinase domain and at least one phosphorylation site, (117). The α and β isoforms are phosphorylated at Thr³⁰⁸ and Ser⁴⁷³ but PKB- γ is only phosphorylated at Thr³⁰⁸ due to it having a truncated C-terminal, (116).

Current information regarding any differences in function and cell specificity between the three isoforms is sparse. In a variety of human tumour cell lines different isoforms of PKB appear to be predominantly responsible for cell proliferation and survival but no single isoform was essential, (118). In concurrence with this both PKB- α and PKB- β knockout mice suffer from impaired growth, but double knockout mice (PKB- α and PKB- β) suffer from *severely* impaired growth suggesting that the functions of PKB- α and PKB- β overlap somewhat, (119). In contrast, differences between PKB- α , PKB- β and PKB- γ null mice do suggest some differences in function between different isoforms or cell lines, (119). PKB- β knockout mice show a tendency towards diabetes suggesting that PKB- β may play a greater role in glucose

homeostasis that the other PKB isoforms, (120). PKB- γ knockout mice were found to suffer from a small brain suggesting that PKB- γ may be predominantly localised to the cells of the central nervous system, (119).

Upon PI3K activation and PIP₃ generation the PH domain of PKB binds to PIP₃, bringing PKB to the plasma membrane and into close proximity to PIP₃-dependent protein kinase 1 (PDK1) which also features a PIP₃ binding PH domain, (116). In order to become fully active PKB must be phosphorylated at both Threonine³⁰⁸ and Serine⁴⁷³. Phosphorylation at Thr³⁰⁸ by PDK1 is dependent on prior phosphorylation of Ser⁴⁷³, (121), leading to easier recognition of PKB by PDK1, and increased phosphorylation of Thr³⁰⁸, (122). The kinase which phosphorylates Ser⁴⁷³ is often referred to as PDK2 due to the assumption that this, as yet uncloned, kinase would share homology with PDK1, (116), especially as localisation of PKB to the plasma membrane is key to efficient phosphorylation of Ser⁴⁷³, (121), suggesting that its kinase might also have a PH domain, (116). However, it has now been elucidated that the Ser⁴⁷³ kinase is the mammalian target of rapamycin (mTOR), functioning as part of the mTOR complex 2, discussed in Section 1.6.2.5.2, (122).

Once it has been dual-phosphorylated PKB is able to translocate within the cytosol or into the nucleus and mediate phosphorylation of its downstream targets, (117).

1.6.2.4 Downstream targets of PKB.

Immediately downstream of PKB are the tuberous sclerosis complex proteins TSC1 (Hamartin) and TSC2 (Tuberin), (123). Phosphorylation of TSC2 by PKB leads to their inactivation. When active the TSC1/TSC2 complex inhibits the activity of a G-protein called Rheb, (Ras homolog enriched in brain), as TSC2 acts as a GTPase activating protein for Rheb, (114). Rheb is thought to directly interact with and activate mammalian target of rapamycin (mTOR), (112), so PKB phosphorylation and inhibition of the TSC1/2 complex indirectly activates mTOR, (123).

Another downstream target of PKB is the protein kinase glycogen synthase kinase-3 (GSK-3), which is inhibited when phosphorylated by PKB, thus relieving its inhibition of eukaryotic initiation factor 2B, (124), discussed further in Section 1.6.2.12.1. PKB can also phosphorylate mTOR directly on Ser²⁴⁴⁸ and Thr²⁴⁴⁶, (123), but evidence suggests that this is not required for mTOR activation, (114).

1.6.2.5 Mammalian Target of Rapamycin.

Mammalian target of rapamycin (mTOR) is a serine/threonine kinase with a molecular weight of around 280kDa, (112), which plays a central role in cellular growth responses to nutrients, hormones and growth factors, (125), by regulating mRNA translation, ribosome biogenesis and nutrient metabolism, (126). mTOR exists in two different complexes, mTOR complex 1 (mTORC1) and mTOR complex 2 (mTORC2), (127,128).

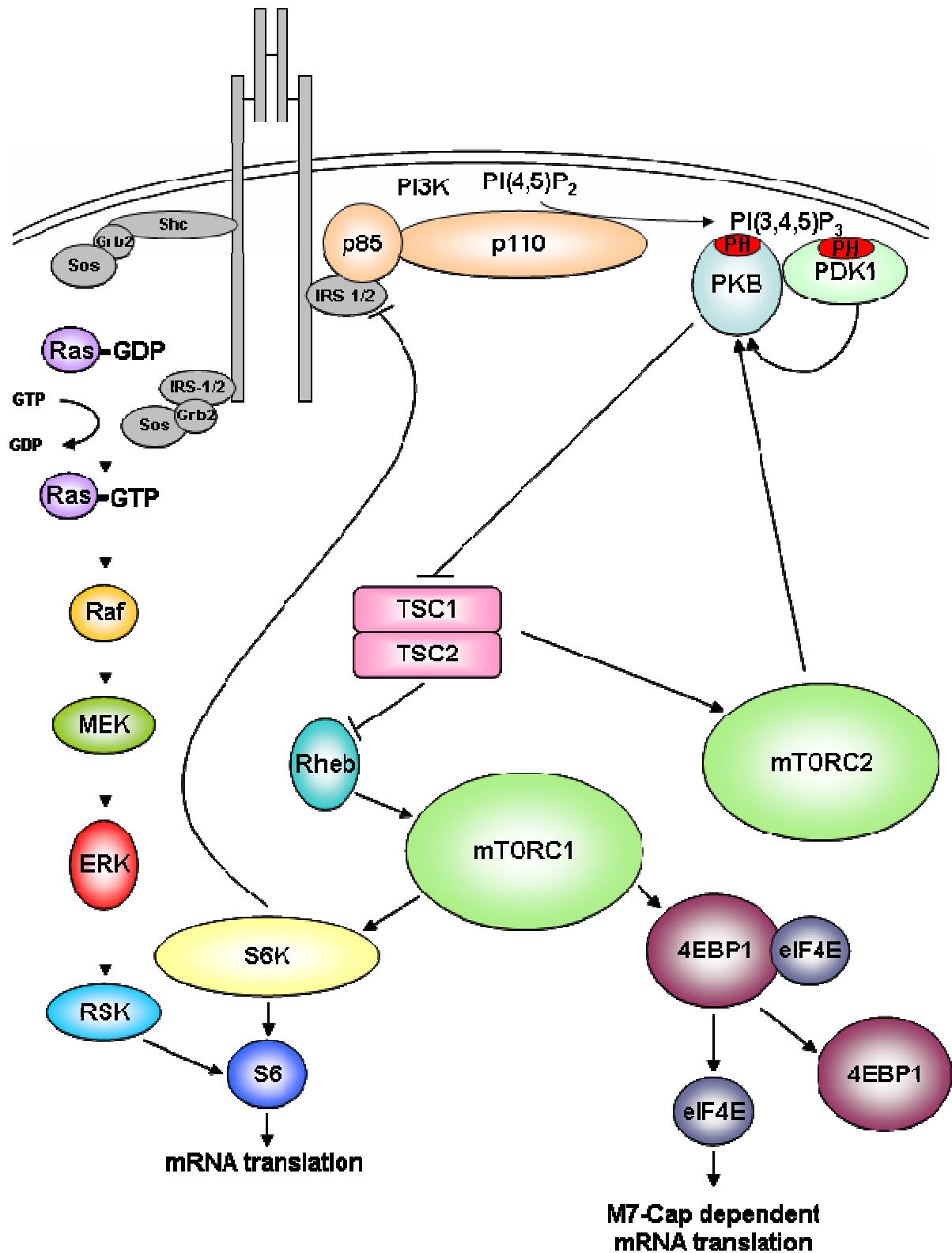


Figure 1.9: The PI3K-mTOR and MEK-ERK signalling pathways

This figure depicts the PI3K-mTOR and MEK-ERK branches of the insulin signalling pathway, described in the text in sections 1.6.2.2 to 1.6.2.11.1.

Proteins are shown schematically as individually labelled coloured circles. This diagram is drawn from information obtained from sources referenced in the main text and items are not drawn to relative scale.

1.6.2.5.1 mTORC1

mTORC1 is a rapamycin sensitive complex consisting of mTOR bound to G protein β -subunit-like protein (G β L), (also called mammalian LST8), (114,127,128), and regulatory associated protein of mTOR (Raptor), (114,127,128). This complex binds to the downstream effectors of mTOR; S6 kinase 1 (S6K1) and eukaryotic initiation factor 4E binding protein 1 (4EBP1), via Raptor which recognises TOR signalling (TOS) domains on downstream effectors and binds to them bringing mTOR into close proximity to its substrates and therefore facilitating mTOR mediated phosphorylation of S6K1 and 4EBP1, (112). Raptor has been found to be an absolute necessity for 4EBP1 phosphorylation, and to greatly enhance S6K1 phosphorylation, by mTOR, (129). G β L is also an important part of this complex and is thought to stabilise the mTOR-raptor interaction and increase the kinase activity of mTOR, in fact decreased levels of G β L lead to decreased phosphorylation of S6K1, (125).

Rapamycin inhibits mTORC1 by destabilising the mTOR-raptor interaction leading to a decrease in the phosphorylation of downstream targets, (114).

1.6.2.5.2 mTORC2

The second mTOR complex, mTORC2, is a rapamycin insensitive complex, (127,124) and includes a greater number of proteins than mTORC1. It is currently thought to include; mTOR and G β L, (as in mTORC1), PRR5, mSin1, Hsp70 and a protein called rapamycin insensitive companion of mTOR (Rictor), (130).

It was determined by Sarbossov et al (2005) (122), that mTORC2 is actually the kinase often referred to as PDK2, (see Section 1.6.2.3), which is responsible for phosphorylating PKB on Serine⁴⁷³. In order for mTOR to phosphorylate PKB it must be in association with Rictor, Raptor can not act as a substitute, (122), illustrating that the association of mTOR within the two different protein complexes, mTORC1 and mTORC2, allows it to carry out two very different roles within the cell.

As phosphorylation of S6K1 and 4EBP1 are often used as a measure of mTOR activity, mTORC1 has been studied much more extensively than mTORC2, (127). As such, the method of activation of mTOR outlined in Section 1.6.2.4 refers to mTORC1 and not to mTORC2.

It has been reported that mTORC2 is activated in a growth factor sensitive manner, although exact mechanisms have not been determined, (122,126,128). However, recent work by Huang et al (2008) in various cell types has proposed a mechanism whereby the TSC1/2 complex is able to interact directly with mTORC2 and positively regulate it when active. This suggests a mechanism whereby the TSC1/2 complex in its constitutively active state inhibits Rheb, and therefore mTORC1, but activates mTORC2 leading to the permissive Ser⁴⁷³ phosphorylation of PKB. Subsequent full activation of PKB by phosphorylation of Threonine³⁰⁸ when insulin and other growth factors are present then leads to inactivation of TSC1/2 and activation of Rheb and mTORC1, (131). In this way mTORC2 may mediate an increase

in the activation of mTORC1 and growth rate when the cell is stimulated with insulin and other growth factors.

Subsequent mention of mTOR in this thesis will refer to mTORC1 unless otherwise stated.

1.6.2.5.3 *mTOR as an amino acid sensor.*

In addition to its ability to respond to hormones, such as insulin, it has also been well documented that mTOR is able to respond to nutrient availability, (112,114), being especially sensitive to amino acid, glucose and ATP availability, (125). The regulatory effect that amino acids have on mTOR mediated signalling shall be the main focus of this discussion.

Amino acids were first noted as possible signalling molecules in the early 1980's, when increases in protein synthesis were observed upon amino acid stimulation, (112). It became apparent in the late 1990's that the mTOR pathway was involved in this process as phosphorylation of S6K1 and 4EBP1 was found to be decreased in conditions of amino acid deprivation, (112). Both raptor and GβL have been implicated in conveying nutrient sensitivity to mTOR. Raptor is generally thought to have a positive effect on mTOR signalling, bringing mTOR into close proximity to its downstream substrates by acting as an adaptor protein, (114,127,129). GβL increases the kinase activity of mTOR, and it has been suggested that it may play an important role in nutrient activation of mTOR by stabilising the mTOR-raptor association, (125). However there have also been reports that raptor binding to mTOR in a

very stable association during amino acid deprivation may inhibit mTOR mediated activation of S6K1 and 4EBP1, (125,132), and that overexpression of raptor can lead to decreased phosphorylation of 4EBP1, (129).

A model of raptor and mTOR association in amino acid deprivation proposed by Kim et al (2002), (132) appears to explain this discrepancy by suggesting that mTOR and raptor exist in different “nutrient determined” states. They describe a loose association in a nutrient rich environment, allowing normal mTOR-raptor associated phosphorylation of downstream targets, and a tight association in a nutrient deprived environment which led to decreased phosphorylation of S6K1 and 4EBP1, (132). In a more recent study by the same group it was also suggested that this, nutrient deprivation induced, inhibitory association between mTOR and raptor may reverse the positive effect of GβL on mTOR kinase activity, (125). However, a more recent study by Oshiro et al (2004), (133), has refuted this model, stating that rapamycin induces mTOR and raptor dissociation and decreases phosphorylation of S6K1 and 4EBP1, but amino acids do not induce a weaker association between mTOR and raptor than that seen in amino acid deprivation.

This implies that Rapamycin and amino acid deprivation have different sites of action when it comes to inhibition of mTOR. This idea is supported by two observations:

- 1) Over-expression of Rheb can overcome the decreased S6K1 phosphorylation observed during amino acid deprivation, but not the corresponding decrease observed in response to Rapamycin, (134)

2) Decreased expression of TSC1/TSC2 can reverse the observed decrease in S6K1 phosphorylation during amino acid depletion, (135), but not during Rapamycin treatment, (133).

This suggests that amino acid deprivation is not sensed by mTOR or its associated proteins and does not inhibit mTOR kinase activity by destabilising the mTOR-raptor relationship but instead that there must be amino acid sensors upstream from Rheb.

It appears to be unlikely that TSC1/2 are involved in amino acid sensing as constitutive activation of S6K1, observed in TSC2 siRNA knockdown cells, was abolished in amino acid starvation, (113), determining that amino acid deprivation is able to down-regulate S6K1 activity without a requirement for a functioning TSC1/2 complex. In agreement with observation number one above siRNA knockdown of Rheb blocks the amino acid induced increase in S6K phosphorylation, (113), suggesting that Rheb may act as an amino acid sensor, especially as it is ideally situated to regulate the activity of mTOR. However amino acid treatment alone is not sufficient to increase the amount of GTP bound Rheb, (112), suggesting that stimulation via the insulin signalling pathway may also be required, and that the amino acid and insulin mediated effects on mTOR signalling may not be mediated via the same pathway.

This observation is concurrent with further observations that insulin and amino acid deprivation inhibited the phosphorylation of both PKB and S6K1,

but the re-addition of amino acids only restored the phosphorylation of S6K1, and in a wortmannin sensitive manner, (112). The lack of PKB phosphorylation appeared to rule out a role for the class I PI3Ks in amino acid sensitivity, but the wortmannin dependent nature of the amino acid mediated response led to the investigation of the class III PI3K, mammalian vacuolar protein sorting 34 homologue (hVPS34), as a potential amino acid sensor, (112).

The class III PI3K, as noted in Table 1.5, is widely expressed and phosphorylates its substrate PI to produce PI(3)P, (meaning it is not involved in PIP₃ dependent insulin signalling), in a wortmannin sensitive manner, (111). The potential of hVPS34 as an amino acid sensor was investigated by Nobukuni et al, (113). They determined that amino acid starvation led to a decrease in the activity of hVPS34 and a decrease in PI(3)P levels, with an increase in hVPS34 activity, and PI(3)P levels, being observed upon re-addition of amino acids in HeLa, HEK293 and MEF cells. In addition to this, separate siRNA knockdown of both hVPS34, and its associated protein hVPS15 (which catalyses hVPS34s kinase activity), led to significant inhibition of amino acid stimulated S6K phosphorylation, (112). This data strongly supports the idea that hVPS34 acts as a, wortmannin sensitive, nutrient sensor, which then regulates mTORC1 activity and protein synthesis rates dependent on nutrient availability, and that activation of hVPS34 is required for activation of mTORC1 and its downstream targets. The exact regulatory mechanisms of this process remain to be determined.

Paradoxically, activation of hVPS34 is also required for induction of the catabolic process of autophagy, a cell protective mechanism which involves the lysosomal degradation of non-vital cytosolic components, thus allowing the continuation of vital cellular functions, in times of nutrient starvation. In conditions of nutrient sufficiency mTORC1 inhibits autophagy by phosphorylating components of the autophagy pathway. It has been suggested that these two conflicting processes are able to occur as a result of hVPS34 activation due to the existence of several different complexes containing hVPS34 thought to control different cellular processes, (136).

In addition to Rheb and hVPS34, several other proteins involved in the sensing of amino acid status and signalling to mTORC1 have also recently been proposed, including Rag GTPases, (137), the kinase MAP4K3, (138), and prolyl hydroxylases whose substrate α -ketoglutarate may respond to changes in amino acid (L-Glu and L-Gln) concentration through the action of transaminases, (139).

The Rag family of GTPases consists of 4 proteins; RagA, RagB, RagC and RagD, which exist in hetero-dimers of either RagA or RagB and RagC or RagD, (137). Very recently described studies in HEK293 cells have shown that expression of mutant Rag-GTPases, permanently bound to GDP (Rag^{GDP}), decreased the activity of mTORC1, while mutants permanently bound to GTP (Rag^{GTP}) increased the activity of mTORC1 and made it resistant to inhibition by amino acid starvation. Furthermore shRNA knockdown of Rag GTPases decreased amino acid stimulation of S6K1

activity. Decreased expression of Rag GTPases also suppressed the anabolic effects of insulin on S6K1 activity, but the observed increase in mTORC1 activity in the presence of Rag^{GTP} mutants was only apparent in the presence of insulin. This implies that there are two separate pathways mediating activation of mTORC1 by insulin and amino acids, possibly via activation of Rag-GTPases, (137). The authors, (137), therefore suggest that amino acids, signalling through Rag GTPases, mediate the translocation of mTORC1 into close-proximity to Rheb, thus explaining why insulin cannot activate mTORC1 in the absence of amino acids, (137). The precise mechanism through which amino acids might regulate Rag GTPases remains to be determined.

Two other proteins which have been suggested as potential amino acid sensors are the translationally controlled tumour protein (TCTP) and FK506-binding protein, 38kDa (FKBP38). TCTP was described as being a guanine-nucleotide exchange factor for Rheb in *Drosophila* and would therefore be expected to activate mTORC1, (140). FKBP38 has also been described as playing a role in Rheb mediated activation of mTORC1, although in this case in an inhibitory role where FKBP38 binds to and inhibits mTORC1 activity, but is also able to bind to Rheb in its GTP bound form therefore removing FKBP38 from its inhibitory association with mTORC1, (140). A role for both of these proteins in sensing amino acids and mediating the downstream effects on mTORC1 has recently been contested due to studies in HEK293 cells, (140), which determined that over-expression of TCTP does not reverse the inhibitory effect of amino acid starvation on phosphorylation of 4EBP1, (140), and, although FKBP38 can bind to mTORC1 it does so with the same affinity

in both anabolic (insulin treatment), and catabolic (amino acid starvation), conditions, (140).

1.6.2.6 Downstream of mTOR

Directly downstream of mTOR are the S6 kinases and eukaryotic initiation factor 4E binding proteins (4EBPs).

1.6.2.7 4EBP1

Eukaryotic initiation factor 4E binding proteins (4EBPs) are important translational repressors that inhibit translation initiation by tightly binding to eIF4E (see Section 1.6.1.1) in their hypo-phosphorylated state, (114). When bound to a 4EBP eIF4E is unable to bind to eIF4G as both eIF4G and the 4EBP compete for the same binding site on eIF4E, (141).

There are three different 4EBP isoforms; 4EBP1, 4EBP2 and 4EBP3, (142), but the majority of studies have focused on 4EBP1, (114). Hyper-phosphorylation of 4EBP1 by mTOR leads to its inactivation and release of eIF4E, (142). There are seven different phosphorylation sites on 4EBP1; Thr³⁷, Thr⁴⁶, Thr⁷⁰, Ser⁶⁵, Ser⁸³, Ser¹⁰¹ and Ser¹¹², and of these the first four listed are especially important, (114). In 293 cells phosphorylation is known to proceed in a particular order, with phosphorylation of Thr³⁷ and Thr⁴⁶ occurring before phosphorylation of Thr⁷⁰ and then finally Ser⁶⁵, (114). Upon phosphorylation of Ser⁶⁵ eIF4E is released from 4EBP1, possibly due to electrostatic repulsion between phosphorylated sites on 4EBP1 and closely situated acidic amino acids on eIF4E, (114). Once released eIF4E is able to

bind to eIF4G, thus completing the eIF4F complex and promoting initiation of translation in mRNAs with a m⁷G-capped 5' end, see Section 1.6.1.1.

1.6.2.8 S6 Kinases

There are two distinct S6 kinase genes in mammals, S6K1 and S6K2, both of which have two isoforms, (143); S6K1, p70(α II) and p85(α I), and S6K2, p54(β II) and p60(β I), which all have highly conserved functional domains, (144). The S6K2 variant was characterised much later than S6K1, (114), and therefore the majority of studies looking at S6 kinases have focused on S6K1 which will be the main focus here.

In its inactive state S6K1 (and 4EBP1) is bound to the scaffold protein eIF3, but dissociates from this initiation factor once phosphorylated by mTOR, (127), allowing PDK1 mediated phosphorylation of S6K1 at Thr²²⁹ to occur leading to complete activation of S6K1. Despite the fact that PDK1 is resistant to rapamycin, activation of S6K1 occurs in a rapamycin sensitive manner, as S6K1 must be phosphorylated at five serine-threonine phosphorylation sites in a specific order, (Ser⁴¹¹, Ser⁴¹⁸, Thr⁴²¹, Ser⁴²⁴, Ser³⁷¹), (144), and then by mTOR at Thr³⁸⁹, prior to PDK1 mediated phosphorylation of Thr²²⁹, (145). The phosphorylation of Thr³⁸⁹ by mTOR correlates most closely with S6K activity, (127,145), suggesting that it is the most vital phosphorylation event in S6K activation. As phosphorylation at some of the other Ser/Thr residues is rapamycin sensitive it appears likely that their phosphorylation also occurs in an mTOR regulated manner, (145).

Once activated S6K1, like mTOR, is able to stimulate protein synthesis, (144), and regulate cell mass by controlling mRNA translation, (114,126,144), via its downstream targets.

1.6.2.9 Phosphorylation targets of S6K1

One phosphorylation target of S6K1 is IRS-1 (see Section 1.6.2.1), which it inhibits via a negative feedback mechanism. S6K1 phosphorylates IRS-1 on Ser³⁰⁷, (144), leading to an inhibition of the interaction between IRS-1 and the insulin receptor and ultimately to down regulation of the PI3K signalling pathway, (112).

There are also several downstream targets of the S6 kinases which could mediate their effects on protein synthesis, the most extensively studied of these is ribosomal protein S6 (rpS6), which was the first substrate of S6K1 to be discovered.

1.6.2.10 Ribosomal protein S6

Ribosomal protein S6 is one of the 33 40S ribosomal subunit proteins, (146), and is located at the mRNA and tRNA binding site at the interface between the large and small ribosomal subunits, (143). Activation of rpS6 occurs upon the phosphorylation of five serine residues with Ser²³⁶ phosphorylation occurring first followed by phosphorylation of Ser²³⁵, Ser²⁴⁰, Ser²⁴⁴ and Ser²⁴⁷ in that order, (146). Both S6K1 and S6K2 are able to phosphorylate rpS6 at all of these phosphorylation sites and ribosomal S6 kinase (RSK), a

downstream target of the mitogen activated protein kinase (MAPK) pathway is able to phosphorylate the Ser^{235/236} residues, (147).

A correlation between the activation of rpS6 and translation of a mRNA subset called 5' tract of pyrimidines (TOP) mRNAs, (114), which contain a short pyrimidine sequence at their 5' end, (101,114), and encode proteins that are involved in translation, such as ribosomal proteins and elongation factors, (143,145), led to the belief that S6K1 activation by mTOR and subsequent activation of rpS6 could control translation of 5' TOP mRNAs. This was supported by observations of rapamycin sensitivity in the translation of 5' TOP mRNAs, which could be overcome in cells expressing a rapamycin resistant S6K1, (101,114).

However, this theory has recently been challenged as translation of 5' TOP mRNA translation was found to be unaffected, as compared to wild-type (wt), in S6K1^{-/-}/S6K2^{-/-} deficient mice, (148). In addition to this, studies on mouse embryonic fibroblast (MEF) cells, where the phosphorylatable serine residues in rpS6 were replaced with alanine residues, showed that 5' TOP mRNA translation was not decreased in these cells as compared to wt, (149). Ruvinsky et al also considered the effect of rpS6 phosphorylation on global protein synthesis and found that total inhibition of rpS6 in mouse embryonic fibroblasts (MEFs) from rpS6^{P-/-} mice did not lead to a decrease in protein synthesis, (149). However, it was determined that MEF cells containing non-phosphorylatable rpS6 were significantly smaller than their wt counterparts and did not reduce further in size in the presence of rapamycin, an

observation matched in β -cells and myoblasts, (149). This suggests that rpS6 is an important downstream effector of mTOR, playing a role in determining cell growth via, as yet, un-elucidated mechanisms.

1.6.2.10.1 eIF4B, eEF2 kinase and SKAR

There are several other less studied targets of S6K1 which could contribute to the effects of S6K1 and S6K2 activation on cell growth.

The initiation factor eIF4B, for example, enhances the activity of the RNA helicase eIF4A, part of the eIF4F complex, which unwinds secondary structures in the 5' UTR of mRNA, (see Section 1.6.1.1). Direct phosphorylation of eIF4B by S6K1 increases its activity and therefore leads to an increase in the translation of mRNAs with a large amount of secondary structure in the 5' UTR, (143). Furthermore it has been observed that S6K1 phosphorylation of a tumour suppressor protein, which under basal conditions binds to eIF4A and inhibits its activity, can lead to degradation of the suppressor protein resulting in increased activity of eIF4A, (144). Thus S6K1 has a role in increasing the activity of both eIF4A and eIF4B and therefore in increasing mRNA translation.

Although initiation is the most highly regulated step in translation there are also substrates of S6K1 which determine the rate of translation elongation. The elongation factor eEF2 mediates the translocation phase of translation elongation, (see Section 1.6.1.2), but in basal conditions is phosphorylated by its kinase eEF2 kinase. Once activated, S6K1 phosphorylates eEF2 kinase

leading to inactivation of the kinase and increased activation of eEF2 and therefore an accelerated rate of elongation, (143,144).

There is also evidence to suggest that S6K1 may phosphorylate nuclear proteins, such as SKAR, which have a role in transcription, pre-mRNA splicing and mRNA export from the nucleus, (112,144). As siRNA knockdown of SKAR led to a decrease in cell size similar to that observed in S6K1 knockdown it is thought that SKAR could play a role in S6K1 mediated control of cell growth, although confirmation of this idea is still required, (144).

1.6.2.11 The MEK-ERK signalling pathway

The core proteins involved in the mitogen activated ERK kinase, (MEK), (82), extracellular signal-regulated kinase (ERK), (150), mitogen activated protein kinase (MAPK) pathway are Ras, Raf, MEK and ERK, each of which phosphorylates the next protein in the sequence upon activation, (82), (see Figures 1.8 and 1.9).

Activation of a receptor tyrosine kinase (RTK), such as the insulin receptor, leads to the exchange of GDP for GTP on the G-protein Ras, as described in Section 1.6.2.1, and ultimately to activation of the Raf family of proteins by Ras-GTP. The activation of Raf by Ras-GTP is a complex multi-step process reviewed in, (82,150), and will not be discussed in detail here.

There are three members of the Raf family; A-Raf, B-Raf and C-Raf, all of which are able to phosphorylate two serine residues in the activation loop on

MEK1 and MEK2, (Ser²¹⁸ and Ser²²² on MEK1), (151), thus triggering the signal amplifying MEK-ERK phosphorylation cascade, (82,150). The MEK proteins are able to phosphorylate their downstream targets, predominantly ERK, on serine, threonine and tyrosine residues leading to their activation, (82,151).

1.6.2.11.1 ERK

The serine/threonine kinase, ERK, is encoded by two different genes giving rise to two isoforms of ERK. The 44kDa ERK isoform, ERK1 and the 42kDa isoform, ERK2 are both phosphorylated exclusively by the MEKs on a threonine and a tyrosine residue, (151). Activation of ERK positively regulates protein synthesis, an effect which is mediated via a large number of downstream cytosolic and nuclear substrates.

In the nucleus activated ERK, either directly or indirectly, (via phosphorylation of intermediate substrates such as RSK), phosphorylates and activates a number of transcription factors leading to increased transcription, (82).

The activity of ERK in the cytoplasm brings about increases in translation via two substrate families; ribosomal S6 kinases 1-4 (RSK1-4) and map kinase-interacting kinases Mnk1 and Mnk2, (151). The Mnk proteins increase translation by phosphorylating eIF4E which some studies suggest increases the rate of translation initiation by as yet unknown mechanisms, (145). The RSK family of proteins are thought to provide crosstalk between the MEK-ERK and mTOR signalling pathways, (145,151). One mechanism by which

this is thought to occur is through the inhibitory phosphorylation of TSC2, mediated by either ERK or the RSKs, which leads to mTOR activation, (145). This crosstalk also occurs due to RSK mediated phosphorylation of downstream targets of S6K, such as eEF2 kinase and eIF4B, (145), discussed in Section 1.6.2.10.1. RSK mediated phosphorylation of rpS6 on Ser^{235/236}, two of its five phosphorylation sites, has also been observed, (147), suggesting that ERK mediated RSK activity may play a role in increased cell growth via rpS6 phosphorylation, however activated S6Ks are also required for complete rpS6 phosphorylation, (147). These pathways are functionally important in skeletal muscle because they mediate the anabolic effect of the β_2 -adrenergic agonist Clenbuterol, (152).

1.6.2.12 Insulin signalling to translation initiation via eIF2

The eukaryotic initiation factor eIF2 is one of the components of the ternary complex (eIF2.GTP.Met-tRNA_i) which mediates binding of the initiator tRNA to the 40S ribosome in translation initiation, as discussed in Section 1.6.1.1.

eIF2 is a multimeric protein, (153), consisting of three subunits; α , β and γ . The α -subunit has a phosphorylatable serine residue, Ser⁵¹, the β -subunit binds to eIF2B and eIF5, which control the binding and dissociation of GTP to eIF2, and the γ -subunit binds GTP and Met-tRNA_i, (153).

Initially eIF2 exists in a GDP bound form, in order to bind to the initiator tRNA eIF2 must first dissociate from GDP and bind to GTP. This process is mediated by the guanine nucleotide exchange factor, (GEF), eIF2B. The binding of eIF2.GTP to Met-tRNA_i is then promoted by the protein ABC50,

(Figure 1.10), after which formation of the 43S pre-initiation complex occurs. Upon start codon recognition the GTPase activator protein (GAP), eIF5, hydrolyses the eIF2 bound GTP to GDP leading to eIF2.GDP release from the ribosome and the transition to translation elongation, (153,154).

1.6.2.12.1 eIF2B

The main regulatory protein in this cyclic pathway is the GEF eIF2B which can be phosphorylated by the kinase GSK-3, (Figure 1.10), (124). In basal conditions the kinase GSK-3 phosphorylates and inhibits eIF2B, which is active in its de-phosphorylated state. Upon insulin stimulation phosphorylation of eIF2B is attenuated as GSK-3 is inhibited by PKB phosphorylation, leading to an increase in eIF2B activity, an increase in eIF2.GTP complexes and ultimately an increase in global protein synthesis, (154).

1.6.2.12.2 eIF2- α

Once phosphorylated on Ser⁵¹ eIF2- α becomes a potent competitive inhibitor of eIF2B, preventing exchange of GDP for GTP on eIF2, and therefore preventing ternary complex production. Even low levels of eIF2- α phosphorylation can inhibit eIF2B and translation initiation because the intracellular concentration of eIF2B is much lower than that of eIF2, (154).

1.6.2.12.3 eIF2 kinases

There are currently four known eIF2 kinases that exist in mammalian cells; 1) haem-regulated inhibitor (HRI), which is activated in haem deprivation, 2) RNA dependent protein kinase (PKR), which becomes activated in response

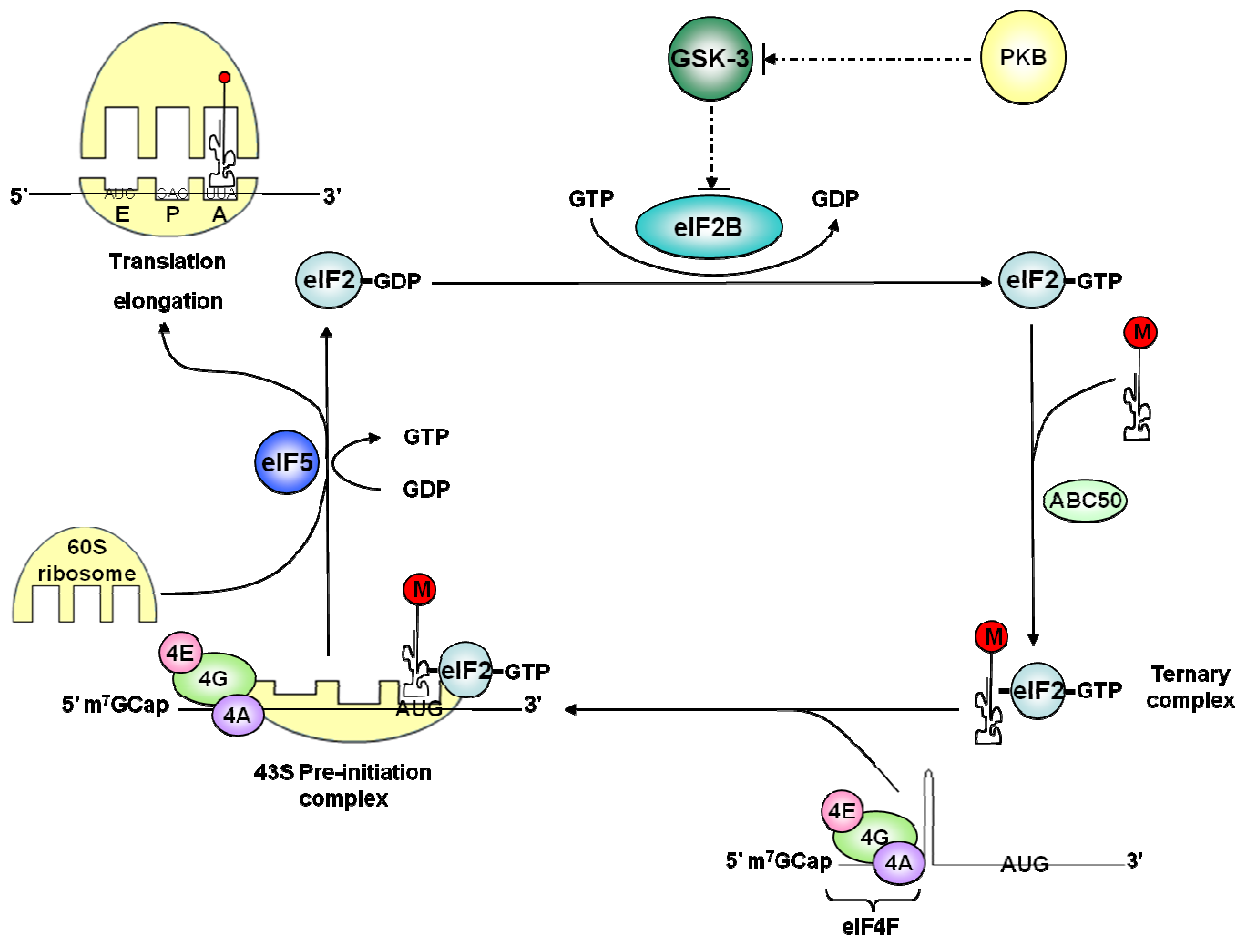


Figure 1.10: Signalling to eIF2

This figure depicts signalling to eIF2, described in the text in sections 1.6.2.12. Enzymes and initiation factors are shown schematically as individually labelled coloured circles or ellipses. This diagram is re-drawn from Proud (2005), (154).

to double stranded RNA, such as may be encountered in viral replication, 3) PKR-like endoplasmic reticulum (ER) kinase (PERK), activated in response to ER stress, and 4) general control non-derepressible-2 (GCN2), which is activated in amino acid starvation due to the accumulation of un-charged t-RNA, (all reviewed in (154)).

Activation of each of these eIF2 kinases occurs due to different cellular stresses. As they all phosphorylate the same target the activation of each will elicit a similar response through eIF2, with the possibility of further stress-specific responses occurring, dependent on the phosphorylation of additional downstream substrates of the particular eIF2 kinase that is activated in that stress response. This gives rise to an integrated response when cells are subjected simultaneously to multiple stresses, and is known as the integrated stress response, (154). This inhibition of eIF2/eIF2B simultaneously decreases global protein synthesis levels and increases the rate of translation of transcriptional activators, such as activating transcription factor 4 (ATF4), leading to up-regulation of specific proteins, such as those containing an amino acid response element (AARE), (76), with the ability to provide the appropriate stress response, (155). This mechanism is also important in providing negative feedback to switch off the eIF2- α phosphorylation signal, as it leads to increased expression of the protein GADD34 (growth arrest and DNA damage 34) which recruits protein phosphatase 1 (PP1) to dephosphorylate eIF2- α , (156). It has recently been suggested, (157), that GADD34 may also directly act as a phospho-eIF2- α phosphatase.

1.7 Control of proteolysis.

As discussed in Section 1.4.4, cachexia is a major problem in a number of chronic illnesses including CKD, (24). Control of protein degradation is critical as a slight increase in proteolysis (or decrease in protein synthesis) can lead to negative protein balance and, over time, significant protein depletion because of the high rate of cellular protein turnover, (3.5-4.5g of protein/kg per day), (32,158). From the viewpoint of sub-cellular compartmentation there are three major proteolytic systems which mediate the breakdown of cellular proteins. These are lysosomal proteolysis, mitochondrial proteolysis and cytoplasmic/nuclear proteolysis, (159). Cytoplasmic/nuclear proteolysis occurs principally through the ATP-dependent ubiquitin-proteasome system (UPS) Figure 1.11, (158,159), through the ATP-independent Ca-dependent proteases known as Calpains, and through caspases which have a major role in apoptotic cells, (158). In most cells the majority of proteolysis occurs through the UPS, and increased activity of the UPS is responsible for the increase in proteolysis observed in uraemia, and muscle wasting in rats with CKD can be inhibited by inhibitors of the proteasome, (32,158).

The breakdown of proteins via the UPS is mainly regulated by three enzymes, E1, E2 and E3, that mediate the ubiquitination of proteins targeted for degradation (Figure 1.11), (158). Initially an ATP-utilising enzyme, E1, activates ubiquitin (Ub), a small protein co-factor of 76 amino acid residues, by converting its critical carboxy terminal glycine residue into a thiol ester. E1 then transfers the activated Ub to an E2 carrier protein and E3, an ubiquitin ligase, then mediates the coupling of the Ub carboxyl group to a lysine

residue in the protein substrate. This cycle is repeated, with subsequent Ub residues being attached to a lysine residue in the previously attached Ub, until a poly-ubiquitin chain of 4-5 ubiquitin residues has been synthesised and attached to the protein substrate, at which stage the substrate protein can be recognised and degraded by the 26S proteasome, (158).

The 26S proteasome is a multicatalytic protease complex of approximately 60 sub-units which breaks down proteins into small peptides, and occurs in the nucleus and cytosol of all cells. Typically 1-2% of cell mass is proteasome, (158). The two main functional units of the 26S proteasome are the 20S core, where proteolysis occurs, and the regulatory 19S proteasome, which is responsible for recognising the poly-ubiquitin chain attached to substrate proteins, removing the Ub chain to allow Ub recycling, and unfolding of the tertiary structure of the substrate protein in order to allow the protein to fit through the narrow entrance into the 20S proteasome, (24). The 20S proteasome is a barrel shaped structure consisting of 4 ring shaped subunits which appear to be stacked on top of each other. Each of these rings has seven distinct, yet related, subunits, (24). The subunits of the two inner rings have proteolytic activity and break the protein substrate down into peptides 6-12 amino acids in length until the whole polypeptide chain has been degraded, (159). Once the protein has been digested and the resulting peptides of 3-25 residues have been released from the 20S proteasome they are either broken down by cytoplasmic exopeptidases to produce amino acids, (159), or, in antigen-presenting cells, are presented on major histocompatibility complex class I proteins (MHC I), (159).

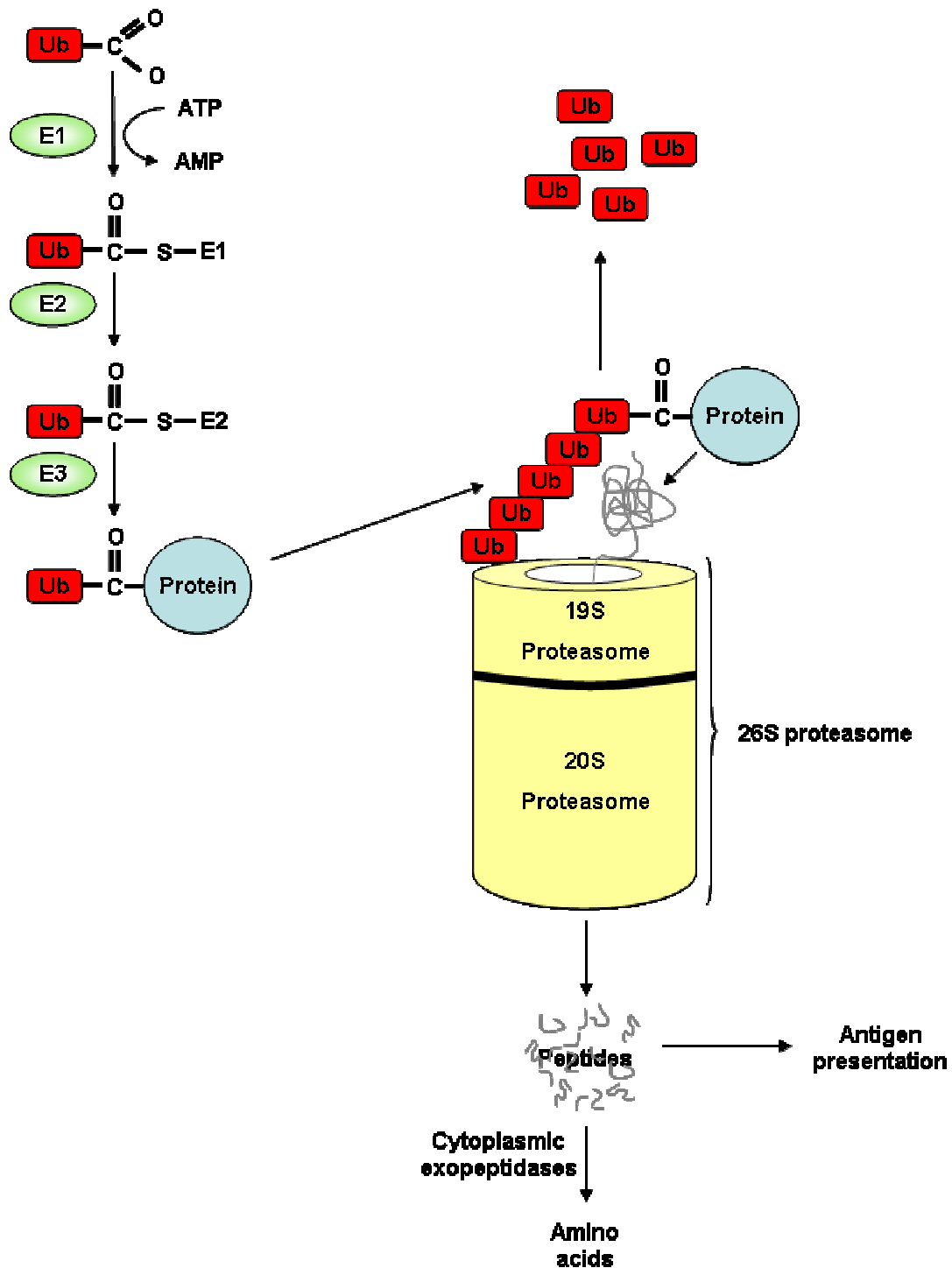


Figure 1.11: Schematic representation of Ub Conjugation of a protein and its subsequent degradation via the ubiquitin proteasome system.

This figure depicts the ubiquitination of a protein targeted for degradation, catalysed by E1, E2 and E3, and shows the entry of the unfolded protein in the 26S proteasome and describes the subsequent breakdown of resultant peptides into amino acids or their role in antigen presentation. Discussed in the text in section 1.7.

Figure re-drawn from information from references cited in the text.

In contrast to the large amount of information available on the regulation of translation (Section 1.6) much remains to be learned about how the increased muscle proteolysis that occurs via the UPS is regulated. Elevated levels of mRNA encoding Ub, (1), and encoding subunits of the 26S proteasome have been observed in uraemic patients, (160), indicating that, in cachexia, part of the regulation is transcriptional. The UPS must display a high level of control because it is responsible for regulating the total quantity of; cellular protein (cell mass) and individual proteins, (24). This control is maintained by the E1, E2 and E3 enzymes, which undertake the ubiquitination of substrate proteins, especially the E3 Ub-ligase group. There is only one form of the E1 protein expressed, but around forty different E2 and over a thousand different E3 Ub ligases, in multiple gene families, have been described, (32,158). Structurally the E3 ligases are of two main types: those with HECT domains (Homologous to E6-AP Carboxy Terminus), and those with RING finger domains. Each E3 ligase is thought to be able to recognise a specific E2-Ubq conjugate, and a protein substrate, and catalyse the transfer of Ub from the E2 protein to that specific protein substrate, (32). Two E3 ligases that are specific to muscle are the F-box protein atrogin-1/MAFbx, and MuRF-1 (muscle ring finger-1), both of which show increased expression during skeletal muscle atrophy, (160). Recent evidence also suggests that tissue-specific activation of proteasome activity in skeletal muscle occurs through proteolytic cleavage of the Rpt6 sub-unit of the proteasome by Caspase-3, (161). This cleavage fails to occur in proliferating cell lines such as myoblasts, and may explain why catabolic stimuli such as metabolic acidosis stimulate global proteolysis in differentiated myotubes but fail to do so in myoblasts, ((161) and Chapters 3 and 4).

Muscle proteolysis has an additional complication in that complexes such as actomyosin, in myofibrils that make up the majority of the protein content of skeletal muscle, are too large to be degraded by the UPS and must first be broken down into actin and myosin fragments by Caspase-3, (162). One of the products of this proteolytic reaction is a characteristic insoluble 14kDa actin fragment which is seen in increased quantities in the atrophying muscle of uraemic rats, (162), and of haemodialysis patients, (163). Caspase-3 mediated actomyosin cleavage only appears to occur in response to a catabolic condition, such as uraemia, and was undetectable in the muscle of control rats. The accumulation of the 14kDa actin fragment and the rate of skeletal muscle proteolysis are both decreased in the presence of a Caspase-3 inhibitor, (162).

In view of the possible role of SNAT2 in regulation of muscle proteolysis in cachexia, it is important to consider whether the SNAT2 protein itself is degraded in such catabolic states. Little is known about the mechanism of SNAT2 degradation in muscle, but evidence in 3T3-L1 adipocytes suggests that it is regulated by NEDD4-2, a HECT E3 Ub ligase, (81).

1.7.1 Coupling of Proteolysis to the Insulin-PI3K-PKB Signalling Pathway.

If there are reduced local concentrations of insulin or IGF-I, or insulin resistance (for example in metabolic acidosis) there is good evidence that signalling through the Insulin/PI-3Kinase/PKB pathway is impaired, (30,164).

In addition to the downstream phosphorylation targets of PKB discussed in

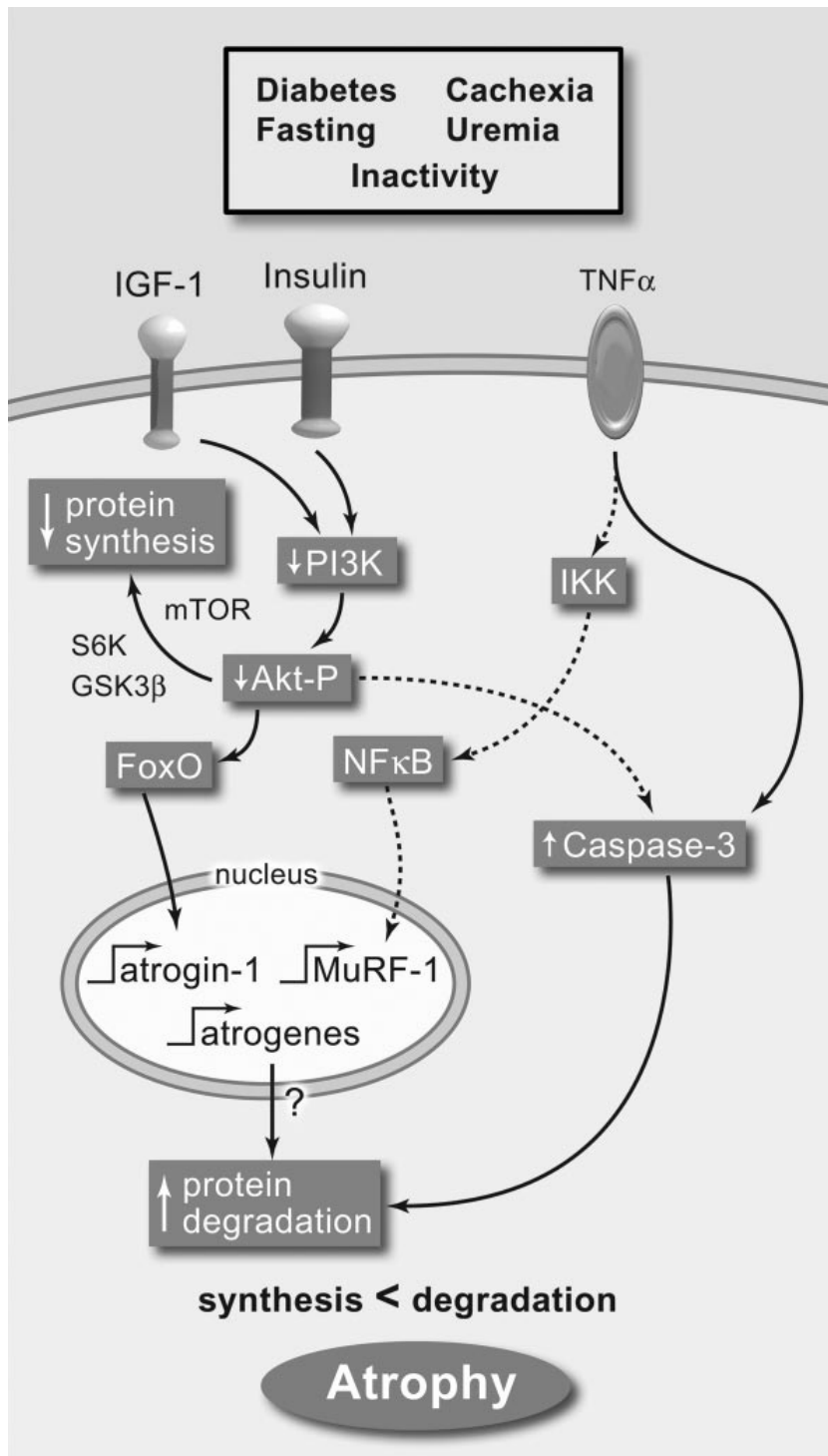


Figure 1.12: The role of impaired PI3K/Akt (PKB) signalling in activation of proteolysis in skeletal muscle in cachexia

This figure depicts the role of the insulin signalling pathway in activating proteolysis in conditions where PI3K/PKB activation are inhibited, such as acidosis, as explained in the text in section 1.7.1.

Taken from Lecker, 2006, (158).

Section 1.6.2.4, another key target is the transcription factor FOXO. When this is under-phosphorylated because of impaired PKB signalling, it is translocated into the nucleus where it activates expression of the E3 ligases atrogin-1/MAFbx and MuRF-1, (164), as shown in Figure 1.12. This is thought to be an important mechanism through which metabolic acidosis stimulates global proteolysis, (30,164).

1.8 Thesis Aims

In view of the probable functional importance of the SNAT2 transporter, its sensitivity to extracellular pH, and the observed coupling between acidosis, insulin signalling and global protein metabolism in skeletal muscle, reviewed above, the principal aim of the work described in this thesis was to determine in L6-G8C5 rat skeletal muscle cells whether SNAT2 might mediate the effects of metabolic acidosis on protein metabolism. The specific objectives of the work were:

In Chapter 3:

- To investigate by selective silencing of SNAT2 gene expression whether inhibition of SNAT2 alone is sufficient to deplete intracellular L-Gln and other anabolic amino acids
- To determine whether SNAT2 is consequently a functionally significant regulator of protein metabolism; in particular whether it is a potential regulator of amino acid-dependent signalling to mTOR and hence to protein synthesis.

In Chapter 4:

- To determine whether the effect of metabolic acidosis or SNAT2 inhibition on intracellular amino acid levels shows an adaptive response consistent with harvesting of amino acids by proteolysis as a compensatory response to restore intracellular amino acid concentrations
- To determine whether metabolic acidosis or SNAT2 inhibition in the presence of insulin activates proteolysis by signalling through mTOR or PI3K
- To determine whether coupling between SNAT2 and PI3K/PKB signalling can be detected by selectively impairing the activity or expression of SNAT2.

In Chapter 5:

- To impose depletion of specific amino acids (particularly L-Gln) on L6-G8C5 cells, and determine whether depletion alone is sufficient to account for the effects of SNAT2 inhibition on intracellular signalling and global protein synthesis.

1.9 Summary

Uraemia in ESRD patients is frequently seen to lead to cachexia, wasting of lean tissue, due to the effects of acidosis, (2), that induce negative protein balance, (33). Insulin resistance in both diabetic and non-diabetic ESRD patients is a major cause of muscle wasting, (165), implying that low pH has a significant effect on insulin signalling in uraemic muscle.

The SNAT2, System A, transporter is an important regulator of intracellular amino acid concentrations in cell stress, (62,74), and its activity is inhibited at low pH, (73). Low intracellular amino acid levels lead to decreases in protein synthesis and increases in proteolysis, potentially mediated by the amino acid sensitive mTOR pathway, (87). These effects are also observed in L6-myotubes at low pH or during SNAT2 inhibition by the non-metabolisable System A substrate MeAIB, (56), suggesting that acidosis, resulting in SNAT2 inhibition, negatively regulates insulin signalling pathway(s). Proteolysis, occurring as a result of PI3K/PKB inhibition, is an important mechanism by which metabolic acidosis increases protein breakdown, (30,164). This process might also be regulated by decreased SNAT2 activity, in low pH, and the resultant inhibition of insulin signalling.

The aims of this thesis are to determine the effects of amino acid, (especially L-Gln), starvation and acidosis on insulin signalling and global protein synthesis/proteolysis rates, to determine whether these effects are mimicked by selective inhibition of SNAT2, and to determine whether SNAT2 inhibition leads to decreases in intracellular amino acid levels similar to those observed in amino acid starvation and acidosis. The majority of the experiments were carried out in the presence of insulin to facilitate this aim.

Chapter 2: Materials and methods

Note: For convenience, throughout this thesis microcentrifuge speeds have been quoted in rpm, because all microcentrifuges used have approximately the same rotor radius (7cm). All other centrifuge speeds have been quoted as the maximum g force generated at the outer edge of the rotor.

2.1 General reagents and materials

Unless otherwise stated, plastic consumables were purchased from Sarstedt, and chemicals and biochemicals were from Sigma and were of analytical grade.

Sterile Petri dishes and 35mm 6-well culture plates were purchased from NUNC and 22mm 12-well culture plates were from Costar.

2.2 Cell culture

Cells used in this study were L6-G8C5 rat skeletal muscle cells, (57), from the European Collection of Animal Cell Cultures (ref. 92121114) and were used at passage number 16 – 28.

L6-G8C5 cells have previously been determined to be a suitable model for this study as they showed a lower rate of acid production in culture compared to other cell lines, (31), hence allowing a stable pH to be obtained in the medium. In addition to this, L6-G8C5 cells are a proven skeletal muscle

model and have been shown to undergo spontaneous differentiation to myotubes when the percentage of serum in the growth media is decreased as described below, (166). It has also been determined, (166), that L6-G8C5 cells showed clearer acid-induced protein wasting when spontaneously differentiated rather than treated with additional differentiation promoting factors, (167).

2.3.1 Maintenance of cell lines

Routine propagation of L6-G8C5 cells was performed in Growth Medium comprising Dulbecco's Modified Eagle's Medium (DMEM) (Invitrogen 11880-028) (components listed in Appendix A), supplemented with batch-tested 10% v/v heat-inactivated foetal bovine serum (FBS; Invitrogen), 1% v/v Penicillin-Streptomycin (Invitrogen 15140-122), 2mM L-Glutamine (Invitrogen 25030-024) and 10mg/l w/v Phenol Red (Merck-BDH).

2.3.2 Routine cell passaging

To prevent over-confluence, proliferating stock cultures on 9cm Petri dishes were passaged approximately every four days. Growth Medium was aspirated and cells were rinsed with 5ml Hank's Balanced Salts Solution (HBSS) (Invitrogen 24020-133) then incubated for 10 min at 37°C in 2ml Trypsin-EDTA (Invitrogen 25300-054). Cells were then centrifuged at 200g for 5 min at 20°C, re-suspended in Growth Medium and plated on 9cm Petri dishes at a density of 1.6×10^3 cells / cm² and cultured at 37°C under humidified 95% air / 5% CO₂.

2.3.3 Differentiation to myotubes

Cells plated for experimental purposes were seeded at a higher density ($5 \times 10^4 / \text{cm}^2$) and were cultured for 3 days in Growth Medium. At this stage, differentiation of the near-confluent myoblasts into myotubes was promoted by replacing Growth Medium with Minimum Essential Medium (MEM) (Invitrogen 21090-022) (components listed in Appendix A), supplemented with only 2% v/v heat-inactivated FBS, 1% v/v Penicillin-Streptomycin and 2mM L-Glutamine. Fresh MEM / 2% FBS was added after a further 24h. Myoblast fusion to form myotubes was then allowed to continue for a further 3 days before commencing experiments.

2.3 Experimentation

Myoblasts or confluent myotubes were washed with HBSS and incubated at 37°C, under humidified 95% air / 5% CO₂, in test media consisting of MEM supplemented with 1% v/v Penicillin-Streptomycin at pH 7.4, unless otherwise stated. The composition of the test media was dependent on experimental conditions required, and is described in detail in the figure legends in the Results Sections (Chapters 3,4 and 5) of this thesis. In test media, serum was replaced with 2% v/v Dialysed Foetal Bovine Serum (Invitrogen 26400) or, for most of the intracellular signalling studies, with 100nM Bovine Insulin. Test media for amino acid free treatments were made from Earl's Balanced Salts Solution (Sigma E2888 or Gibco 24010) supplemented with 1% v/v Penicillin-Streptomycin and 1% MEM vitamins (11120-037) at pH 7.4, unless otherwise stated. Concentrations of amino acids added to these test media are stated in Appendix A.

2.4 Protein Assays

Protein content of cell lysates or membrane preparations for Western blotting was assayed using the Bio-Rad detergent-compatible (DC) protein assay kit (Bio-Rad 500-0116). Protein content of Trichloro-acetic Acid (TCA) precipitates was determined using the Bradford assay or the Lowry (Folin) protein assay, (168).

2.4.1 Lowry protein determination

Reagent A (1 litre)

20g Anhydrous Na_2CO_3

4g NaOH

0.2g K, Na-tartrate.4 H_2O

Reagent B (1 litre)

5g $\text{CuSO}_4 \cdot 5\text{H}_2\text{O}$

Just before use, Reagent A and Reagent B were mixed with a ratio of 50:1 v/v (A: B) to make Reagent C. Folin Ciocalteu's Phenol reagent (Sigma F-9252) was diluted with a 2:1 v/v dilution ratio of water to Folin Ciocalteu Reagent.

Samples or BSA standards were diluted to achieve a final total protein concentration of 0 – 500 $\mu\text{g}/\text{ml}$ in 0.5 M NaOH in a total volume of 50 μl . Diluted Folin Ciocalteu reagent (60 μl) was then added followed by immediate vortexing. Reagent C (600 μl) was added after 10 min, again followed immediately by vortexing. The resulting mixture was then incubated at room temperature for 40 minutes after which the OD 660 was read on a Titertek Multiskan Plus MKII spectrophotometer. The protein contents of the samples

were calculated relative to the measured optical density of the protein standards.

2.4.2 Bio-Rad DC Assay

Reagent A (1ml) and Reagent S (20 μ l) were mixed immediately prior to carrying out the assay to produce reagent A'.

BSA protein standards (0 – 2000 μ g/ml) and samples (5 μ l) were measured in triplicate by mixing with 25 μ l Reagent A' and 200 μ l Reagent B on a 96-well plate. After a 15 minute incubation at room temperature the OD750 of each well was measured as described above.

2.5 Radio-isotope techniques

2.5.1 Protein synthesis measurements

Global protein synthesis rates were determined by measuring incorporation of L-[2,6 3 H]-phenylalanine ([2,6 3 H]-Phe; Amersham TRK552) into cell protein, (56).

After being washed thrice in HBSS, cultures were incubated in test medium (as stated in figure legends) followed by a 30 min incubation in the same medium with 2mCi (74MBq)/L 3 H-L-Phe and a total L-Phe concentration of 200 μ mol/L for 30 min. Cultures were then washed on ice with ice-cold 0.9% w/v NaCl, to remove extracellular 3 H-Phe, and scraped in 1ml of ice-cold 10% w/v Trichloro-acetic acid (TCA). Samples were then centrifuged at 13,000rpm

on a microcentrifuge for 10 min at +4°C. The supernatant was aspirated and the protein pellet was dissolved in 200µl of 0.5M NaOH by heating at 70°C for 30 min. A 50µl aliquot was then added to 4ml of Ecoscint A scintillant and mixed by vigorous vortexing. Total ³H-Phe incorporated into acid precipitable protein was then measured using liquid scintillation counting with quench correction. The total protein content of each sample was determined using the Lowry assay described in Section 2.4.1.

In the experiment described in Appendix E, Figure 7, in which the extracellular total L-Phe was partly depleted, the ratio of ³H-Phe to total L-Phe in the medium was adjusted to ensure a constant specific radio activity at the same level as described in the protocol above.

2.5.2 Proteolysis measurements

Global proteolysis rates were determined by measuring the rate of release of acid-soluble radioactivity from cultures in which the cell proteins had been pre-labelled, (56). Cultures were pre-labelled by incubating with MEM / 2% FBS containing 2mCi (74MBq)/L ³H-L-Phe and a total L-Phe concentration of 200 µmol/L for 72 hours, with addition of fresh labelled medium approximately every 24h. The labelled medium was then aspirated and cultures were washed thrice with HBSS to remove non-incorporated ³H-Phe. Cells were then incubated in test media for 2 hours in the culture incubator. All test media contained 2mM unlabelled L-Phe to minimise reincorporation of ³H-Phe from degraded protein into newly synthesised protein, (31). After this incubation an aliquot of the medium was sampled and the remainder

aspirated and replaced with fresh test medium, again with 2mM unlabelled L-Phe. Cells were then returned to the incubator, with further aliquots of medium being sampled at intervals for up to 48 hours. At this point the cultures were placed on ice and were rinsed thrice in ice-cold 0.9% w/v NaCl and stored at -20°C. Subsequently the cultures were thawed and cells were scraped in 1ml of 0.5M NaOH and then heated at 70°C for 30 minutes to dissolve the cell protein. An aliquot of this digest (50µl) was taken for liquid scintillation counting (as described in Section 2.5.1) to determine the residual ³H in the cell protein. The total protein content of each sample was also measured using the Lowry protein assay as described in Section 2.4.1.

Aliquots of medium sampled during the experiment were deproteinised by mixing with an equal volume of 20% w/v TCA, vortexed and incubated at +4°C for at least 1 hour. These samples were then centrifuged on a microcentrifuge at 13,000rpm for 10 minutes at +4°C to pellet any intact labelled protein; and acid-soluble ³H from degraded protein in the supernatant was measured by scintillation counting as above. The pellets were dissolved in 0.05M NaOH and an aliquot from each was counted as a measure of intact protein leakage or cell detachment into the medium (an index of cell viability, (169)).

Proteolysis rates (calculated from acid-soluble ³H released into the medium and residual ³H in the cells at the end of the experiment) are expressed as log₁₀ of the percentage of the total initial cellular ³H per hour. The calculation method is explained in Appendix D.

2.5.3 ¹⁴C- MeAIB uptake measurements

System A transporter activity (which in L6 skeletal muscle cells arises almost entirely from transport through SNAT2, (72,165)), was determined by measuring the rate of uptake of the specific System A substrate [¹⁴C] α-Methyl-aminoisobutyrate (¹⁴C-MeAIB; NEN-Du Pont NEC 671) into intact cells on 22mm diameter culture wells, (171).

After incubation of L6-G8C5 myotubes in test media, the medium was aspirated and cells were washed twice in Hepes Buffered Saline (HBS) to remove extracellular amino acids. Fresh HBS (500μl) was then added to each 22mm well. Aliquots of ¹⁴C-MeAIB were rapidly pipetted into the HBS to give a final concentration of 10μmol/L ¹⁴C-MeAIB at 0.5mCi (18.5MBq)/L, followed by incubation at room temperature for exactly 5 minutes. Cultures were then placed on ice and the cells were washed thrice in ice-cold 0.9% w/v NaCl to remove extracellular ¹⁴C-MeAIB, and stored at -20°C. Subsequently cells were thawed and scraped in 200μl 0.05M NaOH followed by heating at 70°C for 30 minutes to dissolve the cell protein and release ¹⁴C-MeAIB into solution. A 150μl aliquot of this digest was then mixed with 4ml Ecoscint A and counted on a liquid scintillation counter with quench correction. Total protein in the digest was also assayed using the Lowry assay described in Section 2.4.1.

Transporter activity in sub-confluent myoblasts was assayed in the same way but the concentration of ¹⁴C-MeAIB during the incubation in HBS was increased to 40μmol/L at 2mCi (74MBq)/L.

In each experiment non-specific binding or trapping of ^{14}C -MeAIB in the cell layer was measured by incubating control cultures with ^{14}C -MeAIB as above, but with 10mM unlabelled MeAIB also present in the medium. The radioactivity measured in these control wells was subtracted from the uptake measured in all of the other cultures.

From the known specific radioactivity of the ^{14}C -MeAIB added in the transport assays (112 dpm per pmol) the net uptake of MeAIB was calculated as pmol of MeAIB per mg protein per 5 min.

2.6 Protein techniques

2.6.1 Cell Membrane Preparation

After incubation in test media, (Section 2.3) cultures were placed on ice and rinsed thrice with ice cold 0.9% w/v NaCl. Intact cells were then immediately scraped off the plate using a plastic cell scraper in 3ml of UIC3 lysis buffer (Appendix B) per 9cm Petri. Cells were then centrifuged at 200g for 5 minutes at $+4^{\circ}\text{C}$. Supernatant was aspirated and pellets were re-suspended in UIC3 and incubated on ice for 30 minutes. This suspension was then syringed twice through a 23 gauge needle to ensure total cell lysis. Lysates were then centrifuged on a microcentrifuge at 7500rpm for 10 minutes at $+4^{\circ}\text{C}$. Pellets of nuclei and other large debris were discarded, and supernatants were centrifuged at 170,000g on a Beckman L8-60M ultracentrifuge for 60 minutes at $+4^{\circ}\text{C}$. The resulting membrane pellets were dissolved in UIC3 with 1% v/v IGEPAL CA-630 detergent (Sigma I-3021) and stored at -80°C . Protein in

these membrane preparations was assayed using the Bio-Rad DC assay as described in Section 2.4.2. Samples containing approximately 30µg of protein were then mixed with an equal volume of SDS-PAGE reducing sample buffer and run on SDS-PAGE gels as described in Section 2.4.3.

2.6.2 Sodium Dodecyl Sulphate Polyacrylamide Gel electrophoresis (SDS- PAGE) gels.

Both the Bio-Rad Mini Protean 2 and the Mini Protean 3 electrophoresis systems were used during this study.

2.6.2.1 Casting the gels

The resolving gel (see Table 2.1) was poured between two glass plates and over-layered with H₂O. Once the resolving gel had set, the H₂O was removed and the stacking gel (see Table 2.2) was poured on top and well combs were immediately inserted in the stacking gel to produce defined sample loading wells. The gel was then left to set fully before sample loading could proceed. Volumes of acrylamide and water were adjusted as shown in the tables below to give the required final percentage of acrylamide in the gels.

Table 2.1: SDS-PAGE resolving gel (volumes stated are per gel)

Final Acrylamide (% w/v)	8%	12%	12.5%	15%
Water	4.7ml	3.35ml	3.19ml	2.35ml
Acrylamide (30%w/v)	2.65ml	4.0ml	4.17ml	5.0ml
1.5M Tris HCl, pH 8.8	2.5ml	2.5ml	2.5ml	2.5ml
SDS ¹ (10% w/v)	100µl	100µl	100µl	100µl
APS ² (10% w/v)	50µl	50µl	50µl	50µl
TEMED ³	5µl	5µl	5µl	5µl

Table 2.2: SDS-PAGE stacking gel (volumes stated are per gel)

Water	3.03ml
Acrylamide (30%w/v)	0.65ml
0.5M Tris HCl, pH 6.8	1.25ml
SDS¹ (10% w/v)	50µl
APS² (10% w/v)	25µl
TEMED³	5µl

1- Sodium Dodecyl Sulphate

2- Ammonium Persulfate.

3- Tetramethylethylenediamine

2.6.2.2 Preparation of samples for SDS-PAGE

After incubation of cultures with test media, the culture plates were placed on ice and media were aspirated. Cells were immediately scraped in SDS-PAGE Lysis Buffer (Appendix B) and lysates were centrifuged on a microcentrifuge at 13,000rpm for 10 minutes at +4°C to remove nuclear debris. Supernatants were then assayed for protein content using either the Bio-rad assay, (Section 2.4.2). A quantity of lysate containing 30µg protein was then mixed with an equal volume of SDS-PAGE reducing sample buffer, heated on a Grant QBT2 heating block at 100°C for 5 min and then briefly centrifuged on a microcentrifuge at 13,000 rpm.

2.6.2.3 Running the gels

Gels were transferred to a tank of running buffer (Appendix B), and samples, prepared as described in Section 2.6.2.2, along with molecular weight markers, (Broad Range Markers (NEB) or Kaleidoscope Prestained Standards, (Bio-Rad 161-0324)), were loaded into the sample wells.

Electrophoresis was performed at 200 volts until the Bromophenol Blue dye front had reached the bottom of the gel (approximately 40 min). Gels for S6K1 mobility shift assays were run for an extended period (approximately 80 min) to allow separation of the phospho-activated and non-activated isoforms of the protein to be more easily visualised.

2.6.3 Western Blotting

Proteins separated by SDS-PAGE as described above were blotted onto nitrocellulose membranes (Amersham). The SDS-PAGE gel and a nitrocellulose membrane were pre-equilibrated in Transfer Buffer (Appendix B) for 15 minutes at +4°C before insertion into the cassette of a Bio-Rad Mini Transblot Electrophoretic Transfer Cell, care being taken to exclude trapped bubbles. Electrophoretic transfer was carried out at 80 volts for 2 hours with continuous stirring, with an ice block inserted in the transfer cell to avoid overheating.

2.6.3.1 Blocking the membranes

After the transfer had taken place, membranes were blocked for 1 hour at room temperature in 5% w/v milk powder in TBST or PBST (Appendix B), followed by 3 washes in TBST or PBST. (Membranes to be probed for P-4EBP1 or total 4EBP1 were fixed in 1% glutaraldehyde in PBST for half an hour at room temperature prior to blocking).

2.6.4 Immunostaining

Blocked membranes were then probed with primary antibodies as shown in Table 2.3. Membranes were incubated in the primary antibody solution with rocking at +4°C overnight. To achieve optimum results with a given Primary Antibody, antibodies were diluted in either TBST or PBST with 5% milk powder or BSA (see Table 2.3). For primary antibodies diluted in 5% milk powder, the washing step prior to primary antibody incubation was omitted.

Membranes were then washed thrice in TBST or PBST and primary antibodies were detected by probing membranes with a horseradish-peroxidase conjugated goat anti-rabbit (Dako P0448), rabbit anti-mouse (Dako P0260) or Rabbit anti Goat (Sigma A5420) IgG at a dilution of 1:1500 in TBST or PBST with 5% milk powder for 2 hours at room temperature. Membranes were again washed thrice in TBST or PBST for at least 10 minutes per wash. Then horseradish peroxidase-labelled proteins were detected on Kodak scientific imaging films (Sigma) by chemiluminescence using an ECL detection kit (Amersham). The identity of protein bands detected was confirmed by comparing their positions relative to the molecular weight markers. The bands were quantified as described in Section 2.11.

Table 2.3: Details of Antibodies

Antibody	Source	Ref No	Dilution	TBST/ PBST	Blocking agent	Secondary Antibody
P ^{Ser235/236} -rpS6	NEB	2211L	1:1000	PBST	5% BSA	R
Total rpS6	NEB	2217	1:1000	PBST	5% Milk powder	R
P ^{Ser473} -PKB	NEB	4058	1:1000	TBST	5% BSA	R
Total PKB	NEB	4685	1:1000	TBST	5% BSA	R
P ^{Ser52} -eIF2 α	Bio- source	44- 728G	1:1000	TBST	5% BSA	R
Total eIF2 α	Bio- source	AHO- 0802	1:1000	TBST	5% BSA	M
P ^{Ser65} -4EBP1	NEB	9451	1:1000	TBST	5% BSA	R
Total 4EBP1	AW ⁺	-	1:1000	PBST	5% Milk Powder	R
S6K1	AW ⁺	-	1:1000	PBST	5% Milk Powder	R
P ^{Thr202} -ERK1/ P ^{Tyr204} -ERK2	NEB	9101S	1:1000	PBST	5% BSA	R
Total ERK2	NEB	9108	1:1000	TBST	5% BSA	R
β -Actin	Insight Bio-tech- nology	Ab6276	1:5000	TBST	5% Milk powder	M
SNAT2 Ab1	JE*	-	1:4000	TBST	5% Milk powder	R
SNAT2 Ab2	JE*	-	1:4000	TBST	5% Milk powder	R
Na,K, ATPase	Abcam	ab7671	1:5000	TBST	5% Milk powder	M
Annexin II	Santa Cruz	Sc-1924	1:4000	TBST	5% Milk powder	G
β -O-Glc-NAc glycos-ylated proteins	Pierce Perbio Science	24565 (MAbCTD 110.6)	1:5000	-	Manu- facturers blocker	GM

*A gift from J. Erickson, Louisiana State University Health Sciences Center. *A gift from A. Willis, Nottingham University.

R – HRP conjugated Goat anti Rabbit IgG (Dako P0448).

M - HRP conjugated Rabbit anti Mouse IgG (Dako P0260).

G - HRP conjugated Rabbit anti Goat IgG (Sigma A5420).

GM- HRP conjugated Goat anti Mouse IgM (μ)

Anti-SNAT2 antibody 1 was raised against the N-terminal peptide MKKTEMGRFNISPDEDSC of rat SNAT2 and anti-SNAT2 antibody 2 was raised against the N-terminal hydrophilic portion of rat SNAT2 (AA 1-65) and has been characterised previously by Yao et al, (66). Both antibodies were raised by the same laboratory.

2.7 Assay of Phosphatidylinositol-3-kinase (PI3-K) Activity

Activity of PI3K was assessed using an *in vitro* lipid kinase assay based on the method described by Howells et al, (172). This assay was originally designed to determine the activity of Class 1 PI3Ks, capable of signalling to PKB, but the possibility that Class 3 PI3Ks are also present in the immunoprecipitate used in this assay cannot be ruled out.

Activity of phosphorylated PI3K, immunoprecipitated from cell lysates, was assayed by catalytic transfer of ^{32}P from labelled ATP to phosphatidyl inositol, followed by autoradiography of the product (phosphatidylinositol-3-phosphate, PI(3)P). As shown in Figure 2.1 this differs slightly from the *in vivo* reaction in which activated Class 1 PI3Ks catalyse the conversion of PI(4,5)P₂ to PI(3,4,5)P₃ (as described in Section 1.6.2.2).

After incubation in test media, cells were washed with 1mM w/v Na₃VO₄ in PBS and scraped in PI3K Lysis Buffer (Appendix C). Lysates were centrifuged in a microcentrifuge at 13,000rpm for 5 min at + 4°C and the pellets were discarded. PI3K was immuno-precipitated from the supernatants using an anti-phospho-tyrosine antibody (Santa Cruz PY99) and Protein A-sepharose CL4B beads (Pharmacia). The immuno-precipitation reaction was performed at +4°C for 2 hours with rocking, after which the Protein A-sepharose beads were sedimented by centrifugation on a microcentrifuge at 2000rpm for 15s at +4°C.

The immunoprecipitate on the beads was washed as follows; 3x in PI3K Lysis Buffer, 2x in Wash 1, 1x in Wash 2 and 1x in Wash 3. (The Wash solutions are described in Appendix C). Centrifugation between washes was performed as described above. The immunoprecipitate / Protein A sepharose beads were then re-suspended in 40 μ l of Kinase Assay Buffer (Appendix C) and 20 μ l of phosphatidylinositol / cholate substrate (3mg of phosphatidylinositol in 1ml of 1% w/v sodium cholate). In control conditions the PI3K inhibitor LY294002 was also added at this stage at a final concentration of 12.5 μ M. In a separate tube, 39 μ l of water was mixed with 5 μ l of 30 μ M Na₂ATP, 5 μ l of 75mM MgCl₂ and 1.25 μ Ci (46kBq) of [γ -³²P]-ATP (Amersham PB10168). Both tubes were warmed to 37°C for 5 minutes, then the kinase reaction was started by adding 40 μ l of the γ -³²P-ATP mixture to the tube containing the immunoprecipitate. The reaction was allowed to proceed at 37°C for 5 minutes. The kinase assay reaction was stopped by chilling on ice and immediately adding 450 μ l of Chloroform: Methanol 1:1 v/v and vortexing. Chloroform (150 μ l) and 0.1M HCl (150 μ l) was then added, followed by vortexing and centrifugation on a microcentrifuge at 5000rpm for 10 min at room temperature. The lower phase and interphase were retained and mixed with 300 μ l of synthetic upper phase (chloroform:0.1M HCl 1:1 v/v). Samples were vortexed and centrifuged again as above, and the lower phase was removed and vacuum dried. The resulting lipid film was re-dissolved in 25 μ l of Chloroform: Methanol: 0.1M HCl in the ratio 200:100:1 v/v/v, and spotted onto an oxalate treated (Appendix C) thin layer chromatography (TLC) plate (VWR Kieselgel 60 F-254 Ref 1.05715.0001- see Appendix C), as shown in Figure

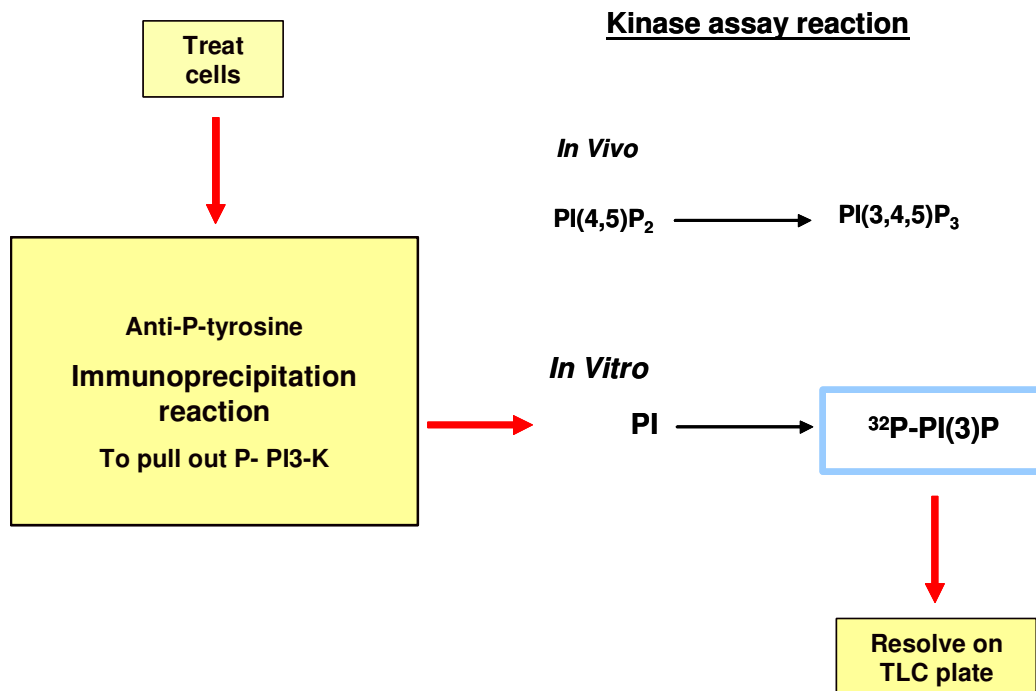


Figure 2.1: The principles of the *in vitro* PI3K assay

See text section 2.7 for further details.

2.2. The lipid extract tube was washed out with a further 25ul of Chloroform: Methanol: 0.1M HCl 200:100:1, and this was then spotted onto the TLC plate in the same position as the original sample. Samples on the TLC plate were then resolved in a chromatography tank containing a pre-equilibrated mixture of; 42.9ml methanol, 30 ml chloroform, 7.65ml 15M ammonia and 9.45ml H₂O, until the solvent front was approximately 1cm from the top of the TLC plate. The plate was then removed from the tank and left to dry in air.

2.7.1 Autoradiography of radio labelled lipids

The ³²P-labelled PI(3)P which had migrated on the TLC plate with an Rf value of approximately 0.85 was visualised by autoradiography. The dried TLC plate was placed face down on an X-OMAT LS Kodak scientific imaging film in a developing cassette and exposed at -80°C for approximately 72 hours. The PI(3)P bands were later quantified as described in Section 2.11.

2.7.2 Quantifying PI(3)P by liquid scintillation counting

In addition to autoradiography, the ³²P-PI(3)P on the TLC plates was also measured in some experiments by liquid scintillation counting. A 1cm grid was ruled on the TLC plate and the silica from each square was scraped off the plate and transferred to a scintillation vial. Radioactivity was counted by liquid scintillation counting in Ecoscint A scintillant. Samples were counted until at least 1000 counts had accumulated.

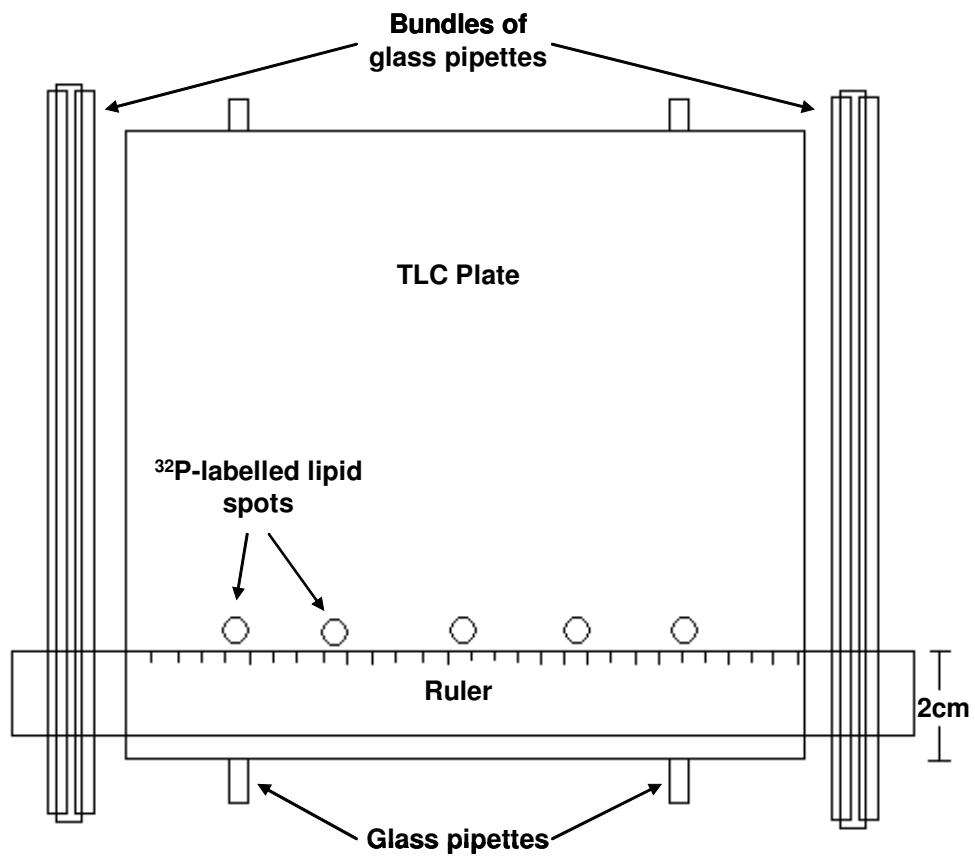


Figure 2.2: Sample loading onto the Oxalate treated TLC plate

See text section 2.7 for further details

2.8 L-Glutamine Synthetase assay

For determination of L-Glutamine synthetase (Glutamate-ammonia ligase E.C. 6.3.1.2), cultures were washed twice with PBS and stored at -80°C in 50mM Imidazole pH 6.8 before colorimetric determination of enzyme activity with hydroxylamine as described, (173).

2.9 RNA techniques

2.9.1 Preparation and Screening of siRNA for Silencing of SNAT2

SNAT2-silencing siRNAs had been prepared previously in this laboratory (by Dr A. Bevington and Mr J. Brown) using the following procedure:

With the siRNA design tool:

http://www.ambion.com/techlib/misc/siRNA_finder.html

70 potential target sequences for siRNA silencing within rat SNAT2 mRNA were identified. A siRNA design request to:

<http://www.eurogentec.com/product/research-custom-sirna.html> confirmed 6 of these sequences as particularly strong candidates for silencing.

After BLAST searching to confirm minimal similarity to sequences in other rat genes, three of these sequences, widely separated throughout the SNAT2 mRNA sequence, were selected for custom synthesis by Eurogentec:

Table 2.4

Candidate sequence	Directed against the following position in the SNAT2 gene sequence:
5'- aacaguugggacauaaggcau	Base position 404 onwards
5'- aacugacauuccuccucgu (SIL)	Base position 1095 onwards
5'- aaccaugagauccgugcaaa	Base position 1388 onwards

The custom-synthesised oligonucleotides were supplied as pairs of single-stranded siRNAs (forward and reverse strands) which were dissolved in sterile diethylpyrocarbonate (DEPC) - treated water to give 50µM stock solutions.

Forward and reverse stocks (180µl of each) were then mixed with 90µl of annealing buffer (500mM NaCl, 250mM Tris, pH 7.5-8.0) and heated to 92°C, followed by slow cooling to room temperature. An Annealing Blank was also prepared by mixing 360µl of DEPC-treated water with 90µl of annealing buffer and heating and cooling as above. The resulting annealed 20µM ds siRNAs and blank were stored in aliquots at -20°C.

The double-stranded siRNA (SIL) that gave the most effective silencing of SNAT2 transporter activity (¹⁴C-MeAIB uptake into myoblasts) was used for subsequent experiments. This siRNA had the forward sequence 5'- CUGACAUUCUCCUCCUCGUdTdT directed against base position 1095 onward in the gene sequence. A scrambled control siRNA (SCRAM) (forward sequence 5'-CGCUCAACUCUACUUGUCCdTdT sharing the same base

sequence as the SNAT2 silencing siRNA but in a random sequence) was also prepared and annealed exactly as above.

2.9.2 Calcium Phosphate mediated siRNA transfection

2.9.2.1 Transfection of unfused myoblasts

Transfections were initially carried out in unfused myoblasts (40 – 70% confluent) because gene silencing with siRNA using oligonucleotides is generally thought to be more effective in sub-confluent proliferating cells. Cells were seeded at 1.3×10^4 / cm² and incubated in Growth Medium (DMEM, with the additions described in Section 2.2.1), for 24 hours. The Growth Media were then aspirated and replaced with half the usual volume of fresh Growth Media. Cells were then treated with a blank generated from the annealing buffer, or transfected with SIL or SCRAM siRNA oligonucleotides at a final concentration of 30nM.

The Transfection kit used was the Promega Profection Calcium Phosphate Transfection kit (Promega E1200). A solution consisting of the relevant siRNA or annealing blank, sterile DEPC water and a 2M CaCl₂ reagent was made up as shown in Table 2.5 and added dropwise to the vortexing 2 X HEPES-buffered Saline (HBS) reagent.

The resulting CaPi transfection mixture was incubated at room temperature for 30 minutes and then added dropwise to the cell culture plates, as shown in Figure 2.3, which were then rocked to ensure even distribution of the

Table 2.5: Transfection mixture

Transfection mixture label	Solution 1		Solution 2			
	2 X HBS (μl)	Annealing Blank B (μl)	20μM ds scrambled siRNA SCRAM (μl)	20μM Ds silencing siRNA SIL (μl)	Filter-sterilised DEPC H ₂ O (μl)	2M CaCl ₂ (μl)
BLANK	5000	113	-	-	4274	613
SCRAM	5000	-	113	-	4274	613
SIL	5000	-	-	113	4274	613

transfection reagent and then incubated overnight at 37°C under humidified 95% air / 5% CO₂. After this 16 hour incubation media were aspirated and cells were incubated for 24 hours in twice the normal volume of Growth Medium. Experiments were then carried out on the fourth day after cells had been plated.

2.9.2.2 Transfection of myotubes

As some functional effects of acidosis and of SNAT2 are only observed in differentiated myotubes (see Results Section 3.2.3.1) transfection was also performed in myotubes, (Section 2.3.3), 9 days after seeding the cells, using exactly the same transfection procedure described above. For the duration of the transfection and the subsequent 24h incubation, Growth Medium was used, rather than the MEM / 2% FBS medium that was normally used for myotube culture.

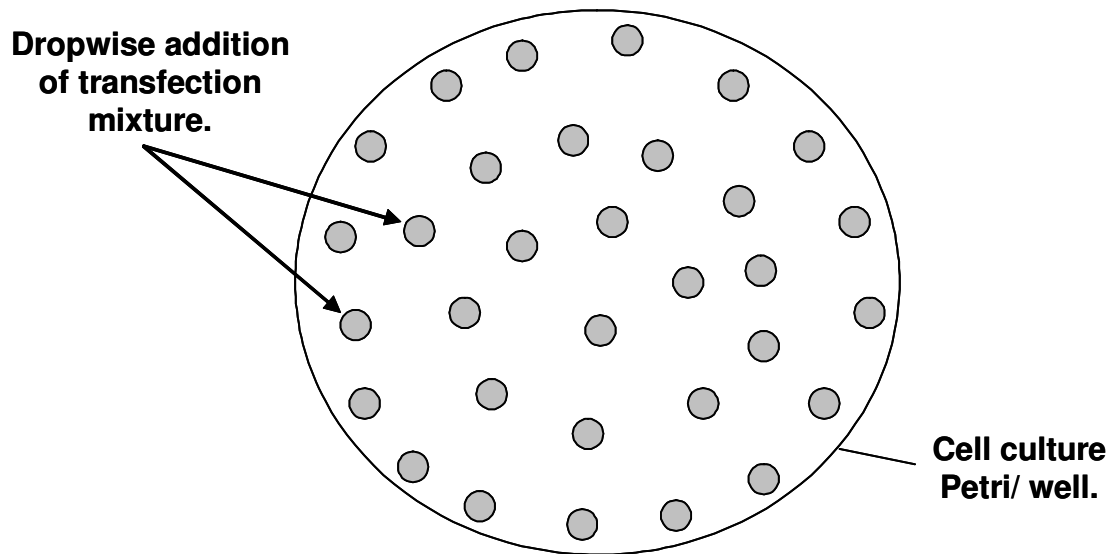


Figure 2.3: Dropwise addition of CaPi transfection mixture and subsequent rocking ensured even distribution throughout cell layer.

CaPi Transfection mixture was added in the following volumes: 60 μ l per 22mm well (12-well plate), 150 μ l per 35mm well (6-well plate), 395 μ l per 25cm² flask and 2500 μ l per 90mm Petri dish.

2.9.3 SNAT2 mRNA determination

2.9.3.1 RNA isolation and RT-PCR

Total RNA was isolated from myotube cultures on 25cm² flasks using an acid phenol-guanidinium reagent (Trizol, Life Technologies 15596) and was quantified by measuring absorption at 260nm. RNA was reverse-transcribed using an AMV Reverse Transcription System (Promega A3500) and was amplified by PCR using gene-specific primers: Rat SNAT1, (74), (493-bp product): forward 5'-CTGATCGGGAGAGTAGGAGGAGTC-3' and reverse 5'-AGCGGGAGAATTATGCCAAAGGTT-3'; rat SNAT2, (74), (693-bp product): forward 5'-TACGAACAGTTGGGACATAAGG-3' and reverse 5'-AGTTCCCACGATCGCAGAGTAG-3'; rat SNAT3, (174), (337-bp product): forward 5'-TTGGGCATATTTGGGATCATTGGTG-3' and reverse 5'-TCCCCTGTCTTTCTCCCCTTCCTTA-3'; rat SNAT4, (175), (187-bp product): forward 5'-ACCCTGGAACGACCTCTTTT-3' and reverse 5'-CCTTCCTTGGCTGTCTTCAG-3'; rat SNAT5, (174), (424-bp product): forward 5'-TCAGCCCCTAGCCTCATCTTCATCC-3' and reverse 5'-AGCTGGCCTCCCTTCCTCCTCTC-3'; rat Cyclophilin A, (176), (369-bp product): forward 5'-CAACCCCACCGTGTTCTTCG-3' and reverse 5'-TTGCCATCCAGCCACTCAGTC-3'. Amplification was performed using Abgene Reddymix System (Abgene AB-0575/LD/b), with the following PCR amplification conditions: 94°C for 4 min, then 25 cycles comprising 94°C for 30 sec, 55°C for 1 min, 68°C for 1 min, followed by a final single extension step of 68°C for 7 min, (74). RT-PCR products were resolved on 1.5% w/v agarose in 40mM Tris-Acetate, 1mM EDTA, pH 8.3, with 0.5µg/ml ethidium bromide, and visualised by ultraviolet fluorescence.

2.9.3.2 Northern Blotting

Total RNA was isolated and quantified as described above. RNA (30 µg per sample) was separated by electrophoresis in a 1% agarose 1.9% formaldehyde gel, transferred to a nylon membrane (Hybond, Amersham RPN 203N) and cross-linked to the membrane by ultraviolet irradiation. Membranes were incubated at 42°C for 4h in a pre-hybridization solution containing 5x SSPE (Sigma S2015), 5x Denhardt's solution (1x = 0.02% Ficoll, 0.02% polyvinylpyrrolidone, 0.02% bovine serum albumin), 50% deionized formamide, 1% sodium dodecyl sulphate (SDS), and 200 µg/ml salmon sperm DNA. Membranes were then hybridized sequentially with ³²P-dCTP-labelled cDNA probes (Promega "Prime-a-Gene) for rat SNAT2 (generated as described in Yao et al, (66)) and rat cyclophilin (from Dr Izabella Pawluczyk, University of Leicester, Department of Infection, Immunity and Inflammation). Hybridization was performed in a hybridization solution of the same composition as above at 42°C overnight. After hybridization, membranes were washed twice with 2x SSPE, 0.2% SDS, at room temperature for 10 min, followed by two washes with 0.2x SSPE, 0.2% SDS at 65°C for 30 min each. The hybridization signal was detected by autoradiography as described in Section 2.7.1.

2.10 Measurement of intracellular amino acids and their derivatives by High Performance Liquid Chromatography (HPLC)

After incubation in test media as described in Section 2.3, cultures on 35mm wells were placed on ice and the cells were washed thrice in ice-cold 0.9% w/v NaCl to remove extracellular amino acids. The rinsed cells were

immediately scraped in 150µl of 0.3M Perchloric acid (PCA). The resulting lysate was transferred to microcentrifuge tubes on ice, followed by incubation for 30 minutes to allow as much protein as possible to precipitate. Samples were then centrifuged at 3000rpm on a microcentrifuge for 10 minutes at +4°C. The resulting pellets were dissolved in 1ml of 0.5M NaOH, by heating at 70°C for 30 minutes, and assayed for protein content using the Lowry assay described in Section 2.4.1. The deproteinised supernatants were placed on ice and then vortexed vigorously for 60 seconds with an equal volume of a Freon-Tri-octylamine mixture, (22% v/v Tri-n-octylamine, 78% v/v 1,1,2-trichlorotrifluoroethane, pre-chilled and mixed immediately prior to use), then centrifuged briefly to separate the phases. The top (aqueous) phase was removed and stored at -80°C. These neutralised extracts were subsequently filtered through a 0.45µm microfilter and analysed by HPLC. Amino acid and glutathione levels were determined on an Agilent 1100 high performance liquid chromatograph with a Zorbax Eclipse AAA column (4.6x75 mm, 3.5µM) at +40°C with o-phthalaldehyde / 3-mercaptopropionate/9-fluorenylmethylchloroformate pre-column derivitisation and ultra-violet post-column detection.

2.11 Quantification of bands in blots and autoradiographs

Band intensity on films was quantified using a Bio-rad GS700 densitometer and Molecular Analyst v1.4 software

2.12 Statistical analyses

Data are presented as mean + SEM. In blotting and autoradiography experiments, densitometry intensity data are expressed as percentage of the intensity of the control band measured on the same film. Statistical significance was assessed by ANOVA and post hoc testing with Duncan's multiple range test, using SPSS 14.0 software (SPSS, Chicago, IL). Changes were regarded as significant at $P < 0.05$. Correlation was expressed as the Spearman Rank Correlation Coefficient, R_s .

Chapter 3: The effect of the SNAT2 transporter on mammalian target of Rapamycin (mTOR) signalling and global protein synthesis

3.1 Introduction

As explained in Section 1.4.2, uraemic metabolic acidosis is an important cause of the wasting of soft tissue, particularly skeletal muscle, which is a frequent occurrence in patients with end-stage renal disease, (177-179). Depletion of intramuscular free amino acids is thought to be an important early step in muscle wasting in uraemia, (180), and depletion is reversed if acidosis is corrected, (181). It is well documented that intracellular amino acid depletion regulates the activity of mTORC1, (87), however, the exact mechanism of amino acid sensing by the mTOR pathway is currently uncertain, see Section 1.6.2.5.3. Impaired protein synthesis is an early consequence of metabolic acidosis in humans, (37), and is partly compensated by harvesting of amino acids at the expense of proteolysis, (182,183), but precisely how acidosis leads to the initial amino acid depletion is poorly understood.

Availability of the free amino acid L-Glutamine (L-Gln) limits protein synthesis, (184), proteolysis, (185), and nucleotide and nucleic acid biosynthesis, (186), in some cell types. Consequently L-Gln has been proposed as a key factor in growth and maintenance of mammalian tissues, (187), and L-Gln availability and losses from muscle may be important contributors to wasting illness and clinical outcome in seriously ill patients, (188). A crucial factor is active

transport of L-Gln across the plasma membrane, (188), maintaining an intracellular concentration at least 20 times higher than the 0.5-1mM found in extracellular fluid, (189). In muscle the molecular identity of the transporter(s) involved has been obscure but, as outlined in Sections 1.5.2 to 1.5.4, studies in cultured L6 skeletal muscle cells, (56,190), have implicated System A neutral amino acid transporters of the SNAT/Slc38 transporter family, in particular SNAT2, (64). SNAT2 is also a possible mediator of the effects of acidosis because it is strongly inhibited at low pH ((73) and Section 1.5.6).

3.1.1 SNAT2 inhibition depletes intracellular amino acids

During the early stages of the work described in this thesis, results were obtained by other workers in this laboratory which implicated SNAT2 in maintaining intracellular L-Gln concentration (Appendix E Figure 1). When this transporter was subjected to selective competitive inhibition by incubating L6 myotubes with a saturating dose of the specific Slc38 substrate MeAIB, intracellular L-Gln was strongly depleted (by 75%) after only 2h (Appendix E Figure 1A). Partial, (approximately 40%), inhibition of SNAT2 transporter activity was also achieved by acidosis i.e. by lowering the pH of the medium to 7.1 (Appendix E Figure 1C). As expected, this inhibitory effect on SNAT2 led to a commensurate depletion of L-Gln (Appendix E Figure 1A).

SNAT2 inhibition also led to significant depletion of L-Leucine (L-Leu) (Appendix E Figure 1B), another amino acid that exerts a protein anabolic effect in human muscle, (191), and L6 cells (192,193). L-Leu is not a substrate for SNAT2, (66), and MeAIB is not a substrate for the System L

transporters of the Slc7 family that carry L-Leu, (57). This implied that coupling occurs between SNAT2 and System L transporters, possibly mediated by the trans-membrane L-Gln gradient and 1:1 exchange of L-Gln for L-Leu (see Figure 1.4 and the discussion in Section 3.3.2 below). To demonstrate that the L-Gln gradient is involved in active accumulation of L-Leu inside the cells, L-Gln was removed from the extracellular medium. This depleted intracellular L-Gln, but after 2h the concentration inside the cells was still appreciable – approximately 4nmol/mg protein (Appendix E Figure 1A). The inside/outside concentration gradient (4 divided by zero i.e. tending to infinity) was therefore considerably larger than in the control cultures and led to the predicted enhanced accumulation of L-Leu in the cells (Appendix E Figure 1B). This effect of extracellular L-Gln depletion on intracellular L-Leu was dose-dependent (Appendix E Figure 2 A,B) and also led to the expected intracellular accumulation of other System L substrates with bulky side chains such as L-Phe (Appendix E Figure 2C) and L-Ile, L-Val, L-Tyr and L-Trp (Appendix E Table 1).

Taking these observations as the starting point, the work described in this Chapter was performed with two aims:

- Firstly to investigate by selective silencing of SNAT2 gene expression whether inhibition of SNAT2 alone is sufficient to deplete intracellular L-Gln and other anabolic amino acids
- Secondly to determine whether SNAT2 is consequently a functionally significant regulator of protein metabolism; in particular whether it is a

potential regulator of amino acid-dependent signalling to mTOR and hence to protein synthesis.

3.2 Results

3.2.1 Silencing of SNAT2 gene expression

To confirm that the predominant System A/Slc38 transporter gene expressed in L6-G8C5 cells is SNAT2, expression of all five Slc38 family transporters (excluding the “orphan” genes Slc38A6 to Slc38A11) was examined using gene-specific PCR primers. In agreement with earlier studies in L6 myotubes, (74), and in rat skeletal muscle *in vivo*, (66), only SNAT2 was detected (Figure 3.1A). The dominant role of SNAT2 in L-Gln and L-Leu homeostasis was confirmed in L6-G8C5 myoblasts by silencing SNAT2 expression using siRNAs. SNAT2 silencing was demonstrated by RT-PCR (Figure 3.1B) and Western blotting (Figure 3.1C) and by functional assay of transporter activity (Figure 3.2A). While the silencing siRNA significantly reduced SNAT2 expression, (Figure 3.1B, Figure 3.1C), transfection agent or scrambled control siRNA had no effect.

In Figure 3.2A the severity of SNAT2 transporter inhibition with the silencing siRNA was comparable with that observed during acidosis (Appendix Figure 1C). As expected, depletion of L-Gln, of branched-chain amino acids (L-Leu, L-Ile, L-Val), of aromatic amino acids (L-Phe, L-Tyr, L-Trp) and of L-His, L-Met and L-Thr (Figure 3.2 and Table 3.1) was similar to that observed in

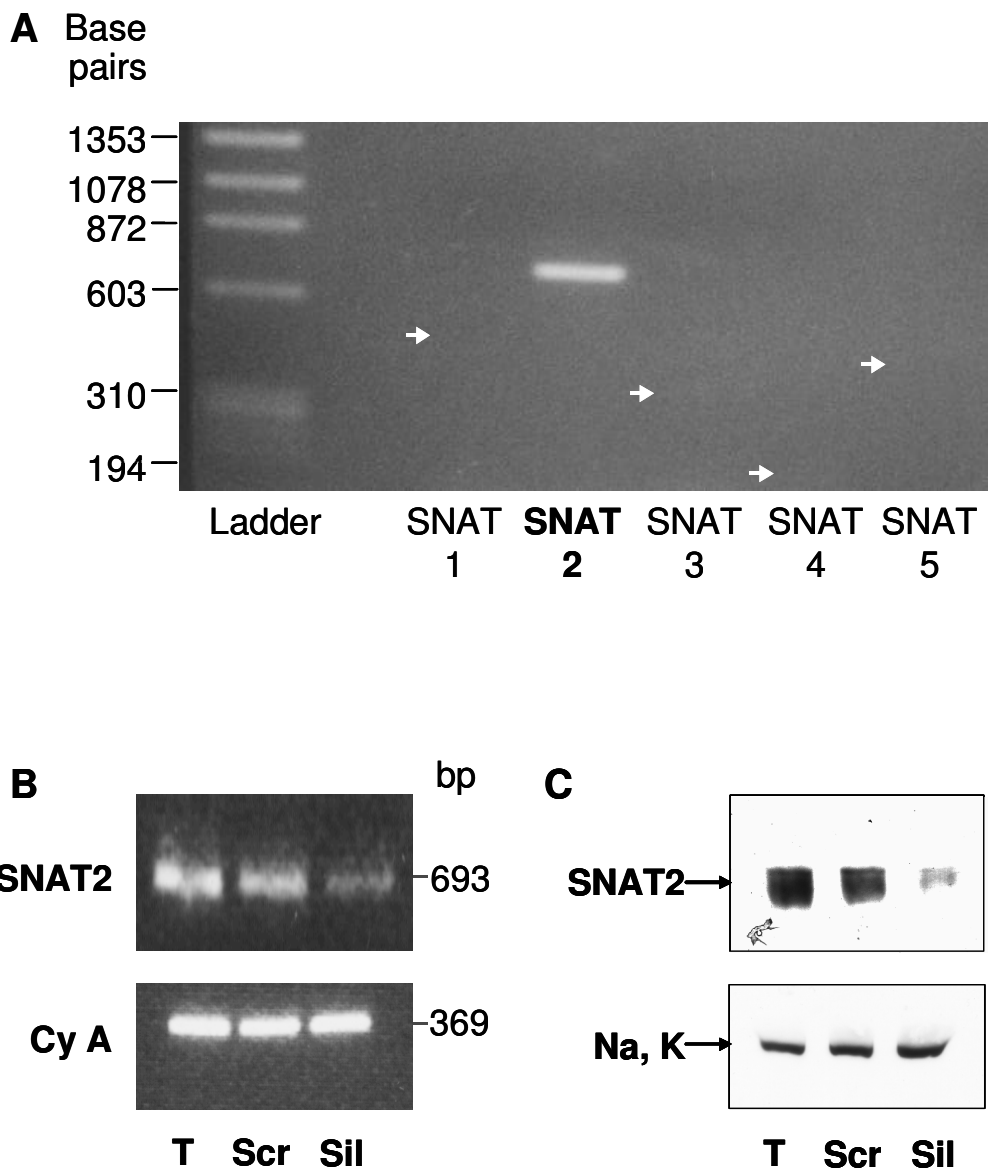


Figure 3.1. (A) Detection of SNAT (slc38 gene family) expression in L6-G8C5 myoblasts by RT-PCR using specific oligonucleotide primers (see Materials and Methods Section). Only SNAT2 expression was detected. White arrows denote the size of the PCR products expected with the primers for SNAT1 and SNAT 3-5. "Ladder" is a PhiX174 Hae III DNA digest (Sigma D-0672). (B) Confirmation of siRNA silencing of SNAT2 expression in L6-G8C5 myoblasts by RT-PCR using the same SNAT2-specific PCR primers as in (A) and Cyclophilin A primers "CyA" as a loading control. "T" denotes transfection blank (cells exposed to calcium phosphate transfection agent only), "Scr" denotes cells exposed to scrambled control siRNA, and "Sil" denotes cells exposed to SNAT2-silencing siRNA. (C) Confirmation of siRNA silencing of SNAT2 expression by immunoblotting of proteins separated by SDS-PAGE from a 170,000g membrane fraction derived from L6-G8C5 myoblasts incubated with siRNAs or transfection agent as in (B). Proteins were probed with SNAT2-specific antibody 2 (see Materials and Methods Section) or α_1 -Na, K-ATPase antibody "Na,K" as a loading control. Results are representative of 3 independent experiments.

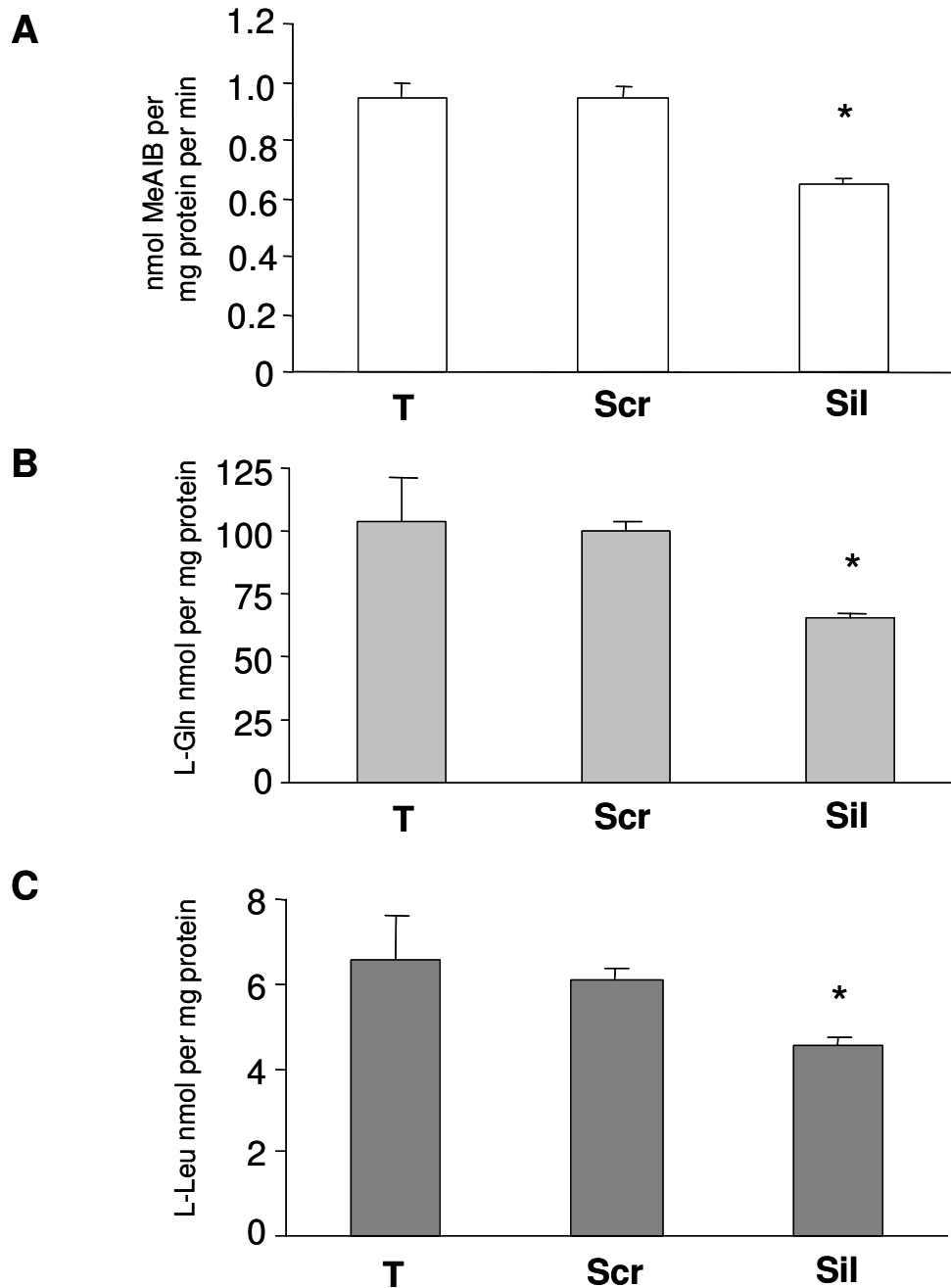


Figure 3.2. Effect of SNAT2 silencing with siRNA on amino acids in L6-G8C5 myoblasts. SNAT2 protein expression in this experiment is shown in Figure 3.1C. (A) SNAT2 transporter activity assessed from the rate of uptake of ^{14}C -MeAIB. (B) Intracellular L-Gln concentration. (C) Intracellular L-Leu concentration. (Data for other amino acids are presented in Table 3.1). "T" denotes transfection blank (cells exposed to calcium phosphate transfection agent only), "Scr" denotes cells exposed to scrambled control siRNA, and "Sil" denotes cells exposed to SNAT2-silencing siRNA. Twenty-four hours after removal of transfection agent, cultures were incubated for a further 3h in serum-free MEM pH 7.4 with 2% dialysed serum before preparation of amino acid extracts. * $P < 0.05$ versus Scr. Results from 1 experiment representative of 3 independent experiments are shown (with $n = 3$ to 4 replicate culture wells for each treatment).

myotubes at pH 7.1 (Appendix E Figure 1 and Appendix E Table 1). In contrast scrambled siRNA, when compared with transfection agent alone, had a negligible effect, exerting a statistically significant effect only on Gly (Table 3.1).

Table 3.1. Effect of SNAT2 Silencing with siRNA on Intracellular Free Amino Acid Profile in L6-G8C5 Myoblasts

(Data for L-Gln and L-Leu are presented in Figure 3.2).

Amino acid	Conc. in fresh MEM $\mu\text{mol/L}$	Intracellular Free Amino Acid Concentration (nmol per mg protein)		
		Transfection blank	Scrambled siRNA	Silencing siRNA
L-Ala	Nil	50.8 \pm 7.7	38.9 \pm 1.0	61.8 ^b \pm 3.3
L-Arg	600	6.5 \pm 1.0	5.7 \pm 0.2	5.7 \pm 0.3
L-Asn	Nil	1.01 \pm 0.11	0.99 \pm 0.03	0.96 \pm 0.04
L-Asp	Nil	16.6 \pm 2.2	14.0 \pm 0.7	16.5 \pm 0.6
L-Cys	200 ^a	UD	UD	UD
L-Glu	Nil	94.4 \pm 13.2	88.9 \pm 3.8	80.3 \pm 3.9
L-Gly	Nil	7.4 \pm 1.3	3.9 ^c \pm 0.8	3.2 ^c \pm 0.3
L-His	200	5.6 \pm 0.7	4.2 \pm 0.9	1.9 ^{bc} \pm 0.1
L-Ile	400	5.7 \pm 0.4	5.4 \pm 0.3	3.9 ^b \pm 0.2
L-Lys	400	3.7 \pm 0.1	3.8 \pm 0.2	3.9 \pm 0.2
L-Met	100	2.6 \pm 0.4	2.9 \pm 0.1	1.6 ^b \pm 0.1
L-Phe	200	4.3 \pm 0.6	4.1 \pm 0.2	3.1 ^b \pm 0.1
L-Pro	Nil	4.2 \pm 0.1	4.2 \pm 0.5	4.8 \pm 0.4
L-Ser	Nil	1.26 \pm 0.15	1.27 \pm 0.04	1.31 \pm 0.16
L-Thr	400	29.0 \pm 3.0	25.7 \pm 1.0	19.8 ^b \pm 0.9
L-Trp	50	1.39 \pm 0.21	1.34 \pm 0.06	1.00 ^b \pm 0.05
L-Tyr	200	4.6 \pm 0.7	4.4 \pm 0.2	3.2 ^b \pm 0.2
L-Val	400	5.6 \pm 0.9	5.2 \pm 0.2	4.0 ^b \pm 0.2

Results from 1 experiment representative of 3 independent experiments are shown (with n= 4 replicate culture wells for each treatment). Silencing of SNAT2 protein expression in this experiment is shown in Figure 3.3c. **UD** - Undetectable, ^aAdded as Cystine, ^bP<0.05 versus scrambled siRNA, ^cP<0.05 versus transfection blank.

3.2.2 SNAT2 is a potential regulator of mTOR signalling to protein synthesis

Stimulation of protein phosphorylation events downstream of mTOR has been demonstrated previously in L6 myotubes in response to L-Leu, (192), and

may respond to other amino acids. Depletion of amino acids by SNAT2 inhibition would therefore be predicted to blunt such phosphorylation signals. For phosphorylation of ribosomal protein S6 (rpS6) this was clearly demonstrated when SNAT2 was inhibited with MeAIB or by low pH in L6 myotubes which had been stimulated with 2% serum or 100nM insulin (Figure 3.3A, 3.4B). A similar result was obtained for S6 kinase activation detected by mobility shift (Figure 3.3B) and for 4E-BP1 phosphorylation (Figure 3.3C).

Experiments were also performed in cultures pre-incubated for 4h with MeAIB, followed by thorough rinsing and incubation with medium without MeAIB. After 4h pre-incubation with 10mM MeAIB, SNAT2 transporter activity was strongly inhibited (Figure 3.4A), and detectable inhibition persisted for a further 2h in medium without MeAIB (Figure 3.4A). As expected, this inhibition also led to impairment of rpS6 phosphorylation (Figure 3.4B). However, pre-incubation with 10mM MeAIB spiked with ¹⁴C-MeAIB, followed by measurement of intracellular radio-activity after washing away the extracellular MeAIB, demonstrated that approximately 50% of the MeAIB remained associated with the cells, (results not shown), (presumably in the intracellular space), even after a further 2h in medium without MeAIB. In principle this might mean that MeAIB exerts its effects in Figure 3.3 and 3.4 by acutely blocking intracellular amino acid sensing by mTOR, rather than through its actions on SNAT2. The role of SNAT2 in regulation of mTOR signalling was therefore also examined by silencing SNAT2 with siRNA (Figure 3.3D). Again strong impairment of rpS6 phosphorylation was observed, confirming the original conclusion that MeAIB was impairing mTOR

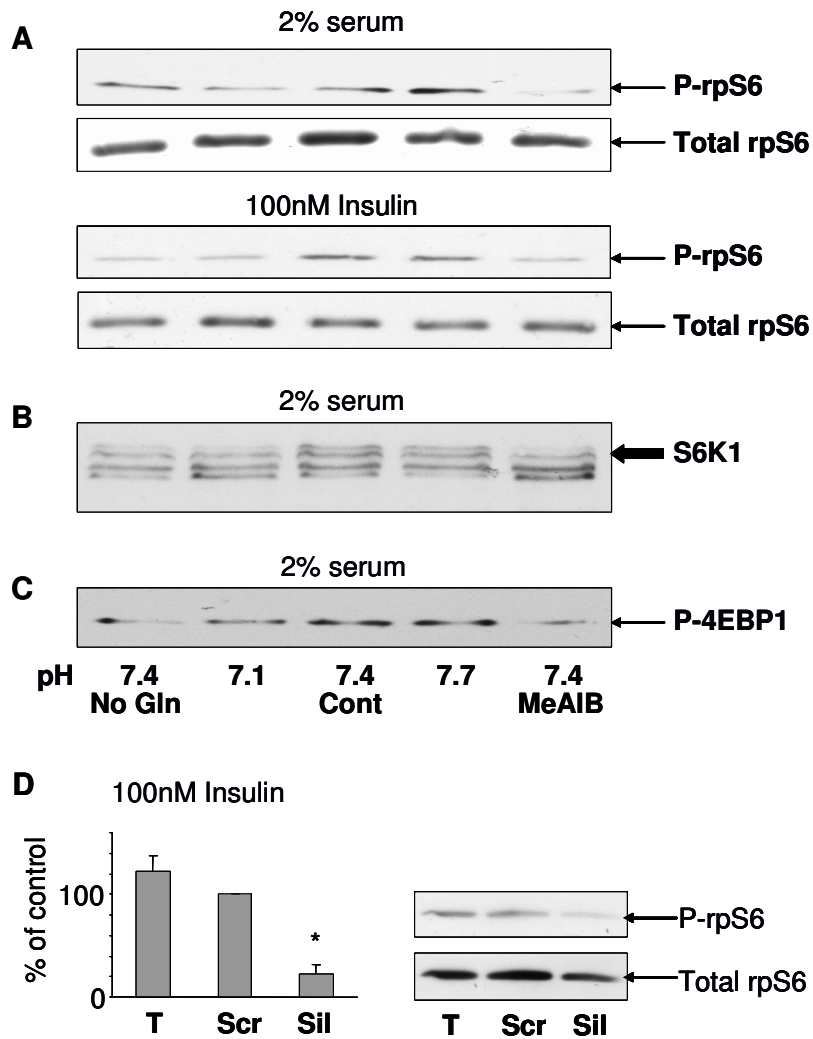


Figure 3.3. (A – C) Effect of 2h of extracellular L-Gln starvation, pH variation or inhibition of SNAT2 transporters with 10mM MeAIB on mTORC1-dependent (and therefore rapamycin sensitive) signalling in L6-G8C5 myotubes incubated in MEM with 2% dialysed serum, or serum-free medium with 100nM bovine insulin. Proteins were separated by SDS-PAGE and immunoblotted using specific antibodies. Blots representative of at least 3 independent experiments are presented as follows: (A) Ribosomal protein S6 (rpS6) phosphorylated at Ser residue 235/6. Quantification of rpS6 phosphorylation by densitometry is presented in Figure 3.4. (B) Ribosomal protein S6 kinase (irrespective of its state of phosphorylation). Mobility shifting of the main bands in MeAIB-treated cultures (black arrow) relative to the pH 7.4 control cultures indicates impaired phosphorylation/activation of rpS6 kinase. (C) Eukaryotic initiation factor 4E binding protein 1 (4E-BP1) phosphorylated at Ser residue 65. In 4 independent experiments the phosphorylation signal with MeAIB (quantified by densitometry) was 53 ± 9 % of the pH 7.4 Control value, $P < 0.05$. **(D) Effect of SNAT2 silencing with siRNA on rpS6 phosphorylation.** "T" denotes transfection blank (cells exposed to calcium phosphate transfection agent only), "Scr" denotes cells exposed to scrambled control siRNA, and "Sil" denotes cells exposed to SNAT2-silencing siRNA. Twenty-four hours after removal of transfection agent, cultures were incubated for a further 2h in serum-free MEM pH 7.4 with 100nM bovine insulin. The bar chart denotes quantification of phosphorylation by densitometry from 5 independent experiments expressed as % of the Scr control value. * $P < 0.05$ versus Scr.

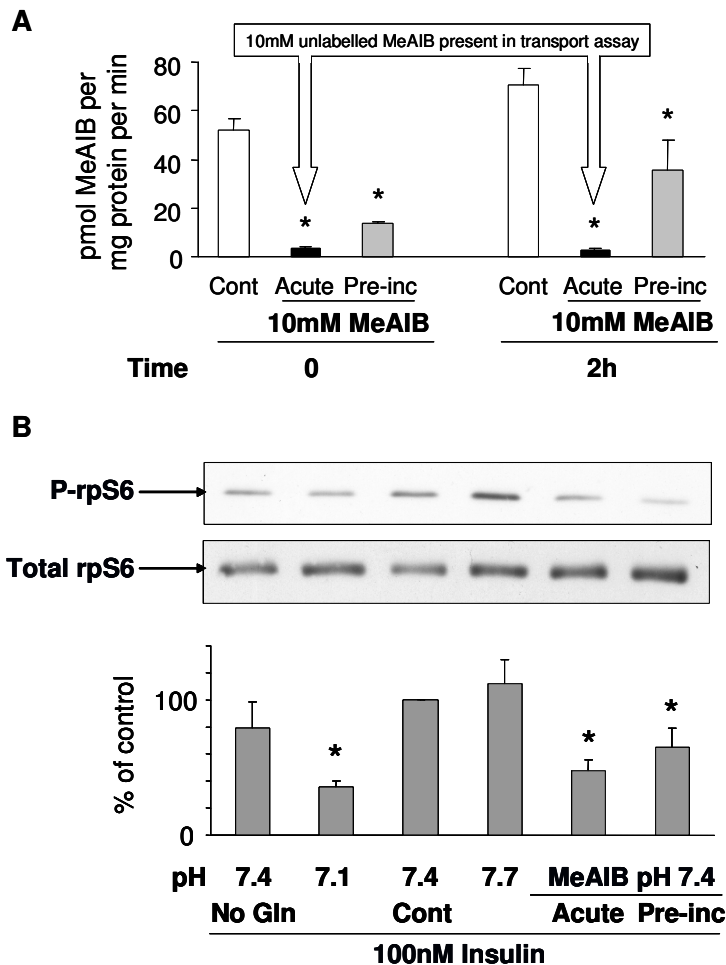


Figure 3.4. (A) Effect on SNAT2 transporter activity of acute incubation (Acute) or prolonged pre-incubation (Pre-inc) with MeAIB. L6-G8C5 myotubes were incubated for 4h in MEM/2% FBS with (Pre-inc) or without (Cont and Acute) 10mM MeAIB. Time 0 cultures were then rinsed three times with Hanks Balanced Salt Solution, and SNAT2 transporter activity (uptake of ^{14}C -MeAIB calculated using a specific radio-activity of 50mCi (1.85GBq) per mmol) was immediately measured (see Materials and Methods). Time 2h cultures received a further 2h incubation in serum-free MEM at pH 7.4 with 100nM bovine insulin with (Acute) or without (Cont and Pre-inc) 10mM MeAIB. Uptake of ^{14}C -MeAIB was then measured immediately at the end of the 2h incubation. In Acute cultures 10mM MeAIB was present throughout the 2h incubation and during both the Time 0 and 2h ^{14}C -MeAIB uptake assays: ^{14}C -MeAIB uptake in these cultures reflects non-specific binding rather than transport into the cells. * $P < 0.05$ versus the corresponding Cont cultures. Results from 1 experiment representative of 3 independent experiments are shown (with $n = 3$ replicate culture wells for each treatment).

(B) Effect on rpS6 phosphorylation of acute incubation (Acute) or prolonged pre-incubation (Pre-inc) with MeAIB. Cultures were incubated as in the experiment with bovine insulin in Figure 3.3(A), but those with MeAIB were either incubated acutely (Acute) for 2h, or pre-incubated (Pre-inc) for 4h followed by removal of MeAIB for the last 2h, exactly as described in (A) in the present figure. Immunoblotting was performed as in Figure 3.3(A). The bar chart denotes quantification of rpS6 phosphorylation by densitometry from 15 independent experiments (6 for Pre-inc) expressed as % of the pH 7.4 Control value. * $P < 0.05$ versus Control.

signalling through SNAT2 inhibition rather than through some other action of MeAIB on mTOR.

3.2.3 Functional effects of SNAT2 on protein metabolism

3.2.3.1 Effects of pH and MeAIB

In myotubes, the effect of low pH on mTOR signalling in Figure 3.3 and 3.4 was accompanied by a sustained 48h impairment of global protein synthesis (Figure 3.5C) and a decrease in total protein (10 ± 2 % decrease in 48h versus pH 7.4 cultures, $P < 0.05$). Similarly, in myoblasts, 24h of incubation at pH 7.1 decreased total protein content and impaired protein synthesis (Table 3.2). The acidosis effect on protein synthesis in myotubes was blunted by 10nM Rapamycin, a dose which almost abolishes signalling to rpS6 (Figure 3.5A and 3.5C), suggesting that signalling through mTOR is involved. The effect was also blunted by extracellular L-Gln deprivation (Figure 3.5C) implying that it is mediated at least partly by effects on L-Gln, a possibility which is investigated further in Chapter 5.

It has been shown previously in L6 myotubes that antagonism of amino acid influx through SNAT2 with as little as 1mM MeAIB in the presence of 2mM L-Gln stimulates global proteolysis within 7h, (56), an effect which is blunted by extracellular L-Gln deprivation or L-Gln loading, implying that MeAIB acts at least partly by antagonising L-Gln influx, (56). In the present study with myotubes in the presence of 2mM L-Gln, MeAIB also significantly impaired

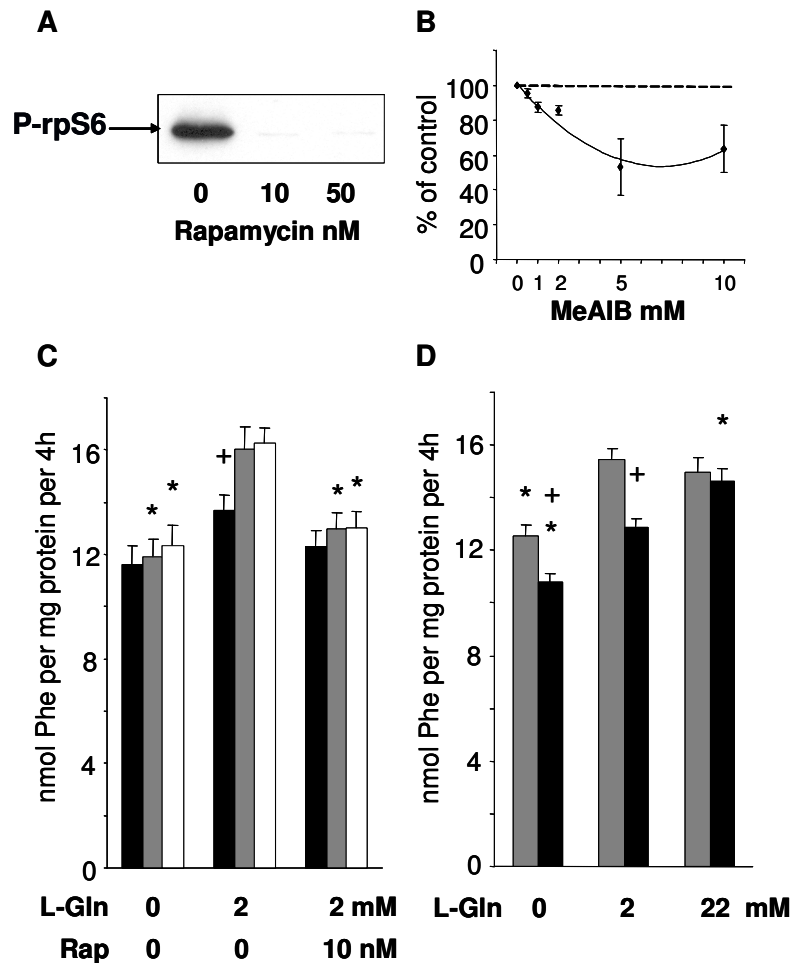


Figure 3.5. (A) Inhibition of mTOR signalling with Rapamycin in L6-G8C5 myotubes. Phosphorylation of rpS6 after 2h in MEM pH 7.4 with 2% dialysed serum and the specified dose of Rapamycin was detected exactly as described in Figure 3.3A. Identical results were obtained with 100nM bovine insulin in place of serum.

(B-D) Effects of pH or SNAT2 inhibition on protein synthesis rate ($^3\text{H-L-Phe}$ incorporation) in L6-G8C5 myotubes. Pooled data from 3 independent experiments (with $n=3$ replicate culture wells for each treatment). (B) Dose-response curve for acute inhibition of protein synthesis by MeAIB. Myotubes were incubated for 2h in MEM pH 7.4 with 2% dialysed serum and the specified dose of MeAIB. $^3\text{H-L-Phe}$ was present in the medium for the final 30 min of the incubation. Synthesis rate is expressed as % of the rate in control cultures without MeAIB. Significant ($P < 0.05$) inhibition was observed at all doses above 0.5mM. (C) Effect of prolonged acidosis on protein synthesis rate. Myotubes were incubated for 48h in MEM with 2% dialysed serum and the specified concentrations of L-Gln or Rapamycin at pH 7.1 (black bars), pH 7.4 (grey bars) or pH 7.7 (white bars). * $P < 0.05$ versus the corresponding value at the same pH with 2mM L-Gln and without Rapamycin. + $P < 0.05$ versus the corresponding value at pH 7.4 (D) Effect of prolonged SNAT2 inhibition with MeAIB on protein synthesis rate. Myotubes were incubated for 48h in MEM pH 7.4 with 2% dialysed serum and the specified concentrations of L-Gln in medium with 10mM MeAIB (black bars), or no MeAIB (grey bars). * $P < 0.05$ versus the corresponding value with 2mM L-Gln. + $P < 0.05$ versus the value at the same L-Gln concentration without MeAIB.

global protein synthesis within 2h at doses down to 1mM (Figure 3.5B). This impairment was sustained for at least 48h (Figure 3.5D), was comparable in magnitude with the impairment seen with Rapamycin or L-Gln starvation (Figure 3.5C,D) and was accompanied by a decline in total protein ($16 \pm 2\%$ decrease in 48h, $P < 0.05$).

Table 3.2. Functional Effects on Global Protein Metabolism of Inhibiting SNAT2 for 24h with Low pH or MeAIB in L6-G8C5 Myoblasts.

		Composition of the Experimental Medium			
		Control			
	pH	7.1	7.4	7.7	7.4
	L-Gln (mmo/L)	2	2	2	2
	MeAIB (mmol/L)	0	0	0	10
Total Protein t=28h	$\mu\text{g per 35mm well}$	174 ± 17	212 ± 11	195 ± 15	$165^* \pm 18$
	<i>% of pH 7.4 Control value</i>	$81^* \pm 6$	100	92 ± 5	$77^* \pm 7$
Protein Synthesis Rate t=24-28h	$\text{nmol L-Phe per mg protein in 4h}$	$8.8^{**} \pm 0.3$	9.9 ± 0.5	10.3 ± 0.3	$8.15^* \pm 0.12$
	<i>% of pH 7.4 Control value</i>	$89^* \pm 3$	100	104 ± 3	$82^* \pm 1$
Proteolysis Rate t=26-33h	$\log_{10}\% \text{ per h} \times 10^3$	10.8 ± 0.9	10.5 ± 0.9	10.4 ± 1.1	13.6 ± 1.0
	<i>% of pH 7.4 Control value</i>	102 ± 2	100	98 ± 2	$130^* \pm 2$
Intact Protein Leakage (Cell damage indicator) t=26-33h	$\% \text{ per h}$	0.13 ± 0.01	0.16 ± 0.01	0.17 ± 0.02	0.15 ± 0.02
	<i>% of pH 7.4 Control value</i>	80 ± 8	100	102 ± 8	94 ± 8

Pooled data from 3 experiments are shown (with 3 replicate culture wells for each treatment). Cells were incubated in the Experimental Media (MEM + 2% Dialysed Foetal Bovine Serum with the additions stated) for 24h. All measurements were then made in parallel at the times (t) indicated using fresh samples of the same Experimental Media.

$P < 0.05$ versus pH 7.4 Control, $^* P < 0.05$ versus pH 7.7

The magnitude of this inhibition of protein synthesis was blunted by extracellular L-Gln deprivation ($30 \pm 4\%$ decrease, $P < 0.05$, Figure 3.5D) and abolished in medium loaded with 22mM L-Gln (Figure 3.5D), again implying that antagonism of L-Gln by MeAIB was a contributor. In myoblasts, complete inhibition of SNAT2 with 10mM MeAIB impaired protein synthesis, stimulated global proteolysis and decreased total protein without loss of cell viability (Table 3.2).

However, unlike myotubes, (56), partial inhibition of SNAT2 with low pH had no effect on proteolysis (Table 3.2), and partial competitive inhibition of SNAT2 with lower doses of MeAIB (0.5 – 2mM) gave negligible stimulation of proteolysis (data not shown), suggesting that proteolysis in myoblasts is less responsive to SNAT2 than in myotubes.

3.2.3.2 Effects of SNAT2 silencing

The functional importance of SNAT2 in protein metabolism was confirmed by silencing SNAT2 in L6 myoblasts with siRNA (Table 3.3). SNAT2 silencing significantly decreased the protein content of the cultures (Table 3.3). This was not attributable to cell toxicity (protein leakage or cell detachment) because protein release into the medium decreased rather than increased when SNAT2 was silenced (Table 3.3). In agreement with the lack of effect of low pH on proteolysis in myoblasts (Table 3.2), the partial silencing of SNAT2 activity (76% inhibition) had no stimulatory effect on proteolysis (Table 3.3). However, the protein synthesis rate was lower in the silenced cultures (Table

3.3), commensurate with the decline in synthesis observed with low pH or MeAIB in Table 3.2.

Table 3.3. Functional Effects on Global Protein Metabolism of 24h of SNAT2 Silencing with siRNA in L6-G8C5 Myoblasts.

		Control		
		Transfection blank	Scrambled siRNA	Silencing siRNA
SNAT2 Transporter Activity t=24h	pmol MeAIB per mg protein per min	227 ± 48	249 ± 56	63* ± 19
	% of Control value	97 ± 10	100	24* ± 7
Total Protein t=28h	µg per 35mm well	316 ± 55	284 ± 40	203 ± 31
	% of Control value	106 ± 15	100	71* ± 5
Protein Synthesis Rate_{t=24-28h}	nmol L-Phe per mg protein in 4h	9.1 ± 1.2	9.2 ± 1.2	8.2 ± 1.1
	% of Control value	99 ± 1	100	88* ± 2
Proteolysis Rate t=26-33h	log₁₀% per h x 10³	7.3 ± 0.4	7.7 ± 0.4	7.4 ± 0.4
	% of Control value	94 ± 6	100	97 ± 5
Intact Protein Leakage (Cell damage indicator) t=26-33h	% per h	0.11 ± 0.02	0.14 ± 0.03	0.09 ± 0.01
	% of Control value	84* ± 6	100	73* ± 6

Pooled data from 3 experiments are shown (with 3 replicate culture wells for each treatment). Cells were transfected with SNAT2 silencing siRNA or Scrambled Control siRNA as described in Methods. Transfection was followed by a 24h incubation in DMEM + 10% foetal bovine serum. All measurements were then made in parallel at the times indicated in MEM at pH 7.4 with 2% dialysed foetal bovine serum. The times (t) denote the time elapsed since removal of the transfection agent. *P<0.05 versus Scrambled Control siRNA

In spite of the failure to detect effects of SNAT2 silencing on proteolysis described above, subsequent work showed that coupling does in fact exist between SNAT2 and proteolysis, but that this is only detectable in differentiated myotubes. This is described in detail in the next Chapter.

3.3 Discussion

3.3.1 SNAT2 determines L-Gln concentration in L6-G8C5 cells

The SNAT2 silencing experiments described in this chapter are the first demonstration that selective inhibition of a single transporter protein, SNAT2 (Slc38A2), leads to marked depletion of L-Gln in cultured skeletal muscle cells. At first sight this is surprising because a wide range of amino acid transporter genes are expressed in muscle and a number of these transport L-Gln, (57). Not all of these however directly accumulate L-Gln inside cells against its concentration gradient. For example ASC transporters (Slc1 A4 and A5) and System L transporters (Slc7 A5 and A8) are primarily amino acid exchangers, (57), and consequently have only secondary effects on the intracellular L-Gln concentration. Members of the SNAT/Slc38 transporter family, other than SNAT2, can transport L-Gln against a gradient, (64), but are unlikely to contribute to L-Gln accumulation in L6 cells because they are expressed only at low levels (Figure 3.3A). A similar situation applies in muscle *in vivo* where the predominant SNAT transporter expressed is again SNAT2, (66,74). Of the other System A transporters, SNAT1 is only expressed at low level, (64), and SNAT4 is unlikely to be a major contributor because L-Gln is only a weak substrate for this transporter, (194). The role of the N-type transporters SNAT3 and SNAT5 in muscle is currently unknown, but it should be noted that, in addition to driving intracellular L-Gln accumulation, they can also perform L-Gln efflux, (70).

3.3.2 Inhibition of SNAT2 depletes amino acids not transported on SNAT2

Selective silencing of SNAT2 led to depletion of other amino acids which are not regarded as SNAT2 substrates (Figure 3.2C, Table 3.1) suggesting that SNAT2 also exerts indirect effects. This is consistent with reports that System A transporters, particularly SNAT2, (84), "energise" the active accumulation of amino acids through other transporters, notably System L, by building a transmembrane L-Gln gradient which then drives active uptake of other amino acids such as L-Leu by exchange of intracellular L-Gln for extracellular L-Leu (see Section 1.5.3.1). This suggests that SNAT2 is an important determinant of the intracellular concentration of amino acids thought to exert a protein anabolic effect in muscle (i.e L-Gln, L-Leu, L-Ile and L-Val).

3.3.3 SNAT2 regulates mTOR and influences protein metabolism

Signalling effects through amino acid transporters are now a well-established concept in mammalian cell biology, (57). While much remains to be learned about signalling pathways affected by SNAT2, the data in Figure 3.3 and 3.4 suggest that the level of SNAT2 inhibition by acidosis exerts functionally significant effects on mTOR, consistent with an earlier report of co-regulation of SNAT2 and mTOR in L6 cells treated with ceramide, (190). Acute inhibition of the flux through SNAT2 by treating with MeAIB could in principle exert non-specific effects (independent of SNAT2) because MeAIB is itself an amino acid analogue and might influence amino acid sensing by the cell. This is unlikely to be the full explanation, however, because a similar impairment of rpS6 signalling was obtained by silencing SNAT2 with siRNA (Figure 3.3D)

and these effects on mTOR were followed by sustained effects on protein metabolism (Figure 3.5 and Table 3.3). These observations are functionally important because System A/SNAT2 transporters up-regulate in muscle in response to exercise, (195), (and presumably down-regulate in sedentary renal patients), and mTOR signalling is a key link between mechanical loading of muscle and the resulting stimulation of protein synthesis, (196,197). The experiments presented here did not determine however which amino acid(s) affected by SNAT2 were mediating the effects of SNAT2 on mTOR and protein metabolism. This problem is investigated further in Chapter 5.

3.3.4 SNAT2 inhibition mimics the effects of acidosis in vivo

A recent site-directed mutagenesis study showed that SNAT2 inhibition by low pH is largely a consequence of protonation of an extracellular C-terminal histidine residue, (73). The fall in interstitial fluid pH which occurs even during compensated metabolic acidosis in vivo, (198,199), would therefore be expected to inhibit SNAT2 directly. Inhibition of System A/SNAT2 activity has been reported in vivo in skeletal muscle of patients with chronic renal failure, (200), and persistent inhibition has been demonstrated during ex vivo incubation of muscles from uraemic rats, (201), suggesting that uraemic factors other than protonation also inhibit SNAT2. The pattern of amino acid depletion observed in the present study resembles the changes in intramuscular amino acid concentrations and muscle/plasma concentration gradients reported in haemodialysis patients, (180,181). The mechanisms reported here may therefore be relevant to the initiation of amino acid

depletion and impaired protein metabolism *in vivo*. Finally these effects may be particularly important in renal patients with diabetes mellitus. In view of their pre-existing insulin deficiency or insulin resistance, the inhibition of amino acid-dependent insulin signalling through mTOR following SNAT2 inhibition may explain why muscle protein metabolism is so badly impaired in these patients, (18). This leads to the interesting question of whether other pathways of insulin signalling in addition to mTOR are impaired by inhibiting SNAT2, and this is the subject of the next chapter.

Chapter 4: The effect of the SNAT2 transporter on phosphatidylinositol-3-kinase (PI3K) signalling and global proteolysis.

4.1 Introduction

There is now strong evidence that, even in non-diabetic patients, insulin resistance in end-stage renal disease is a major cause of muscle wasting, (165,202). As an important contributor to this problem is uraemic metabolic acidosis, (177), this implies that low pH has a significant impact on insulin signalling in uraemic muscle, and raises the question of whether pH sensing through SNAT2 might be involved.

In the previous chapter it was shown that inhibition of SNAT2 rapidly depletes intracellular amino acids and thereby strongly impairs insulin signalling to protein synthesis through mTOR. While this provides a plausible explanation for the inhibition of muscle protein synthesis that occurs during acute metabolic acidosis in humans, (37), the response of muscle to chronic uraemic metabolic acidosis in renal patients usually involves increased proteolysis, (28,183). A possible rationale for this chronic proteolysis is that it is an adaptation to the initial amino acid depletion, whereby amino acids are harvested from muscle protein to restore intracellular amino acid levels, (182), thereby minimising impairment of protein synthesis but at the expense of chronically elevated proteolysis.

The stimulation of proteolysis by low pH in L6 myotubes has been attributed to a defect in insulin signalling through Insulin Receptor Substrate-1

associated Phosphatidylinositol-3-Kinase (IRS-1-associated PI3K) leading to impaired activation of Protein Kinase B (PKB), (30), (see Section 1.7.1) and a similar defect has been demonstrated in acidotic and uraemic rat skeletal muscle *in vivo*, (164). Unlike mTOR signalling, Type I PI3K signalling to PKB is not traditionally regarded as an amino acid sensitive pathway, implying that inhibition of SNAT2 by acidosis is not responsible for this effect. However, a Type III PI-3-kinase (Section 1.6.2.5.3) has been implicated in amino acid sensing by the mTOR pathway, (113). There is also recent evidence from amino acid starved L6 myotubes that extracellular amino acid concentration is sensed through SNAT2 which acts as a signalling protein in its own right – a so-called “transceptor”, (80), which signals to SNAT2 gene expression, (80). This signal is blunted by inhibitors of PI3K, (80), implying that coupling exists between SNAT2 and this enzyme. It is not known however whether such coupling influences PI3K signalling to PKB and proteolysis.

4.1.1 Increased proteolysis arising from insulin resistance during acidosis can be modelled *in vitro* using L6-G8C5 myotubes

Prior to the start of the work described in this thesis, it was shown by other workers in this laboratory that L6-G8C5 myotubes are a suitable cell culture model in which to study these effects. Increased global proteolysis is readily demonstrable in L6-G8C5 myotubes after as little as 7h of exposure to medium at pH 7.1 ((56) and Appendix E Figure 3A), and this pH-dependence is still observed in the presence of Actinomycin D (Appendix E Figure 3A), implying that its initiation requires only post-transcriptional events. If, as proposed above, (30), proteolysis induced by acidosis arises from insulin

resistance, the dose-response curve for suppression of proteolysis by insulin or IGF-I should be right-shifted by acid, with the effect of acid disappearing both in insulin-free medium and when excess insulin or IGF-I is added to overcome the resistance. In serum-free medium with insulin or IGF-I as the sole anabolic factor, L6-G8C5 myotubes clearly showed this hypothetical right-shift (Appendix E Figure 3B and 3C). No pH effect was observed in serum-free medium alone, and the effect of pH was abolished with high dose IGF-I.

Therefore, using this culture model, the aims of the work described in this chapter were:

- Firstly to determine whether the effect of metabolic acidosis or SNAT2 inhibition on intracellular amino acid levels shows an adaptive response consistent with compensatory harvesting of amino acids by proteolysis
- Secondly, to determine whether metabolic acidosis or SNAT2 inhibition in the presence of insulin activates proteolysis by signalling through mTOR or PI3K, and
- Thirdly to determine whether coupling between SNAT2 and PI3K/PKB signalling can be detected by selectively impairing the activity or expression of SNAT2.

4.2 Results

4.2.1 Time course of intracellular L-Gln depletion by SNAT2 inhibition

As shown in Chapter 3, the 40% inhibition of the activity of the SNAT2 transporter that occurs on lowering the pH to 7.1 (Appendix E Figure 1C) leads within 2h to a fall in the concentration of many amino acids in L6-G8C5 myotubes, most notably a 25% fall in the large L-Gln pool (Figure 4.1A). However, in longer incubations of 7 or 24h duration the L-Gln depleting effect of low pH was blunted, no longer achieving statistical significance (Figure 4.1B and 4.1C). When amino acid influx through SNAT2 was completely inhibited with a saturating competing dose of the SNAT2 substrate MeAIB, strong L-Gln depletion was observed at 2h (Appendix E Figure 1A and Figure 4.1A) but no subsequent recovery occurred (Figure 4.1B and 4.1C). The cells therefore apparently possess mechanism(s) to bolster L-Gln levels in the face of partial SNAT2 inhibition in chronic acidosis, but not when SNAT2 is saturated with MeAIB.

4.2.2 Role of SNAT2 up-regulation and L-Gln synthetase in restoring L-Gln levels during acidosis

Complete amino acid starvation of L6 myotubes leads within a few hours to up-regulation of SNAT2, (80). A possible explanation therefore for the apparent L-Gln adaptive response to acidosis (and its failure on complete SNAT2 inhibition with MeAIB) is that intracellular amino acid depletion during acidosis up-regulates SNAT2 thus increasing L-Gln influx. However no significant increase in expression of the SNAT2 protein was detected in

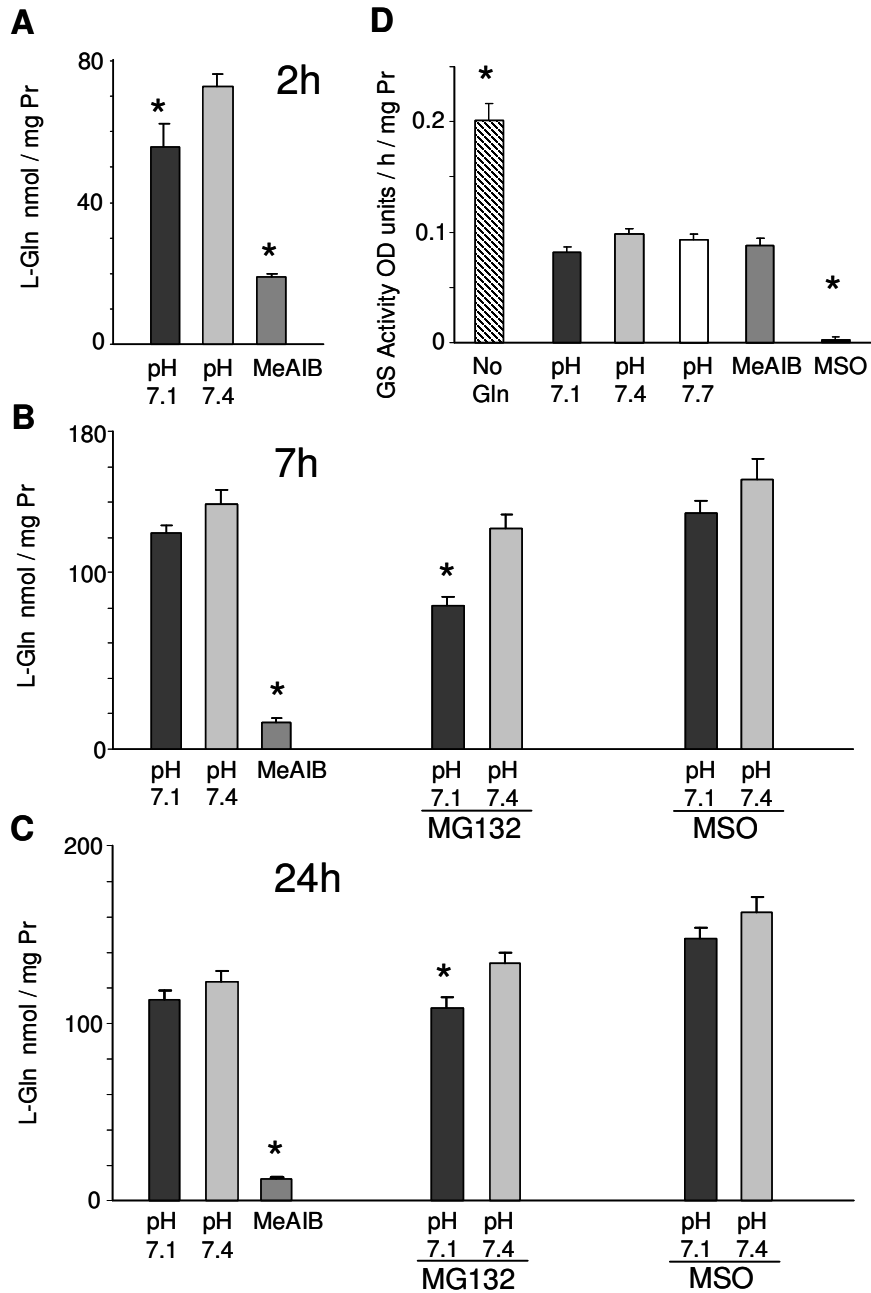


Figure 4.1. (A) – (C) Time course of the effect of low pH or methylaminoisobutyrate (MeAIB) (10mM) on the intracellular concentration of L-Gln in L6-G8C5 myotubes, with MG132 (10 μ M) or Methionine Sulfoximine (MSO) (1mM). Media were based on MEM and contained 2mM L-Gln with 2% dialysed foetal bovine serum. Pooled data from 3 independent experiments are shown (with at least 3 replicate culture wells for each treatment). In 24h incubations, MG132 and MSO were present only for the last 7h. (D) L-Glutamine Synthetase catalytic activity in lysates from L6-G8C5 myotubes incubated for 48h at pH 7.4 without L-Gln, or with 2mM L-Gln at the specified pH or with 2mM L-Gln at pH 7.4 with 10mM MeAIB or 1mM MSO. Fresh medium of the same composition was added after 24h. Pooled data from 5 independent experiments are shown (with at least 3 replicate culture wells for each treatment). *P<0.05 versus the corresponding control value at pH 7.4.

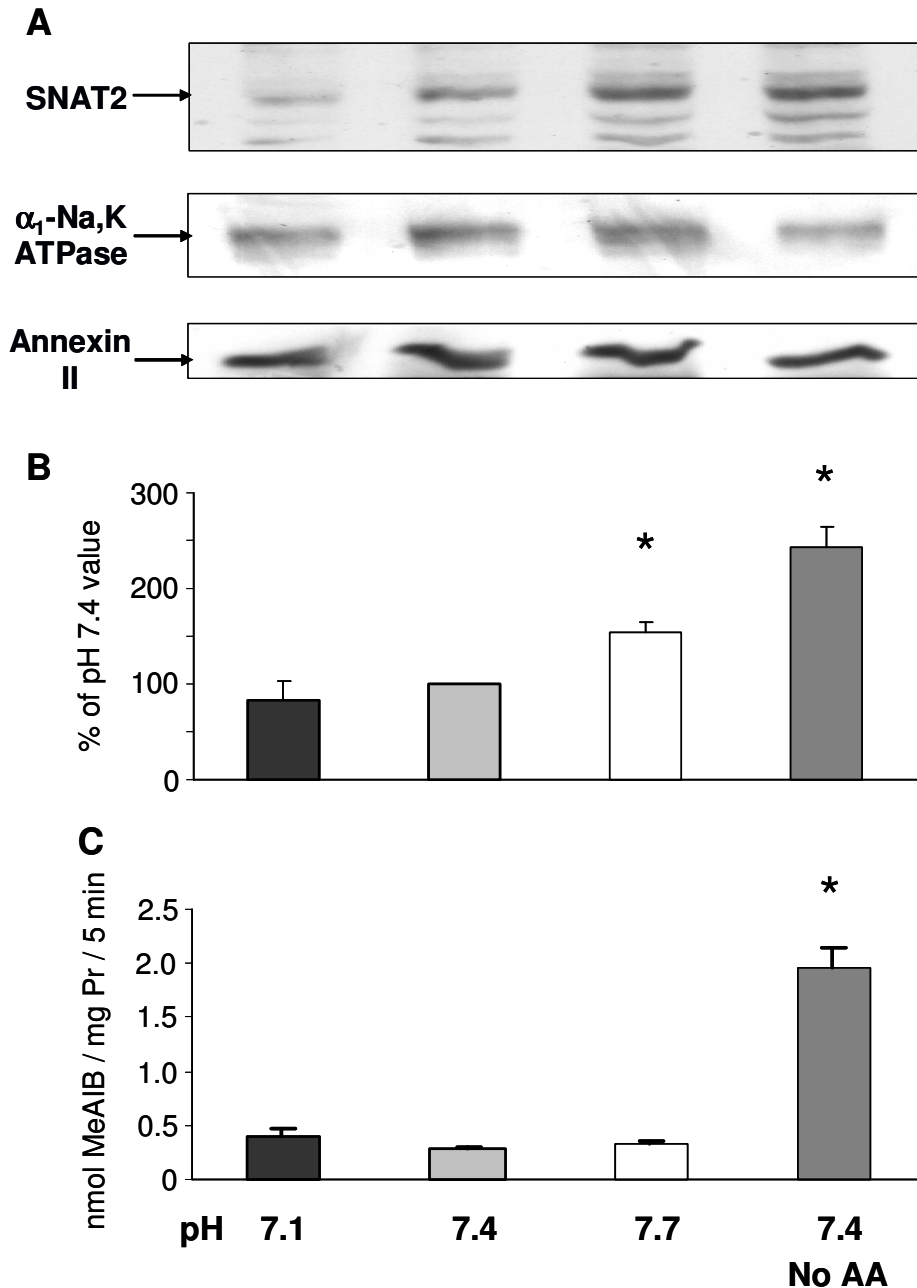


Figure 4.2. Effect of 6h of incubation in MEM with 2% dialysed foetal bovine serum at the specified pH, or at pH 7.4 with no amino acids (“No AA”), on SNAT2 expression in L6-G8C5 myotubes. (A) Immunoblots of proteins separated by SDS-PAGE from a 170,000g membrane preparation, probing with SNAT2-specific antibody (or α_1 -Na,K-ATPase antibody or Annexin II antibody as loading controls). (B) Quantification by densitometry of the principal 65kDa SNAT2 band in blots like (A). Pooled data are presented from 4 independent experiments. (C) Assay of SNAT2 transporter activity. After 6h incubation, cultures were rinsed with Hepes-buffered balanced salt solution (at pH 7.4 for all cultures), and uptake of 14 C-labelled methylaminoisobutyrate (MeAIB) was measured at 25°C (see Materials and Methods). Representative assay from 3 independent experiments. *P<0.05 versus the pH 7.4 control value.

response to 6h at low pH, even though a clear increase was observed on complete amino acid starvation (Figure 4.2A and 4.2B). SNAT2 transporter activity across the plasma membrane was also strongly activated by amino acid starvation (Figure 4.2C), but again no significant increase was observed in response to 6h of exposure to acid when transport was assayed immediately after restoring the pH from 7.1 to 7.4 (Figure 4.2C).

Complete removal of L-Gln from the extracellular medium activates the enzyme L-Gln synthetase in these cells (Figure 4.1D). However, no such effect occurred in response to partial depletion of L-Gln with acid or MeAIB (Figure 4.1D). The L-Gln synthetase inhibitor Methionine Sulfoximine (MSO), at a dose which abolishes activity of the enzyme (Figure 4.1D), also gave no detectable depletion of intracellular L-Gln during acidosis (Figure 4.1B and 4.1C) confirming that L-Gln synthesis is not a major factor sustaining L-Gln levels in acidosis.

4.2.3 Proteolysis maintains intracellular L-Gln levels during acidosis

The onset after ~7h of increased proteolysis in L6-G8C5 myotubes in response to acidosis (Appendix Figure 3A) coincides with the time at which the L-Gln depletion effect is blunted (Figure 4.1B). Blockade of proteolysis with the proteasome inhibitor MG132 enhanced the L-Gln depleting effect of low pH, prolonging it to 7h and 24h (Figure 4.1B and 4.1C), demonstrating that the stimulation of proteolysis by acidosis has a significant role in maintaining intracellular L-Gln levels at these time points.

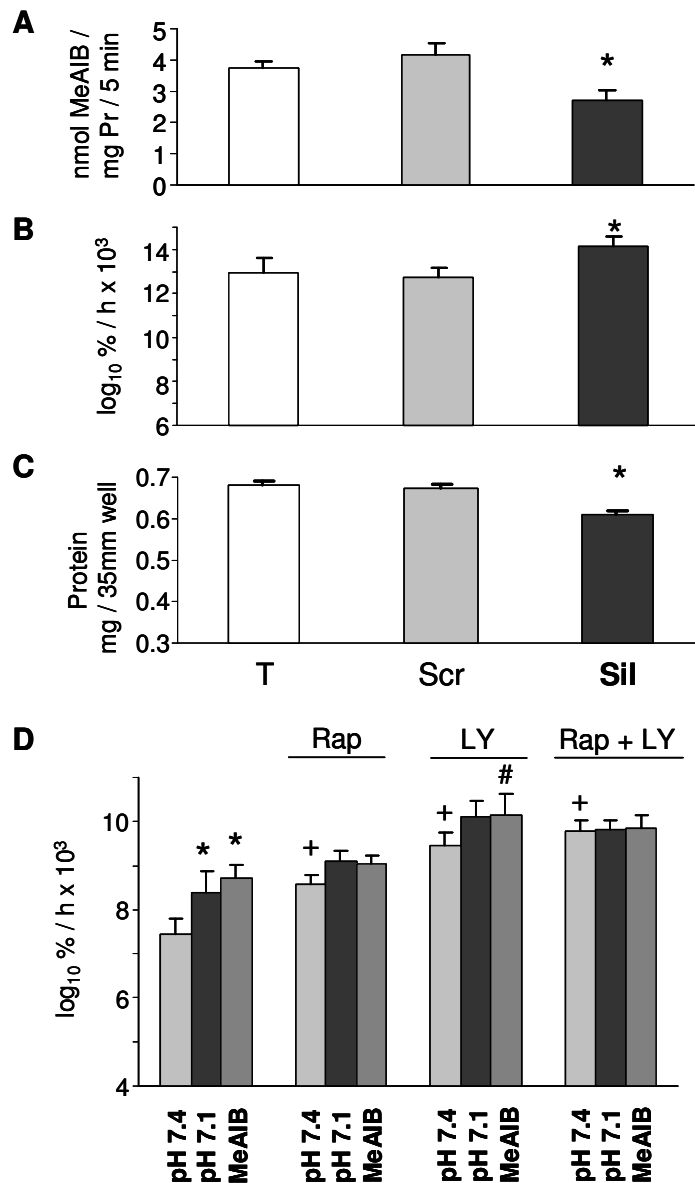


Figure 4.3. (A) – (C) Effect of siRNA silencing of SNAT2 in L6-G8C5 myotubes. Pooled data from 3 independent experiments are shown (with 3 replicate culture wells for each treatment). “T” denotes cultures incubated with calcium phosphate Transfection Blank, “Scr” scrambled control siRNA, and “Sil” SNAT2 silencing siRNA. Transfection was followed by an 8h incubation in DMEM + 10% foetal bovine serum followed by 16h in MEM + 2% dialysed foetal bovine serum. All measurements were then made in parallel as follows: (A) SNAT2 transporter activity (B) Proteolysis rate during 24h in MEM + 2mM L-Phe + 2% dialysed foetal bovine serum at pH 7.4. Cultures were pre-labelled by incubating with ³H-L-Phe for 72h (including the transfection incubation) before the de-labelling measurements. (C) Protein content of the cultures in (B). *P<0.05 versus “Scr” control. **(D) Effect of 100nM Rapamycin (“Rap”) and 12.5µM LY294002 (“LY”) on proteolysis rate in L6-G8C5 myotubes.** As in Appendix Figure 3B during incubation at pH 7.1, pH 7.4, or pH 7.4 with 10mM methylaminoisobutyrate (MeAIB) in serum-free MEM with 100nM insulin. *P<0.05 versus the corresponding pH 7.4 control value. +P<0.05 versus cultures at pH 7.4 without Rapamycin or LY294002. #P<0.05 versus cultures with 10mM MeAIB without LY294002. Pooled data from 4 independent experiments are shown (with 3 replicate culture wells for each treatment).

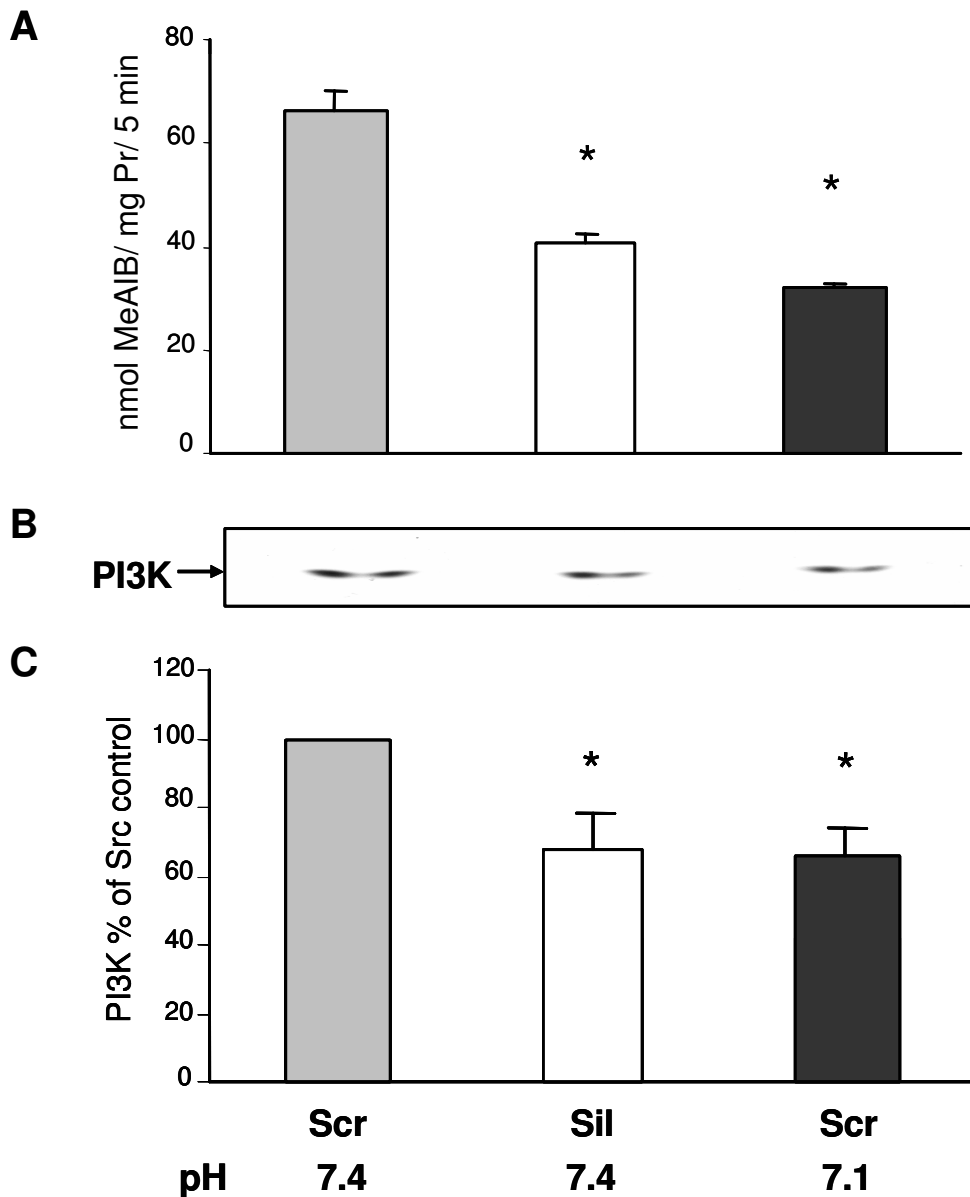


Figure 4.4. Comparison of the effects of siRNA silencing of SNAT2 and of acidosis on phosphatidylinositol-3-kinase (PI3K) activity in L6-G8C5 myotubes. Transfection (see Figure 4.3) was followed by 24h in DMEM + 10% foetal bovine serum. Cells were subjected to a further 2h incubation in serum-free MEM, at the specified pH with 100nM insulin before preparing lysates for PI3K assay.

(A) SNAT2 transporter activity assayed at the specified pH. (B) Representative autoradiograph of thin layer chromatography plate showing ^{32}P -labelled phosphatidylinositol-3-phosphate generated by the PI3K lipid kinase reaction (see Materials and Methods). (C) Quantification by densitometry of data pooled from 3 independent experiments performed as in (B), expressed as % of the pH 7.4 "Scr" control value. * $P < 0.05$ versus the pH 7.4 "Scr" control.

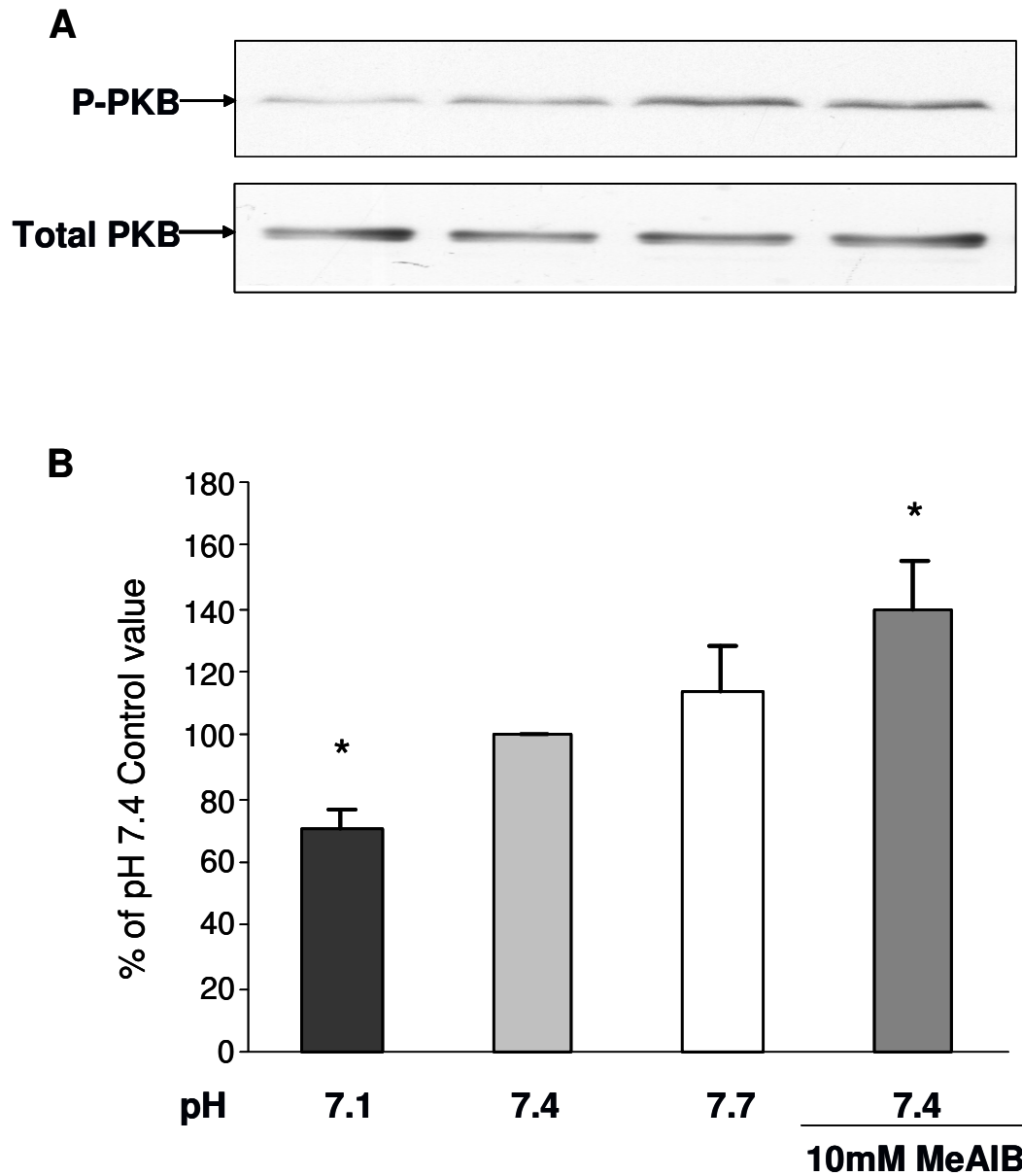


Figure 4.6. Effect on protein kinase B (PKB) activation in L6-G8C5 myotubes of 2h incubations at the specified pH with or without 10mM methylaminoisobutyrate (MeAIB) as in Figure 4.5. All media contained serum-free MEM with 100nM insulin. (A) Representative immunoblot showing PKB activation assessed from phosphorylation of PKB at Ser 473. (B) Pooled quantification data from 18 independent experiments performed as in (A) expressed as % of the control value at pH 7.4. *P<0.05 versus the pH 7.4 control.

4.2.4 Increased proteolysis in response to acid involves SNAT2

The effect of selective inhibition of SNAT2 on proteolysis was tested by selective silencing of SNAT2 expression using the siRNA characterised in the previous chapter. Treatment of differentiated myotubes with the silencing siRNA reduced SNAT2 transporter activity by 35% (Figure 4.3A, Figure 4.4A) a reduction comparable in magnitude with that observed on lowering extracellular pH to 7.1 (Appendix E Figure 1C and Figure 4.4A). This gave a clear stimulation of global proteolysis (Figure 4.3B) and, as predicted, the increase in proteolysis was similar in magnitude to that induced by acidosis (Appendix E Figure 3C) and yielded net protein wasting (Figure 4.3C) like that previously observed in acid-treated myotubes (Chapter 3 and (56)). Furthermore the previously reported stimulation of proteolysis when the amino acid influx through SNAT2 was blocked with MeAIB (Chapter 3 and (56)) was also observed in serum-free medium with insulin (Figure 4.3D).

4.2.5 Involvement of mTOR and PI3K signalling in acid-induced proteolysis

In the presence of insulin, the stimulatory effects of acid or MeAIB on proteolysis were mimicked when insulin signalling through mTOR and PI3K was inhibited with Rapamycin and LY294002 respectively (Figure 4.3D). In the presence of the stimulatory effect on proteolysis of Rapamycin or LY294002 alone, the stimulatory effect of acid or MeAIB no longer reached statistical significance (Figure 4.3D). In the presence of Rapamycin plus LY294002 combined, acidosis or MeAIB exerted no further stimulatory effect

(Figure 4.3D), consistent with the idea that low pH, acting through SNAT2, signals to proteolysis by impairing insulin signalling to mTOR and/or PI3K.

Low pH or selective inhibition of SNAT2 is already known to impair mTOR signalling in these cells (Chapter 3). Inhibition by low pH of PI3K and PKB has also been reported previously, (30), and was confirmed in myotubes in the present study (Figure 4.4C, Figure 4.5A,B and Figure 4.6). The effect of selective SNAT2 inhibition on insulin signalling to PI3K and PKB was investigated by silencing SNAT2 expression with siRNA in myoblasts which efficiently reduced SNAT2 protein expression (Figure 4.7A) and SNAT2 transporter activity (Figure 4.7B and 4.8A). Consistent with the effects of acidosis, silencing of SNAT2 alone significantly impaired both PI3K lipid kinase activity (Figure 4.7C-E) and PKB activation (Figure 4.8B,C). The weaker silencing of SNAT2 obtained in myotubes (Figure 4.3A, 4.4A) (similar in magnitude to the impairment of SNAT2 activity observed with acid (Figure 4.4A)) also gave an impairment of PI3K signalling similar to that observed with acid (Figure 4.4B,C), consistent with the similar stimulation of proteolysis observed in myotubes with SNAT2 silencing (Figure 4.3B) and acid (Appendix Figure 3C).

When the myoblast signalling data from Figures 4.7D and 4.8C were plotted against the degree of SNAT2 silencing in those 8 experiments, signalling was found to decline approximately in proportion to the extent of SNAT2 silencing (Figure 4.8D). Consequently in strongly SNAT2-silenced myoblasts, there is little residual PI3K signal on which low pH can exert an inhibitory effect

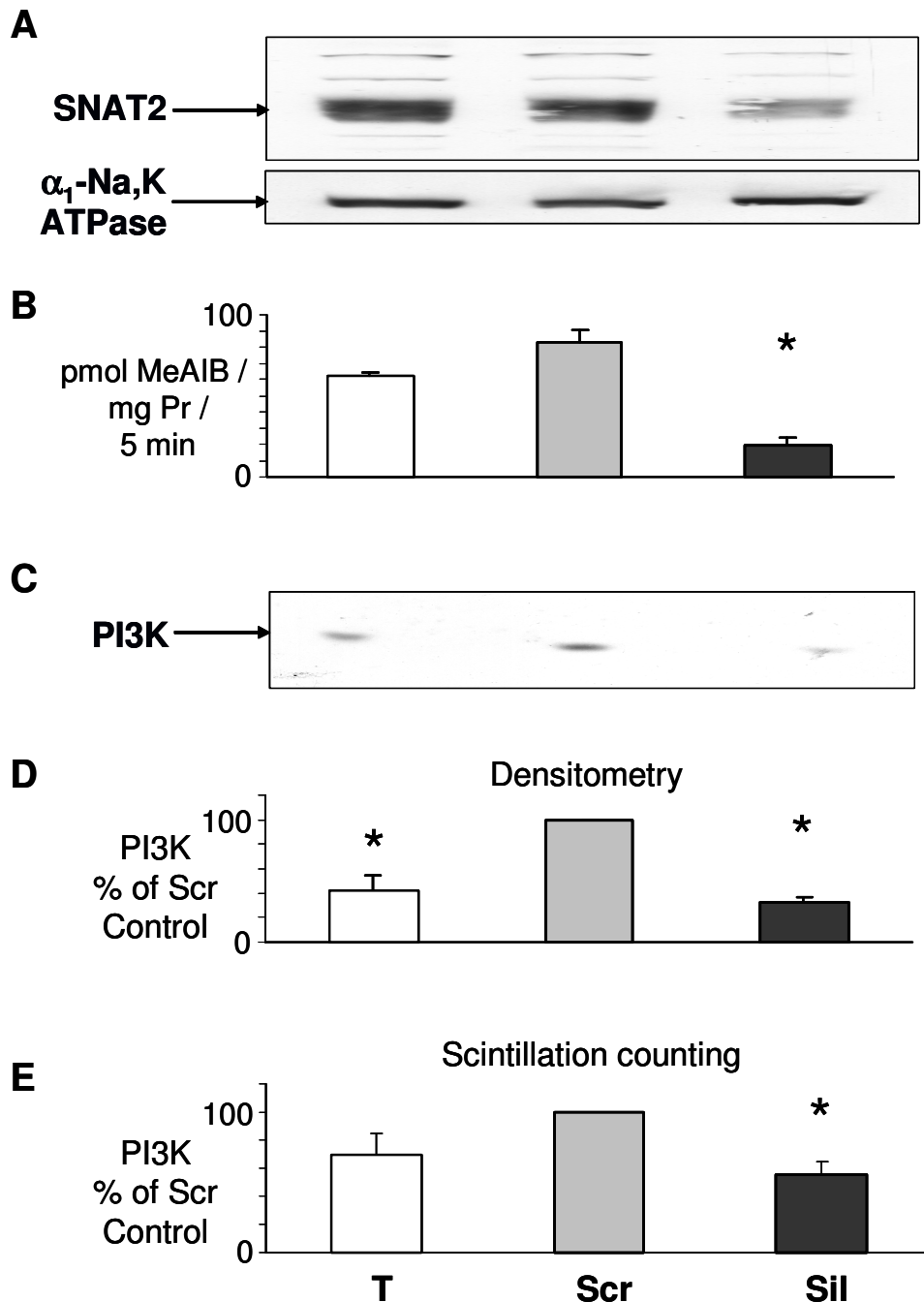


Figure 4.7. Effect of siRNA silencing of SNAT2 on phosphatidylinositol-3-kinase (PI3K) activity as in Figure 4.4, but with L6-G8C5 myoblasts. “T”, “Scr” and “Sil” are as in Figure 4.3. (A) Confirmation by immunoblotting of SNAT2 silencing. Proteins from a 170,000g membrane preparation separated by SDS-PAGE were probed with SNAT2-specific antibody (or α_1 -Na,K-ATPase antibody as a loading control). Experiments in (B) – (E) were run in parallel on the same cells. Pooled data from 3 independent experiments are presented. (B) SNAT2 transporter activity (C) Representative autoradiograph of PI3K assay thin layer chromatography plate (D) Quantification of pooled experiments performed as in (C). (E) Quantification by liquid scintillation counting of 32 P spots scraped from the plates in (D). * $P < 0.05$ versus the “Scr” control.

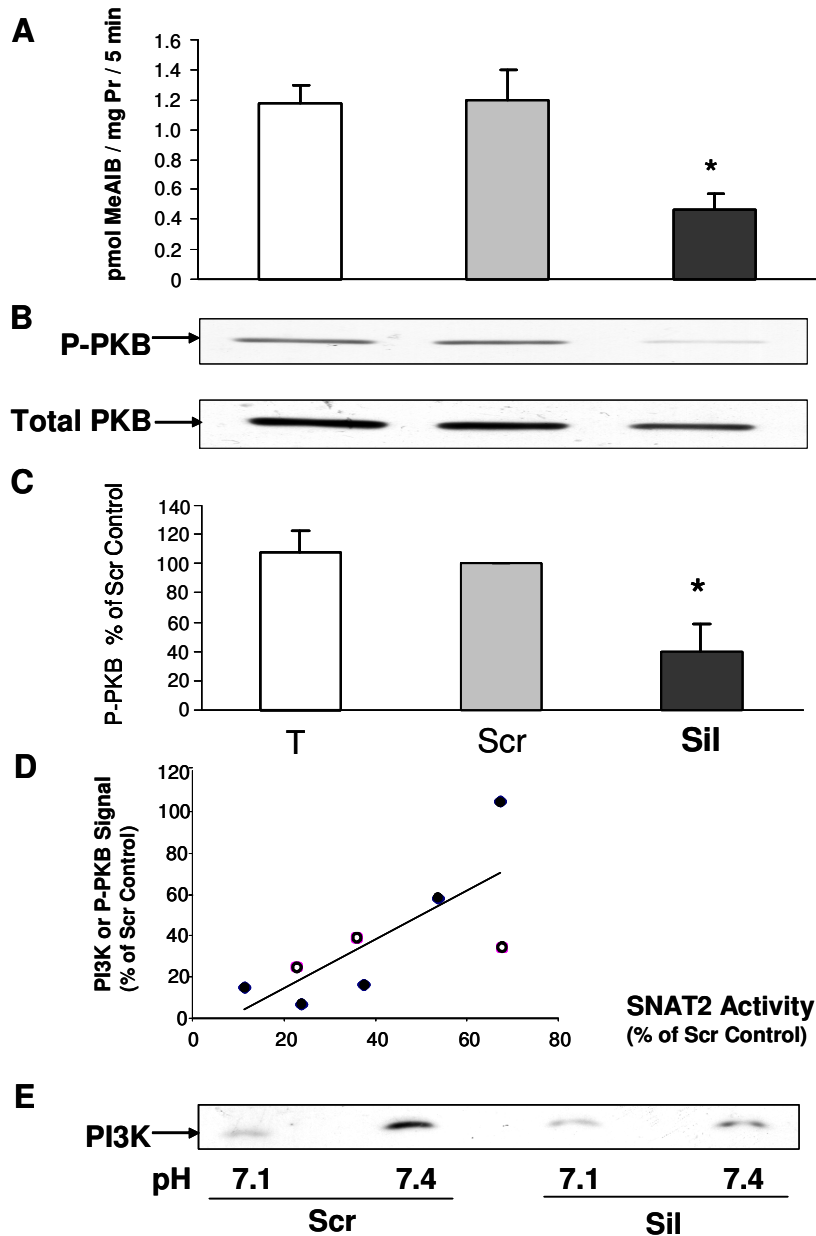


Figure 4.8. (A) – (C) Effect of siRNA silencing of SNAT2 on protein kinase B (PKB) activation in L6-G8C5 myoblasts as in Figure 4.7. Experiments in (A) – (C) were run in parallel on the same cells. Pooled data from 5 independent experiments are presented. (A) SNAT2 transporter activity (B) Representative immunoblot showing PKB activation assessed from phosphorylation of PKB at Ser 473. (C) Quantification by densitometry of pooled experiments performed as in (B), expressed as % of the “Scr” control value. *P<0.05 versus the “Scr” control.

(D) Correlation between the degree of silencing of SNAT2 and the accompanying degree of inhibition of the P-PKB and PI3K signals. Data are plotted from the five PKB experiments in (A) and (C) above (filled symbols) and the three PI3K experiments in Figure 4.7B and 4.7D (open symbols). Spearman Rank Correlation Coefficients: All data $R_s = 0.74$, $P < 0.04$; PKB data only $R_s = 0.90$, $P < 0.04$. (E) Representative experiment showing the effect of pH on the residual PI3K activity in myoblasts in which SNAT2 had been silenced as in Figure 4.7, but the ensuing 2h incubation with 100nM insulin was performed either at pH 7.1 or at pH 7.4.

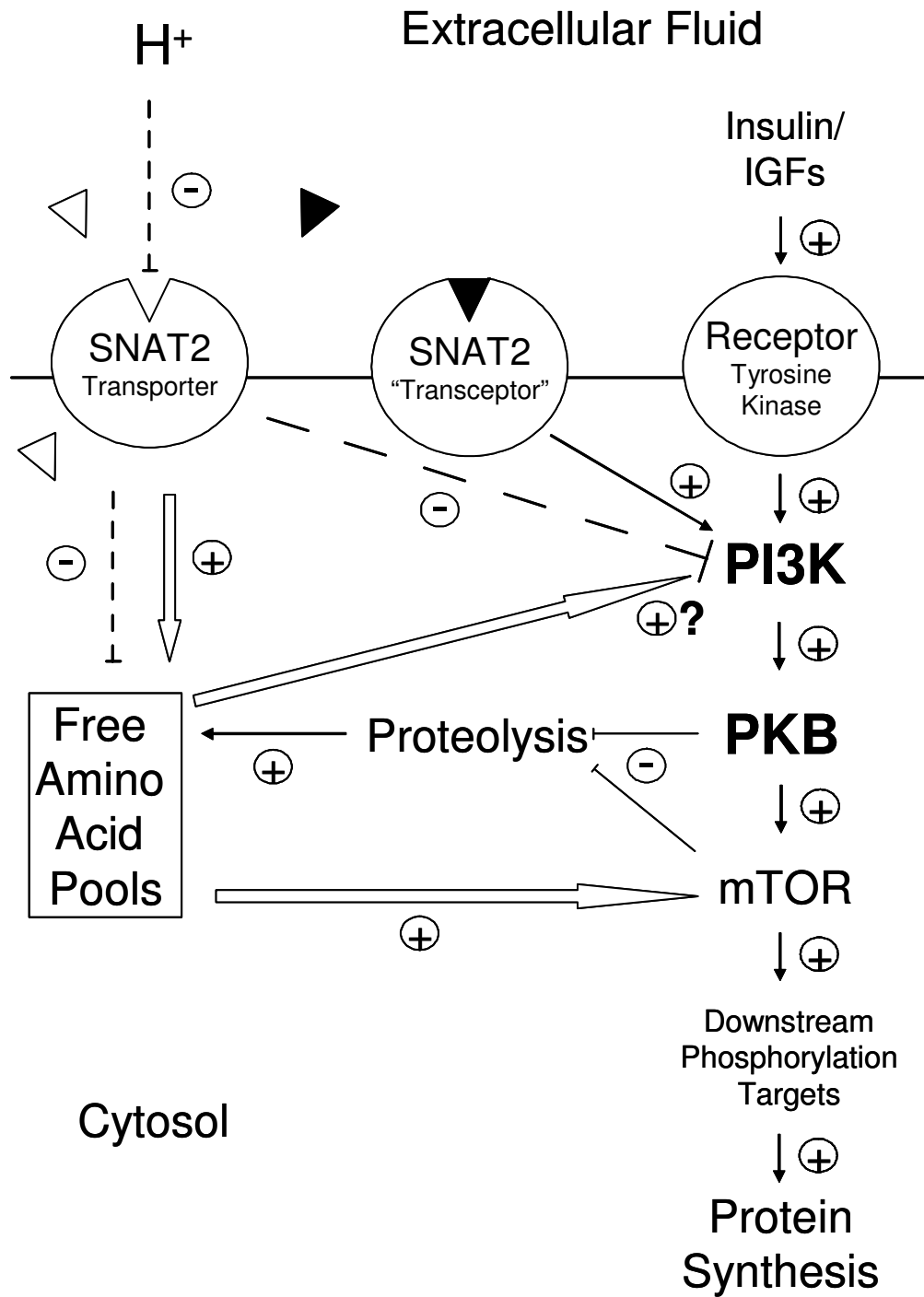


Figure 4.9. Proposed scheme whereby the pH-sensitive SNAT2 amino acid transporter and the putative SNAT2/amino acid substrate "transceptor" complex influence amino acid signalling and global proteolysis in L6-G8C5 rat skeletal muscle cells. Dashed lines denote the inhibitory effect of low extracellular pH on the SNAT2 transporter, and the resulting inhibition of PI3K and depletion of intracellular free amino acid pools. White arrows indicate known or suspected effects of amino acids whose intracellular concentrations are directly (e.g. L-Gln) or indirectly (e.g. L-Leu) regulated by SNAT2 transporter activity. Open triangles represent naturally occurring metabolisable amino acid substrates of SNAT2. Filled triangles represent the synthetic non-metabolisable SNAT2 substrate MeAIB.

(Figure 4.8E). Therefore, at least in myoblasts, inhibition by low pH of SNAT2-independent contributors to PI3K/PKB signalling seems unlikely to be a major contributor to the effect of acid on PI3K/PKB.

4.2.6 Mechanism of SNAT2 effects on PI3K and PKB

The SNAT2 protein is thought to be able to signal in L6 skeletal muscle cells by two mechanisms (Figure 4.9): through SNAT2 acting as a transporter, influencing intracellular amino acid concentration (Chapter 3) (which might then act directly on PI3K); or through the recently proposed SNAT2 “transceptor” mechanism in which a signal is generated by a SNAT2/amino acid substrate complex, (80), acting independently of intracellular amino acid levels. In principle these two mechanisms can be distinguished by saturating SNAT2 with its synthetic substrate MeAIB which should competitively inhibit the first mechanism and stimulate the second (Figure 4.9). The observed stimulation of both PI3K and PKB by MeAIB (Figures 4.5 and 4.6) suggests that the second mechanism rather than the first predominates. This conclusion of acidosis inhibiting PI3K through SNAT2 by a pathway independent of the amino acid influx through SNAT2 is further supported by the failure of amino acids to exert any acute stimulatory effect on the catalytic activity of immunoprecipitated PI3K (Figure 4.5C), the failure of extracellular amino acid starvation to block pH-sensitivity of PI3K (Figure 4.10A,B), and the apparent blunting of pH-sensitivity of PI3K when SNAT2 is saturated with MeAIB (Figure 4.10A,B). It was also noted that, in contrast to metabolisable amino acids, (80), neither acute saturation with MeAIB, nor pre-incubation with MeAIB, achieved down-regulation of SNAT2 protein expression

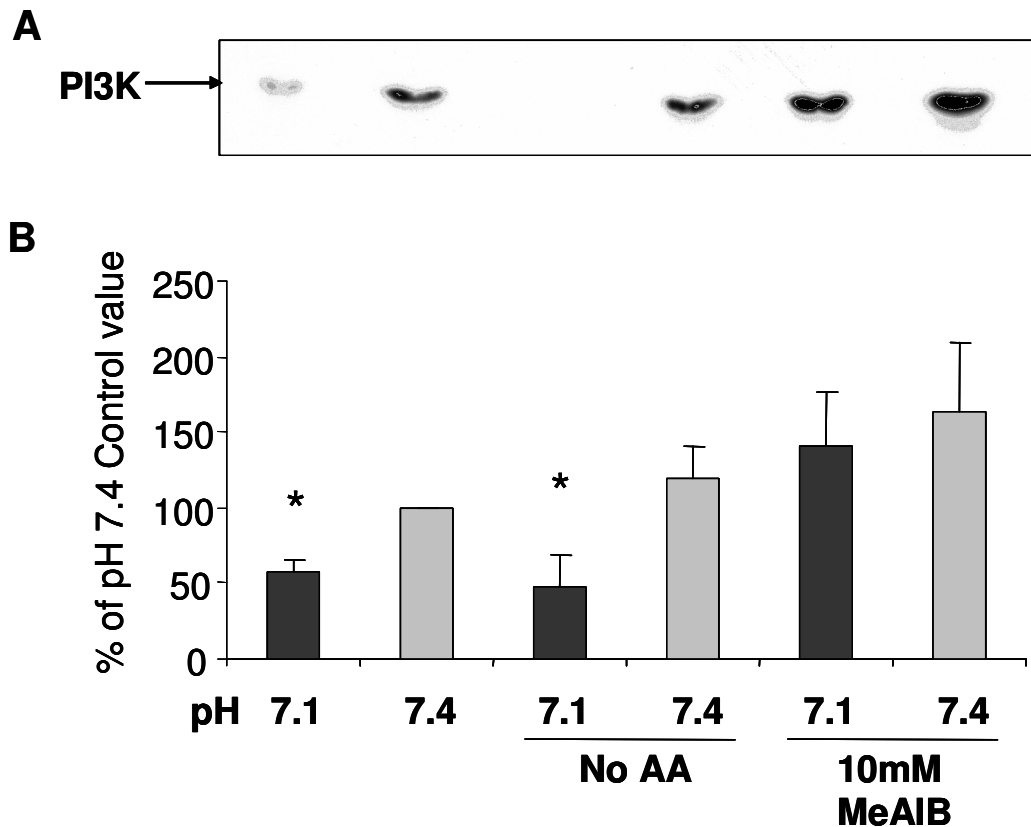


Figure 4.10. Influence of amino acid starvation “No AA”, or saturation of SNAT2 with 10mM MeAIB on the pH-sensitivity of PI3K lipid kinase activity in L6-G8C5 myotubes. Cells were incubated for 2h at the specified pH with or without amino acids or MeAIB. All media contained serum-free MEM with 100nM insulin. For “No AA” cultures, this 2h incubation was preceded by 2h in MEM without amino acids with 2% dialysed foetal bovine serum. (A) Representative PI3K assay autoradiograph (B) Pooled quantification data obtained by densitometry of 3 independent experiments performed as in (A). * $P < 0.05$ versus the corresponding pH 7.4 control.

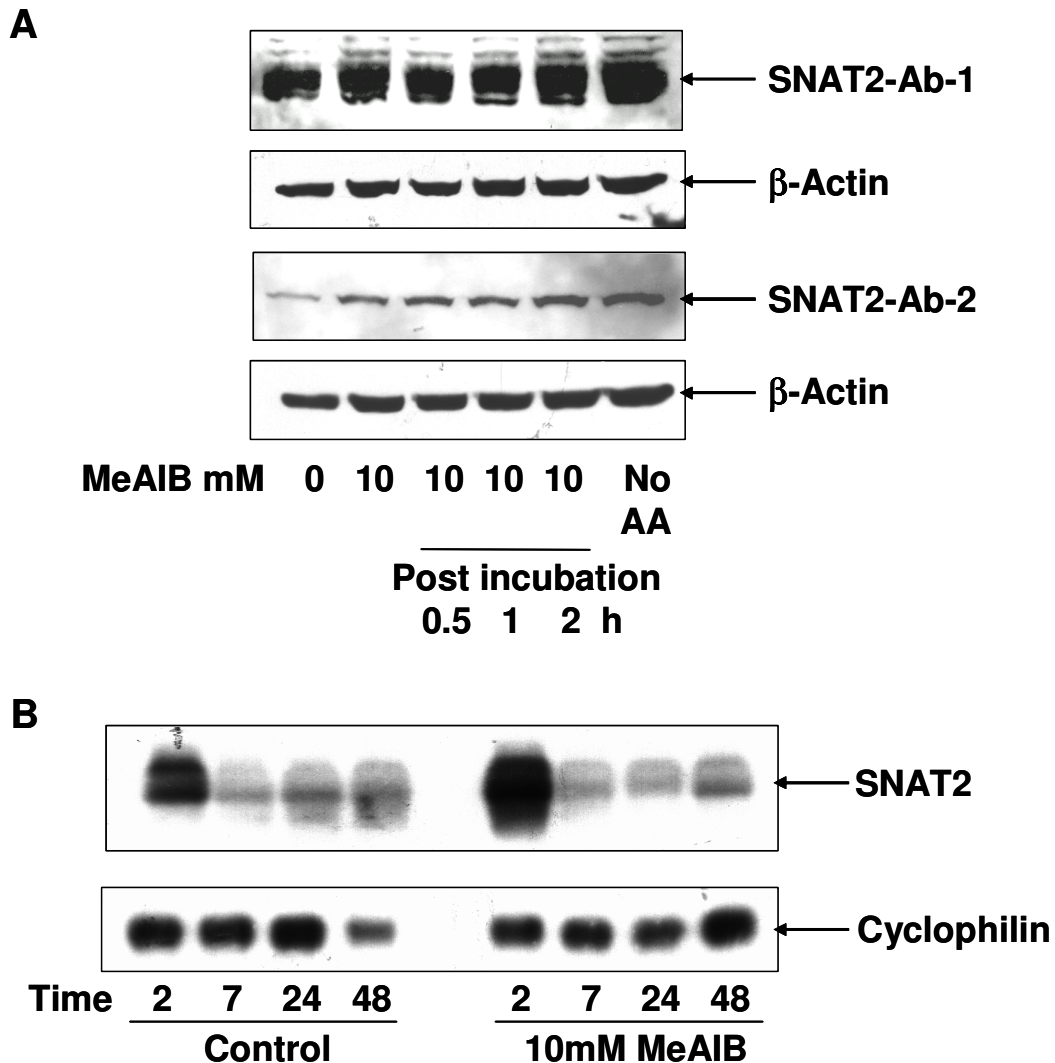


Figure 4.11. A) Effect of amino acid starvation and acute incubation (or pre-incubation) with MeAIB on the expression of SNAT2 protein. The test media consisted of MEM containing 2mM L-Gln and 100nM insulin. L6-G8C5 myotubes were treated under these control conditions or with 10mM MeAIB for 4 hours. After this time the “post-incubation” cultures were washed thrice in HBSS and then treated for 30min, 1h or 2h with the control medium. In the amino acid starved condition myotubes were treated for 4 hours in amino acid free test media, produced as described in section 2.3, which did not contain L-Gln or MeAIB. Immunoblots of proteins separated by SDS-PAGE from a 170,000g membrane preparation, probed with SNAT2-specific antibodies (or a β -actin specific antibody as a loading control) are shown. **B) Time course of the effect of MeAIB on SNAT2 mRNA expression.** L6-myotubes were treated with the control medium or 10mM MeAIB medium described above for 2, 7, 24, or 48 hours. Northern blots for SNAT2 mRNA (and cyclophilin mRNA control) are shown.

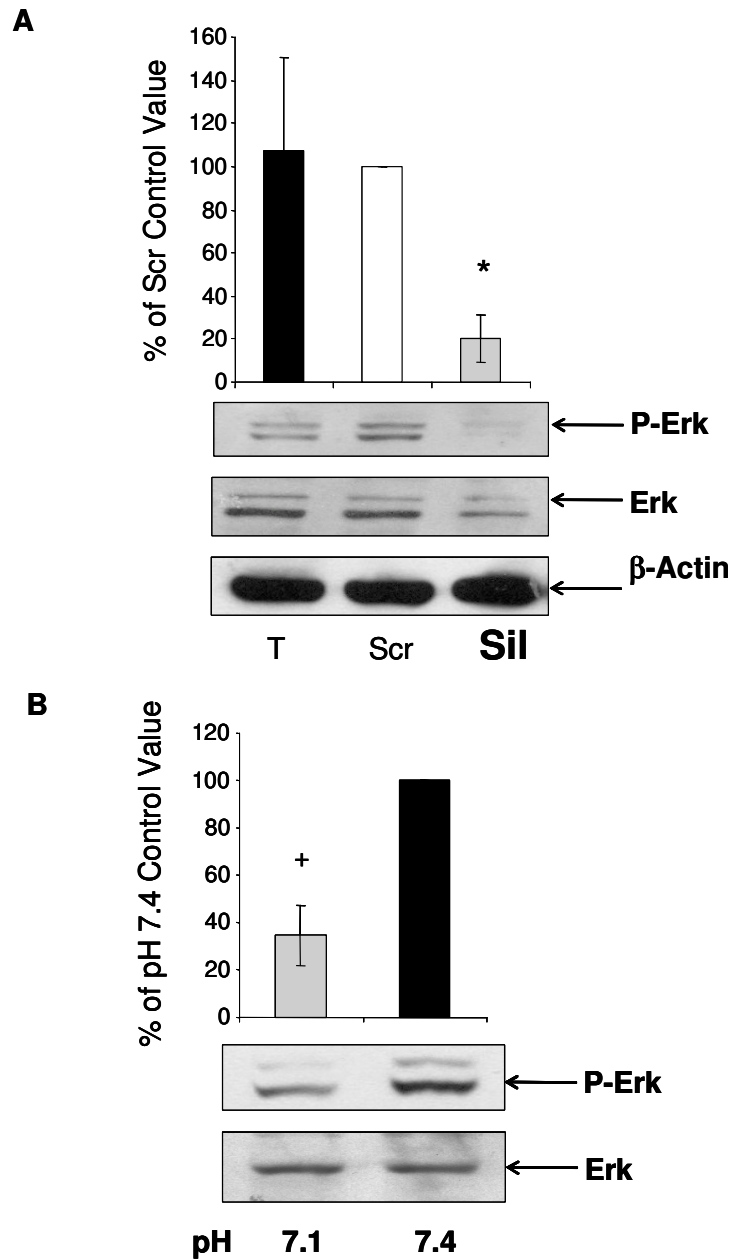


Figure 4.12. A) Effect of siRNA silencing of SNAT2 on Erk activation in L6-G8C5 myotubes. Pooled data from 3 independent experiments are shown (with 2 replicate culture wells for each treatment). “T” denotes cultures incubated with calcium phosphate Transfection Blank, “Scr” scrambled control siRNA, and “Sil” SNAT2 silencing siRNA. Transfection was followed by an 8h incubation in DMEM + 10% foetal bovine serum followed by 16h in MEM + 2% dialysed foetal bovine serum. Cells were then washed thrice in HBSS and incubated in MEM-based media containing 2mM L-Gln and 100nM insulin for 2h. **B) Effect of 2 hour incubation at the specified pH on Erk activation in L6-G8C5 myotubes.** Pooled data from 4 independent experiments are shown. Cells were subjected to a 2h incubation in serum free MEM containing 2mM L-Gln and 100nM insulin either at control pH 7.4 or acidic pH 7.1. *P<0.05 versus “T” and “Scr” controls. *P<0.05 versus pH 7.4 control. Immunoblots of proteins separated by SDS-PAGE were probed with antibodies against Thr202/Tyr204 phosphorylated Erk (or against p42 ERK and β -actin as loading controls).

assessed using two different SNAT2 antibodies (Figure 4.11A). Similarly, acute incubation with MeAIB also failed to down-regulate SNAT2 mRNA over a time course from 2 to 48h (Figure 4.11B).

4.2.7 SNAT2 effects on other insulin signals

The observation of apparent effects of SNAT2 on signalling through mTOR (Chapter 3) and PI3K/PKB also raises the question of whether the other major insulin signalling pathway through Ras/Raf/MEK/Erk is affected. At least in myoblasts, SNAT2 silencing with siRNA did significantly impair Erk activation (Figure 4.12A), consistent with the observation that low pH also impairs signalling through this pathway in L6-G8C5 myotubes (Figure 4.12B).

4.3 Discussion

4.3.1 SNAT2 regulates mTOR, PI3K, PKB and proteolysis

This study is the first to demonstrate that the acidosis-sensitive SNAT2 transporter is coupled to PI3K, PKB and proteolysis in skeletal muscle cells. Viewed in conjunction with the evidence of regulation of mTOR and protein synthesis by SNAT2 in Chapter 3, this strongly suggests that this transporter is a key player in the acid-induced insulin resistance which is regarded as a prime cause of cachexia in acidotic uraemic patients.

In this study (Figure 4.3) 35% silencing of SNAT2 activity in myotubes using siRNA led to a reproducible 11% stimulation of global proteolysis. The data in Chapter 3 showed that a similar degree of silencing also leads to a 12%

decrease in global protein synthesis. Together these effects impose negative nitrogen balance on the cells, leading to a significant but non-toxic decline in the protein content of the cultures (Chapter 3, (56), and Figure 4.3C). From ^{11}C -MeAIB positron emission tomography of skeletal muscle *in vivo*, SNAT2 transport activity in patients with chronic renal failure has been estimated to be 23% lower than in healthy controls, (200). The effects reported here therefore seem comparable with those *in vivo* and are of sufficient magnitude to contribute to uraemic cachexia.

4.3.2 Linkage between protein synthesis and degradation during acidosis

Evidence from inhibition of proteolysis with MG132 (Figure 4.1) suggests that the SNAT2-mediated depletion by acidosis of intracellular amino acids noted in Chapter 3 (leading to impaired mTOR signalling and impaired protein synthesis during acidosis) may be blunted by amino acids generated by subsequent degradation of cell protein (Figure 4.9). Such a mechanism may explain why impaired protein synthesis is observed in response to *acute* metabolic acidosis in humans, (37), but not during prolonged acidosis (e.g. in chronic renal failure) in which degradation of large myofibrillar protein pools, and hence liberation of amino acids in the cytosol, is chronically stimulated, (28).

This raises the important mechanistic question of whether proteolysis during metabolic acidosis is stimulated exclusively by intracellular amino acid depletion triggered by inhibition of SNAT2 activity (which might therefore be

amenable to amino acid supplementation therapy), or through some other mechanism for sensing of low extracellular pH (for example through effects of pH on SNAT2 other than inhibition of the amino acid influx through the transporter). Evidence presented in this chapter and Chapter 3 suggests that both mechanisms may contribute as follows (Figure 4.9).

4.3.3 SNAT2 signalling to proteolysis through amino acid depletion

The inhibitor studies in Figure 4.3D suggest that both mTOR signalling and PI3K signalling are involved in the regulation of proteolysis in these cells. Inhibition of SNAT2 leads to significant intracellular depletion of L-Gln and also indirectly to depletion of the branched chain amino acids L-Leu, L-Ile and L-Val (Chapter 3) which are well established as activators of mTOR signalling in skeletal muscle cells, including L6, (192). While mTOR signalling is probably an important contributor, other amino acid sensing pathways also possibly contribute, for example the recently described L-Leu suppressible activation of proteolysis in muscle that occurs through the dsRNA-dependent protein kinase PKR, (203). The involvement of pathways other than PI3K/PKB in regulation of proteolysis is also shown by the effect of MeAIB which clearly activates proteolysis (Chapter 3, (56), and Figure 4.3D) even though it fails to inhibit PI3K and PKB (Figures 4.5 and 4.6). This failure of MeAIB to generate one of the potentially catabolic signals that is generated by low pH, leading to a disproportionately small generation of amino acids from proteolysis, presumably explains the failure of MeAIB-induced proteolysis to rectify L-Gln depletion during treatment with MeAIB in Figures 4.1B and 4.1C.

Selective silencing of SNAT2 with siRNA led to significant impairment of PI3K and PKB activation in the presence of insulin (Figures 4.4, 4.7 and 4.8). Near-complete silencing of SNAT2 was only achieved in myoblasts (Figures 4.7 and 4.8), but a proportionate decrease in PI3K activity was also observed with the partial silencing of SNAT2 achieved in myotubes (Figure 4.4). Unlike mTOR, PI3K and PKB are not routinely regarded as responsive to amino acids. Nevertheless precedents do exist for amino acid effects on PI3K. Activation of the Type III PI3 kinase hVPS34 by amino acids is well documented, (113), and, under PI3K assay conditions like those described in the present study, PI3K activity in L-Leu starved L6 cells was strongly activated in response to 2mM L-Leu, (204). Even though L-Leu is a poor SNAT2 substrate, and the L-Leu effect was short-lived, and no PKB activation resulted from it, (192,204), this earlier report is relevant to the present study because L-Leu loading of L-Leu starved L6 cells is a potent activator of SNAT2, (204).

4.3.4 SNAT2 signalling independent of amino acid transport

While the intracellular amino acids supplied through SNAT2 may have a role in the coupling between SNAT2 and PI3K, this is unlikely to be the full explanation. Direct addition of amino acids did not activate immunoprecipitated PI3K (Figure 4.5C), blocking amino acid influx through SNAT2 with MeAIB did not inhibit PI3K (Figure 4.5), and amino acid starvation in intact cells has consistently failed to inhibit insulin signalling to PKB, (205,206), (the latter possibly because of the strong countervailing up-regulation of SNAT2 that occurs on complete amino acid starvation (Figure

4.2 and (80)). This leads to the interesting possibility that the SNAT2 protein signals to PI3K and PKB through a pathway independent of intracellular amino acid levels (Figure 4.9), analogous to the mechanisms that have been postulated to explain signal generation by the Ssy1 protein in yeast, (207), signalling from the Path amino acid transporter to dTOR in Drosophila, (208), and sensing of amino acid availability in L6 myotubes, (80). Of particular relevance is the latter study which proposes that part of the signal that suppresses SNAT2 gene expression, when SNAT2 amino acid substrates are added to L6 cells, arises not from amino acids carried into the cell by SNAT2, but from the SNAT2/amino acid substrate complex. Signalling through such a complex (Figure 4.9) may explain why PI3K and PKB in the present study were inhibited by siRNA silencing of SNAT2 (Figures 4.4, 4.7 and 4.8) but activated when the cells were saturated with SNAT2 substrate MeAIB (Figures 4.5 and 4.6).

This apparent activation of PI3K by substrate (MeAIB) saturation seems inconsistent however with the failure of amino acid starvation to influence PI3K in Figure 4.10. A possible explanation for this discrepancy is that naturally occurring metabolisable amino acids exert two opposing effects through SNAT2 on PI3K: activation by a transceptor-like mechanism, opposed by inhibition through down-regulation of the SNAT2 protein as described by Hyde et al 2007, (80). With MeAIB only the first effect seems to occur in L6-G8C5 cells because, unlike metabolisable amino acids, MeAIB failed to down-regulate SNAT2 (Figure 4.11).

4.3.5 Mechanism(s) of SNAT2 coupling to PI3K

The molecular basis of SNAT2s apparent effect on insulin signalling to PI3K is currently unknown, but the observation of similar apparent coupling to Erk signalling (Figure 4.12) may mean that SNAT2 influences insulin signalling at a site proximal to both PI3K and Erk. A possible site is the insulin receptor tyrosine kinase which has been shown to be inhibited by acidosis in rat heart, (209). A further finding of possible relevance is that System A type transporters (which include SNAT2) associate with integrin $\alpha_3\beta_1$, (210), and therefore may co-localise with adhesion kinases which are potent activators of PI3K, (211).

4.3.6 Implications for SNAT2 signals to mTOR and protein synthesis

The unexpected finding of SNAT2 effects on the largely amino acid – insensitive PI3K/PKB pathway in the present chapter raises the important question of whether the effects of SNAT2 on mTOR signals and protein synthesis in Chapter 3 arose exclusively from the sensing of changes in intracellular amino acid concentration brought about by SNAT2. Comparison of the effects of externally imposed amino acid depletion with those of SNAT2 inhibition on mTOR signalling and protein synthesis is therefore the subject of the next chapter.

Chapter 5: The role of free amino acids in the effect of SNAT2 on global protein synthesis.

5.1 Introduction

The data presented in Chapter 3 showed that in L6-G8C5 myoblast or myotube cultures, inhibition or silencing of SNAT2 depleted intracellular free amino acid pools, significantly impaired mTOR signalling, and slowed the rate of global protein synthesis. Whether SNAT2 was acting on mTOR exclusively through the changes in the intracellular amino acid concentration and, if so, which specific amino acid pools were involved, was left as an open question.

It has been shown in *Xenopus laevis* oocytes that micro-injecting free amino acids (especially L-Leu) to raise the cytosolic concentration by ~50% is sufficient to stimulate Rapamycin-sensitive signalling to S6 kinase 1, (212). Administration of extracellular amino acid was only effective when the oocytes were made to over-express the System L heterodimer 4F2hc/IU12, implying that amino acid entry into the cells was required, (212). In a mammalian system (Chinese Hamster Ovary cells – CHO-K1) it has also been shown, (213), that targets of mTOR can be regulated by manipulation of intracellular free amino acid pools (achieved by inhibiting global protein synthesis or global proteolysis). However, whether such effects of intracellular amino acids also explain the effects of SNAT2 inhibition on global protein synthesis and mTOR signalling observed in Chapter 3 is unknown.

If intracellular amino acid concentration is the sole mediator of SNAT2's effects on translation initiation through mTOR in L6-G8C5 myotubes, it should

be possible to reconstruct the effects of SNAT2 inhibition on these parameters by depleting the relevant intracellular amino acid pools. The most marked effect on intracellular amino acids following inhibition or silencing of SNAT2 was depletion of L-Gln (Figure 4.1 and Appendix E Figure 1A). This therefore seemed the most promising initial target for such experiments, especially in view of the observation in Figure 3.5C that L-Gln starvation impaired protein synthesis; and in Figure 3.5D that removal of extracellular L-Gln, or addition of an excess of L-Gln, blunted the inhibitory effect of SNAT2 antagonism by MeAIB on protein synthesis (implying that MeAIB was acting by competing with L-Gln for entry on SNAT2).

5.1.1 Pathways of L-Gln metabolism

In addition to incorporation into protein and oxidation as a metabolic fuel, L-Gln plays an important role in mammalian cells as the nitrogen donor for amidotransferase enzymes involved in the biosynthesis of nucleotides, (214), and biosynthesis of hexosamines for protein glycosylation, (215). Of possible relevance to translation initiation is the hexosamine pathway (Figure 5.1A) which uses L-Gln to generate UDP N-acetylglucosamine, which is the substrate for regulatory β -O-Glc-NAc glycosylation of a series of cytoplasmic and nuclear regulatory proteins. It has been proposed that this pathway promotes translation initiation by increasing O-Glc-NAc glycosylation of p67 (an eIF2 binding protein), (216). Glycosylation of p67 is reported to protect the binding protein from degradation and thus maintains sequestration of eIF2, protecting it from phosphorylation which would suppress translation initiation (Figure 5.1B). There has also been a preliminary report that, like L-Gln,

intermediates in the hexosamine pathway can stimulate protein synthesis in isolated rat skeletal muscle preparations, (217).

Through conversion to L-Glu, a metabolic precursor of glutathione, L-Gln is also an important determinant of glutathione pool size in skeletal muscle, (218), and L-Gln itself is a major intracellular osmolyte and, in some cell types, its effects on protein metabolism have been attributed to osmotic induction of cell swelling, (219), a phenomenon which may further enhance L-Gln influx, (220).

5.1.2 Previous work on the metabolic effects of L-Gln starvation in L6-G8C5 myotubes

Prior to the start of this project, an initial study was made by other workers in this laboratory of pathways of L-Gln metabolism and their effect on global protein synthesis rate in L6-G8C5 myotubes [J.R. Brown, Z. Nasim and A. Bevington, unpublished observations]. At early time points (up to 2h) depletion of intracellular L-Gln by extracellular L-Gln starvation had negligible effect on the major ribonucleotide pools (ATP, GTP, UTP and CTP) (data not shown). Furthermore, cell swelling, induced by lowering extracellular osmolarity to values which did not trigger cell lysis or decrease cell viability, had no stimulatory effect on protein synthesis, indeed a decrease was observed (Appendix E Figure 4), suggesting that, in these cells, osmotic swelling by intracellular L-Gln was unlikely to mediate stimulation of protein synthesis by L-Gln. Stimulation of flux through the hexosamine pathway by incubation with glucosamine, (219), also failed to stimulate protein synthesis

(Appendix E Figure 5), on the contrary synthesis was decreased. It was however noted that several metabolic stresses (L-Gln starvation, D-glucose starvation and Glucosamine treatment) all yielded a similar degree of non-additive impairment of protein synthesis (Appendix E Figure 5) suggesting that these stresses might be acting through a common signalling pathway in these cells.

The aim of the work described in this chapter was therefore to extend these observations by imposing depletion of specific amino acids on L6-G8C5 cells, and determining whether depletion alone is sufficient to account for the effects of SNAT2 inhibition on intracellular signalling and global protein synthesis. The specific aims were:

- To determine the effects of L-Gln depletion on signalling and protein synthesis
- To determine which pathways of L-Gln metabolism are involved in initiating these signals
- To refine the amino acid depletion model by superimposing depletion of other amino acid pools on L-Gln depletion (as would occur during SNAT2 inhibition); followed by monitoring of the response of the anabolic signal from mTOR to protein synthesis through phosphorylation of ribosomal protein S6, a signal which had previously shown strong dependence on SNAT2 in Chapter 3.

5.2 Results

In agreement with the L-Gln starvation experiments in Figure 3.5, incubation of L6-G8C5 myotubes in medium without L-Gln rapidly led to significant impairment of global protein synthesis rate, reaching statistical significance within 2h (Figure 5.2). This time course was closely mimicked by the L-Gln anti-metabolite Acivicin (Figure 5.2), implying that metabolism of L-Gln was required for the response. The effect of L-Gln deprivation was strongly blunted by removal of serum from the medium, but was restored in completely defined serum-free medium supplemented with insulin or IGF-I as the only anabolic factors (Figure 5.3A). Consequently the 28% stimulation of protein synthesis by insulin which was observed in the presence of L-Gln was abolished (or even reversed) in L-Gln depleted medium (Figure 5.3B), suggesting that L-Gln deprivation (like SNAT2 inhibition in Chapter 4) might be impairing the signalling effects of insulin (or related growth factors in serum).

To determine whether L-Gln depletion was directly acting through insulin signalling pathways, selective inhibitors of these pathways were screened to determine whether they could influence the magnitude of the L-Gln deprivation effect on protein synthesis. The effect was blunted when PI3K was inhibited with LY294002 (Figure 5.4A) or when Ras/Raf/MEK/Erk signalling was inhibited with PD98059 (Figure 5.5A). However, screening of downstream phosphorylation events (phospho-activation of PKB or Erk respectively) (Figures 5.4B and 5.5B) failed to confirm any direct impairment of signalling through PKB or Erk by L-Gln deprivation, suggesting that there

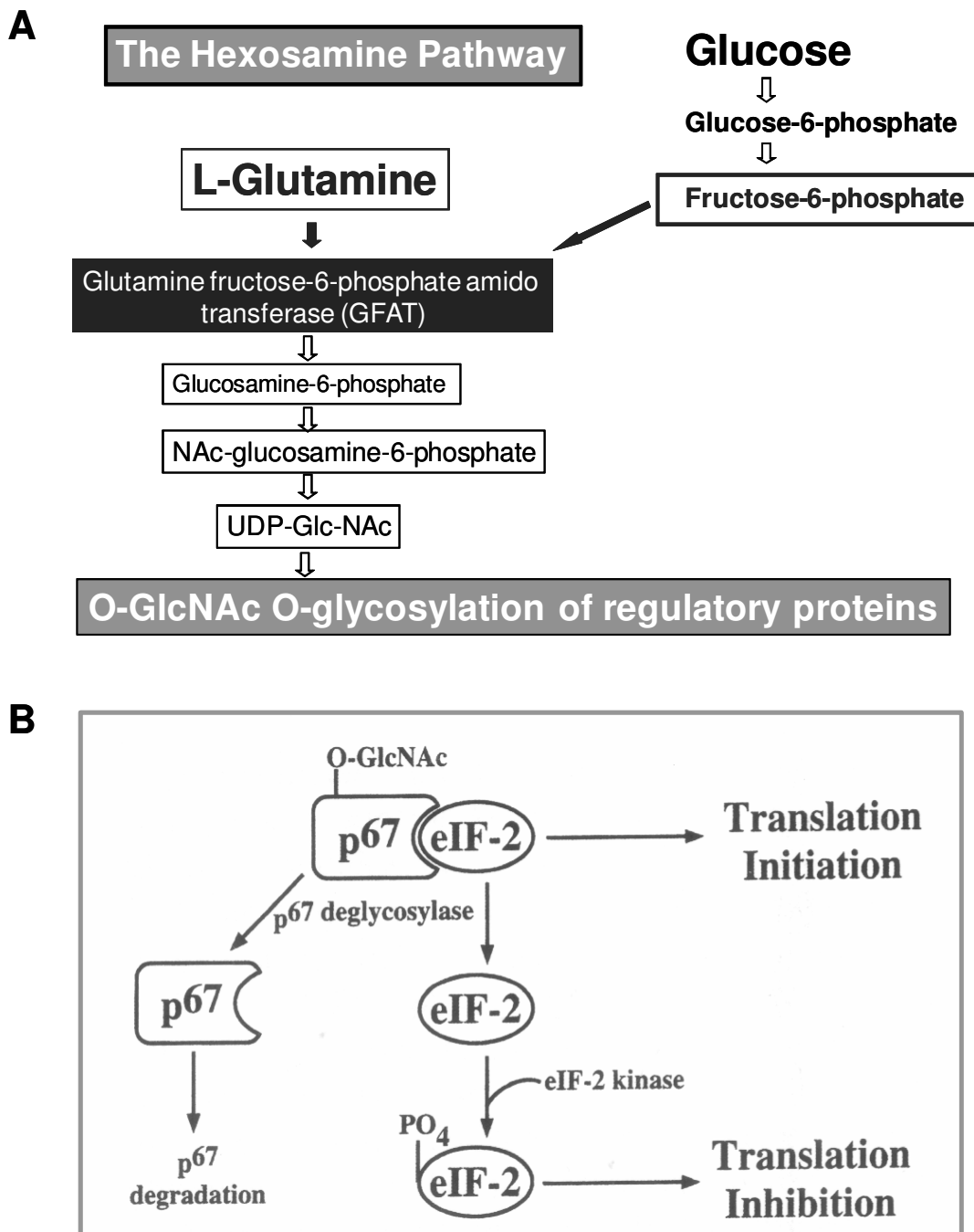


Figure 5.1. A) Schematic diagram of the hexosamine pathway. B) Proposed scheme for regulation of translation initiation by O-Glc-NAc glycosylation of p67 (an eIF2 binding protein). Taken from Comer FI, Hart GW: *Biochim Biophys Acta* 1473:161, 1999, (216).

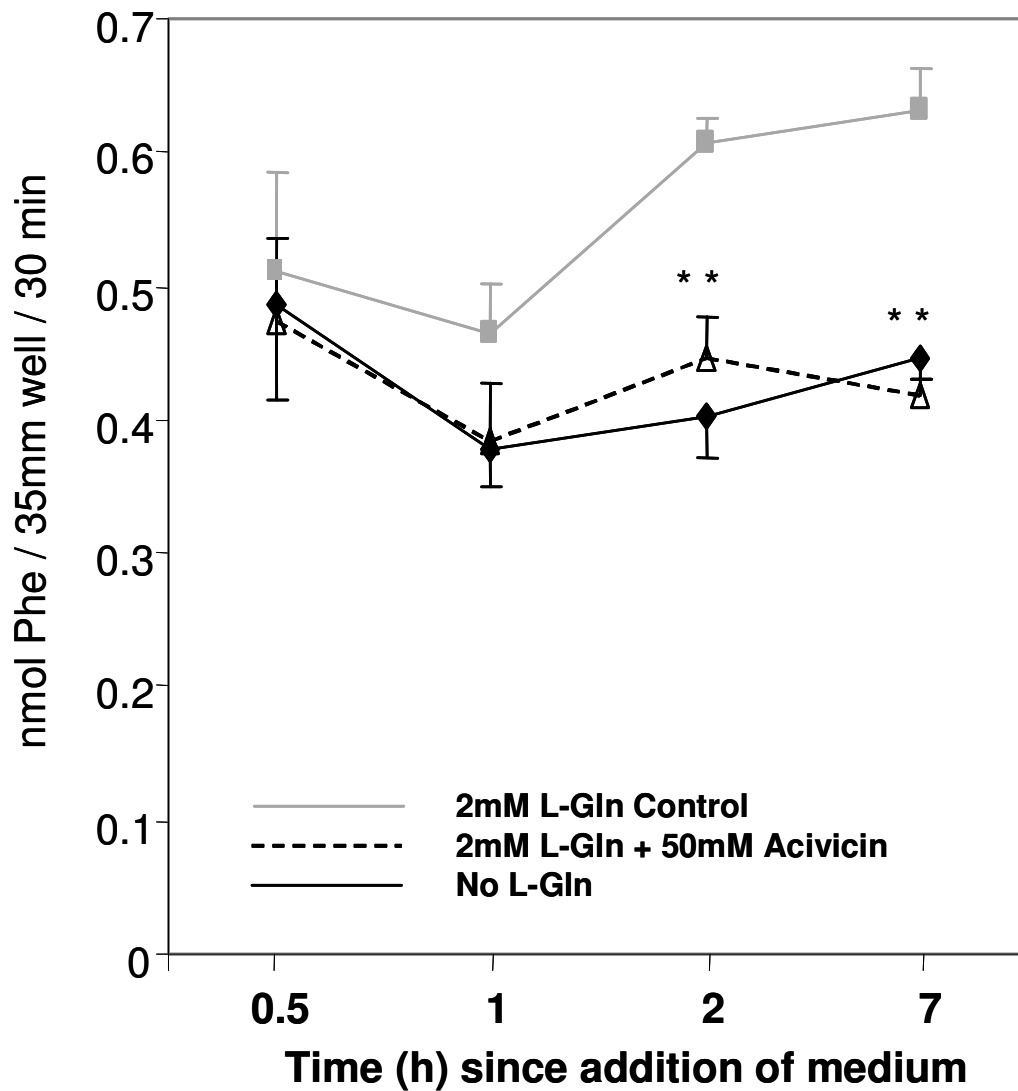


Figure 5.2. Time course of the effect of L-Gln depletion or acivicin on global protein synthesis rate ($^3\text{H-L-Phe}$ incorporation) in L6-G8C5 myotubes. Pooled data from 3 independent experiments are shown (with 3 replicate culture wells for each experiment). Cells were incubated in MEM-based test media containing 2% dialysed foetal bovine serum and the specified concentration of L-Gln and acivicin for 0.5, 1, 2, or 7 hours. $^3\text{H-L-Phe}$ was present in the medium for the final 30 min of the incubation. **P < 0.05 versus control medium at the same time point.

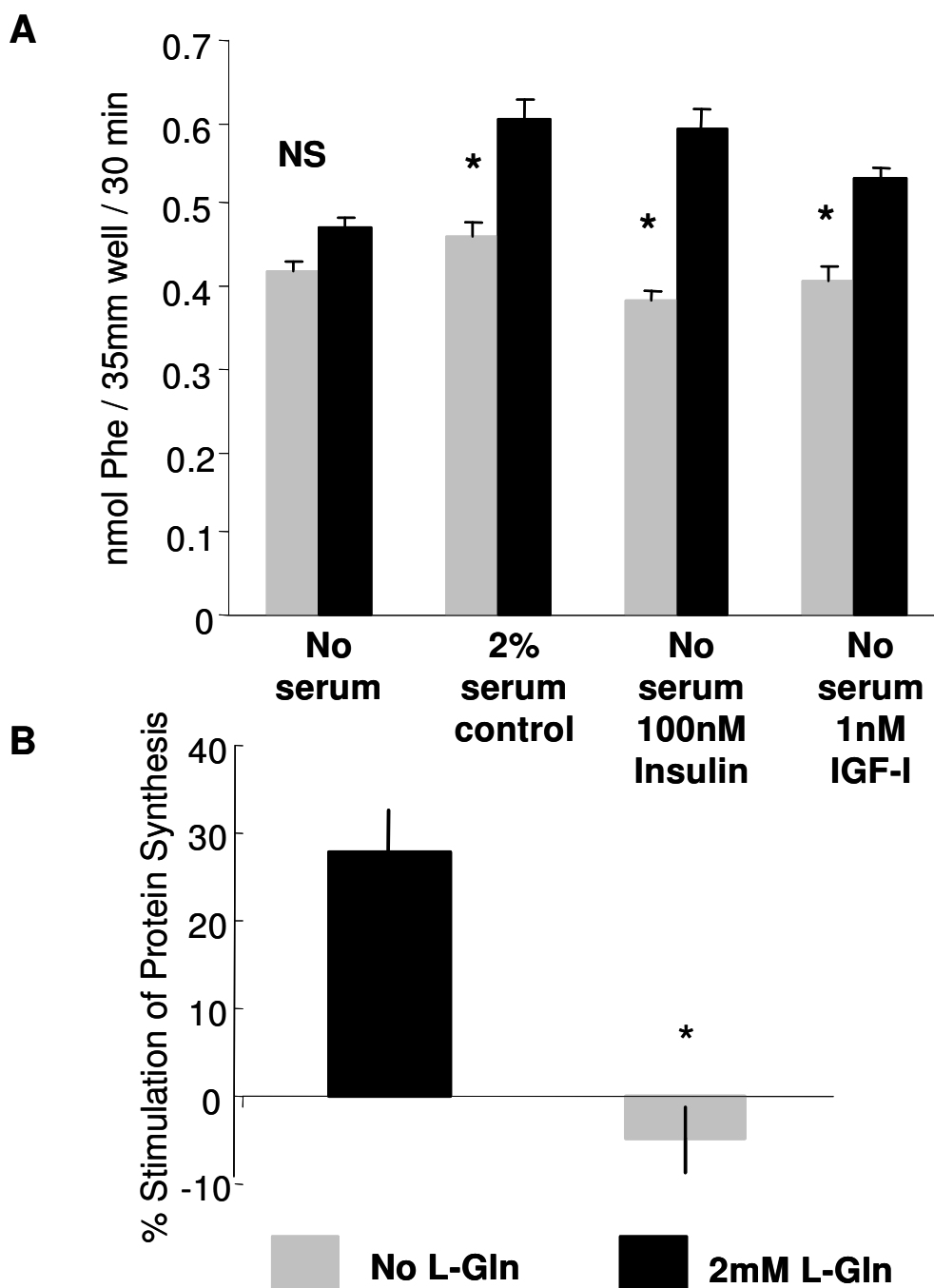


Figure 5.3. A) Effect of 2h L-Gln depletion in defined (serum-free) media on global protein synthesis rate ($^3\text{H-L-Phe}$ incorporation) in L6-G8C5 myotubes. Cells were incubated in MEM with the specified additions for 2 hours. $^3\text{H-L-Phe}$ was present in the medium for the final 30 min of the incubation. **B) Effect of L-Gln depletion on the net stimulation of protein synthesis by 100nM insulin in L6-G8C5 myotubes.** Data are derived from (A) above. Stimulation of protein synthesis by insulin is expressed as percentage of the value in the serum free control (see A). In A) and B) pooled data from 4 independent experiments are shown (with 3 replicate culture wells for each experiment). * $P < 0.05$ versus the corresponding medium with L-Gln.

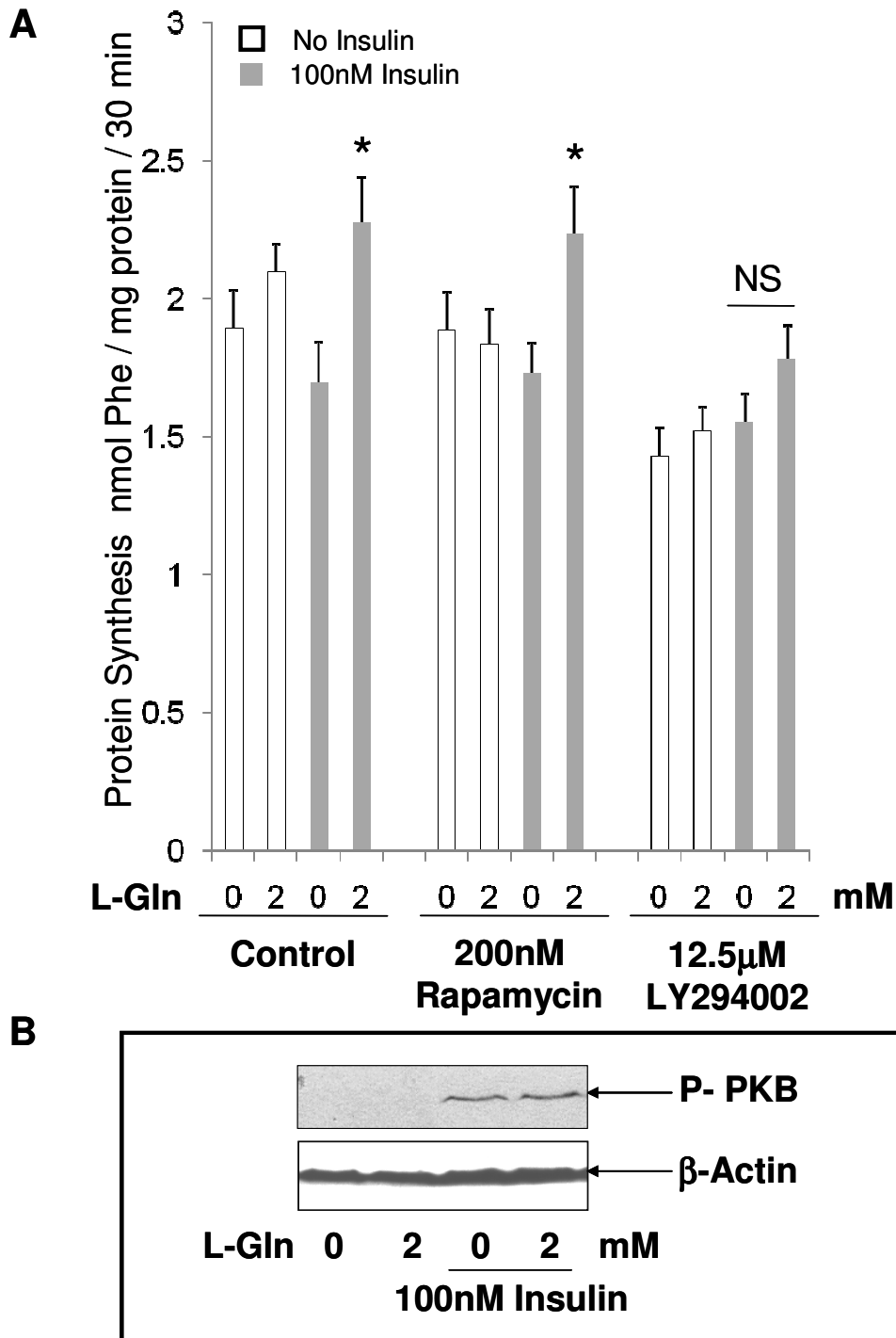


Figure 5.4. A) Effect of inhibition of PI3-K and mTOR on the L-Gln dependence of global protein synthesis rate ($^3\text{H-L-Phe}$ incorporation) in L6-G8C5 myotubes. Myotubes were incubated in MEM with the specified concentrations of insulin, L-Gln and PI3K inhibitor LY294002 or mTORC1 inhibitor Rapamycin for 2 hours. $^3\text{H-L-Phe}$ was present in the medium for the final 30 min of the incubation. Pooled data from 3 independent experiments are shown (with 3 replicate culture wells for each experiment). * $P < 0.05$ versus the corresponding medium without L-Gln. **B) Effect of L-Gln depletion on the activation of PKB by insulin.** Myotubes were incubated as described in A) in the presence or L-Gln or insulin for 2 hours. Immunoblots of proteins separated by SDS-PAGE were probed with antibodies against phosphorylated PKB (or β -actin as a loading control).

was only an indirect permissive requirement for PI3K and MEK in the L-Gln dependence of protein synthesis.

5.2.1 Role of mTOR signalling in the L-Gln deprivation effect

In isolated rat hepatocytes, activation of S6 kinase (S6K), a downstream target of mTOR, has been reported in response to L-Gln, (221). However, in L6-G8C5 myotubes the magnitude of the L-Gln deprivation effect on protein synthesis was not significantly altered when mTOR signalling was blocked with Rapamycin (Figure 5.4A). L-Gln deprivation also had no reproducible effect on signals downstream of mTOR. Activation of S6K (detected by mobility shift), phosphorylation of ribosomal protein S6 (rpS6), and phosphorylation of eukaryotic initiation factor 4E binding protein 1 (4E-BP1) all showed no significant change in response to L-Gln (Figure 5.6).

As inhibition of SNAT2 is accompanied by partial depletion of System L amino acids in addition to L-Gln depletion (Appendix E Figure 1 and Appendix E Table 1), and SNAT2 inhibition had previously caused clear impairment of rpS6 phosphorylation (Figure 3.3 and 3.4), the effect of superimposing partial extracellular depletion (down to 25%) of the System L amino acids L-Ile, L-Leu, L-Phe, L-Trp, L-Tyr plus L-Val on L-Gln starvation was also investigated (Figure 5.7). With these depleted media, a significant depletion of the L-Leu concentration inside the cells (a known regulator of mTOR) was observed (Appendix E Figure 6), and was accompanied (not shown) by L-Gln depletion identical to that observed previously. These depleted media also led to impairment of global protein synthesis (Appendix E Figure 7) but, this showed

no dependence on the concentration of System L amino acids. Furthermore, even though a decrease in rpS6 phosphorylation comparable with that achieved on SNAT2 inhibition with MeAIB was sometimes observed in the amino acid depleted media (Figure 5.7 A), the average response over 11 such experiments was weak, showed poor dose-dependence, and (in contrast to MeAIB) did not achieve statistical significance (Figure 5.7 B,D).

5.2.2 Phosphorylation of eukaryotic initiation factor 2 α (eIF2 α)

In spite of the lack of effect on the signalling pathways above, L-Gln depletion reproducibly led to phosphorylation of eIF2 α (Figure 5.8 and Figure 5.9), an event which strongly inhibits translation initiation (Section 1.6.2.12.2) and would be expected to over-ride the stimulatory effect of insulin on translation (Figure 5.3B). The time course of phosphorylation (Figure 5.8A) closely mirrored the time course of inhibition of protein synthesis (Figure 5.2). The effect was mimicked (Figure 5.8C and Figure 5.9) by a series of other metabolic stresses which have previously been shown to impair global protein synthesis in these and other cells including L-Leu deprivation, (222), D-glucose deprivation (Appendix E Figure 5 and, (223)), stimulation of the flux through the hexosamine pathway with D-glucosamine and uridine (Appendix E Figure 5 and, (220)), Acivicin (Figure 5.2), and inhibition of glutathione biosynthesis with L-Buthionine-[S,R]-Sulfoximine (BSO) (see below).

Two pathways through which L-Gln depletion potentially influences eIF2 α phosphorylation are the hexosamine pathway, culminating in β -OGlcNAc

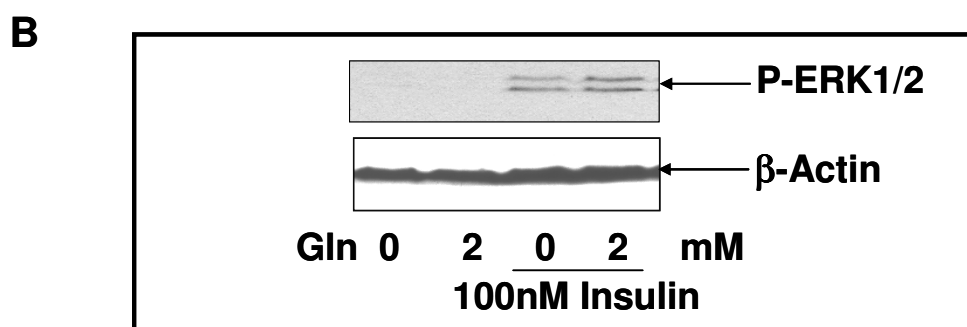
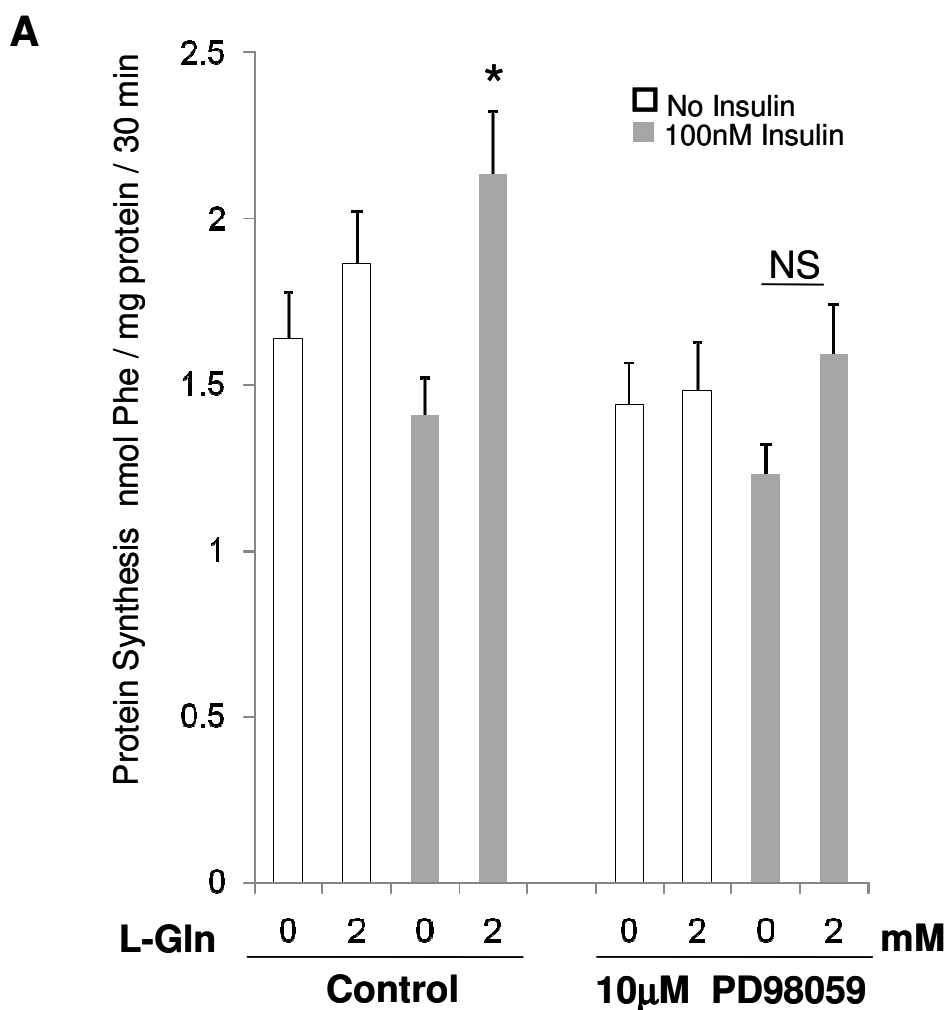


Figure 5.5. A) Effect of inhibition of MEK on the L-Gln dependence of global protein synthesis rate ($^3\text{H-L-Phe}$ incorporation) in L6-G8C5 myotubes. Myotubes were incubated in MEM with the specified concentrations of insulin, L-Gln and MEK inhibitor PD98059 for 2 hours. $^3\text{H-L-Phe}$ was present in the medium for the final 30 min of the incubation. Pooled data from 3 independent experiments are shown (with 3 replicate culture wells for each experiment). * $P < 0.05$ versus the corresponding medium without L-Gln. **B) Effect of L-Gln depletion on the activation of Erk by insulin.** Myotubes were incubated as described in A) in the presence or L-Gln or insulin for 2 hours. Immunoblots of proteins separated by SDS-PAGE were probed with antibodies against phosphorylated Erk (or β -actin as a loading control).

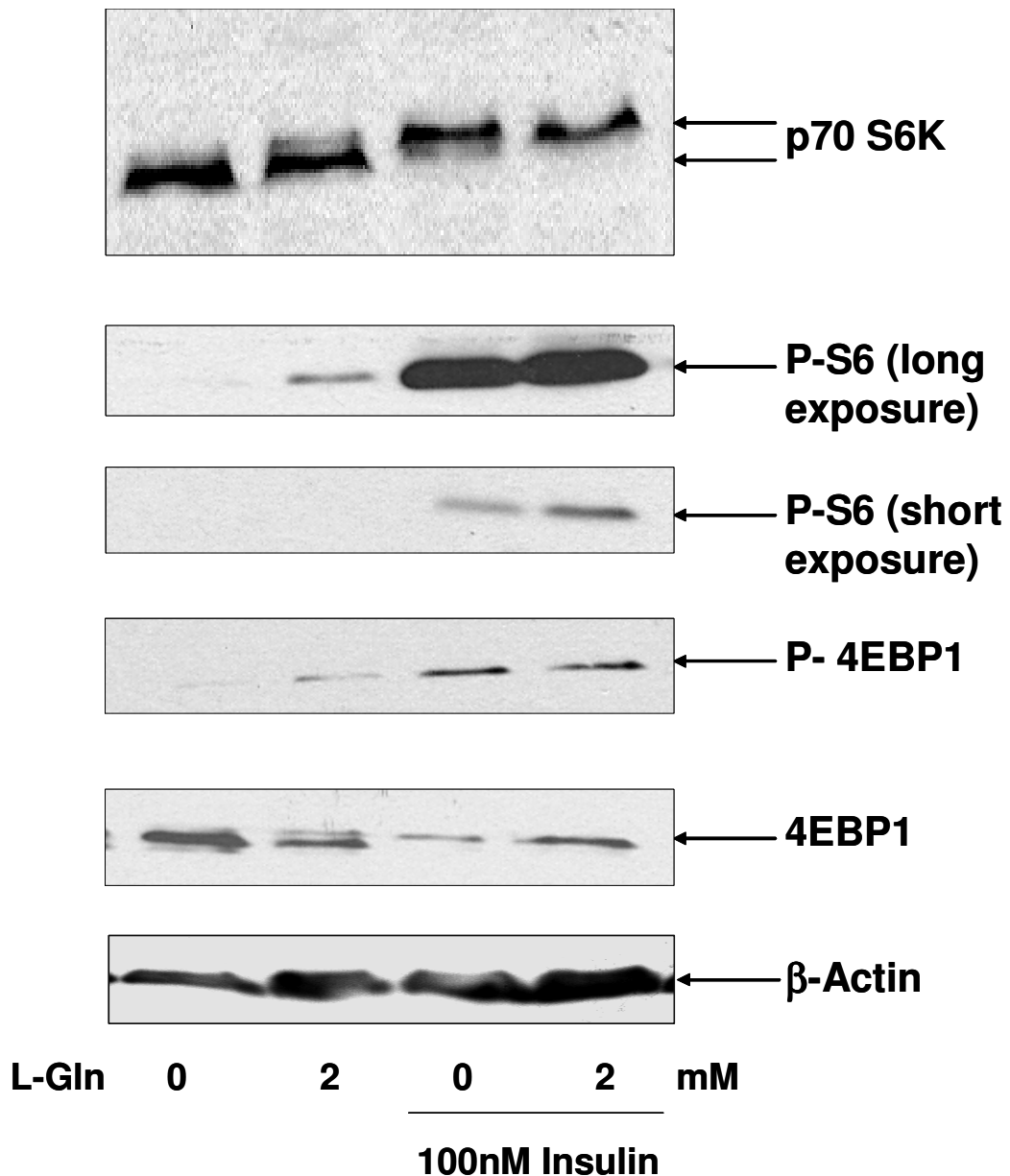


Figure 5.6. Effect of L-Gln depletion on the activation of downstream targets of mTOR in L6-G8C5 myotubes. Cells were incubated in MEM with or without 100nM insulin and 2mM L-Gln for 2 hours. Immunoblots of proteins separated by SDS-PAGE were probed with antibodies against p70 S6K, Ser235/6-phosphorylated rpS6, and Ser65-phosphorylated 4EBP1 (and total 4EBP1 and β -actin as loading controls). The apparent mobility shift of p70 S6K observed with insulin showed no reproducible response to L-Gln starvation.

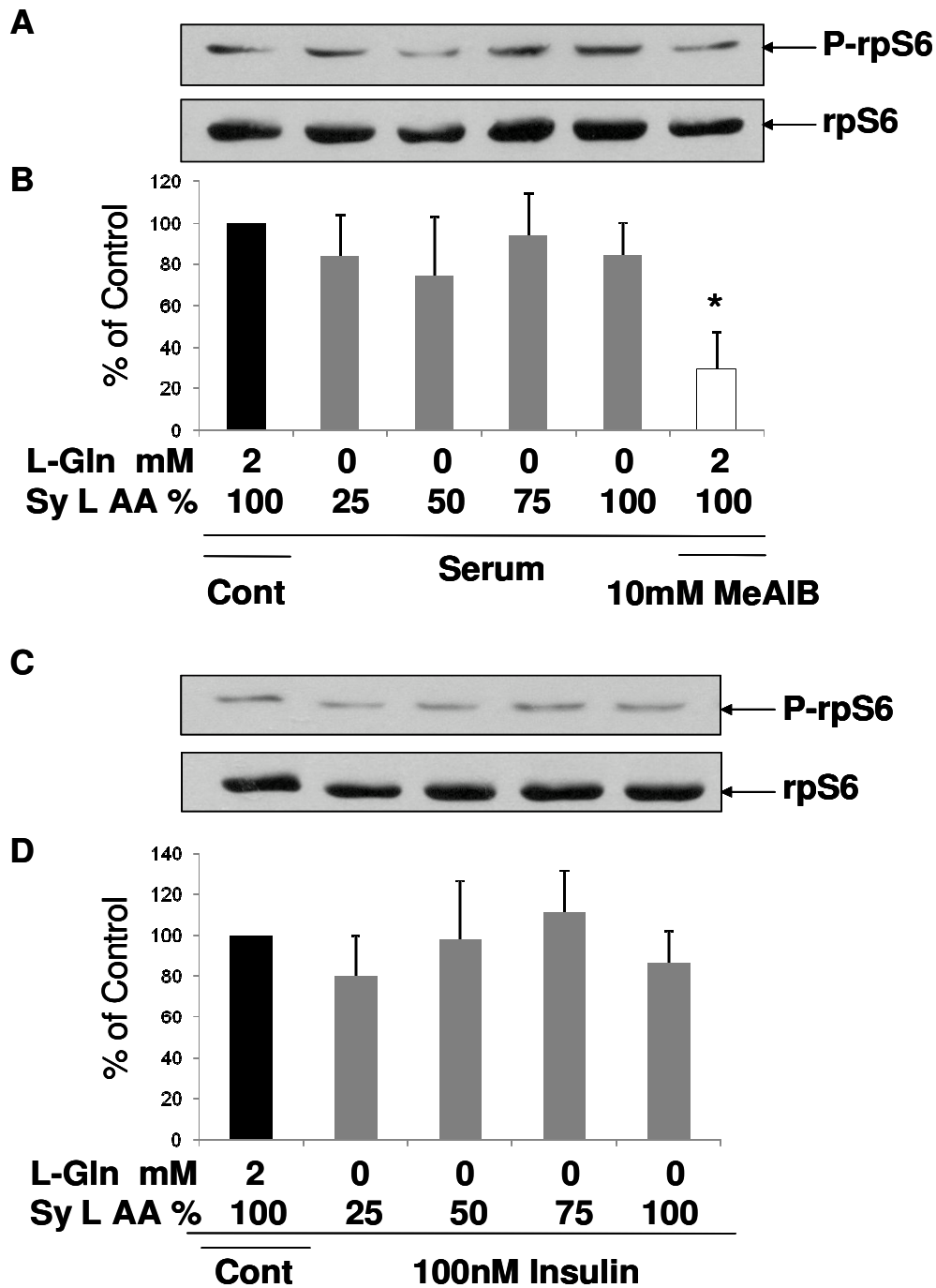


Figure 5.7. The effect on rpS6 phosphorylation of partial System L amino acid depletion superimposed on L-Gln starvation in L6-G8C5 myotubes. Cultures were incubated for 2 hours in complete MEM with 2mM L-Gln (Control) with or without 10mM MeAIB (positive control); or modified MEM without L-Gln in which the concentration of the System L amino acids (L-Ile, L-Leu, L-Phe, L-Trp, L-Tyr plus L-Val) was 25, 50, 75 or 100% of the normal value in MEM. Media were supplemented with either 2% dialysed foetal bovine serum (A,B) or 100nM insulin (C,D). Immunoblots of proteins separated by SDS-PAGE were probed with antibody against Ser235/6-phosphorylated rpS6 (or total rpS6 as a loading control). Pooled quantification data are shown from 11 experiments (3 experiments for MeAIB), expressed as a percentage of the Control value. *P < 0.05 versus the corresponding Control value.

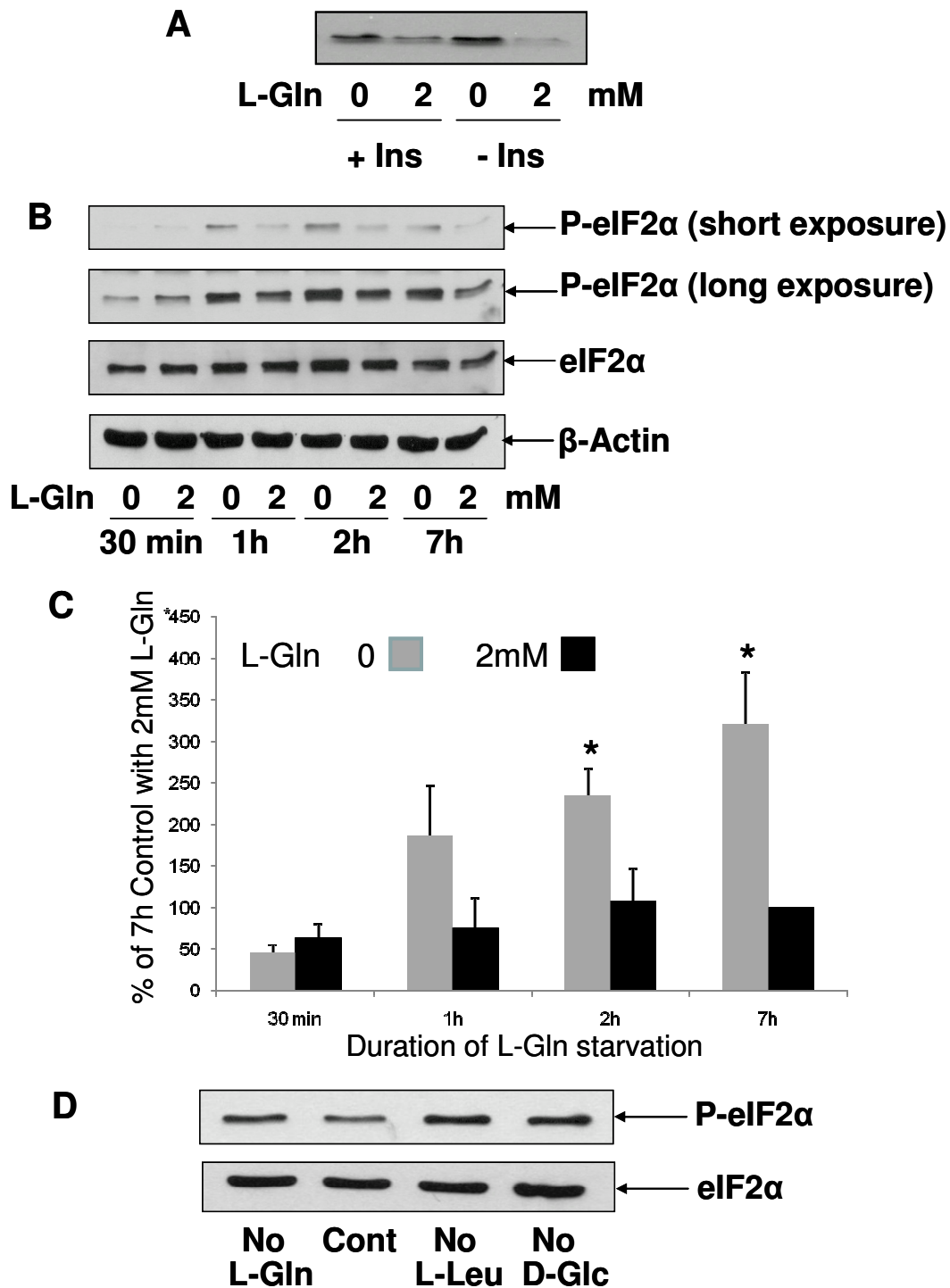


Figure 5.8. The effects of nutrient starvation on phosphorylation of eIF2- α in L6-G8C5 myotubes in the absence (A) and presence (B, C, D) of insulin. (A) the effect of L-Gln starvation on eIF2- α phosphorylation in the presence and absence of insulin at 2 hours. (B) and (C) time course of the effect of L-Gln starvation. (D) Effect of incubation without L-Gln, L-Leu or D-glucose (D-Glc) for 2h. Cultures were incubated in MEM (modified as shown) with or without 100nM insulin for the time stated. Immunoblots of proteins separated by SDS-PAGE were probed with antibody against Ser52-phosphorylated eIF2- α (or total eIF2- α or β -actin as loading controls). Pooled quantification data from 3 experiments are shown in (C) expressed as percentage of the L-Gln control value at 7h. *P < 0.05 versus the L-Gln control at the same time point.

glycosylation of proteins (Figure 5.1), and glutathione biosynthesis via L-Glu, (214). In L6-G8C5 myotubes, 2h of L-Gln deprivation depleted both β -OGlcNAc glycosylated proteins (Figure 5.10B) and intracellular L-Glu (Figure 5.11A), followed by a slower decline in glutathione itself (Figure 5.11B).

The L-Gln-dependent hexosamine pathway has been implicated in suppression of eIF2 α phosphorylation, (216). Stimulation of the pathway with D-glucosamine or treatment with O-(2-Acetamido-2-deoxy-D-glucopyranosylidene) amino N-phenyl carbamate (PUGNAc - a selective inhibitor of the glycosidase which removes β -OGlcNAc glycosylation from proteins, (224), clearly increased β -OGlcNAc protein glycosylation in L6-G8C5 myotubes (Figure 5.10A). In spite of this, these agents neither suppressed eIF2 α phosphorylation (Figure 5.9) nor stimulated protein synthesis (5.10B and Appendix Figure 5), suggesting that this pathway was not the mechanism of L-Gln's effect on eIF2 α . This was further supported by the observation that L-Gln deprivation failed to deplete the key UDP-GlcNAc pool (Figure 5.1A) directly assayed in these cells by HPLC (A. Bevington and Z. Nasim personal communication).

In contrast, forcing glutathione depletion on the cells by incubation with BSO (Figure 5.11C) did stimulate eIF2 α phosphorylation (Figure 5.9A and 5.12A) and detectably impaired protein synthesis (Figure 5.12B). An additional pathway linking L-Gln and protein synthesis must also occur however, because even high dose BSO is a less potent inhibitor of protein synthesis than is L-Gln deprivation (Figure 5.12B); and L-Gln-dependence of protein

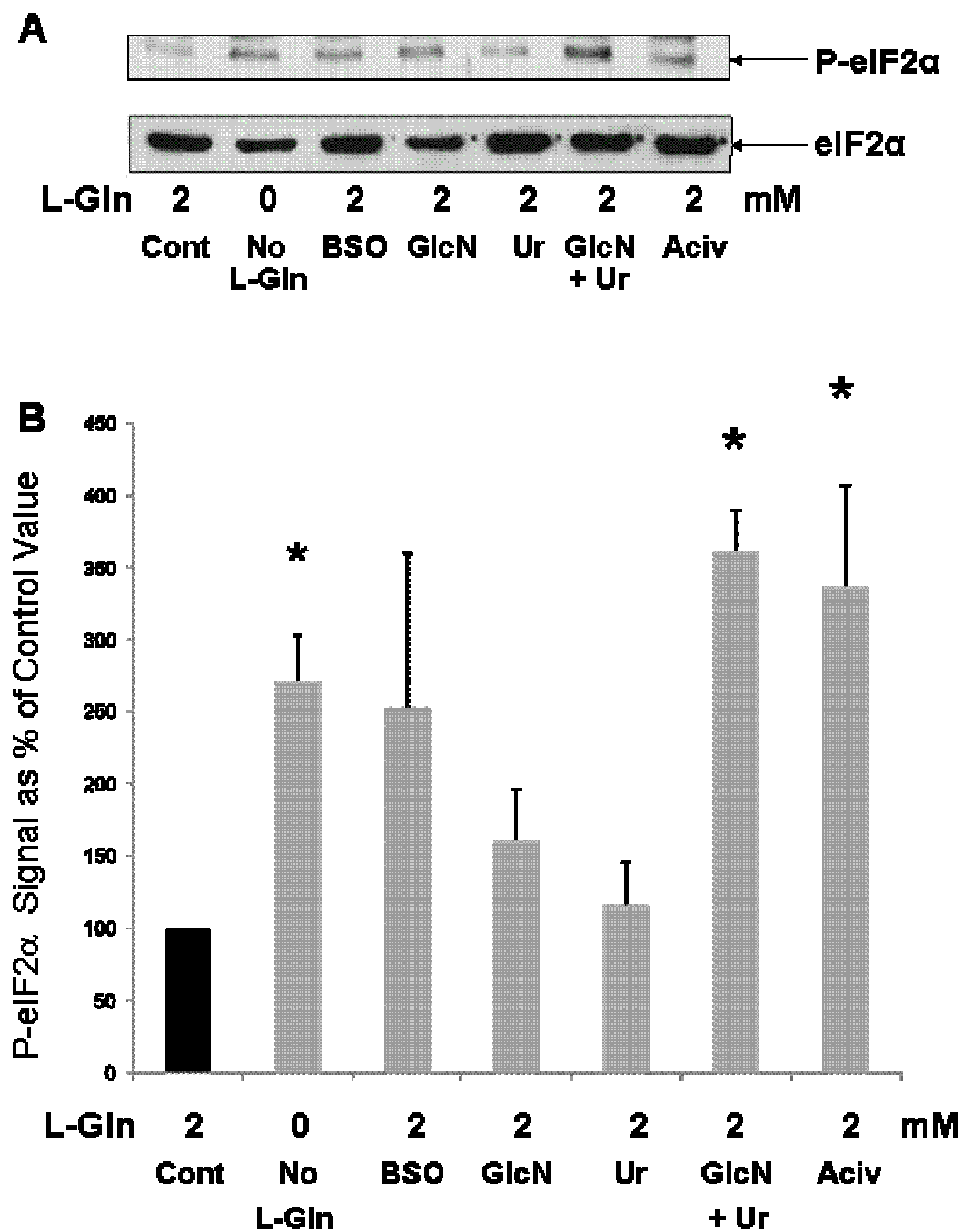
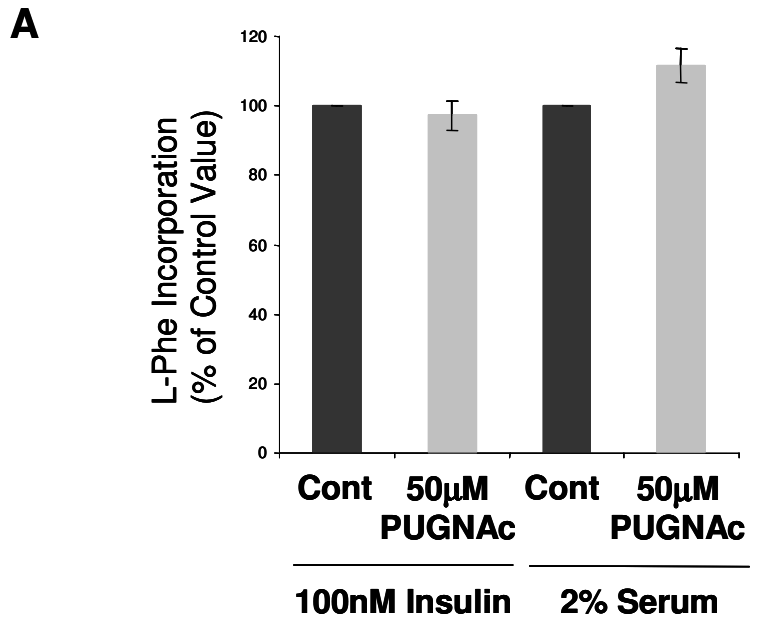


Figure 5.9. A) and B) The effect of metabolic stressors on phosphorylation of eIF2 α in L6-G8C5 myotubes. Control (Cont) cultures were incubated for 2 hours in MEM with 100nM insulin and 2mM L-Gln. Other cultures were L-Gln starved or incubated with glutathione biosynthesis inhibitor L-Buthionine-[S,R]-Sulfoximine (BSO, 100 μ M); hexosamine pathway precursors D-glucosamine (GlcN, 5mM) and/or uridine (Ur, 500 μ M), or L-Gln antimetabolite acivicin (Aciv, 50 μ M). Immunoblots of proteins separated by SDS-PAGE were probed with antibody against Ser52-phosphorylated eIF2 α (or total eIF2 as a loading control). Pooled quantification data are shown in (B) expressed as percentage of the control value. Data are from 3 independent experiments (except for BSO (n=6) and L-Gln starvation and Control (both n=9)). *P < 0.05 versus the control value.



B β -O-GlcNAc Glycosylated Proteins

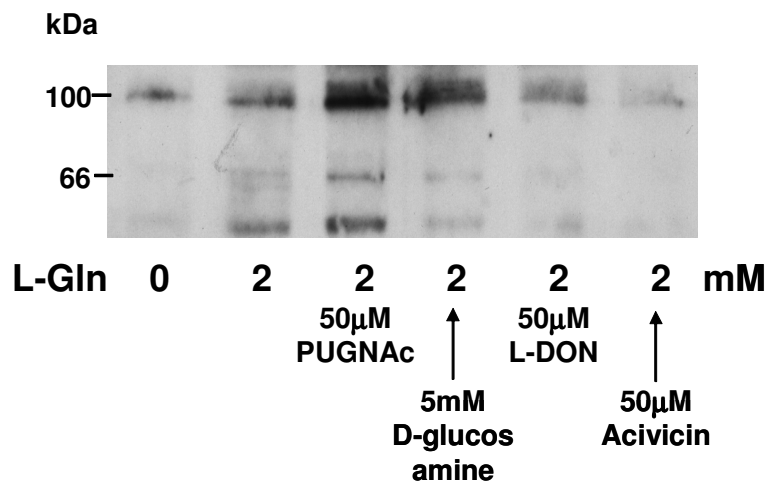


Figure 5.10. Effect of the β -OGlcNAc glycosidase inhibitor O-(2-Acetamido-2-deoxy-D-glucopyranosylidene) amino N-phenyl carbamate (PUGNAc) on global protein synthesis in L6-G8C5 myotubes. Cultures were incubated for 2h in MEM with 2mM L-Gln and either 2% dialysed foetal bovine serum or 100nM insulin, with or without PUGNAc. (A) Protein synthesis rate (3 H-L-Phe incorporation). 3 H-L-Phe was present in the medium for the final 30 min of the incubation. Pooled data from 3 independent experiments are shown (with 3 replicate culture wells for each experiment). (B) **Positive control. Demonstration that PUGNAc leads to the expected accumulation of β -OGlcNAc glycosylated proteins in cultures incubated with insulin as described in (A).** Parallel cultures were incubated in L-Gln depleted medium, medium with the hexosamine pathway precursor D-glucosamine, or media containing the L-Gln anti-metabolites L-Diazo-oxo-norleucine (L-DON) or Acivicin. Immunoblots of proteins separated by SDS-PAGE were probed with an antibody specific for β -O-GlcNAc glycosylated proteins.

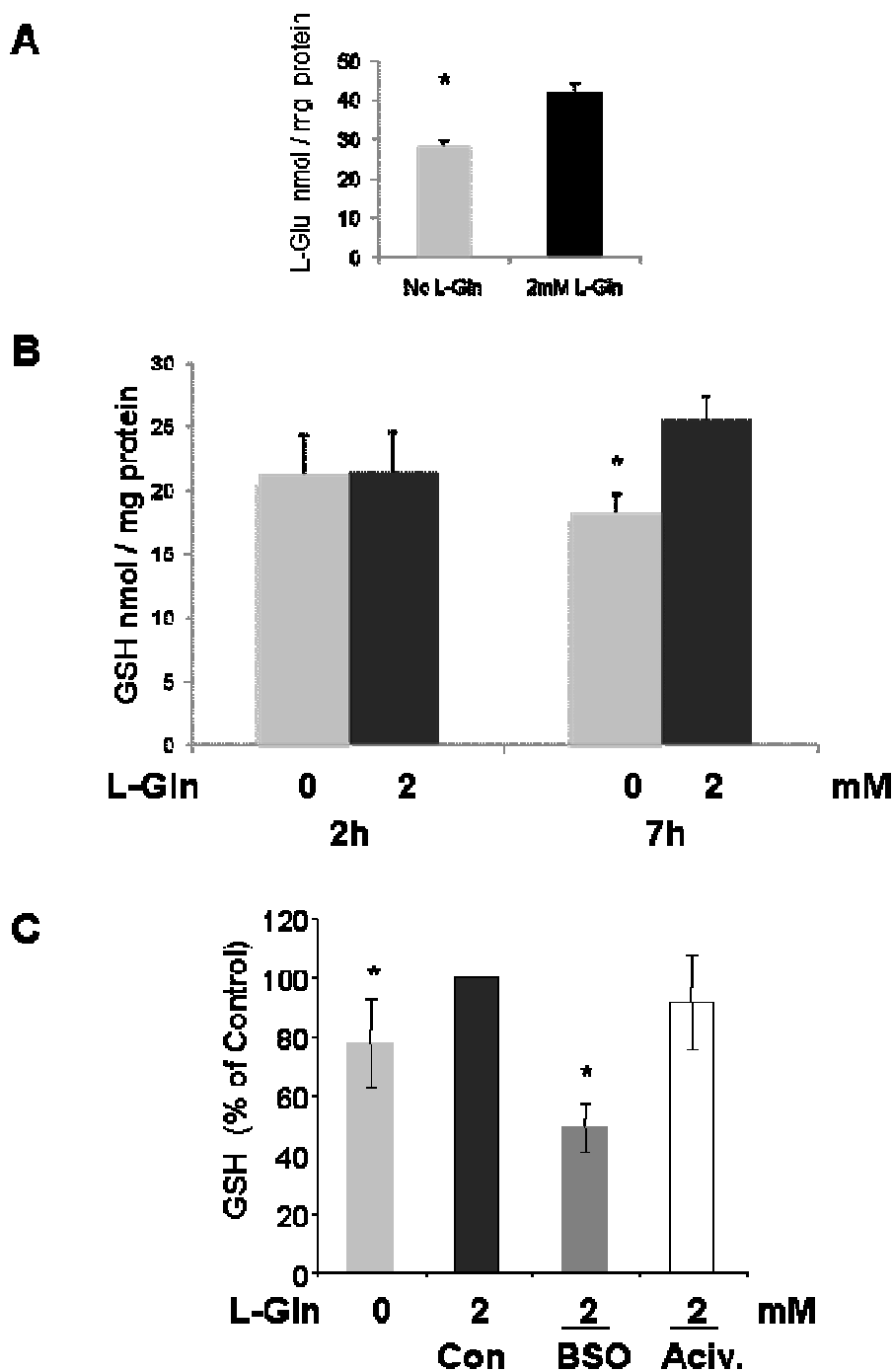


Figure 5.11. Effect of L-Gln starvation on the concentration of L-Glu and reduced glutathione (GSH) in L6-G8C5 myotubes. Unless otherwise stated, cultures were incubated for 2h in MEM with or without 2mM L-Gln and 100nM insulin. L-Glu and GSH were determined at the end of the incubations by HPLC. The effect of incubation with glutathione biosynthesis inhibitor L-Buthionine-[S,R]-Sulfoximine (BSO, 100 μ M); or L-Gln antimetabolite acivicin (Aciv, 50 μ M) is also shown. L-Glu data in (A) are from 1 experiment representative of 4 independent experiments with n=4 replicate culture wells for each treatment). GSH data in (B) and (C) are pooled from 3 experiments with 3 replicate wells for each condition. *P<0.05 versus control with 2mM L-Gln.

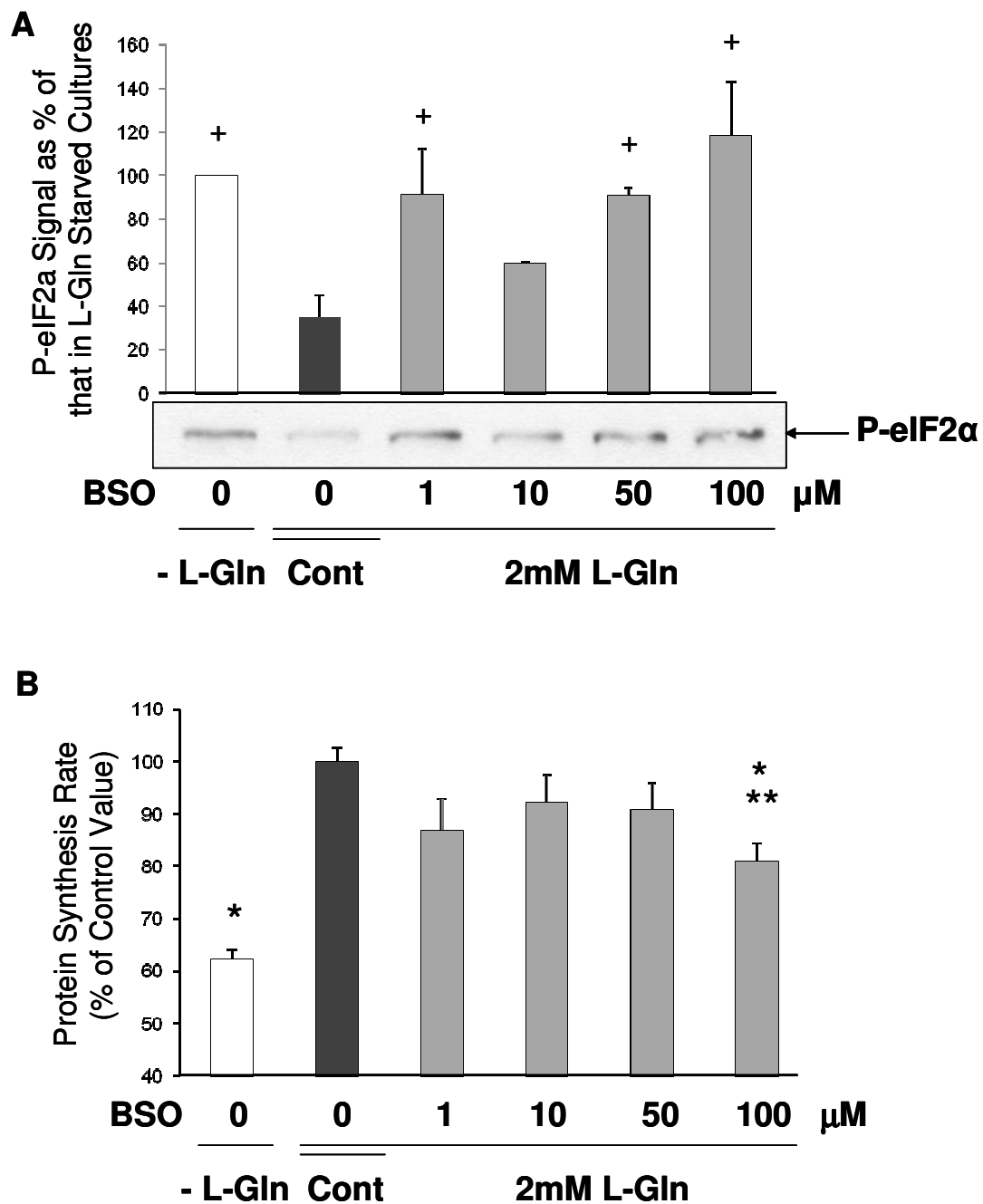


Figure 5.12. Comparison of the effect of L-Gln starvation and of incubation with glutathione biosynthesis inhibitor L-Buthionine-[S,R]-Sulfoximine (BSO) on (A) phosphorylation of eIF2 α and (B) global protein synthesis ($^3\text{H-L-Phe}$ incorporation) in L6-G8C5 myotubes. Cultures were incubated for 2h in MEM with or without 2mM L-Gln and 100nM insulin. In (A) immunoblots of proteins separated by SDS-PAGE were probed with antibody against Ser52-phosphorylated eIF2 α . Pooled blot quantification data are combined from 3 independent experiments, $^+P < 0.05$ versus control. In (B) $^3\text{H-L-Phe}$ was present in the medium for the final 30 min of the incubation. Protein synthesis rate is expressed as percentage of the control value. Pooled data from 3 independent experiments are shown (with 3 replicate culture wells for each experiment), $^*P < 0.05$ versus control, $^{**}P < 0.05$ versus L-Gln starved condition.

synthesis is detectable within 2h and is mimicked by the L-Gln anti-metabolite Acivicin (Figure 5.2) whereas L-Gln-dependent glutathione depletion is not (Figure 5.11B and C).

5.2.3 Relevance of L-Gln deprivation effects to SNAT2

In contrast to the effect of extracellular L-Gln deprivation which gave a roughly 2.5-fold stimulation of eIF2 α phosphorylation (Figure 5.8B and Figure 5.9B), depletion of intracellular L-Gln by inhibiting SNAT2 transporters in L6G8C5 myotubes gave no statistically significant stimulation of this signal (Figure 5.13A). Partial inhibition with low extracellular pH had almost no detectable effect, and the effect was still statistically insignificant even when SNAT2 was completely inhibited with a saturating dose of MeAIB (Figure 5.13A). Furthermore, chronic siRNA silencing of SNAT2 in myoblasts led to an apparent decrease in the basal eIF2 α phosphorylation (Figure 5.13B). It was also noted that the level of L-Gln depletion needed to impair protein synthesis in the myotube cultures was <0.1mM extracellular L-Gln (Figure 5.14A). Comparison with the data previously presented in Appendix E Figure 2A (and shown again in Figure 5.14B) indicates that this level of L-Gln restriction is sufficient to decrease intracellular L-Gln by more than 90% - more severe than the ~75% depletion obtained on complete inhibition of SNAT2 with MeAIB (Figure 4.1A) .

Therefore to achieve closer matching of the intracellular amino acid profile obtained by extracellular amino acid depletion, to the profile observed on inhibiting SNAT2 with MeAIB (Appendix E Figure 1 and Appendix E Table 1),

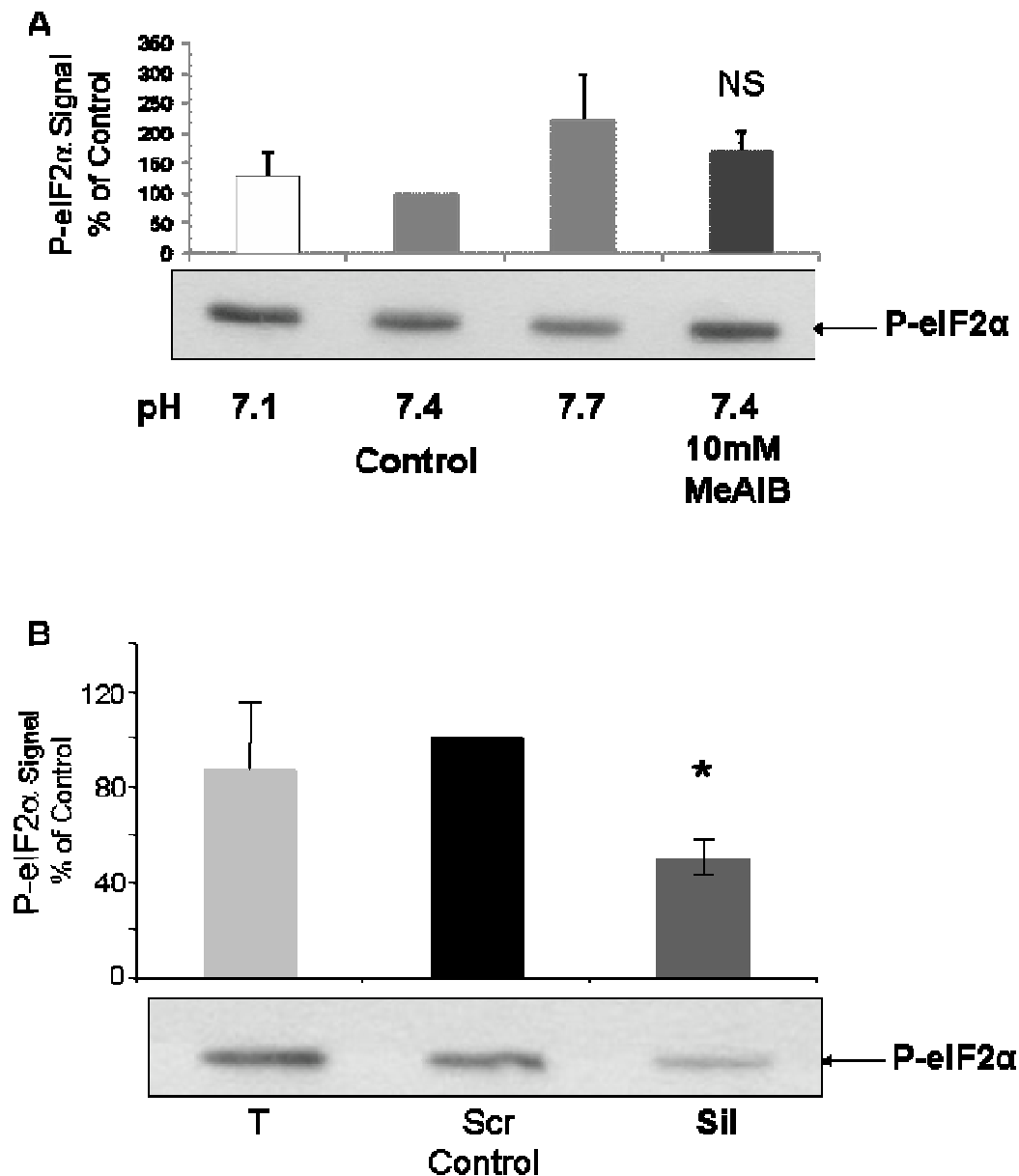


Figure 5.13. Effect of SNAT2 inhibition or silencing on eIF2 α phosphorylation. (A) L6-G8C5 myotubes were incubated for 2h in MEM containing 2mM L-Gln and 100nM insulin either at acidic pH 7.1 or at control pH 7.4 (with or without 10mM MeAIB). **(B)** Effect of SNAT2 silencing with siRNA in L6-G8C5 myoblasts. Transfection was followed by an 8h incubation in DMEM + 10% foetal bovine serum followed by 16h in MEM + 2% dialysed foetal bovine serum. Cells were then washed thrice in HBSS and incubated in MEM based media containing 2mM L-Gln and 100nM insulin for 2h. "T" denotes transfection blank (cells exposed to calcium phosphate transfection agent only), "Scr" denotes cells exposed to scrambled control siRNA, and "Sil" denotes cells exposed to SNAT2-silencing siRNA. Immunoblots of proteins separated by SDS-PAGE were probed with antibody against Ser52-phosphorylated eIF2- α . The bar charts denote quantification of phosphorylation by densitometry. (A) Pooled data from 7 independent experiments expressed as percentage of the pH 7.4 control value. The apparent increase in response to MeAIB did not achieve statistical significance. (B) Pooled data from 2 independent experiments with duplicate cultures under each set of conditions. Data are expressed as percentage of the Scr control value. *P<0.05 versus Scr.

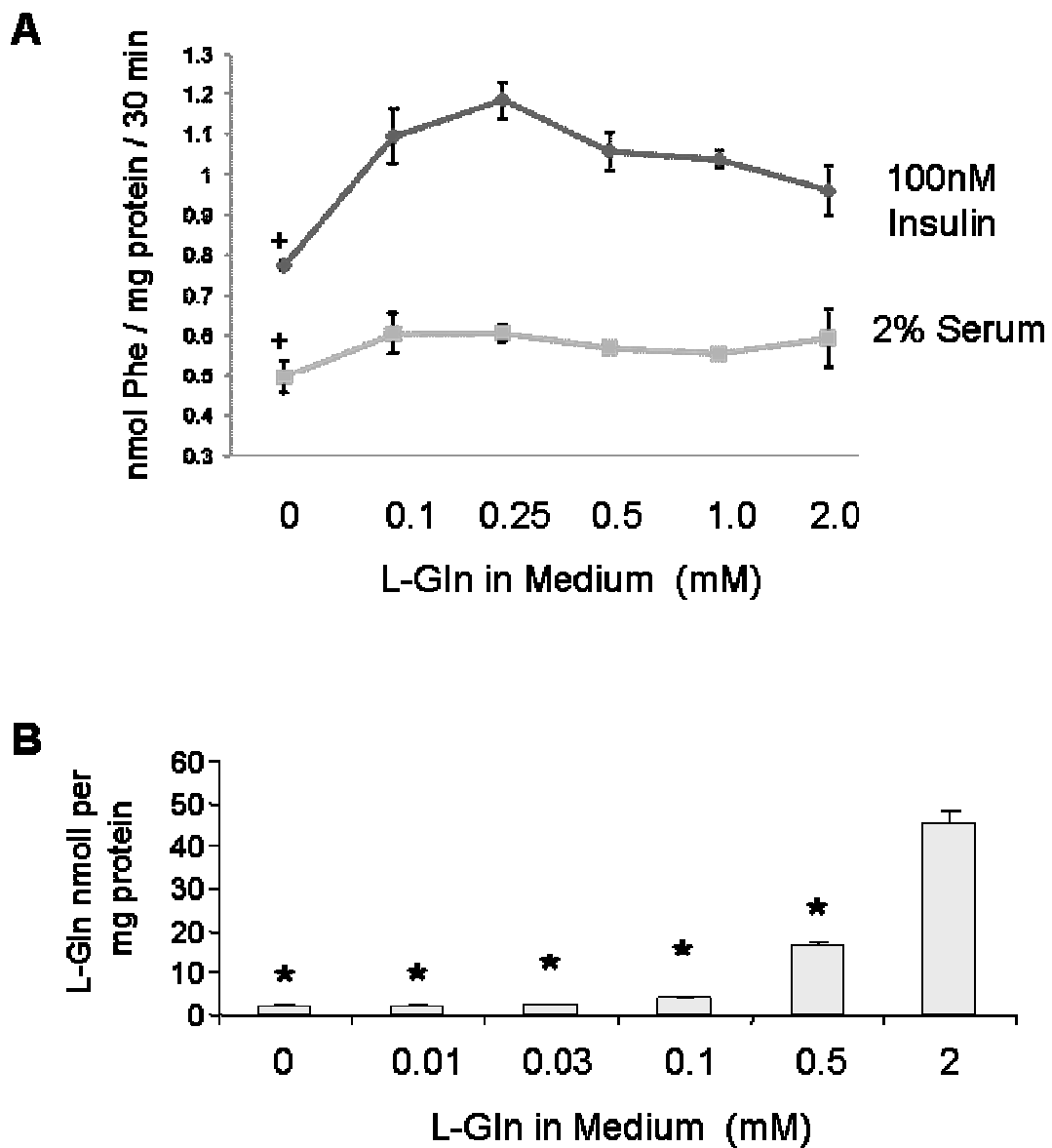


Figure 5.14. A) Dependence of the global protein synthesis rate ($^3\text{H-L-Phe}$ incorporation) in L6-G8C5 myotubes on the extracellular L-Gln concentration. Cultures were incubated in MEM with either 2% dialysed foetal bovine serum or 100nM insulin at the specified L-Gln concentration for 2 hours. $^3\text{H-L-Phe}$ was present in the medium for the final 30 min of the incubation. Pooled data from 3 independent experiments are shown (1 for serum) with 3 replicate culture wells for each experiment. * $P < 0.05$ versus medium with 2mM L-Gln. B) From Appendix Figure 2. Effect of extracellular L-Gln concentration on intracellular concentrations of L-Gln, after 2h at pH 7.4. * $P < 0.05$ versus medium with 2mM L-Gln. Results from 1 experiment representative of 3 independent experiments are shown with $n = 3$ replicate culture wells for each treatment.

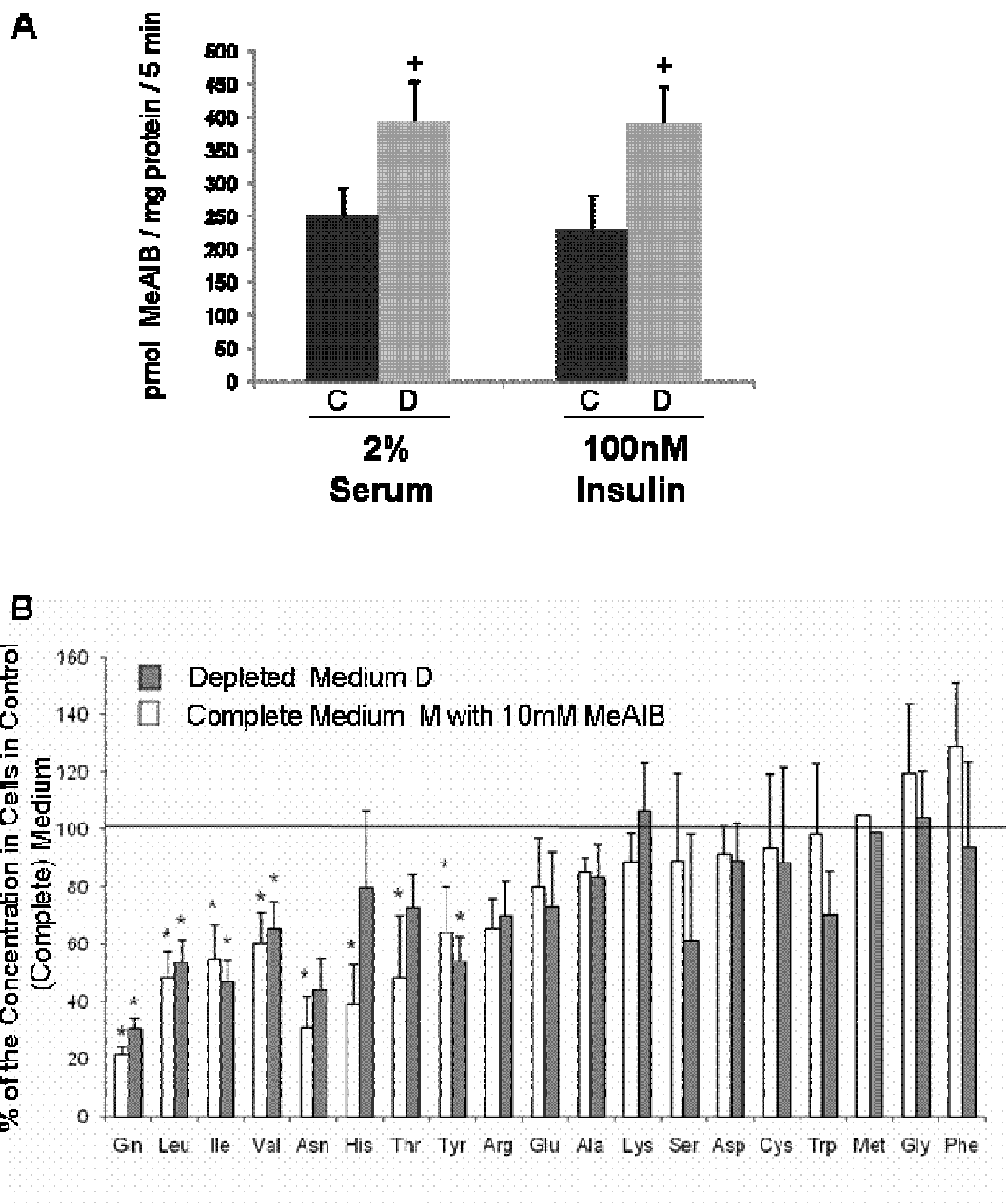
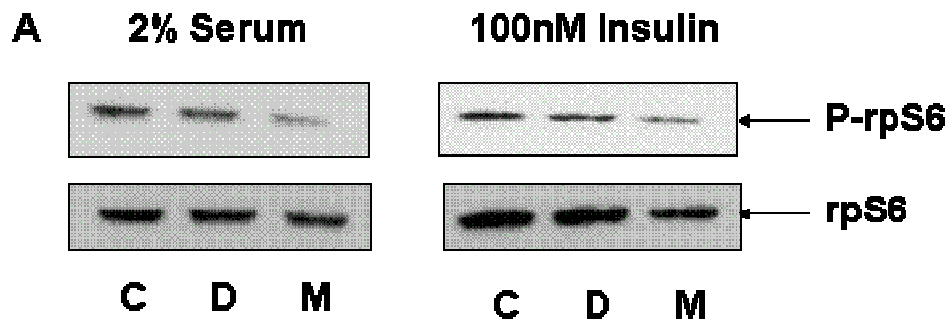


Figure 5.15. The effects of 2 hours of partial amino acid depletion or SNAT2 inhibition on (A) SNAT2 transporter activity and (B) intracellular amino acid concentrations in L6-G8C5 myotubes. Cultures were incubated for 2 hours in complete MEM (Control medium “C”) with 2mM L-Gln; in partly depleted medium (“D”) containing 15% of the L-Gln and 25% of all the other amino acids present in C; and in medium “M” which was derived from “C” by adding 10mM MeAIB. (A) After the 2h incubation, SNAT2 transporter activity was immediately assessed from the rate of uptake of ^{14}C -MeAIB in Hepes buffered saline. * $P < 0.05$ versus the control, C. (B) Parallel cultures were rinsed thrice in ice-cold 0.9% NaCl (to remove extracellular amino acids) and free amino acids were extracted for determination by HPLC. Results are expressed as percentage of the concentration in control medium “C”. * $P < 0.05$ versus control C. Pooled data from 3 independent experiments are shown with 3 replicate culture wells for each treatment.



B Densitometry on P-rp S6 Signal

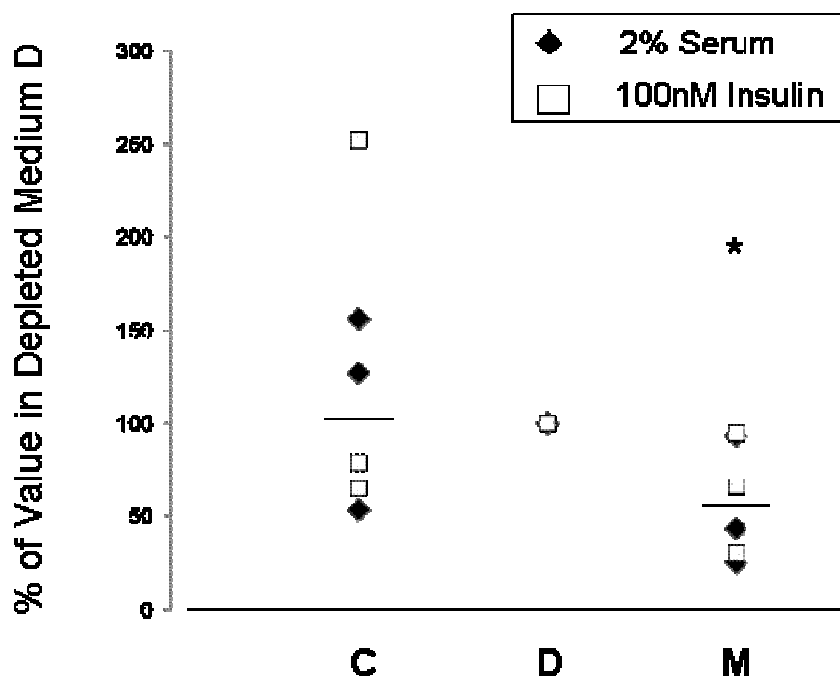


Figure 5.16 The effect of 2 hours of partial amino acid depletion or SNAT2 inhibition on rpS6 signalling in L6-G8C5 myotubes. Experiments were performed in parallel with those in Figure 5.15. Immunoblots of proteins separated by SDS-PAGE were probed with antibody against Ser235/6-phosphorylated rpS6 (and a total rpS6 antibody as a loading control). Pooled quantification data from 3 experiments are shown with results expressed as percentage of those in the partially depleted medium “D” control. *P < 0.05 versus medium “D”.

L6-G8C5 myotubes were incubated in a partial depletion medium (designated “Medium D” in Figures 5.15 and 5.16) in which extracellular L-Gln was reduced to 15% and all other amino acids to 25% of the concentration in the control medium. After 2h in this medium, the intracellular free amino acid profile was compared with that in parallel SNAT2-inhibited cultures incubated with MeAIB. In spite of the compensatory up-regulation of SNAT2 transporter activity that occurred in cells incubated in the partial depletion medium (Figure 5.15A), the intracellular amino acid profile for the potentially anabolic amino acids L-Gln, L-Leu, L-Ile and L-Val with this medium was comparable with that obtained in cultures with MeAIB (Figure 5.15B). In spite of this, the mTOR signal to rpS6 phosphorylation was noticeably weaker in MeAIB cultures than in the cultures with a comparable anabolic amino acid profile in partially depleted Medium D (Figure 5.16); consistent with the failure of intracellular amino acid depletion to mimic the effect of SNAT2 inhibition previously observed in Figure 5.7.

5.3 Discussion

5.3.1 L-Gln restriction is an imperfect model for the effect of SNAT2 inhibition on protein synthesis

SNAT2 inhibition strongly depletes intracellular L-Gln in L6-G8C5 myotubes and this depletion is therefore an appealingly simple explanation for the functional effects of SNAT2 inhibition on the cells. Superficially the effect of L-Gln restriction on protein metabolism does resemble the effect of SNAT2 inhibition: it impairs global protein synthesis (Figure 5.2), activates global proteolysis (56), and blunts the effects of SNAT2 inhibition on protein

synthesis (Figure 3.5 C,D) and proteolysis, (56). L-Gln deprivation also abolishes the insulin sensitivity of protein synthesis (Figure 5.3), thus apparently mimicking the impairment of insulin signalling to protein metabolism observed when SNAT2 is inhibited (Chapters 3 and 4). Detailed examination of the signalling pathways influenced by L-Gln deprivation however showed only weak mimicry of the effects of SNAT2 inhibition on signalling through mTOR, PI3K/PKB and Ras/Raf/MEK/Erk. Instead L-Gln deprivation activated eIF2 α phosphorylation – a signal more frequently associated with endoplasmic reticulum stress (ER stress) and the unfolded protein response, (156).

5.3.2 L-Gln restriction is a metabolic stress

L-Gln restriction has previously been associated with ER stress, (225), and associated transcriptional responses, (226), in breast tumour cell lines, but the mechanism of that response is still unclear. The present study indicates that glutathione depletion is probably a contributor to the increased eIF2 α phosphorylation observed in L-Gln-deprived L6-G8C5 myotubes, but some additional factor of more rapid onset, apparently mimicked by Acivicin, also seems to be involved. The failure of SNAT2 manipulation to mirror this eIF2 α response, and the failure of L-Gln deprivation, even when accompanied by partial System L amino acid depletion, to reproduce the inhibitory effect of SNAT2 manipulation on rpS6 phosphorylation, strongly suggests that L-Gln deprivation and effects mediated by SNAT2 effects on protein metabolism occur by radically different pathways. The failure of L-Gln deprivation to impair protein synthesis, except when deprivation is severe

(Figure 5.15), also supports the conclusion that L-Gln depletion is a metabolic stress and not the basis of SNAT2's effect on protein synthesis.

5.3.3 Partial depletion of L-Gln and branched chain amino acids fails to mimic the effect of SNAT2 inhibition

Even though it is well established that ~50% changes in intracellular amino acid pools can regulate (m)TOR signalling in some cell types, (212,213), and even though strong depletion of L-Leu can influence such signals in L6 cells, (192), in the present study **partial** depletion of amino acid pools, to mimic the effect of SNAT2 inhibition, gave only a surprisingly weak effect on rpS6 phosphorylation (Figures 5.7 and 5.16). In contrast, in parallel cultures (Figure 5.16), as in Chapter 3, this signal showed a clear inhibitory response to treatment of SNAT2 with MeAIB – a disparity which is particularly surprising in view of the tendency of MeAIB to stimulate PI3K in Chapter 4, an effect which would be expected to send a stimulatory signal to mTOR.

This leads to the question of whether free amino acids (other than L-Gln and the branched chain amino acids which have previously been shown to influence signalling to global protein synthesis in L6 cells) might be exerting an effect. Examination of the intracellular amino acid profiles in Figure 5.15B shows that even though SNAT2 inhibition with MeAIB depleted intracellular L-His and L-Thr, significant depletion of these pools was not achieved with the amino acid depleted culture medium. A role for these amino acids in mediating the functional effects of SNAT2 cannot therefore be excluded. However, L-His and L-Thr have not previously been implicated in mTOR

signalling in skeletal muscle cells, which raises the question of whether SNAT2 can influence mTOR signalling through some mechanism in addition to its effects on amino acid pools. This possibility is considered in more detail in the final chapter that follows.

Chapter 6: General Discussion

6.1 SNAT2 Coupling to Amino Acid Dependent Proteins

The data presented in Chapter 3 of this thesis suggest that SNAT2 is coupled to at least two important amino acid-dependent systems in L6-G8C5 myoblasts and myotubes: plasma membrane amino acid exchangers (probably System L transporters) and mTOR. Therefore a straightforward explanation of SNAT2's functional effects is that it acts primarily by maintaining an intracellular/extracellular concentration gradient of its neutral amino acid substrates, notably L-Gln. Then, through utilisation of this gradient by amino acid exchangers, SNAT2 indirectly maintains an intracellular/extracellular gradient of other amino acids such as L-Leu that are not directly transported by SNAT2, (see Figure 6.1). There is good evidence in L6 cells that, when compared with cells incubated in medium without L-Leu, addition of this amino acid is sufficient to activate mTOR and its downstream targets, (192,204).

If SNAT2's effects on intracellular amino acid pools alone explain the functional consequences of SNAT2 inhibition in Chapter 3, it should be possible to reconstruct these effects by amino acid depletion alone. However, even though severe L-Leu depletion, (192,204), and severe L-Gln depletion, (Chapter 5), exerted significant effects on signalling and global protein metabolism in these cells, partial depletion of these pools in Chapter 5 (comparable with that achieved by SNAT2 inhibition), did not completely

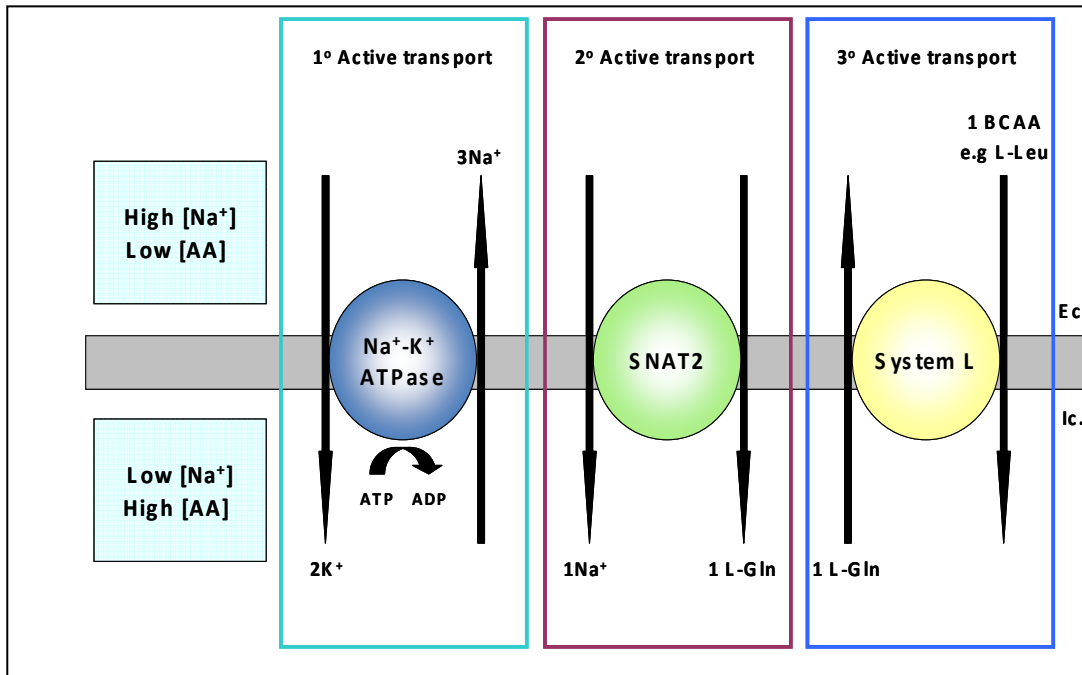


Figure 6.1: Coupling between SNAT2 and System L transporters.

This figure depicts the coupling of that occurs between SNAT2 and other transporters, using System L as an example. SNAT2 functions as a L-Gln pump setting up a L-Gln gradient which allows the BCAA carried on System L to accumulate within the cell as they are exchanged for L-Gln.

mimic the effects of SNAT2 inhibition with MeAIB. At present there seem to be at least two possible explanations for this discrepancy:

1) As discussed in Chapter 5, a possible explanation is that SNAT2 inhibition acts on mTORC1 through depletion of some previously unsuspected intracellular amino acid pool such as L-His which was not significantly depleted by the partly amino acid depleted medium used in Figure 5.15 and 5.16.

2) However, the larger inhibition of rpS6 phosphorylation observed with MeAIB than with partial amino acid depletion, (Figure 5.16), raises again the question posed in Chapter 3 of whether MeAIB is directly blocking amino acid sensing by mTORC1 (Figure 6.2). A possible explanation is that the SNAT2 protein itself is part of that sensing mechanism, and that saturation of the transporter with MeAIB, in addition to depleting intracellular amino acids, augments the effects of amino acid depletion on mTORC1 by blocking the hypothetical amino acid sensor upstream of mTOR (Figure 6.2).

In addition to evidence for an amino acid sensing role for SNAT2 presented previously, (80), there is also considerable evidence that amino acid sensing by (m)TOR in eukaryotes can occur through a Class III PI-3-kinase, hVPS34, (113). The evidence for coupling between SNAT2 and Class I PI3K and PKB presented in Chapter 4, leads to the important question of whether a similar coupling might exist between SNAT2 and Class III lipid kinases (Figure 6.2),

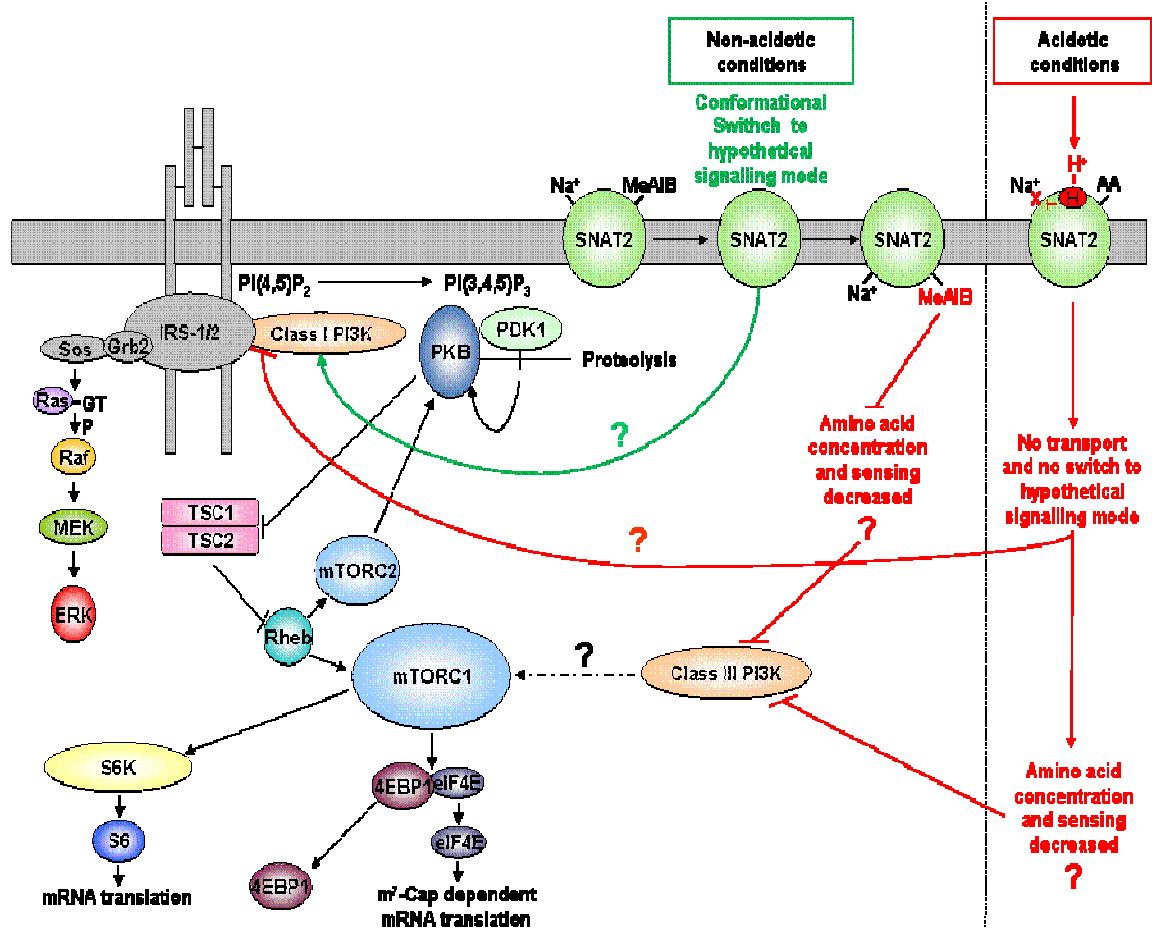


Figure 6.2: Proposed mechanisms via which SNAT2 inhibition may mediate increases in proteolysis and decreases in protein synthesis by regulation of the activity of the insulin signalling pathway.

Green lines show the positive effect of SNAT2 in its hypothetical signalling mode on PI3K. Red lines indicate a negative effect of SNAT2 inhibition of insulin signalling.

The acidotic effect on SNAT2 is shown by protonation of the histidine residue which allosterically prevents Na⁺ binding and pushes the transporter into its “off” mode, thus preventing amino acid influx and decreasing the intracellular amino acid concentration. The same effect observed due to MeAIB inhibition of SNAT2 is also shown.

The Class III PI3K is shown as a potential sensor of intracellular amino acid levels, which regulates (possibly via other proteins) mTORC1 activity, and may be blocked by SNAT2 saturation with MeAIB, thus leading to further decreases in mTORC1 activity as suggested in section 6.1.

These signalling pathways have not been confirmed but are suggested as a result of previous results from other researchers and from the results of this study, and are discussed in the text throughout chapter 6.

Proteins are shown schematically as coloured shapes and are not drawn relative to scale.

and whether this contributes to the apparent effects on signalling downstream of mTORC1 observed in Chapter 3 and Chapter 5.

It should also be noted that, although partial depletion of extracellular amino acids did mimic the changes in intracellular amino acid levels observed during SNAT2 inhibition with MeAIB (Figure 5.15B), it does not mimic all of the changes to the cellular environment that occur when SNAT2 is inhibited. Firstly, extracellular amino acid depletion ultimately produces a decrease in the amino acid concentration on both sides of the plasma membrane, whereas SNAT2 inhibition only decreases the intracellular concentration, to which the cytosolic face of the plasma membrane is exposed. If cell surface amino acid sensors exist (as has been proposed previously in hepatocytes, (227)) extracellular amino acid depletion might exert effects radically different from those achieved by SNAT2 inhibition. Secondly, depletion of extracellular amino acids initially increases the intracellular/extracellular amino acid gradient, whereas during SNAT2 inhibition this gradient initially decreases. However, there is no evidence yet that mTORC1 can sense amino acid gradients as opposed to amino acid concentrations.

6.2 SNAT2 Coupling to Proteins Independent of Amino Acids

The observations in Chapter 4 of a functional link between SNAT2 and PI3K and PKB are at present difficult to explain in terms of known properties of the SNAT2 protein. The well-documented pH sensitivity of PI3K and PKB, apparently mediated by SNAT2, and its apparent modulation by substrate binding, implies that SNAT2 may exist in at least two states: an “on” state

which can transport amino acids and activate PI3K/PKB (and also possibly Erk); and an “off” state in which both of these functions are impaired (Figure 6.2). Stimulation of PI3K/PKB activity by MeAIB (observed in chapter 4) may mean that they are activated by a signalling function of the SNAT2 “transceptor”, as proposed by Hyde et al, (80), rather than indirectly, as a result of a SNAT2-dependent change in intracellular amino acid levels. This proposal is consistent with the accepted view that Class I PI3Ks are not directly sensitive to amino acid concentration or pH, and the observation from Hyde et al that pharmacological inhibition of PI3K blunts adaptive regulation of SNAT2, (80), again suggesting a link between the SNAT2 transceptor signal and the PI3K pathway.

A possible biochemically testable explanation for the effects observed in Chapter 4 is that the transition between the “on” and “off” states is modulated by phosphorylation of the SNAT2 protein. Phosphorylation of the N-terminal cytoplasmic tail of SNAT2 has recently been reported in HeLa cells, (228,229). It will be of considerable interest in future to determine if such phosphorylation also occurs in L6 cells, and whether this phosphorylation is influenced by acidosis and by substrate binding to SNAT2.

6.3 Temporal Relationships

The precise temporal relationships between the signals described here are still uncertain as detailed time courses of the effects described in this thesis have not yet been performed. However, if low pH acts on the SNAT2 protein primarily through direct protonation of the protein, this is probably an early

and rapid event, because proton transfer in aqueous solution is an extremely rapid chemical process. Effects mediated by changes in amino acid concentration are presumably slower than this, but clear effects of System L amino acid deprivation or MeAIB on mTOR signalling have been detected in L6-G8C5 myotubes in as little as 30 minutes (A Bevington and J Brown personal communication), and activation of eIF2- α phosphorylation by L-Gln starvation was detected in Figure 5.8B within 1 hour.

6.4 Summary

In conclusion metabolic acidosis is known to occur in ESRD patients and lead to increased wasting of the lean tissue. This study has demonstrated that the pH sensitive SNAT2 transporter is coupled to PI3K, PKB and proteolysis, and, can regulate mTOR activation and protein synthesis, in skeletal muscle cells. This strongly suggests that this transporter is a key player in the acid-induced insulin resistance which is regarded as a prime cause of cachexia in acidotic uraemic patients, (165). It has also been determined that amino acid depletion does not necessarily mimic these signalling effects, suggesting that amino acid repletion treatment in uraemic patients may not fully suppress the catabolic effect of metabolic acidosis. Finally these effects may be particularly important in renal patients with diabetes mellitus. In view of their pre-existing insulin deficiency or insulin resistance, (18,165), the inhibition of insulin signalling following pH inhibition of SNAT2 may explain why muscle protein metabolism is so badly impaired in these patients.

Appendix A: DMEM and MEM Components

MEM Invitrogen 21090-022 Components

COMPONENTS	Molecular Weight	Concentration (mg/L)	Molarity
Amino Acids			
L-Arginine hydrochloride	211	126	0.597156
L-Cystine	240	24	0.1
L-Histidine hydrochloride-H2O	210	42	0.2
L-Isoleucine	131	52	0.396947
L-Leucine	131	52	0.396947
L-Lysine hydrochloride	183	73	0.398907
L-Methionine	149	15	0.100671
L-Phenylalanine	165	32	0.193939
L-Threonine	119	48	0.403361
L-Tryptophan	204	10	0.04902
L-Tyrosine	181	36	0.198895
L-Valine	117	46	0.393162
Vitamins			
Choline chloride	140	1	0.007143
D-Calcium pantothenate	477	1	0.002096
Folic Acid	441	1	0.002268
Niacinamide	122	1	0.008197
Pyridoxal hydrochloride	204	1	0.004902
Riboflavin	376	0.1	0.000266
Thiamine hydrochloride	337	1	0.002967
i-Inositol	180	2	0.011111
Inorganic Salts			
Calcium Chloride (CaCl ₂ -2H ₂ O)	147	264	1.795918
Magnesium Sulfate (MgSO ₄ -7H ₂ O)	246	200	0.813008
Potassium Chloride (KCl)	75	400	5.333334
Sodium Bicarbonate (NaHCO ₃)	84	2200	26.190475
Sodium Chloride (NaCl)	58	6800	117.24138
Sodium Phosphate monobasic (NaH ₂ PO ₄ ·2H ₂ O)	156	158	1.01282
Other Components			
D-Glucose (Dextrose)	180	1000	5.555555

Phenol Red	376.4	10	0.026567
------------	-------	----	----------

http://www.invitrogen.com/site/us/en/home/support/Product-Technical-Resources/media_formulation.197.html

Last accessed 19.01.09

DMEM Invitrogen 11880-028 Components

COMPONENTS	Molecular Weight	Concentration (mg/L)	Molarity
Amino Acids			
Glycine	75	30	0.4
L-Arginine hydrochloride	211	84	0.398104
L-Cystine 2HCl	313	63	0.201278
L-Histidine hydrochloride-H ₂ O	210	42	0.2
L-Isoleucine	131	105	0.801527
L-Leucine	131	105	0.801527
L-Lysine hydrochloride	183	146	0.797814
L-Methionine	149	30	0.201342
L-Phenylalanine	165	66	0.4
L-Serine	105	42	0.4
L-Threonine	119	95	0.798319
L-Tryptophan	204	16	0.078431
L-Tyrosine	181	72	0.39779
L-Valine	117	94	0.803419
Vitamins			
Choline chloride	140	4	0.028571
D-Calcium pantothenate	477	4	0.008386
Folic Acid	441	4	0.00907
Niacinamide	122	4	0.032787
Pyridoxine hydrochloride	204	4	0.019608
Riboflavin	376	0.4	0.001064
Thiamine hydrochloride	337	4	0.011869
i-Inositol	180	7.2	0.04

Inorganic Salts			
Calcium Chloride (CaCl ₂ ·2H ₂ O)	147	264	1.795918
Ferric Nitrate (Fe(NO ₃) ₃ ·9H ₂ O)	404	0.1	0.000248
Magnesium Sulfate (MgSO ₄ ·7H ₂ O)	246	200	0.813008
Potassium Chloride (KCl)	75	400	5.333334
Sodium Bicarbonate (NaHCO ₃)	84	3700	44.04762
Sodium Chloride (NaCl)	58	6400	110.34482
Sodium Phosphate monobasic (NaH ₂ PO ₄ ·2H ₂ O)	154	141	0.915584
Other Components			
D-Glucose (Dextrose)	180	1000	5.555555
Sodium Pyruvate	110	110	1

http://www.invitrogen.com/site/us/en/home/support/Product-Technical-Resources/media_formulation.183.html

Last accessed 19.01.09

Concentrations of amino acids added back to EBSS based amino acid free media

Amino acid	mg/L
L-Arginine.HCl	126
L-Cystine	24
L-Histidine.HCl.H ₂ O	42
L-Lysine.HCl	73
L-Methionine	15
L-Threonine	48
L-Isoleucine	52
L-Leucine	52
L-Phenylalanine	32
L-Tryptophan	10
L-Tyrosine	36
L-Valine	46

Appendix B: Buffers and Reagents

SDS-PAGE reducing sample buffer

4ml np H₂O
1ml 0.5M Tris HCl pH 6.8
0.8ml Glycerol
1.6ml 10% w/v Sodium Dodecyl Sulphate (SDS)
0.4ml β-Mercaptoethanol
0.2ml 0.05% w/v Bromophenol Blue

Western Transfer buffer (1litre)

3.03g Tris-base
14.4g Glycine
200ml Methanol

SDS-PAGE Running buffer (1litre)

3.03g Tris-base
14.4g glycine
50ml 20% w/v SDS

Lysis buffer for Western blotting

10mM β-glycerophosphate pH 7.4
1mM Ethylenediaminetetraacetic acid (EDTA) pH 8
1mM Ethylene glycol tetraacetic acid (EGTA)
50mM Tris HCl pH 7.5
1mM Benzamidine
1mM Sodium Orthovanadate
0.2mM Phenylmethylsulphonyl fluoride (PMSF)
1ug/ml Pepstatin A
1ug/ml Leupeptin
0.1% v/v β-Mercaptoethanol
1% v/v Triton X-100
50mM Sodium Fluoride

Lysis Buffer for Isolation of Cell Membranes (UIC3)

250mM Sucrose
20mM Hepes
5mM Sodium Azide
2mM EGTA
1% v/v Calbiochem Protease Inhibitor Cocktail set 3
Adjust to pH 7.4 with 0.5M NaOH.

10 X Tris-buffered saline (TBS) (1 litre)

6.055g Trizma Base
8.766g NaCl
Adjust to pH 7.6 with HCl

1 X TBS-Tween (1 litre)

100ml 10X TBS

900ml De-ionised H₂O
1ml Tween 20

10 X Phosphate-buffered saline (PBS) (1 litre)

3g KCl
100g NaCl
14g Na₂HPO₄
3g KH₂PO₄
Adjust to pH 7.4 with HCl

1 X PBS-Tween (1 litre)

100ml 10X PBS
90ml DI H₂O
1% Tween 20

Hepes buffered saline (HBS)

140mM NaCl
20mM Hepes acid
2.5mM MgSO₄.7H₂O
5mM KCl
1mM CaCl₂.2H₂O
10mg/l Phenol red
Adjust to pH 7.4 with NaOH.

Appendix C: Buffers and Reagents used in PI3K assays

PI3K Lysis Buffer

137mM NaCl
2.7mM KCl
1mM MgCl₂
1mM CaCl₂
1% v/v IGEPAL CA-630
10% v/v Glycerol
1mg/ml BSA
20mM Tris-Base
0.5mM Na₃VO₄
0.2mM PMSF
10ug/ml Leupeptin
10ug/ml Antipain
10ug/ml Pepstatin A
10ug/ml Aprotinin
Adjust pH to 8.0 with HCl

Wash1/2

0.5M LiCl
0.1M Tris-Base
Adjust pH to 8.0 with HCl

Wash 3

0.15M NaCl
10mM Tris-Base
1mM EDTA
Adjust pH to 7.6 with HCl

Wash 4

20mM Hepes
1mM Dithiothreitol (DTT)
5mM MgCl₂
Adjust pH to 7.6 with HCl

Kinase Assay Buffer

20mM Beta-Glycerophosphate
5mM Sodium Pyrophosphate
30mM NaCl
1mM DTT
Adjust pH to 7.2 with HCl

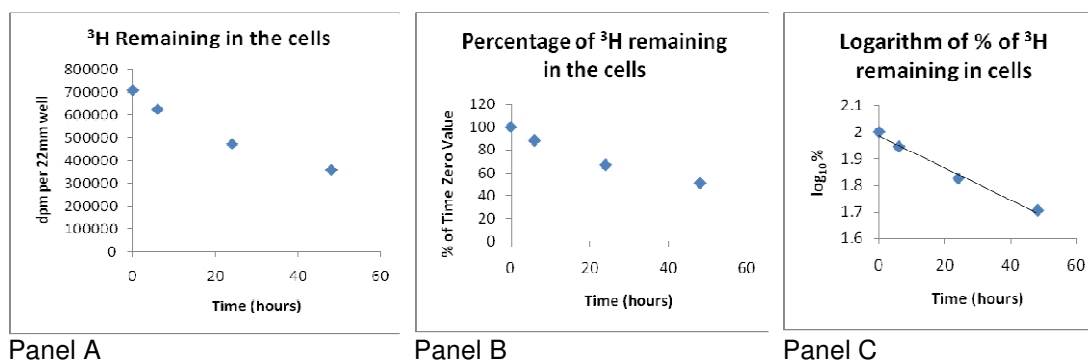
Oxalate-treated TLC plates

A 20 x 20cm VWR Kieselgel 60 F-254 plate (Ref 1.05715.0001) was immersed in a solution containing an equal volume of a 1% w/v Potassium Oxalate, 2mM EDTA solution and methanol, allowed to dry in air, and then baked at 150°C for 2 hours. The plate was then used immediately after cooling.

Appendix D: Specimen Calculation of Global Proteolysis Rate of Cultures of L6-G8C5 Myotubes

Principle

Cell protein is pre-labelled with ^3H -L-Phe in cultures on 22mm diameter culture wells as described in Materials and Methods. The medium containing ^3H -L-Phe is rinsed away and fresh unlabelled medium is added and incubated for 2h to allow rapidly degraded proteins to release ^3H . This medium is then discarded and fresh unlabelled medium is added (time zero). Aliquots of medium are removed after a further 6, 24 or 48h and are deproteinised with trichloroacetic acid. Residual ^3H in the cells after 48h is digested in NaOH. From the activity of ^3H counted in the deproteinised medium and in the final NaOH cell digest, the total ^3H in cell protein at time zero and after 6, 24 or 48h is calculated (Panel A) and expressed as a percentage of the initial total ^3H in cell protein (Panel B). This approximately exponential curve is then rendered linear by re-plotting the percentages as a logarithm (Panel C). The slope of the linear regression through the data in Panel C is then taken as a measure of the global proteolysis rate averaged over the 48h experiment. Alternatively the slopes of the individual sections of the curve between the data points are taken as an indicator of how the proteolysis rate has varied throughout the experiment.



Procedure

At time zero 2ml of unlabelled medium is added to the culture. Aliquots of 300 μl are drawn from the medium after 6, 24 or 48h. Each aliquot is mixed with 300 μl of 20% w/v trichloroacetic acid and centrifuged. From the supernatant 500 μl is counted. After 48h the cultures are rinsed and the residual ^3H in the cells is digested in 1ml of 0.5M NaOH and 50 μl of the digest is counted.

Specimen Data

Time	Sample	Count in the aliquot taken (dpm)
6h	Culture Medium	Count a = 10 518
24h	Culture Medium	Count b = 32 889
48h	Culture Medium	Count c = 53 229
48h	Residual Cell Digest	Count d = 18 022

Background Count (BG) = 19dpm

Calculation (using the counts **a**, **b**, **c**, **d** and **BG** above)

Total ³H in the cells at Time Zero = T₀

= ³H in the cells at the end of the experiment (48h)
+ ³H remaining in the medium at the end of the experiment (48h)
+ ³H sampled in the 300μl aliquot of medium at 24h
+ ³H sampled in the 300μl aliquot of medium at 6h

= (d - BG) x (1000/50)
+ (c - BG) x (600/500) x (1400/300)
+ (b - BG) x (600/500)
+ (a - BG) x (600/500)

= 710 000 dpm

³H in the cells at 6h

= T₀ (Total ³H in the cells at Time Zero) - ³H in the Medium at 6h
= T₀ - [(a - BG) x (600/500) X (2000/300)]

= 626 000 dpm

³H in the cells at 24h

= T₀ (Total ³H in the cells at Time Zero) - ³H sampled in the 300μl aliquot of medium at 6h - ³H in the Medium at 24h

= T₀ - [(a - BG) x (600/500)] - [(b - BG) x (600/500) X (1700/300)]

= 474 000 dpm

³H in the cells at 48h

= ³H measured in the cell digest at 48h

= (d - BG) x (1000/50)

= 360 000 dpm

Average Global Proteolysis Rate over the 48h Experiment

(Linear Regression Slope through the data in Panel C)

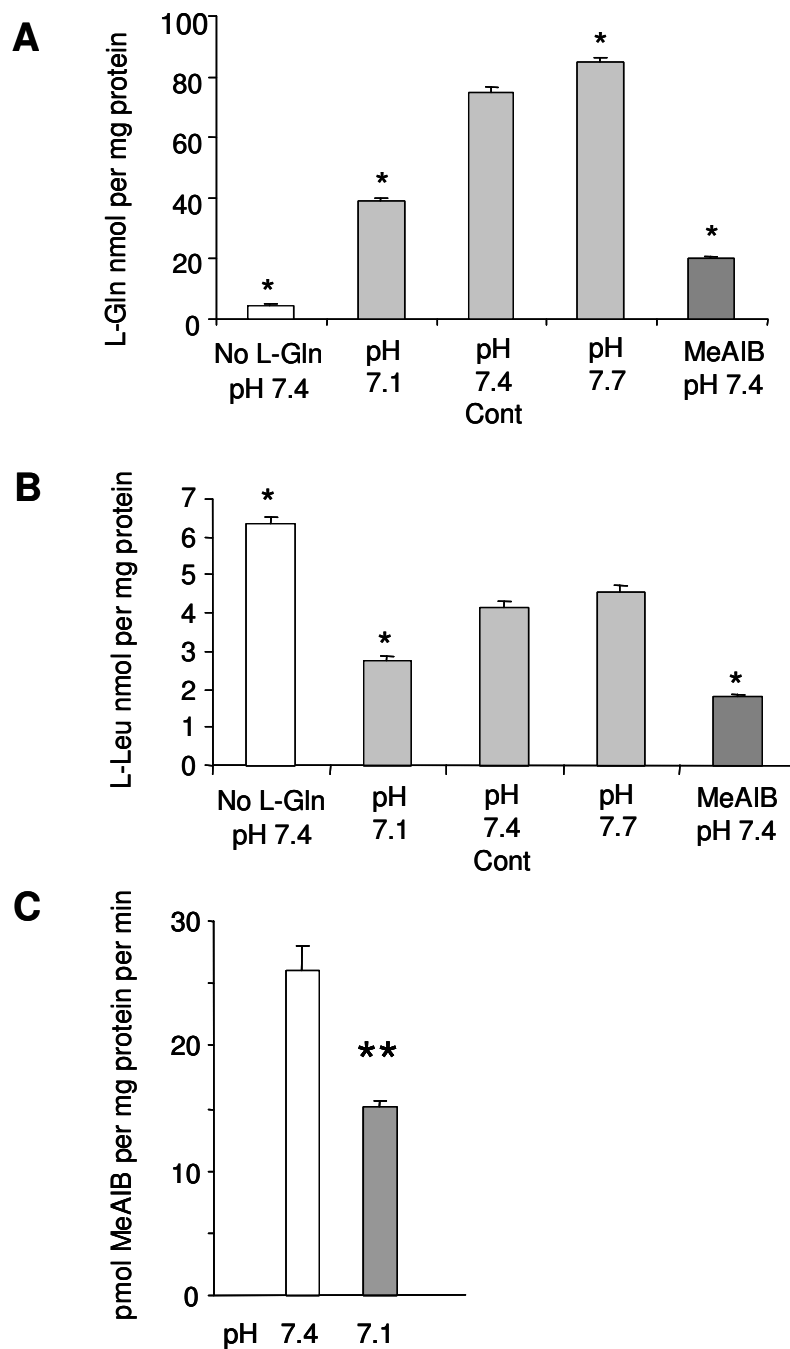
= - 6.06 x 10⁻³ log₁₀ % per hour

Appendix E: Supporting Data

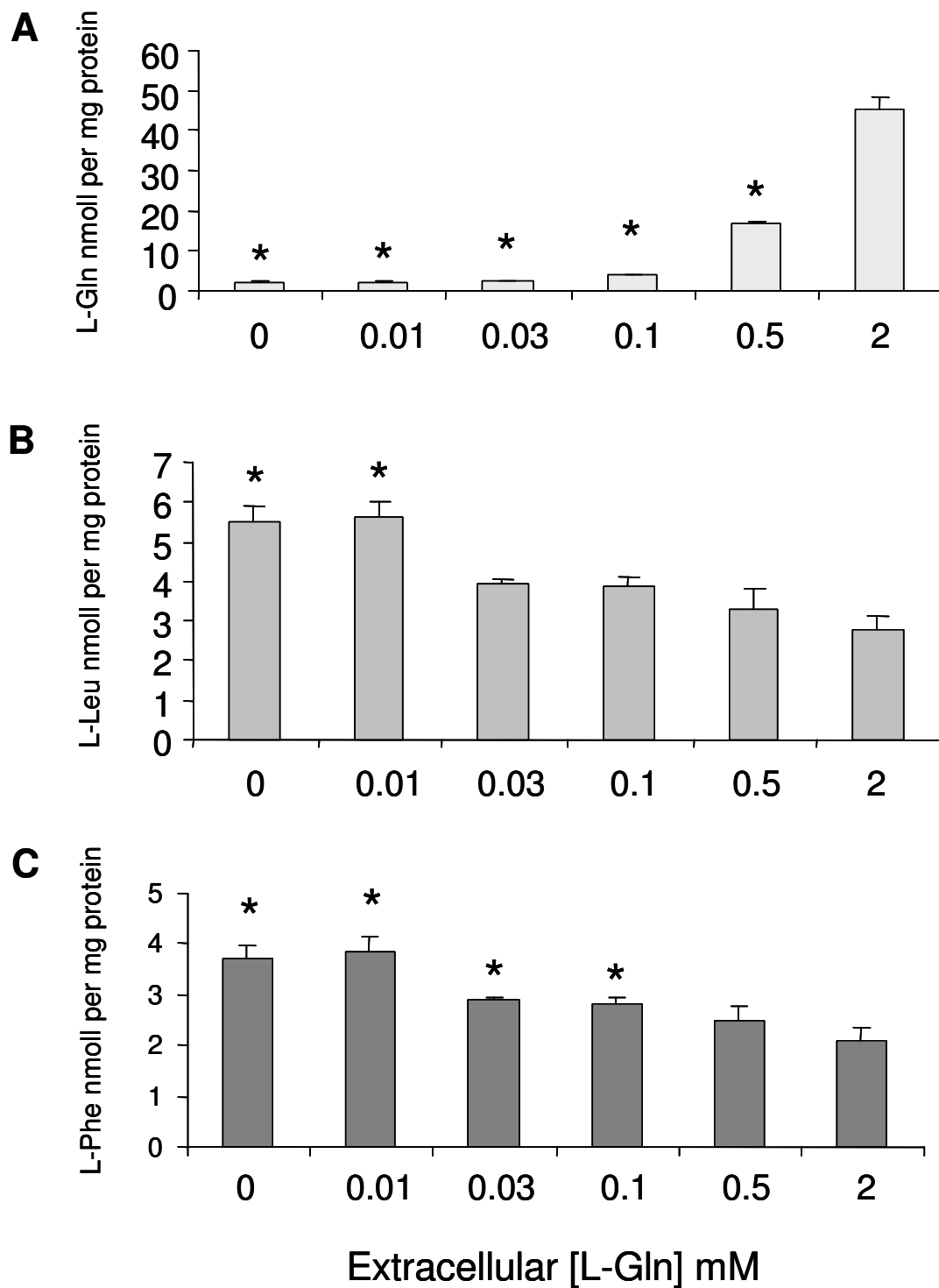
Appendix Table 1. Effect of Extracellular L-Gln Starvation, pH and SNAT2 Inhibition with MeAIB on Intracellular Free Amino Acid Profile in L6-G8C5 Myotubes after 2h incubations. (Data for L-Gln and L-Leu are presented in Appendix Figure 1).

Composition of the Medium						
Control						
pH		7.4	7.1	7.4	7.7	7.4
L-Gln (mmo/L)		0	2	2	2	2
MeAIB (mmol/L)		0	0	0	0	10
Amino acid	Conc. in fresh MEM $\mu\text{mol/L}$	Intracellular Free Amino Acid Concentration (nmol per mg protein)				
L-Ala	Nil	75.9 \pm 2.1	71.3 \pm 1.3	70.0 \pm 1.7	69.3 \pm 2.5	69.4 \pm 1.6
L-Arg	600	5.23* \pm 0.15	3.99* \pm 0.08	4.68 \pm 0.12	4.94 \pm 0.11	3.38* \pm 0.11
L-Asn	Nil	0.54* \pm 0.05	1.28* \pm 0.05	1.43 \pm 0.05	1.34 \pm 0.03	0.92* \pm 0.02
L-Asp	Nil	25.6* \pm 1.3	37.4* \pm 1.2	47.4 \pm 1.5	47.0 \pm 0.6	43.8 \pm 0.7
L-Cys	200 ^a	UD	UD	UD	UD	UD
L-Glu	Nil	28.3* \pm 1.3	37.0** \pm 0.8	42.2 \pm 2.1	48.8* \pm 3.0	38.8 \pm 2.0
L-Gly	Nil	13.1 \pm 0.5	14.4* \pm 0.5	12.1 \pm 0.2	10.4* \pm 0.2	12.9 \pm 0.3
L-His	200	3.6* \pm 0.2	1.2* \pm 0.1	2.4 \pm 0.3	2.7 \pm 0.2	0.8* \pm 0.1
L-Ile	400	5.5* \pm 0.2	2.5* \pm 0.1	3.7 \pm 0.2	3.9 \pm 0.2	1.7* \pm 0.1
L-Lys	400	UD	UD	UD	UD	UD
L-Met	100	3.7* \pm 0.3	1.2** \pm 0.2	1.8 \pm 0.3	2.3 \pm 0.3	1.1 \pm 0.2
L-Phe	200	4.39* \pm 0.12	1.92* \pm 0.08	2.82 \pm 0.09	3.14 \pm 0.07	1.29* \pm 0.04
L-Pro	Nil	1.5* \pm 0.1	3.9 \pm 0.3	3.4 \pm 0.2	3.4 \pm 0.2	2.4* \pm 0.1
L-Ser	Nil	1.81 \pm 0.06	1.53 \pm 0.06	1.60 \pm 0.05	1.58 \pm 0.06	1.29* \pm 0.05
L-Thr	400	36.1* \pm 1.1	15.3* \pm 0.5	20.2 \pm 0.4	25.9* \pm 0.4	9.4* \pm 0.2
L-Trp	50	1.40* \pm 0.05	0.69* \pm 0.05	0.98 \pm 0.05	1.01 \pm 0.04	0.52* \pm 0.02
L-Tyr	200	4.79* \pm 0.15	2.32* \pm 0.38	3.12 \pm 0.15	3.41 \pm 0.14	1.42* \pm 0.06
L-Val	400	6.03* \pm 0.19	3.06* \pm 0.14	4.05 \pm 0.19	4.32 \pm 0.19	2.59* \pm 0.08

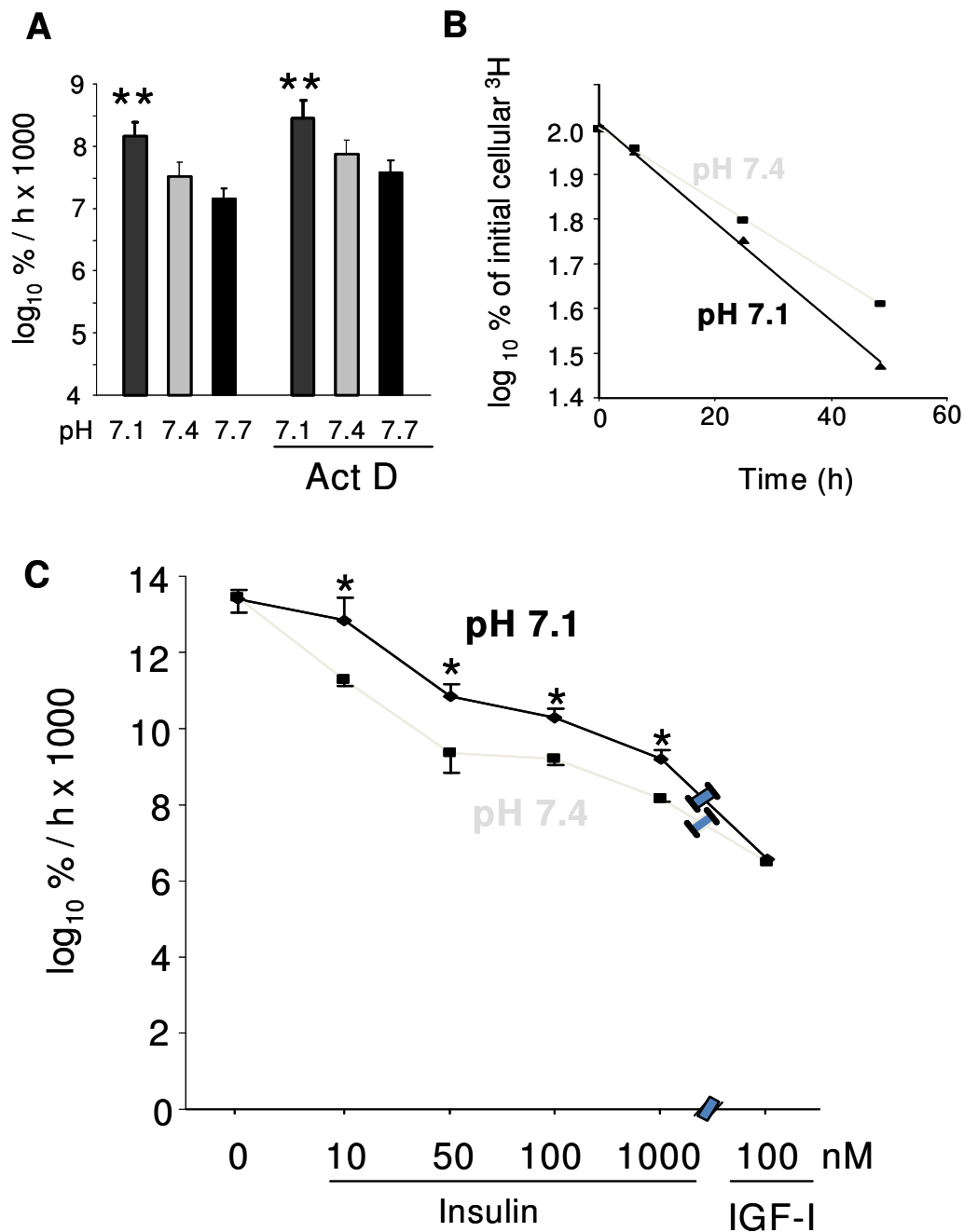
Results from 1 experiment representative of 4 independent experiments are shown (with n= 5 replicate culture wells for each treatment). UD - Undetectable ^aAdded as Cystine, *P<0.05 versus pH 7.4 Control, **P<0.05 versus pH 7.7



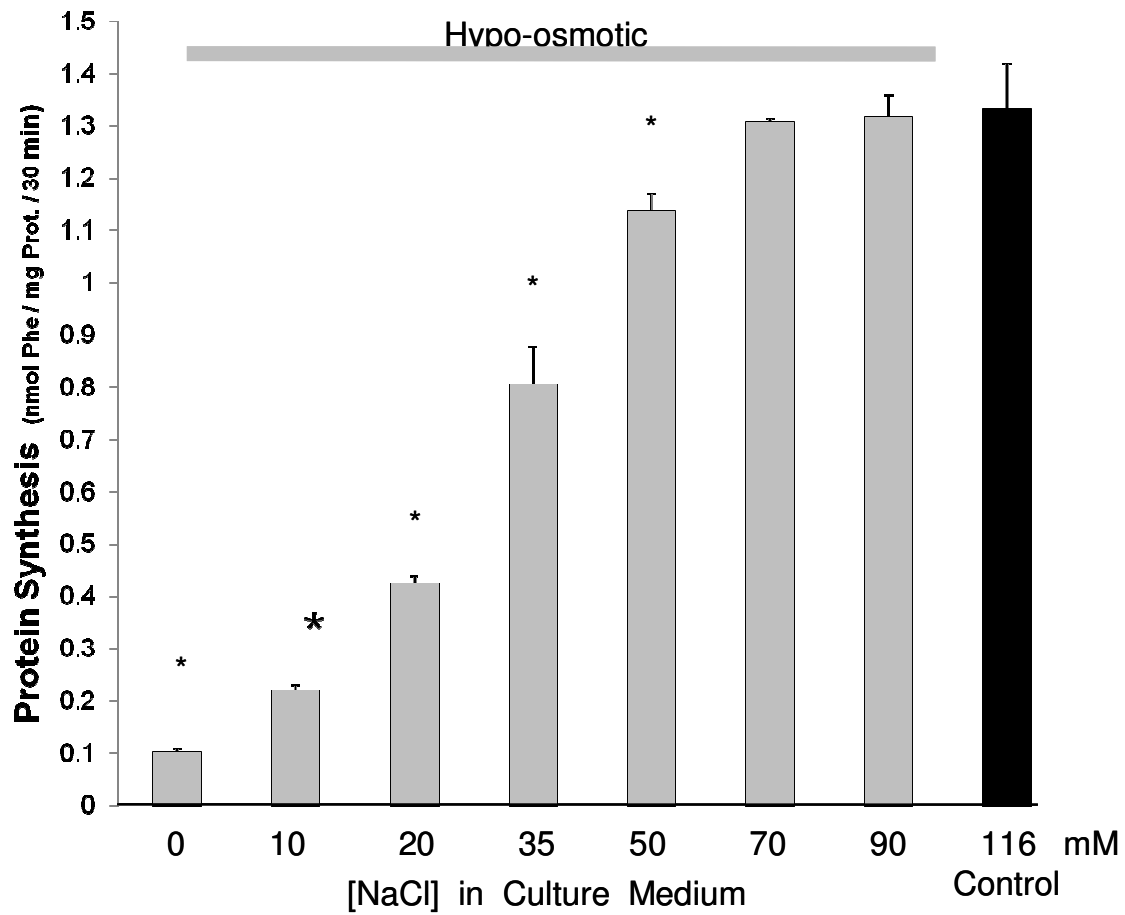
Appendix Figure 1. Effect of 2h of extracellular L-Gln starvation, pH variation or inhibition of SNAT2 transporters with 10mM MeAIB on intracellular concentrations of (A) L-Gln and (B) L-Leu in L6-G8C5 myotubes. (Data for other amino acids are presented in Table 1). All media contained 2mM L-Gln and 0.4mM L-Leu unless otherwise stated. *P<0.05 versus control medium (Cont). Results from 1 experiment representative of 4 independent experiments are shown (with n= 5 replicate culture wells for each treatment). **(C) Effect of extracellular pH on SNAT2 transporter activity after 7h of exposure to experimental media at the specified pH.** Transport was then immediately assessed from the rate of uptake of ¹⁴C-MeAIB in Hepes buffered saline at the same pH as the experimental media. Results from 1 experiment representative of 3 independent experiments are shown with n= 3 replicate culture wells for each treatment. **P<0.05 versus the corresponding medium at pH 7.4.



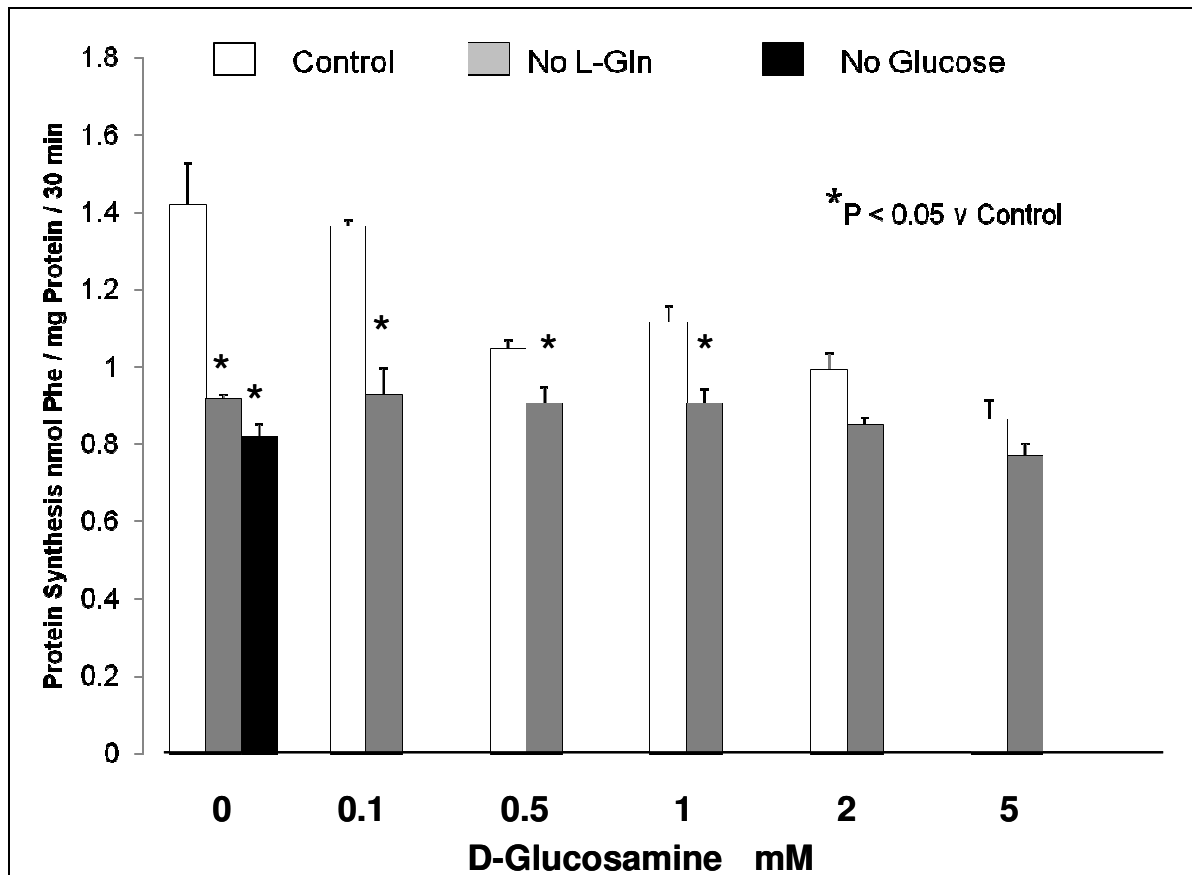
Appendix Figure 2. Effect of extracellular L-Gln concentration on intracellular concentrations of (A) L-Gln, (B) L-Leu and (C) L-Phe after 2h at pH 7.4. *P<0.05 versus medium with 2mM L-Gln. Results from 1 experiment representative of 3 independent experiments are shown with n= 3 replicate culture wells for each treatment.



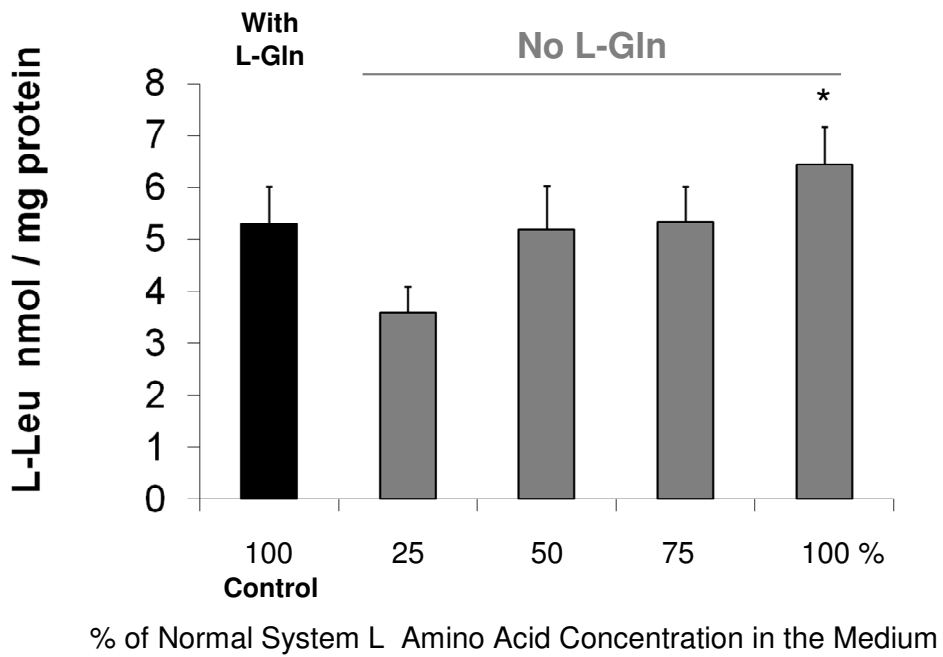
Appendix Figure 3. (A) Effect of 1 μ M Actinomycin D (Act D) on proteolysis rate in L6-G8C5 myotubes during 7-h incubations at the specified pH in MEM + 2 mM L-Phe + 2% dialyzed FBS. Pooled data from 4 independent experiments are shown (with 3 replicate culture wells for each treatment). Proteolysis was assessed from the rate of release of radioactivity into the medium from cultures pre-labeled with ^3H -L-Phe and is expressed as the logarithm of the percentage of the total initial cellular radioactivity per hour ($\log_{10} \% / \text{h} \times 1000$ - see the Materials and Methods Section). (B) Typical delabeling time course of ^3H -L-Phe pre-labeled cells incubated in serum-free MEM + 2mM L-Phe at the specified pH with 100nM insulin. (C) Effect of pH, insulin and high-dosage IGF-I on the rate of proteolysis (delabeling) expressed as $\log_{10} \% / \text{h} \times 1000$ in L6-G8C5 myotubes. Pooled data from 3 independent experiments are shown (with 3 replicate culture wells for each treatment). *P < 0.05 versus the corresponding pH 7.4 control value; **P < 0.05 versus the corresponding pH 7.7 value.



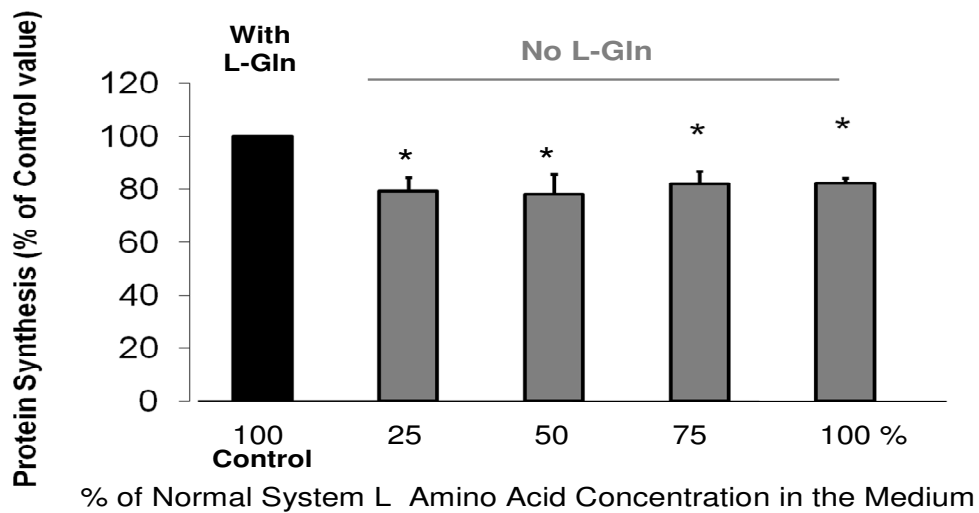
Appendix Figure 4. Effect of hypo-osmotic media on global protein synthesis rate ($^3\text{H-L-Phe}$ incorporation) in L6-G8C5 myotubes. Cultures were incubated in modified MEM (with the specified NaCl concentration) with 2% dialysed foetal bovine serum in the presence of $^3\text{H-L-Phe}$. Data from 1 experiment with 3 replicate culture wells for each treatment are shown. * $P < 0.05$ versus Control medium.



Appendix Figure 5. Effect of metabolic stressors on global protein synthesis rate ($^3\text{H-L-Phe}$ incorporation) in L6-G8C5 myotubes. Cultures were incubated in Control medium (MEM with 2mM L-Gln and 5.5mM D-glucose), or in modified MEM (as stated in the figure) with 2% dialysed foetal bovine serum in the presence of L- $^3\text{H-Phe}$. Data from 1 experiment with 3 replicate culture wells for each treatment are shown. * $P < 0.05$ versus the corresponding Control medium at the same D-glucosamine concentration.



Appendix Figure 6. The effect of L-Gln-free modified MEM containing 25%, 50%, 75% or 100% of control System L amino-acid concentration on intracellular L-Leu concentrations. L6-G8C5 myotubes were incubated with the corresponding modified media for 2h. Media contained 2% dialysed foetal bovine serum. The data are pooled from 4 independent experiments. *P < 0.05 v medium with 25% of normal System L amino-acid concentration.



Appendix Figure 7. The effect of L-Gln-free modified MEM containing 25%, 50%, 75% or 100% of control System L amino-acid concentration on Global Protein Synthesis rate as measured by incorporation of $^3\text{H-L-Phe}$. L6-G8C5 myotubes were pre-incubated with the specified media for 90 min followed by a 30 min incubation with the same media containing $^3\text{H-L-Phe}$. The results are pooled from 6 independent experiments and are expressed as a % of the control value obtained in complete MEM including 2mM L-Gln. * $P < 0.05$ v 2mM L-Gln control. All media contained 2% dialysed foetal bovine serum.

References

- (1) Kovacic V, Roguljic L, Kovacic V. Metabolic acidosis of chronically hemodialyzed patients. *Am.J.Nephrol.* 2003 May-Jun;23(3):158-164.
- (2) Kraut JA, Kurtz I. Metabolic acidosis of CKD: diagnosis, clinical characteristics, and treatment. *Am.J.Kidney Dis.* 2005 Jun;45(6):978-993.
- (3) Koeppen, B.M. and Stanton, B.A. Renal System. In: Berne, R.M. and Levy, M.N., editor. *Principles of Physiology.* 3rd Edition ed.: Mosby; 2000. p. 408-478.
- (4) Haraldsson B, Sorensson J. Why do we not all have proteinuria? An update of our current understanding of the glomerular barrier. *News Physiol.Sci.* 2004 Feb;19:7-10.
- (5) D'Amico G, Bazzi C. Pathophysiology of proteinuria. *Kidney Int.* 2003 Mar;63(3):809-825.
- (6) Aaltonen P, Holthofer H. The nephrin-based slit diaphragm: new insight into the signalling platform identifies targets for therapy. *Nephrol.Dial.Transplant.* 2007 Dec;22(12):3408-3410.
- (7) Suliman ME, Anderstam B, Bergstrom J. Evidence of taurine depletion and accumulation of cysteinesulfinic acid in chronic dialysis patients. *Kidney Int.* 1996 Nov;50(5):1713-1717.
- (8) Sebastian A, Frassetto LA, Sellmeyer DE, Merriam RL, Morris RC, Jr. Estimation of the net acid load of the diet of ancestral preagricultural Homo sapiens and their hominid ancestors. *Am.J.Clin.Nutr.* 2002 Dec;76(6):1308-1316.
- (9) Karim Z, Szutkowska M, Vernimmen C, Bichara M. Renal handling of NH₃/NH₄⁺: recent concepts. *Nephron Physiol.* 2005;101(4):p77-81.
- (10) Stumvoll M, Perriello G, Meyer C, Gerich J. Role of glutamine in human carbohydrate metabolism in kidney and other tissues. *Kidney Int.* 1999 Mar;55(3):778-792.
- (11) Gill N, Nally JV, Jr, Fatica RA. Renal failure secondary to acute tubular necrosis: epidemiology, diagnosis, and management. *Chest* 2005 Oct;128(4):2847-2863.
- (12) Goldberg R, Dennen P. Long-term outcomes of acute kidney injury. *Adv.Chronic Kidney Dis.* 2008 Jul;15(3):297-307.
- (13) St Peter WL. Introduction: chronic kidney disease: a burgeoning health epidemic. *J.Manag.Care.Pharm.* 2007 Dec;13(9 Suppl D):S2-5.
- (14) Gokal R. Renal Failure. *ELS* 2001 April 19, 2001:January 28, 2008.

- (15) Brunskill NJ. Albumin signals the coming of age of proteinuric nephropathy. *J.Am.Soc.Nephrol.* 2004 Feb;15(2):504-505.
- (16) Eyre J, Ioannou K, Grubb BD, Saleem MA, Mathieson PW, Brunskill NJ, et al. Statin-sensitive endocytosis of albumin by glomerular podocytes. *Am.J.Physiol.Renal Physiol.* 2007 Feb;292(2):F674-81.
- (17) Ritz E. Advances in nephrology: successes and lessons learnt from diabetes mellitus. *Nephrol.Dial.Transplant.* 2001;16 Suppl 7:46-50.
- (18) Pupim LB, Heimbürger O, Qureshi AR, Ikizler TA, Stenvinkel P. Accelerated lean body mass loss in incident chronic dialysis patients with diabetes mellitus. *Kidney Int.* 2005 Nov;68(5):2368-2374.
- (19) Mehrotra R, Kopple JD, Wolfson M. Metabolic acidosis in maintenance dialysis patients: clinical considerations. *Kidney Int.Suppl.* 2003 Dec;(88)(88):S13-25.
- (20) Throssell D, Brown J, Harris KP, Walls J. Metabolic acidosis does not contribute to chronic renal injury in the rat. *Clin.Sci.(Lond)* 1995 Dec;89(6):643-650.
- (21) Schiffrin EL, Lipman ML, Mann JF. Chronic kidney disease: effects on the cardiovascular system. *Circulation* 2007 Jul 3;116(1):85-97.
- (22) Brooks SV,. Current topics for teaching skeletal muscle physiology. *Adv. Physiol. Educ.* 2003 Dec; 27(4): 171-182.
- (23) Kotler DP. Cachexia. *Ann.Intern.Med.* 2000 Oct 17;133(8):622-634.
- (24) Mitch WE. Robert H Herman Memorial Award in Clinical Nutrition Lecture, 1997. Mechanisms causing loss of lean body mass in kidney disease. *Am.J.Clin.Nutr.* 1998 Mar;67(3):359-366.
- (25) Morley JE, Thomas DR, Wilson MM. Cachexia: pathophysiology and clinical relevance. *Am.J.Clin.Nutr.* 2006 Apr;83(4):735-743.
- (26) Mehrotra R, Kopple JD. Protein and energy nutrition among adult patients treated with chronic peritoneal dialysis. *Adv.Ren.Replace.Ther.* 2003 Jul;10(3):194-212.
- (27) Mitch WE. Cachexia in chronic kidney disease: a link to defective central nervous system control of appetite. *J.Clin.Invest.* 2005 Jun;115(6):1476-1478.
- (28) Reaich D, Graham KA, Channon SM, Hetherington C, Scrimgeour CM, Wilkinson R, et al. Insulin-mediated changes in PD and glucose uptake after correction of acidosis in humans with CRF. *Am.J.Physiol.* 1995 Jan;268(1 Pt 1):E121-6.
- (29) Isozaki U, Mitch WE, England BK, Price SR. Protein degradation and increased mRNAs encoding proteins of the ubiquitin-proteasome proteolytic

pathway in BC3H1 myocytes require an interaction between glucocorticoids and acidification. *Proc.Natl.Acad.Sci.U.S.A.* 1996 Mar 5;93(5):1967-1971.

(30) Franch HA, Raissi S, Wang X, Zheng B, Bailey JL, Price SR. Acidosis impairs insulin receptor substrate-1-associated phosphoinositide 3-kinase signaling in muscle cells: consequences on proteolysis. *Am.J.Physiol.Renal Physiol.* 2004 Oct;287(4):F700-6.

(31) Bevington A, Brown J, Pratt A, Messer J, Walls J. Impaired glycolysis and protein catabolism induced by acid in L6 rat muscle cells. *Eur.J.Clin.Invest.* 1998 Nov;28(11):908-917.

(32) Rajan VR, Mitch WE. Muscle wasting in chronic kidney disease: the role of the ubiquitin proteasome system and its clinical impact. *Pediatr.Nephrol.* 2008 Apr;23(4):527-535.

(33) Ballmer PE, McNurlan MA, Hulter HN, Anderson SE, Garlick PJ, Krapf R. Chronic metabolic acidosis decreases albumin synthesis and induces negative nitrogen balance in humans. *J.Clin.Invest.* 1995 Jan;95(1):39-45.

(34) May RC, Kelly RA, Mitch WE. Mechanisms for defects in muscle protein metabolism in rats with chronic uremia. Influence of metabolic acidosis. *J.Clin.Invest.* 1987 Apr;79(4):1099-1103.

(35) Bevington A, Poulter C, Brown J, Walls J. Inhibition of protein synthesis by acid in L6 skeletal muscle cells: analogies with the acute starvation response. *Miner.Electrolyte Metab.* 1998;24(4):261-266.

(36) England BK, Chastain JL, Mitch WE. Abnormalities in protein synthesis and degradation induced by extracellular pH in BC3H1 myocytes. *Am.J.Physiol.* 1991 Feb;260(2 Pt 1):C277-82.

(37) Kleger GR, Turgay M, Imoberdorf R, McNurlan MA, Garlick PJ, Ballmer PE. Acute metabolic acidosis decreases muscle protein synthesis but not albumin synthesis in humans. *Am.J.Kidney Dis.* 2001 Dec;38(6):1199-1207.

(38) Bailey JL, England BK, Long RC, Jr, Weissman J, Mitch WE. Experimental acidemia and muscle cell pH in chronic acidosis and renal failure. *Am.J.Physiol.* 1995 Sep;269(3 Pt 1):C706-12.

(39) Nishida A, Kubo K, Nihei H. Impaired muscle energy metabolism in uremia as monitored by ³¹P-NMR. *Nippon Jinzo Gakkai Shi* 1991 Jan;33(1):65-73.

(40) May RC, Kelly RA, Mitch WE. Metabolic acidosis stimulates protein degradation in rat muscle by a glucocorticoid-dependent mechanism. *J.Clin.Invest.* 1986 Feb;77(2):614-621.

(41) Pickering WP, Baker FE, Brown J, Butler HL, Govindji S, Parsons JM, et al. Glucocorticoid antagonist RU38486 fails to block acid-induced muscle wasting in vivo or in vitro. *Nephrology Dialysis Transplantation* 2003 Aug;18(8):1475-1484.

- (42) Ashmole I, Goodwin PA, Stanfield PR. TASK-5, a novel member of the tandem pore K⁺ channel family. *Pflugers Arch.* 2001 Sep;442(6):828-833.
- (43) Kim Y, Bang H, Kim D. TASK-3, a new member of the tandem pore K(+) channel family. *J.Biol.Chem.* 2000 Mar 31;275(13):9340-9347.
- (44) Rajan S, Wischmeyer E, Xin Liu G, Preisig-Muller R, Daut J, Karschin A, et al. TASK-3, a novel tandem pore domain acid-sensitive K⁺ channel. An extracellular histiding as pH sensor. *J.Biol.Chem.* 2000 Jun 2;275(22):16650-16657.
- (45) Yuill K, Ashmole I, Stanfield PR. The selectivity filter of the tandem pore potassium channel TASK-1 and its pH-sensitivity and ionic selectivity. *Pflugers Arch.* 2004 Apr;448(1):63-69.
- (46) Ludwig MG, Vanek M, Guerini D, Gasser JA, Jones CE, Junker U, et al. Proton-sensing G-protein-coupled receptors. *Nature* 2003 Sep 4;425(6953):93-98.
- (47) Alper SL. Molecular physiology of SLC4 anion exchangers. *Exp.Physiol.* 2006 Jan;91(1):153-161.
- (48) Stewart AK, Kurschat CE, Burns D, Banger N, Vaughan-Jones RD, Alper SL. Transmembrane domain histidines contribute to regulation of AE2-mediated anion exchange by pH. *Am.J.Physiol.Cell.Physiol.* 2007 Feb;292(2):C909-18.
- (49) Borza DB, Shipulina NV, Morgan WT. Effects of histidine-proline-rich glycoprotein on plasminogen activation in solution and on surfaces. *Blood Coagul.Fibrinolysis* 2004 Oct;15(8):663-672.
- (50) Borza DB, Morgan WT. Histidine-proline-rich glycoprotein as a plasma pH sensor. Modulation of its interaction with glycosaminoglycans by ph and metals. *J.Biol.Chem.* 1998 Mar 6;273(10):5493-5499.
- (51) Klein JD, Rouillard P, Roberts BR, Sands JM. Acidosis mediates the upregulation of UT-A protein in livers from uremic rats. *J.Am.Soc.Nephrol.* 2002 Mar;13(3):581-587.
- (52) Yamaji Y, Amemiya M, Cano A, Preisig PA, Miller RT, Moe OW, et al. Overexpression of csk inhibits acid-induced activation of NHE-3. *Proc.Natl.Acad.Sci.U.S.A.* 1995 Jul 3;92(14):6274-6278.
- (53) Gunthorpe MJ, Smith GD, Davis JB, Randall AD. Characterisation of a human acid-sensing ion channel (hASIC1a) endogenously expressed in HEK293 cells. *Pflugers Arch.* 2001 Aug;442(5):668-674.
- (54) Wood JN. II. Genetic approaches to pain therapy. *Am.J.Physiol.Gastrointest.Liver Physiol.* 2000 Apr;278(4):G507-12.

- (55) Yiangou Y, Facer P, Smith JA, Sangameswaran L, Eglen R, Birch R, et al. Increased acid-sensing ion channel ASIC-3 in inflamed human intestine. *Eur.J.Gastroenterol.Hepatol.* 2001 Aug;13(8):891-896.
- (56) Bevington A, Brown J, Butler H, Govindji S, M-Khalid K, Sheridan K, et al. Impaired system A amino acid transport mimics the catabolic effects of acid in L6 cells. *Eur.J.Clin.Invest.* 2002 Aug;32(8):590-602.
- (57) Hyde R, Taylor PM, Hundal HS. Amino acid transporters: roles in amino acid sensing and signalling in animal cells. *Biochem.J.* 2003 Jul 1;373(Pt 1):1-18.
- (58) Lingrel JB, Kuntzweiler T. Na⁺,K⁽⁺⁾-ATPase. *J.Biol.Chem.* 1994 Aug 5;269(31):19659-19662.
- (59) Verrey F. System L: heteromeric exchangers of large, neutral amino acids involved in directional transport. *Pflugers Arch.* 2003 Feb;445(5):529-533.
- (60) Meier C, Ristic Z, Klauser S, Verrey F. Activation of system L heterodimeric amino acid exchangers by intracellular substrates. *EMBO J.* 2002 Feb 15;21(4):580-589.
- (61) Ramadan T, Camargo SM, Herzog B, Bordin M, Pos KM, Verrey F. Recycling of aromatic amino acids via TAT1 allows efflux of neutral amino acids via LAT2-4F2hc exchanger. *Pflugers Arch.* 2007 Jun;454(3):507-516.
- (62) Lopez A, Torres N, Ortiz V, Aleman G, Hernandez-Pando R, Tovar AR. Characterization and regulation of the gene expression of amino acid transport system A (SNAT2) in rat mammary gland. *Am.J.Physiol.Endocrinol.Metab.* 2006 Nov;291(5):E1059-66.
- (63) Sundberg BE, Waag E, Jacobsson JA, Stephansson O, Rumaks J, Svirskis S, et al. The evolutionary history and tissue mapping of amino acid transporters belonging to solute carrier families SLC32, SLC36, and SLC38. *J.Mol.Neurosci.* 2008 Jun;35(2):179-193.
- (64) Mackenzie B, Erickson JD. Sodium-coupled neutral amino acid (System N/A) transporters of the SLC38 gene family. *Pflugers Arch.* 2004 Feb;447(5):784-795.
- (65) Bracy DS, Handlogten ME, Barber EF, Han HP, Kilberg MS. Cis-inhibition, trans-inhibition, and repression of hepatic amino acid transport mediated by System A. Substrate specificity and other properties. *J.Biol.Chem.* 1986 Feb 5;261(4):1514-1520.
- (66) Yao D, Mackenzie B, Ming H, Varoqui H, Zhu H, Hediger MA, et al. A novel system A isoform mediating Na⁺/neutral amino acid cotransport. *J.Biol.Chem.* 2000 Jul 28;275(30):22790-22797.
- (67) Dolinska M, Zablocka B, Sonnewald U, Albrecht J. Glutamine uptake and expression of mRNA's of glutamine transporting proteins in mouse cerebellar

and cerebral cortical astrocytes and neurons. *Neurochem.Int.* 2004 Jan;44(2):75-81.

(68) Chaudhry FA, Schmitz D, Reimer RJ, Larsson P, Gray AT, Nicoll R, et al. Glutamine uptake by neurons: interaction of protons with system A transporters. *J.Neurosci.* 2002 Jan 1;22(1):62-72.

(69) Wagner CA. Metabolic acidosis: new insights from mouse models. *Curr. Opin. Nephrol. Hypertens.* 2007 Sep; 16(5): 471-476

(70) Baird FE, Beattie KJ, Hyde AR, Ganapathy V, Rennie MJ, Taylor PM. Bidirectional substrate fluxes through the system N (SNAT5) glutamine transporter may determine net glutamine flux in rat liver. *J.Physiol.* 2004 Sep 1;559(Pt 2):367-381.

(71) Boll M, Daniel H, Gasnier B. The SLC36 family: proton-coupled transporters for the absorption of selected amino acids from extracellular and intracellular proteolysis. *Pflugers Arch.* 2004 Feb;447(5):776-779.

(72) Chen Z, Fei YJ, Anderson CM, Wake KA, Miyauchi S, Huang W, et al. Structure, function and immunolocalization of a proton-coupled amino acid transporter (hPAT1) in the human intestinal cell line Caco-2. *J.Physiol.* 2003 Jan 15;546(Pt 2):349-361.

(73) Baird FE, Pinilla-Tenas JJ, Ogilvie WL, Ganapathy V, Hundal HS, Taylor PM. Evidence for allosteric regulation of pH-sensitive System A (SNAT2) and System N (SNAT5) amino acid transporter activity involving a conserved histidine residue. *Biochem.J.* 2006 Jul 15;397(2):369-375.

(74) Hyde R, Christie GR, Litherland GJ, Hajduch E, Taylor PM, Hundal HS. Subcellular localization and adaptive up-regulation of the System A (SAT2) amino acid transporter in skeletal-muscle cells and adipocytes. *Biochem.J.* 2001 May 1;355(Pt 3):563-568.

(75) Ling R, Bridges CC, Sugawara M, Fujita T, Leibach FH, Prasad PD, et al. Involvement of transporter recruitment as well as gene expression in the substrate-induced adaptive regulation of amino acid transport system A. *Biochim.Biophys.Acta* 2001 May 2;1512(1):15-21.

(76) Pali SS, Thiaville MM, Pan YX, Zhong C, Kilberg MS. Characterization of the amino acid response element within the human sodium-coupled neutral amino acid transporter 2 (SNAT2) System A transporter gene. *Biochem.J.* 2006 May 1;395(3):517-527.

(77) Novak D, Quiggle F, Haafiz A. Impact of forskolin and amino acid depletion upon System A activity and SNAT expression in BeWo cells. *Biochimie* 2006 Jan;88(1):39-44.

(78) Hyde R, Peyrollier K, Hundal HS. Insulin promotes the cell surface recruitment of the SAT2/ATA2 system A amino acid transporter from an endosomal compartment in skeletal muscle cells. *J.Biol.Chem.* 2002 Apr 19;277(16):13628-13634.

- (79) Gaccioli F, Huang CC, Wang C, Bevilacqua E, Franchi-Gazzola R, Gazzola GC, et al. Amino acid starvation induces the SNAT2 neutral amino acid transporter by a mechanism that involves eukaryotic initiation factor 2 α phosphorylation and cap-independent translation. *J.Biol.Chem.* 2006 Jun 30;281(26):17929-17940.
- (80) Hyde R, Cwiklinski EL, MacAulay K, Taylor PM, Hundal HS. Distinct sensor pathways in the hierarchical control of SNAT2, a putative amino acid transceptor, by amino acid availability. *J.Biol.Chem.* 2007 Jul 6;282(27):19788-19798.
- (81) Hatanaka T, Hatanaka Y, Setou M. Regulation of amino acid transporter ATA2 by ubiquitin ligase Nedd4-2. *J.Biol.Chem.* 2006 Nov 24;281(47):35922-35930.
- (82) McCubrey JA, Steelman LS, Chappell WH, Abrams SL, Wong EW, Chang F, et al. Roles of the Raf/MEK/ERK pathway in cell growth, malignant transformation and drug resistance. *Biochim.Biophys.Acta* 2007 Aug;1773(8):1263-1284.
- (83) McGivan JD, Pastor-Anglada M. Regulatory and molecular aspects of mammalian amino acid transport. *Biochem.J.* 1994 Apr 15;299 (Pt 2)(Pt 2):321-334.
- (84) Franchi-Gazzola R, Dall'Asta V, Sala R, Visigalli R, Bevilacqua E, Gaccioli F, et al. The role of the neutral amino acid transporter SNAT2 in cell volume regulation. *Acta Physiol.(Oxf)* 2006 May-Jun;187(1-2):273-283.
- (85) Bevilacqua E, Bussolati O, Dall'Asta V, Gaccioli F, Sala R, Gazzola GC, et al. SNAT2 silencing prevents the osmotic induction of transport system A and hinders cell recovery from hypertonic stress. *FEBS Lett.* 2005 Jun 20;579(16):3376-3380.
- (86) Munoz P, Guma A, Camps M, Furriols M, Testar X, Palacin M, et al. Vanadate stimulates system A amino acid transport activity in skeletal muscle. Evidence for the involvement of intracellular pH as a mediator of vanadate action. *J.Biol.Chem.* 1992 May 25;267(15):10381-10388.
- (87) Proud CG. mTOR-mediated regulation of translation factors by amino acids. *Biochem.Biophys.Res.Commun.* 2004 Jan 9;313(2):429-436.
- (88) Varoqui H, Zhu H, Yao D, Ming H, Erickson JD. Cloning and functional identification of a neuronal glutamine transporter. *J.Biol.Chem.* 2000 Feb 11;275(6):4049-4054.
- (89) Schliess F, Reinehr R, Haussinger D. Osmosensing and signaling in the regulation of mammalian cell function. *FEBS J.* 2007 Nov;274(22):5799-5803.
- (90) Mathews MB, Sonenburg N, Hershey JWB. Origins and principles of translational control. In: Mathews MB, Sonenburg N, Hershey JWB, editors. *Translational control of gene expression*: NY, Cold Spring Harbor Laboratory Press; 2000. p. 1-26.

- (91) Maniatis T, Reed R. An extensive network of coupling among gene expression machines. *Nature* 2002 Apr 4;416(6880):499-506.
- (92) Erkmann JA, Kutay U. Nuclear export of mRNA: from the site of transcription to the cytoplasm. *Exp.Cell Res.* 2004 May 15;296(1):12-20.
- (93) Algire MA, Lorsch JR. Where to begin? The mechanism of translation initiation codon selection in eukaryotes. *Curr.Opin.Chem.Biol.* 2006 Oct;10(5):480-486.
- (94) Merrick WC. Mechanism and regulation of eukaryotic protein synthesis. *Microbiol.Rev.* 1992 Jun;56(2):291-315.
- (95) Janzen DM, Geballe AP. The effect of eukaryotic release factor depletion on translation termination in human cell lines. *Nucleic Acids Res.* 2004 Aug 23;32(15):4491-4502.
- (96) Pisareva VP, Pisarev AV, Hellen CU, Rodnina MV, Pestova TV. Kinetic analysis of interaction of eukaryotic release factor 3 with guanine nucleotides. *J.Biol.Chem.* 2006 Dec 29;281(52):40224-40235.
- (97) Hinnebusch AG. eIF3: a versatile scaffold for translation initiation complexes. *Trends Biochem.Sci.* 2006 Oct;31(10):553-562.
- (98) Hershey, J.W.B. and Merrick, W.C. The pathway and mechanisms of initiation of protein synthesis. In: Mathews MB, Sonenburg N, Hershey JWB, editors. *Translational control of gene expression*: NY, Cold Spring Harbor Laboratory Press; 2000. p. 33-75.
- (99) Oberer M, Marintchev A, Wagner G. Structural basis for the enhancement of eIF4A helicase activity by eIF4G. *Genes Dev.* 2005 Sep 15;19(18):2212-2223.
- (100) Rogers GW,Jr, Richter NJ, Lima WF, Merrick WC. Modulation of the helicase activity of eIF4A by eIF4B, eIF4H, and eIF4F. *J.Biol.Chem.* 2001 Aug 17;276(33):30914-30922.
- (101) Proud CG. Regulation of mammalian translation factors by nutrients. *Eur.J.Biochem.* 2002 Nov;269(22):5338-5349.
- (102) Pittman YR, Valente L, Jeppesen MG, Andersen GR, Patel S, Kinzy TG. Mg²⁺ and a key lysine modulate exchange activity of eukaryotic translation elongation factor 1B alpha. *J.Biol.Chem.* 2006 Jul 14;281(28):19457-19468.
- (103) Keeling PJ, Inagaki Y. A class of eukaryotic GTPase with a punctate distribution suggesting multiple functional replacements of translation elongation factor 1alpha. *Proc.Natl.Acad.Sci.U.S.A.* 2004 Oct 26;101(43):15380-15385.
- (104) Cohen P. The twentieth century struggle to decipher insulin signalling. *Nat.Rev.Mol.Cell Biol.* 2006 Nov;7(11):867-873.

- (105) Sykiotis GP, Papavassiliou AG. Serine phosphorylation of insulin receptor substrate-1: a novel target for the reversal of insulin resistance. *Mol.Endocrinol.* 2001 Nov;15(11):1864-1869.
- (106) Sesti G, Federici M, Hribal ML, Lauro D, Sbraccia P, Lauro R. Defects of the insulin receptor substrate (IRS) system in human metabolic disorders. *FASEB J.* 2001 Oct;15(12):2099-2111.
- (107) Kido Y, Nakae J, Accili D. Clinical review 125: The insulin receptor and its cellular targets. *J.Clin.Endocrinol.Metab.* 2001 Mar;86(3):972-979.
- (108) Dance M, Montagner A, Salles JP, Yart A, Raynal P. The molecular functions of Shp2 in the Ras/Mitogen-activated protein kinase (ERK1/2) pathway. *Cell.Signal.* 2008 Mar;20(3):453-459.
- (109) Kardinal C, Konkol B, Lin H, Eulitz M, Schmidt EK, Estrov Z, et al. Chronic myelogenous leukemia blast cell proliferation is inhibited by peptides that disrupt Grb2-SoS complexes. *Blood* 2001 Sep 15;98(6):1773-1781.
- (110) Shepherd PR. Mechanisms regulating phosphoinositide 3-kinase signalling in insulin-sensitive tissues. *Acta Physiol.Scand.* 2005 Jan;183(1):3-12.
- (111) Shepherd PR, Withers DJ, Siddle K. Phosphoinositide 3-kinase: the key switch mechanism in insulin signalling. *Biochem.J.* 1998 Aug 1;333 (Pt 3)(Pt 3):471-490.
- (112) Dann SG, Thomas G. The amino acid sensitive TOR pathway from yeast to mammals. *FEBS Lett.* 2006 May 22;580(12):2821-2829.
- (113) Nobukuni T, Joaquin M, Rocco M, Dann SG, Kim SY, Gulati P, et al. Amino acids mediate mTOR/raptor signaling through activation of class 3 phosphatidylinositol 3OH-kinase. *Proc.Natl.Acad.Sci.U.S.A.* 2005 Oct 4;102(40):14238-14243.
- (114) Hay N, Sonenberg N. Upstream and downstream of mTOR. *Genes Dev.* 2004 Aug 15;18(16):1926-1945.
- (115) Falasca M, Maffucci T. Role of class II phosphoinositide 3-kinase in cell signalling. *Biochem.Soc.Trans.* 2007 Apr;35(Pt 2):211-214.
- (116) Coffey PJ, Jin J, Woodgett JR. Protein kinase B (c-Akt): a multifunctional mediator of phosphatidylinositol 3-kinase activation. *Biochem.J.* 1998 Oct 1;335 (Pt 1)(Pt 1):1-13.
- (117) Fayard E, Tintignac LA, Baudry A, Hemmings BA. Protein kinase B/Akt at a glance. *J.Cell.Sci.* 2005 Dec 15;118(Pt 24):5675-5678.
- (118) Koseoglu S, Lu Z, Kumar C, Kirschmeier P, Zou J. AKT1, AKT2 and AKT3-dependent cell survival is cell line-specific and knockdown of all three isoforms selectively induces apoptosis in 20 human tumor cell lines [abstract only]. *Cancer.Biol.Ther.* 2007 May;6(5):755-762.

- (119) Somanath PR, Razorenova OV, Chen J, Byzova TV. Akt1 in endothelial cell and angiogenesis. *Cell.Cycle* 2006 Mar;5(5):512-518.
- (120) Garofalo RS, Orena SJ, Rafidi K, Torchia AJ, Stock JL, Hildebrandt AL, et al. Severe diabetes, age-dependent loss of adipose tissue, and mild growth deficiency in mice lacking Akt2/PKB beta. *J.Clin.Invest.* 2003 Jul;112(2):197-208.
- (121) Scheid MP, Marignani PA, Woodgett JR. Multiple phosphoinositide 3-kinase-dependent steps in activation of protein kinase B. *Mol.Cell.Biol.* 2002 Sep;22(17):6247-6260.
- (122) Sarbassov DD, Guertin DA, Ali SM, Sabatini DM. Phosphorylation and regulation of Akt/PKB by the rictor-mTOR complex. *Science* 2005 Feb 18;307(5712):1098-1101.
- (123) Ruggero D, Sonenberg N. The Akt of translational control. *Oncogene* 2005 Nov 14;24(50):7426-7434.
- (124) Lizcano JM, Alessi DR. The insulin signalling pathway. *Curr.Biol.* 2002 Apr 2;12(7):R236-8.
- (125) Kim DH, Sarbassov DD, Ali SM, Latek RR, Guntur KV, Erdjument-Bromage H, et al. GbetaL, a positive regulator of the rapamycin-sensitive pathway required for the nutrient-sensitive interaction between raptor and mTOR. *Mol.Cell* 2003 Apr;11(4):895-904.
- (126) Sarbassov DD, Ali SM, Sabatini DM. Growing roles for the mTOR pathway. *Curr.Opin.Cell Biol.* 2005 Dec;17(6):596-603.
- (127) Corradetti MN, Guan KL. Upstream of the mammalian target of rapamycin: do all roads pass through mTOR? *Oncogene* 2006 Oct 16;25(48):6347-6360.
- (128) Pende M. mTOR, Akt, S6 kinases and the control of skeletal muscle growth. *Bull.Cancer* 2006 May 1;93(5):E39-43.
- (129) Hara K, Maruki Y, Long X, Yoshino K, Oshiro N, Hidayat S, et al. Raptor, a binding partner of target of rapamycin (TOR), mediates TOR action. *Cell* 2002 Jul 26;110(2):177-189.
- (130) Martin J, Masri J, Bernath A, Nishimura RN, Gera J. Hsp70 associates with Rictor and is required for mTORC2 formation and activity. *Biochem.Biophys.Res.Commun.* 2008 Aug 8;372(4):578-583.
- (131) Huang J, Dibble CC, Matsuzaki M, Manning BD. The TSC1-TSC2 complex is required for proper activation of mTOR complex 2 [abstract only]. *Mol.Cell.Biol.* 2008 Jun;28(12):4104-4115.
- (132) Kim DH, Sarbassov DD, Ali SM, King JE, Latek RR, Erdjument-Bromage H, et al. mTOR interacts with raptor to form a nutrient-sensitive

complex that signals to the cell growth machinery. *Cell* 2002 Jul 26;110(2):163-175.

(133) Oshiro N, Yoshino K, Hidayat S, Tokunaga C, Hara K, Eguchi S, et al. Dissociation of raptor from mTOR is a mechanism of rapamycin-induced inhibition of mTOR function. *Genes Cells* 2004 Apr;9(4):359-366.

(134) Manning BD, Cantley LC. Rheb fills a GAP between TSC and TOR. *Trends Biochem.Sci.* 2003 Nov;28(11):573-576.

(135) Marygold SJ, Leever SJ. Growth signaling: TSC takes its place. *Curr.Biol.* 2002 Nov 19;12(22):R785-7.

(136) Backer JM, The regulation and function of Class III PI3Ks: Novel roles for Vps34. *Biochem. J.* 2008 Feb 15; 410(1): 1-17.

(137) Sancak Y, Peterson TR, Shaul YD, Lindquist RA, Thoreen CC, Bar-Peled L, et al. The Rag GTPases bind raptor and mediate amino acid signaling to mTORC1. *Science* 2008 Jun 13;320(5882):1496-1501.

(138) Findlay GM, Yan L, Procter J, Mieulet V, Lamb RF. A MAP4 kinase related to Ste20 is a nutrient-sensitive regulator of mTOR signalling. *Biochem.J.* 2007 Apr 1;403(1):13-20.

(139) Duran R, Boulahbel H, Gottlieb E. Prolylhydroxylases as regulators of cell metabolism. Proceedings of the Biochemical Society Focused Meeting on "mTOR Signalling, Nutrients and Disease", Oxford 15-16 September, 2008. [abstract only]. *Biochemical Society Transactions* 2009 (In Press);37(1).

(140) Wang X, Fonseca BD, Tang H, Liu R, Elia A, Clemens MJ, et al. Re-evaluating the roles of proposed modulators of mammalian target of rapamycin complex 1 (mTORC1) signaling. *J.Biol.Chem.* 2008 Aug 1.

(141) Richter JD, Sonenberg N. Regulation of cap-dependent translation by eIF4E inhibitory proteins. *Nature* 2005 Feb 3;433(7025):477-480.

(142) Sonenberg N. eIF4E, the mRNA cap-binding protein: from basic discovery to translational research. *Biochem.Cell Biol.* 2008 Apr;86(2):178-183.

(143) Wang X, Proud CG. The mTOR pathway in the control of protein synthesis. *Physiology (Bethesda)* 2006 Oct;21:362-369.

(144) Jastrzebski K, Hannan KM, Tchoubrieva EB, Hannan RD, Pearson RB. Coordinate regulation of ribosome biogenesis and function by the ribosomal protein S6 kinase, a key mediator of mTOR function. *Growth Factors* 2007 Aug;25(4):209-226.

(145) Proud CG. Signalling to translation: how signal transduction pathways control the protein synthetic machinery. *Biochem.J.* 2007 Apr 15;403(2):217-234.

- (146) Fumagalli SaT,G. S6 Phosphorylation and Signal Transduction. In: Mathews MB, Sonenburg N, Hershey JWB, editors. Translational control of gene expression: NY, Cold Spring Harbor Laboratory Press; 2000. p. 695-711.
- (147) Roux PP, Shahbazian D, Vu H, Holz MK, Cohen MS, Taunton J, et al. RAS/ERK signaling promotes site-specific ribosomal protein S6 phosphorylation via RSK and stimulates cap-dependent translation. *J.Biol.Chem.* 2007 May 11;282(19):14056-14064.
- (148) Pende M, Um SH, Mieulet V, Sticker M, Goss VL, Mestan J, et al. S6K1(-)/S6K2(-) mice exhibit perinatal lethality and rapamycin-sensitive 5'-terminal oligopyrimidine mRNA translation and reveal a mitogen-activated protein kinase-dependent S6 kinase pathway. *Mol.Cell.Biol.* 2004 Apr;24(8):3112-3124.
- (149) Ruvinsky I, Sharon N, Lerer T, Cohen H, Stolovich-Rain M, Nir T, et al. Ribosomal protein S6 phosphorylation is a determinant of cell size and glucose homeostasis. *Genes Dev.* 2005 Sep 15;19(18):2199-2211.
- (150) McKay MM, Morrison DK. Integrating signals from RTKs to ERK/MAPK. *Oncogene* 2007 May 14;26(22):3113-3121.
- (151) Shaul YD, Seger R. The MEK/ERK cascade: from signaling specificity to diverse functions. *Biochim.Biophys.Acta* 2007 Aug;1773(8):1213-1226.
- (152) Kline WO, Panaro FJ, Yang H, Bodine SC. Rapamycin inhibits the growth and muscle-sparing effects of clenbuterol. *J.Appl.Physiol.* 2007 Feb;102(2):740-747.
- (153) Kimball SR. Eukaryotic initiation factor eIF2. *Int.J.Biochem.Cell Biol.* 1999 Jan;31(1):25-29.
- (154) Proud CG. eIF2 and the control of cell physiology. *Semin.Cell Dev.Biol.* 2005 Feb;16(1):3-12.
- (155) Zhou D, Palam LR, Jiang L, Narasimhan J, Staschke KA, Wek RC. Phosphorylation of eIF2 directs ATF5 translational control in response to diverse stress conditions. *J.Biol.Chem.* 2008 Mar 14;283(11):7064-7073.
- (156) Wek RC, Jiang HY, Anthony TG. Coping with stress: eIF2 kinases and translational control. *Biochem.Soc.Trans.* 2006 Feb;34(Pt 1):7-11.
- (157) Oyadomari S, Harding HP, Zhang Y, Oyadomari M, Ron D. Dephosphorylation of translation initiation factor 2alpha enhances glucose tolerance and attenuates hepatosteatosis in mice. *Cell.Metab.* 2008 Jun;7(6):520-532.
- (158) Lecker SH, Goldberg AL, Mitch WE. Protein degradation by the ubiquitin-proteasome pathway in normal and disease states. *Journal of the American Society of Nephrology* 2006 Jul;17(7):1807-1819.

- (159) Mitch WE, Goldberg AL. Mechanisms of muscle wasting. The role of the ubiquitin-proteasome pathway. *N.Engl.J.Med.* 1996 Dec 19;335(25):1897-1905.
- (160) Sandri M, Sandri C, Gilbert A, Skurk C, Calabria E, Picard A, et al. Foxo transcription factors induce the atrophy-related ubiquitin ligase atrogin-1 and cause skeletal muscle atrophy. *Cell* 2004 Apr 30;117(3):399-412.
- (161) Wang XaM,W.E. Proceedings of the National Academy of Sciences of the USA 2008 (in press).
- (162) Du J, Wang X, Miereles C, Bailey JL, Debigare R, Zheng B, et al. Activation of caspase-3 is an initial step triggering accelerated muscle proteolysis in catabolic conditions. *J.Clin.Invest.* 2004 Jan;113(1):115-123.
- (163) Workeneh BT, Rondon-Berrios H, Zhang L, Hu Z, Ayehu G, Ferrando A, et al. Development of a diagnostic method for detecting increased muscle protein degradation in patients with catabolic conditions. *J.Am.Soc.Nephrol.* 2006 Nov;17(11):3233-3239.
- (164) Bailey JL, Zheng B, Hu Z, Price SR, Mitch WE. Chronic kidney disease causes defects in signaling through the insulin receptor substrate/phosphatidylinositol 3-kinase/Akt pathway: implications for muscle atrophy. *J.Am.Soc.Nephrol.* 2006 May;17(5):1388-1394.
- (165) Lee SW, Park GH, Lee SW, Song JH, Hong KC, Kim MJ. Insulin resistance and muscle wasting in non-diabetic end-stage renal disease patients. *Nephrol.Dial.Transplant.* 2007 Sep;22(9):2554-2562.
- (166) Pickering W, Cheng M, Brown J, Butler H, Wall J, Bevington A. Stimulation of protein degradation by low pH in L6G8C5 skeletal muscle cells is independent of apoptosis but dependent on differentiation state. *Nephrol.Dial.Transplant.* 2003 Aug; 18(8): 1466-1474.
- (167) Elsner P, Quistorff B, Hermann TS, Dich J, Grunnet N. Regulation of glycogen accumulation in L6 myotubes cultured under optimized differentiation conditions. *Am. J. Physiol. Endocrinol. Metab.* 1998 Dec; 275 (6Pt1): E925-933.
- (168) Lowry OH, Rosebrough NJ, Farr AL, Randall RJ. Protein measurement with the Folin phenol reagent. *J.Biol.Chem.* 1951 Nov;193(1):265-275.
- (169) Ballard FJ, Francis GL. Effects of anabolic agents on protein breakdown in L6 myoblasts. *Biochem.J.* 1983 Jan 15;210(1):243-249.
- (170) Evans K, Nasim Z, Brown J, Butler H, Kauser S, Varoqui H, et al. Acidosis-sensing glutamine pump SNAT2 determines amino acid levels and mammalian target of rapamycin signalling to protein synthesis in L6 muscle cells. *Journal of the American Society of Nephrology* 2007 May;18(5):1426-1436.

- (171) Hundal HS, Bilan PJ, Tsakiridis T, Marette A, Klip A. Structural disruption of the trans-Golgi network does not interfere with the acute stimulation of glucose and amino acid uptake by insulin-like growth factor I in muscle cells. *Biochem.J.* 1994 Jan 15;297 (Pt 2)(Pt 2):289-295.
- (172) Howells LM, Hudson EA, Manson MM. Inhibition of phosphatidylinositol 3-kinase/protein kinase B signaling is not sufficient to account for indole-3-carbinol-induced apoptosis in some breast and prostate tumor cells. *Clin.Cancer Res.* 2005 Dec 1;11(23):8521-8527.
- (173) Santoro JC, Harris G, Sitlani A. Colorimetric detection of glutamine synthetase-catalyzed transferase activity in glucocorticoid-treated skeletal muscle cells. *Anal.Biochem.* 2001 Feb 1;289(1):18-25.
- (174) Xiang J, Ennis SR, Abdelkarim GE, Fujisawa M, Kawai N, Keep RF. Glutamine transport at the blood-brain and blood-cerebrospinal fluid barriers. *Neurochem.Int.* 2003 Sep-Oct;43(4-5):279-288.
- (175) Ensenat D, Hassan S, Reyna SV, Schafer AI, Durante W. Transforming growth factor-beta 1 stimulates vascular smooth muscle cell L-proline transport by inducing system A amino acid transporter 2 (SAT2) gene expression. *Biochem.J.* 2001 Dec 1;360(Pt 2):507-512.
- (176) Al-Bader MD, Al-Sarraf HA. Housekeeping gene expression during fetal brain development in the rat-validation by semi-quantitative RT-PCR. *Brain Res.Dev.Brain Res.* 2005 Apr 21;156(1):38-45.
- (177) Mitch WE. Metabolic and clinical consequences of metabolic acidosis. *J.Nephrol.* 2006 Mar-Apr;19 Suppl 9:S70-5.
- (178) Stein A, Moorhouse J, Iles-Smith H, Baker F, Johnstone J, James G, et al. Role of an improvement in acid-base status and nutrition in CAPD patients. *Kidney Int.* 1997 Oct;52(4):1089-1095.
- (179) Szeto CC, Wong TY, Chow KM, Leung CB, Li PK. Oral sodium bicarbonate for the treatment of metabolic acidosis in peritoneal dialysis patients: a randomized placebo-control trial. *J.Am.Soc.Nephrol.* 2003 Aug;14(8):2119-2126.
- (180) Bergstrom J, Alvestrand A, Furst P. Plasma and muscle free amino acids in maintenance hemodialysis patients without protein malnutrition. *Kidney Int.* 1990 Jul;38(1):108-114.
- (181) Lofberg E, Wernerman J, Anderstam B, Bergstrom J. Correction of acidosis in dialysis patients increases branched-chain and total essential amino acid levels in muscle. *Clin.Nephrol.* 1997 Oct;48(4):230-237.
- (182) Vabulas RM, Hartl FU. Protein synthesis upon acute nutrient restriction relies on proteasome function. *Science* 2005 Dec 23;310(5756):1960-1963.

- (183) Du J, Hu Z, Mitch WE. Molecular mechanisms activating muscle protein degradation in chronic kidney disease and other catabolic conditions. *Eur.J.Clin.Invest.* 2005 Mar;35(3):157-163.
- (184) Curi R, Lagranha CJ, Doi SQ, Sellitti DF, Procopio J, Pithon-Curi TC, et al. Molecular mechanisms of glutamine action. *J.Cell.Physiol.* 2005 Aug;204(2):392-401.
- (185) Holecek M. Relation between glutamine, branched-chain amino acids, and protein metabolism. *Nutrition* 2002 Feb;18(2):130-133.
- (186) Lyons SD, Sant ME, Christopherson RI. Cytotoxic mechanisms of glutamine antagonists in mouse L1210 leukemia. *J.Biol.Chem.* 1990 Jul 5;265(19):11377-11381.
- (187) Oehler R, Roth E. Regulative capacity of glutamine. *Curr.Opin.Clin.Nutr.Metab.Care* 2003 May;6(3):277-282.
- (188) Rennie MJ, Hundal HS, Babij P, MacLennan P, Taylor PM, Watt PW, et al. Characteristics of a glutamine carrier in skeletal muscle have important consequences for nitrogen loss in injury, infection, and chronic disease. *Lancet* 1986 Nov 1;2(8514):1008-1012.
- (189) Mittendorfer B, Volpi E, Wolfe RR. Whole body and skeletal muscle glutamine metabolism in healthy subjects. *Am.J.Physiol.Endocrinol.Metab.* 2001 Feb;280(2):E323-33.
- (190) Hyde R, Hajduch E, Powell DJ, Taylor PM, Hundal HS. Ceramide down-regulates System A amino acid transport and protein synthesis in rat skeletal muscle cells. *FASEB J.* 2005 Mar;19(3):461-463.
- (191) Lundholm K, Edstrom S, Ekman L, Karlberg I, Walker P, Schersten T. Protein degradation in human skeletal muscle tissue: the effect of insulin, leucine, amino acids and ions. *Clin.Sci.(Lond)* 1981 Mar;60(3):319-326.
- (192) Kimball SR, Shantz LM, Horetsky RL, Jefferson LS. Leucine regulates translation of specific mRNAs in L6 myoblasts through mTOR-mediated changes in availability of eIF4E and phosphorylation of ribosomal protein S6. *J.Biol.Chem.* 1999 Apr 23;274(17):11647-11652.
- (193) Bevington A, Brown J, Walls J. Leucine suppresses acid-induced protein wasting in L6 rat muscle cells. *Eur.J.Clin.Invest.* 2001 Jun;31(6):497-503.
- (194) Sugawara M, Nakanishi T, Fei YJ, Martindale RG, Ganapathy ME, Leibach FH, et al. Structure and function of ATA3, a new subtype of amino acid transport system A, primarily expressed in the liver and skeletal muscle. *Biochim.Biophys.Acta* 2000 Dec 20;1509(1-2):7-13.
- (195) King PA. Effects of insulin and exercise on amino acid transport in rat skeletal muscle. *Am.J.Physiol.* 1994 Feb;266(2 Pt 1):C524-30.

- (196) Cuthbertson DJ, Babraj J, Smith K, Wilkes E, Fedele MJ, Esser K, et al. Anabolic signaling and protein synthesis in human skeletal muscle after dynamic shortening or lengthening exercise. *Am.J.Physiol.Endocrinol.Metab.* 2006 Apr;290(4):E731-8.
- (197) Hornberger TA, Stuppard R, Conley KE, Fedele MJ, Fiorotto ML, Chin ER, et al. Mechanical stimuli regulate rapamycin-sensitive signalling by a phosphoinositide 3-kinase-, protein kinase B- and growth factor-independent mechanism. *Biochem.J.* 2004 Jun 15;380(Pt 3):795-804.
- (198) Steinhagen C, Hirche HJ, Nestle HW, Bovenkamp U, Hosselmann I. The interstitial pH of the working gastrocnemius muscle of the dog. *Pflugers Arch.* 1976 Dec 28;367(2):151-156.
- (199) Wesson DE. Dietary acid increases blood and renal cortical acid content in rats. *Am.J.Physiol.* 1998 Jan;274(1 Pt 2):F97-103.
- (200) Asola, M.R. Virtanen, K.A. Peltoniemi, P. Nagren, K. Jyrkkio, S. Knutti, J. Nuutila, P.R. Metsarinne, K.P. Amino acid transport into skeletal muscle is impaired in chronic renal failure [abstract]. *J Am Soc Nephrol* 2001;12(64A).
- (201) Maroni BJ, Haesemeyer RW, Kutner MH, Mitch WE. Kinetics of system A amino acid uptake by muscle: effects of insulin and acute uremia. *Am.J.Physiol.* 1990 May;258(5 Pt 2):F1304-10.
- (202) Siew ED, Pupim LB, Majchrzak KM, Shintani A, Flakoll PJ, Ikizler TA. Insulin resistance is associated with skeletal muscle protein breakdown in non-diabetic chronic hemodialysis patients. *Kidney Int.* 2007 Jan;71(2):146-152.
- (203) Eley HL, Russell ST, Tisdale MJ. Effect of branched-chain amino acids on muscle atrophy in cancer cachexia. *Biochem.J.* 2007 Oct 1;407(1):113-120.
- (204) Peyrollier K, Hajduch E, Blair AS, Hyde R, Hundal HS. L-leucine availability regulates phosphatidylinositol 3-kinase, p70 S6 kinase and glycogen synthase kinase-3 activity in L6 muscle cells: evidence for the involvement of the mammalian target of rapamycin (mTOR) pathway in the L-leucine-induced up-regulation of system A amino acid transport. *Biochem.J.* 2000 Sep 1;350 Pt 2:361-368.
- (205) Wang X, Campbell LE, Miller CM, Proud CG. Amino acid availability regulates p70 S6 kinase and multiple translation factors. *Biochem.J.* 1998 Aug 15;334 (Pt 1)(Pt 1):261-267.
- (206) Campbell LE, Wang X, Proud CG. Nutrients differentially regulate multiple translation factors and their control by insulin. *Biochem.J.* 1999 Dec 1;344 Pt 2:433-441.
- (207) Wu B, Ottow K, Poulsen P, Gaber RF, Albers E, Kielland-Brandt MC. Competitive intra- and extracellular nutrient sensing by the transporter homologue Ssy1p. *J.Cell Biol.* 2006 May 8;173(3):327-331.

- (208) Goberdhan DC, Meredith D, Boyd CA, Wilson C. PAT-related amino acid transporters regulate growth via a novel mechanism that does not require bulk transport of amino acids. *Development* 2005 May;132(10):2365-2375.
- (209) Beauloye C, Bertrand L, Krause U, Marsin AS, Dresselaers T, Vanstapel F, et al. No-flow ischemia inhibits insulin signaling in heart by decreasing intracellular pH. *Circ.Res.* 2001 Mar 16;88(5):513-519.
- (210) McCormick JI, Johnstone RM. Identification of the integrin alpha 3 beta 1 as a component of a partially purified A-system amino acid transporter from Ehrlich cell plasma membranes. *Biochem.J.* 1995 Nov 1;311 (Pt 3)(Pt 3):743-751.
- (211) Thamilselvan V, Craig DH, Basson MD. FAK association with multiple signal proteins mediates pressure-induced colon cancer cell adhesion via a Src-dependent PI3K/Akt pathway. *FASEB J.* 2007 Jun;21(8):1730-1741.
- (212) Christie GR, Hajduch E, Hundal HS, Proud CG, Taylor PM. Intracellular sensing of amino acids in *Xenopus laevis* oocytes stimulates p70 S6 kinase in a target of rapamycin-dependent manner. *J.Biol.Chem.* 2002 Mar 22;277(12):9952-9957.
- (213) Beugnet A, Tee AR, Taylor PM, Proud CG. Regulation of targets of mTOR (mammalian target of rapamycin) signalling by intracellular amino acid availability. *Biochem.J.* 2003 Jun 1;372(Pt 2):555-566.
- (214) Flaring UB, Rooyackers OE, Wernerman J, Hammarqvist F. Glutamine attenuates post-traumatic glutathione depletion in human muscle. *Clin.Sci.(Lond)* 2003 Mar;104(3):275-282.
- (215) Haussinger D, Schliess F. Glutamine metabolism and signaling in the liver. *Front.Biosci.* 2007 Jan 1;12:371-391.
- (216) Comer FI, Hart GW. O-GlcNAc and the control of gene expression. *Biochim.Biophys.Acta* 1999 Dec 6;1473(1):161-171.
- (217) Rennie MJ. Recent findings on the mechanism of glutamine stimulation of protein and carbohydrate anabolism. *Clin.Nutr.* 1990 Feb;9(1):33-34.
- (218) Ritchie JW, Baird FE, Christie GR, Stewart A, Low SY, Hundal HS, et al. Mechanisms of glutamine transport in rat adipocytes and acute regulation by cell swelling. *Cell.Physiol.Biochem.* 2001;11(5):259-270.
- (219) Wang J, Liu R, Hawkins M, Barzilai N, Rossetti L. A nutrient-sensing pathway regulates leptin gene expression in muscle and fat. *Nature* 1998 Jun 18;393(6686):684-688.
- (220) Kline CL, Schrufer TL, Jefferson LS, Kimball SR. Glucosamine-induced phosphorylation of the alpha-subunit of eukaryotic initiation factor 2 is mediated by the protein kinase R-like endoplasmic-reticulum associated kinase. *Int.J.Biochem.Cell Biol.* 2006;38(5-6):1004-1014.

- (221) Krause U, Bertrand L, Maisin L, Rosa M, Hue L. Signalling pathways and combinatory effects of insulin and amino acids in isolated rat hepatocytes. *Eur.J.Biochem.* 2002 Aug;269(15):3742-3750.
- (222) Kimball SR, Horetsky RL, Jefferson LS. Implication of eIF2B rather than eIF4E in the regulation of global protein synthesis by amino acids in L6 myoblasts. *J.Biol.Chem.* 1998 Nov 20;273(47):30945-30953.
- (223) Gomez E, Powell ML, Bevington A, Herbert TP. A decrease in cellular energy status stimulates PERK-dependent eIF2alpha phosphorylation and regulates protein synthesis in pancreatic beta-cells. *Biochem.J.* 2008 Mar 15;410(3):485-493.
- (224) Arias EB, Kim J, Cartee GD. Prolonged incubation in PUGNAc results in increased protein O-Linked glycosylation and insulin resistance in rat skeletal muscle. *Diabetes* 2004 Apr;53(4):921-930.
- (225) Bobrovnikova-Marjon EV, Marjon PL, Barbash O, Vander Jagt DL, Abcouwer SF. Expression of angiogenic factors vascular endothelial growth factor and interleukin-8/CXCL8 is highly responsive to ambient glutamine availability: role of nuclear factor-kappaB and activating protein-1. *Cancer Res.* 2004 Jul 15;64(14):4858-4869.
- (226) Abcouwer SF, Schwarz C, Meguid RA. Glutamine deprivation induces the expression of GADD45 and GADD153 primarily by mRNA stabilization. *J.Biol.Chem.* 1999 Oct 1;274(40):28645-28651.
- (227) Mortimore GE, Wert JJ,Jr, Miotto G, Venerando R, Kadowaki M. Leucine-specific binding of photoreactive Leu7-MAP to a high molecular weight protein on the plasma membrane of the isolated rat hepatocyte. *Biochem.Biophys.Res.Commun.* 1994 Aug 30;203(1):200-208.
- (228) Olsen JV, Blagoev B, Gnäd F, Macek B, Kumar C, Mortensen P, et al. Global, in vivo, and site-specific phosphorylation dynamics in signaling networks. *Cell* 2006 Nov 3;127(3):635-648.
- (229) Olsen JV, Blagoev B, Gnäd F, Macek B, Kumar C, Mortensen P, et al. Global, in vivo, and site-specific phosphorylation dynamics in signaling networks. [SNAT2 online database].